

Evaluation of Copernicus MACC-II ensemble products in the ETC/ACM spatial air quality mapping



ETC/ACM Technical Paper 2013/9
April 2014

*Jan Horálek, Leonor Tarrasón, Peter de Smet,
Laure Malherbe, Philipp Schneider, Anthony Ung,
Linton Corbet and Bruce Denby*



The European Topic Centre on Air Pollution and Climate Change Mitigation (ETC/ACM) is a consortium of European institutes under contract of the European Environment Agency
RIVM UBA-V ÖKO AEAT EMISIA CHMI NILU VITO INERIS 4Sfera PBL CSIC

Front page picture:

Left: Satellite image of Europe illustrated with air quality measurement stations and their coloured concentration values; these data are the primary data source of the spatial interpolation mapping method dealt with in this paper.

Top right: Artist's impression of a satellite in Earth orbit, as illustration that satellite imagery (may) contribute to air quality mapping and assessments.

Bottom right: The MACC-II logo, as illustration of the potential role its air quality modelling data may have in improving European spatial interpolated air quality mapping, as tested in this paper.

Author affiliation:

Leonor Tarrasón, Philipp Schneider and Bruce Denby: Norwegian Institute of Air Research (NILU), Norway

Jan Horálek, Linton Corbet: Czech Hydrometeorological Institute (CHMI), Czech Republic

Laure Malherbe, Anthony Ung: National Institute for Industrial Environment and Risk (INERIS), France

Peter de Smet: National Institute for Public Health and the Environment (RIVM), The Netherlands

Refer to this document as:

Horálek J, Tarrasón L, De Smet P, Malherbe L, Schneider P, Ung A, Corbet L, Denby B (2014). Evaluation of Copernicus MACC-II ensemble products in the ETC/ACM spatial air quality mapping. ETC/ACM Technical paper 2013/9.

http://acm.eionet.europa.eu/reports/ETCACM_TP_2013_9_AQmaps_with_MACCproducts

DISCLAIMER

This ETC/ACM Technical Paper has not been subjected to European Environment Agency (EEA) member country review. It does not represent the formal views of the EEA.

© ETC/ACM, 2014.

ETC/ACM Technical Paper 2013/9

European Topic Centre on Air Pollution and Climate Change Mitigation

PO Box 1

3720 BA Bilthoven

The Netherlands

Phone +31 30 2748562

Fax +31 30 2744433

Email etcacm@rivm.nl

Website <http://acm.eionet.europa.eu/>

Contents

1	INTRODUCTION	5
2	CURRENT MAPPING METHODS WITH RELEVANCE FOR ETC/ACM	7
2.1	CURRENT ETC/ACM SPATIAL MAPPING TECHNIQUE	7
2.2	MODEL PRODUCTS FROM MACC-II	10
2.3	MAPPING APPROACH WITHIN EC4MACS	14
3	COMPARISON APPROACH AND DATA USED	15
3.1	SELECTION OF DIFFERENT OPTIONS FOR COMPARISON	15
3.2	DATA USED FOR THE COMPARISON.....	17
3.3	METHODOLOGY USED FOR THE COMPARISON.....	21
4	COMPARISON OF MAPPING RESULTS USING DIFFERENT MODEL OUTPUTS.....	23
4.1	PM ₁₀	24
4.1.1	<i>Mapping using EMEP, MACC-II Ensemble and CHIMERE models</i>	<i>24</i>
4.1.2	<i>Cross-validation results.....</i>	<i>33</i>
4.2	OZONE.....	36
4.2.1	<i>Mapping using EMEP, MACC-II Ensemble and CHIMERE models</i>	<i>36</i>
4.2.2	<i>Cross-validation results.....</i>	<i>43</i>
4.3	CONCLUSIONS	45
5	COMPARISON WITH MODEL RESULTS	47
5.1	COMPARISON WITH HINDCAST MODEL OUTPUTS.....	47
5.2	INITIAL COMPARISON WITH REANALYSIS MODEL RESULTS	53
5.2.1	PM ₁₀	54
5.2.2	Ozone.....	60
6	RECOMMENDATIONS	65
6.1	GENERAL REQUIREMENTS FOR MODELS USED IN ETC/ACM MAPPING	65
6.2	SPECIFIC REQUIREMENTS FOR MACC-II PRODUCTS	68
6.3	RECOMMENDATIONS FOR FUTURE ETC/ACM MAPPING ASSESSMENTS.....	69
7	SUMMARY AND CONCLUSIONS	71
	REFERENCES.....	75
	ANNEX 1. PARAMETERS USED IN ETC/ACM SPATIAL INTERPOLATION METHOD.....	79
	ANNEX 2. CROSS-VALIDATION SCATTER PLOTS.....	83
	ANNEX 3. MAPS OF DIFFERENCES	97
	ANNEX 4. OUTPUTS OF CHEMICAL TRANSPORT MODELS	107
	ANNEX 5. SCATTER PLOTS AND STATISTICAL INDICATORS OF MODELLED VS. MEASUREMENT DATA.....	113
	ANNEX 6. COMPARISON OF SCATTER PLOTS OF REANALYSED MODEL AND ETC/ACM MAPPING RESULTS..	129
	ANNEX 7. EXPLANATION OF TAYLOR DIAGRAM PRINCIPLE.....	147

1 Introduction

The Directive on Ambient Air Quality and Cleaner Air for Europe (EC, 2008) requires that air quality should be assessed throughout the territory of each member state. It requires that the fixed measurements should be used as a primarily source of information for such assessment in the polluted areas. Those measurement data may be supplemented by modelling techniques to provide adequate information on the spatial distribution of the air quality.

The mapping methodology developed at EEA through its ETC/ACM (EEA, 2009) provides such assessments based primarily on air quality measurements. It combines monitoring data, chemical transport model results and ancillary information through spatial interpolation methods in order to provide consistent estimates of air quality across Europe. The mapping results provide regularly a consistent set of information for ozone and particulate matter pollution that exceeds the accuracy achievable from using any single model. It currently provides a unified methodology for estimating background pollution levels in Europe and offers information on the probability of exceedance of limit values with a spatial resolution of $10 \times 10 \text{ km}^2$.

The ETC/ACM spatially interpolated (SI) maps describe different concentration layers, combining observations from AirBase stations and background model information at regional scale (Horálek et al., 2013). The basic dispersion modelling information at the European level, which is used currently at ETC/ACM, is obtained from the EMEP model, a reference regional chemical transport model in Europe with a spatial resolution of $50 \times 50 \text{ km}^2$. The quality and resolution of the EMEP model used as reference for these mapping activities influences the quality of the spatially interpolated maps. The recent availability of a series of Copernicus Atmospheric Service (MACC-II) products opens up the possibility for potential improving the geostatistical mapping technique as it is operationally used at the ETC/ACM.

The Copernicus program is a European initiative to support the development and the implementation of operational services dedicated to environment and security monitoring. They should provide to the general public, decision makers, research laboratories, industries and consulting companies, data they need or request for knowledge and economy development. The projects MACC (2009–2011) and MACC-II (2011–2014) relate to the pre-operational phase of the future Copernicus Atmospheric Services. Such monitoring services aim at describing and forecasting the atmospheric composition at the global to European scales to inform general public and support policy decision. Services result from a wealth of data from ground level monitoring networks, Earth observations systems and model results used to derive operational products such as atmospheric composition forecasts, reanalyses and policy-oriented tools.

In 2012, mapping activities at ETC/ACM were extended to investigate the feasibility of using Copernicus products within the mapping procedure. The potential of using Copernicus (formerly called GMES) satellite data for mapping nitrogen dioxide at European scale was identified as a possible contribution to the mapping activities (Schneider et al., 2012). A second study presented a series of approaches to carry out urban air quality mapping using new methodologies based on the Copernicus services (Rouil, 2012b). This later study proposed the use of the regional scale MACC-II Ensemble as potential alternative modelling

input in the ETC/ACM routine mapping activities. The MACC-II Ensemble model is a combination of the model results provided by the individual regional chemistry transport involved in MACC-II.

The main purpose of the present study is to carry out a comparison of the ETC/ACM mapping results when using either the EMEP model or the MACC-II Ensemble model as an auxiliary variable in the geostatistical interpolation. The results from the comparison are expected to determine the capabilities and needs of the MACC-II ensemble system as input to ETC/ACM mapping activities and its feasibility to become part of the operational ETC/ACM mapping chain. The ultimate goal is to improve the quality of the routine mapping assessments and provide a consistent estimate of rural and urban background levels over Europe. The assessment is also intended for use by national and urban authorities as input for their exposure estimates at urban level.

Next to this, the paper compares the ETC/ACM mapping results and the modelling results, in order to show the added value of the ETC/ACM mapping routines with respect to any of the chemical transport models used.

Chapter 2 describes briefly the mapping methods relevant for ETC/ACM. Chapter 3 documents the comparison approach and the input data. Chapter 4 presents the comparison of the ETC/ACM mapping results using different chemical transport models. Chapter 5 shows the comparison of the mapping results with the model results. Chapter 6 gives the recommendations and Chapter 7 summarizes the conclusions. Annexes provide the details of the comparisons.

2 Current mapping methods with relevance for ETC/ACM

2.1 Current ETC/ACM spatial mapping technique

The current ETC/ACM mapping method was developed with the objective of the European Environmental Agency of having interpolated maps primarily based on air quality measurements as reported by the countries through the Exchange of Information (EoI), next to the model-based European air quality maps (Horálek et al., 2007). In the method, the ground-level measurements are taken as the primarily data and the results from chemistry transport modelling and other auxiliary data (altitude, meteorology) as the secondary sources. By this, the method differs from the data assimilation methods (see Section 2.2) that incorporates monitoring data directly into air quality model calculations during the modelling process itself (EEA, 2011a).

The method used is a linear regression model followed by kriging of the residuals produced by that model (residual kriging). In the linear regression model, the measured data are considered as a dependent variable, while a dispersion model's output and other supplementary data (altitude, meteorology) are used as independent variables. These gridded auxiliary variables provide a spatial perspective to guide the interpolation process. The estimation is calculated according to relation

$$\hat{Z}(s_0) = c + a_1.X_1(s_0) + a_2.X_2(s_0) + \dots + a_n.X_n(s_0) + \eta(s_0)$$

where $\hat{Z}(s_0)$ is the estimated value of the air pollution indicator at a point s_0 ,
 $X_1(s_0), X_2(s_0), \dots, X_n(s_0)$ are n number of individual auxiliary variables at a point s_0 ,
 c, a_1, a_2, \dots, a_n are $n+1$ parameters of the linear regression model calculated based on the data at the points of measurement, and
 $\eta(s_0)$ is the calculated spatial interpolated value of the residuals of the linear regression model at a point s_0 , based on the residuals at the points of measurement.

The spatial interpolation of the regression's residuals is carried out using ordinary kriging, according to equation

$$\hat{R}(s_0) = \sum_{i=1}^N \lambda_i R(s_i), \text{ with } \sum_{i=1}^N \lambda_i = 1$$

where $\hat{R}(s_0)$ is the interpolated value at a point s_0 , derived from the residuals of the linear regression model at the points of measurement $s_i, i = 1, \dots, N$,
 $R(s_i)$ are the residuals of the linear regression model at the points of measurement $s_i, i = 1, \dots, N$,
 N is the number of the measurement stations used in the interpolation, and
 $\lambda_1, \dots, \lambda_N$ are the weights estimated based on the *variogram*, which is a measure of a spatial correlation, see Cressie (1993).

The variogram is estimated as following: first, the *empirical* variogram $2\gamma_e$ is calculated according to equation

$$2\gamma_e(h) = \frac{1}{n} \sum_{i,j;d(i,j)=h\pm\delta} (R(s_i) - R(s_j))^2$$

where $R(s_i), R(s_j)$ are the residuals in the points of the measurement stations s_i and s_j ,
 $d(i,j)$ is the distance between the points s_i and s_j , and
 n is the number of the pairs of stations with the distance $h\pm\delta$ (where δ is the tolerance).

Next step is to fit the empirical variogram using a spherical function according to equation

$$2\gamma_f(h) = (\theta_s - \theta_n) \left(\frac{h}{\theta_r} - \frac{h^3}{\theta_r^3} \right) + \theta_n \quad \text{for } h < \theta_r$$

$$= \theta_s \quad \text{for } h \geq \theta_r$$

where $2\gamma_f(h)$ is the fitted variogram,
 $\theta_n, \theta_s, \theta_r$ are the parameters of the fitted variogram (called *nugget*, *sill*, and *range*), based on the empirical variogram by minimizing RMSE (Section 3.3).

For the illustration of the spherical function and the parameters of variogram, see Figure 2.1.

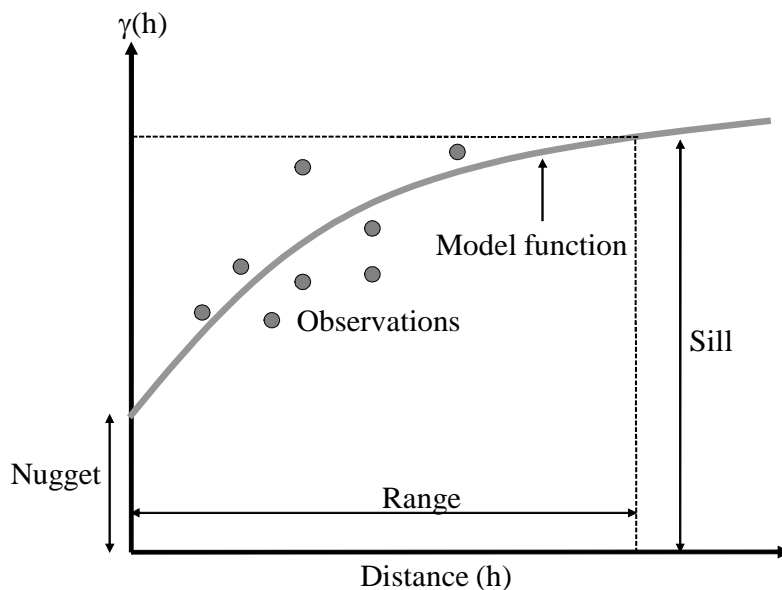


Figure 2.1. Diagram showing the parameters of variogram function

In the case of PM_{10} (and $PM_{2.5}$, however not dealt with in this paper), prior to linear regression and interpolation, a logarithmic transformation to measured and modelled data is applied. After the interpolation, a back-transformation is used.

The maps are constructed for the rural and urban background areas separately on a grid of $10 \times 10 \text{ km}^2$ resolution. The reason for this procedure is that the urban air quality fields are different from the rural ones, i.e. the concentration level for urban areas is in general higher

for PM₁₀ (and many other pollutants) and lower for ozone. The rural map is based on rural background stations and the urban background map is based on urban and suburban background stations. Both the rural and the urban background maps are adapted using the joint rural/urban map, which is constructed based on both rural and urban/suburban background stations. (This adaption applies at a limited set of areas where the estimated urban value is lower, respectively higher, in case of PM₁₀, respectively ozone, than the estimated rural map value; for details, see De Smet et al., 2011.) Subsequently to this, the adapted rural and urban background maps are merged into one combined air quality indicator map using a European-wide population density grid at 1x1 km² resolution. For areas with a population density less than the defined value of α_1 , the rural map is applied, and for areas with a population density grids greater than the defined value α_2 , the urban background map is applied. For areas with population density within the interval (α_1, α_2) , the relation

$$\hat{Z}(s) = \frac{\alpha_2 - \alpha(s)}{\alpha_2 - \alpha_1} \cdot R(s) + \frac{\alpha(s) - \alpha_1}{\alpha_2 - \alpha_1} \cdot UB(s) \text{ is applied,}$$

where $\hat{Z}(s)$ is the resulting estimate of concentration at the point s ,

$R(s)$ is the concentration at the point s for the rural map,

$UB(s)$ is the concentration at the point s for the urban background map, and

$\alpha(s)$ is the population density at the point s .

For the details, see Horálek et al. (2010) and De Smet et al. (2011).

The final merged map in 1x1 km² resolution is used for exposure estimates. The map in 1x1 km² resolution distinguishes better the rural and the urban background areas compared to the map with the lower resolution of 10x10 km² (see Horálek et al., 2010). However, for final presentation of the mapping results on a European scale, a spatial aggregation to 10x10 km² resolution has been chosen. For details on the residual kriging procedure applied by the ETC/ACM, see Horálek et al. (2013).

In this paper, rural and urban background maps are mostly analysed separately. In some cases (namely in Section 5.2), also the merged maps in 1x1 km² resolution are used for analysis.

For different pollutants and area types, different supplementary data are used in the mapping, see Table 2.1. For all indicators of one pollutant, the same set of supplementary data is used.

Table 2.1 Supplementary data used in ETC/ACM mapping

Pollutant and area type		EMEP model output	Altitude	Surface solar radiation	Wind speed	Population density
PM ₁₀	rural	+	+	+	+	-
	urban background	+	-	-	-	-
Ozone	rural	+	+	+	-	-
	urban background	+	-	+	+	-
PM _{2.5}	rural	+	+	+	+	+
	urban background	-	-	-	-	-
NO ₂	rural	+	+	-	+	-
	urban background	+	+	-	+	-
NO _x	rural	+	+	+	+	-
SO ₂	rural	+	+	-	-	-

The specific supplementary data for individual pollutants and area types were selected as being in general the most significant when including them in the mapping, see Horálek et al. (2007 and 2008) and Denby et al. (2011b). The maps of PM₁₀, PM_{2.5} and O₃ are constructed routinely annually (e.g. Horálek et al., 2013), while the maps of other pollutant occasionally.

The mapping domain consists of the areas of all EEA member and cooperating countries, as far as they fall into the EEA map extent *Map_1c* (EEA, 2011b). Due to a lack of observations in Turkey, the interpolation results for Turkey are not presented in the maps.

2.2 Model products from MACC-II

The MACC-II project – Monitoring Atmospheric Composition and Climate – is the current pre-operational Copernicus Atmosphere Service. Copernicus was previously known as GMES (Global Monitoring for Environment and Security). MACC-II includes a European-wide regional air quality service that secures the timely provision of forecasts of up to two days, daily analysed maps, and reanalysed (or data assimilated) maps of air pollutants regulated in Europe by the European Union’s (EU’s) air quality legislation (i.e. for ozone, SO₂, NO₂, PM₁₀, and PM_{2.5}). Further, hindcast maps, i.e. model estimates of the past air quality situations (without the use of the data assimilation) are also calculated, however not as a standard product. Forecasts and near-real time analysis are calculated within the ENS (Air quality forecasting and analysis) subproject of MACC-II, while hindcasts and reanalysis are produced within its EVA (Air quality validated assessments) subproject. For the meaning of the used specific terms, see glossary presented in Table 2.2.

Table 2.2 Glossary of the used specific terms

Term	Meaning
Analyses	Air pollutant concentrations fields issued from numerical model results combined with up-to-date available observation data to improve their accuracy using data assimilation. In MACC-II, they are produced routinely on a daily basis.
Data assimilation (DA)	Mathematical process to incorporate observations in a numerical model of physical systems.
Ensemble model	Combination of various results from various models. This can be a simple average or median, or a weighted average resulting from analysis of models’ behaviour over past periods.
Hindcast	Model result (simulation) of a past situation, without any data assimilation.
In-situ	Ground-level (contrary to satellite).
Raw model data	Model results directly issued from the modelling chain, without any post-treatment process.
Reanalyses	Air pollutant concentrations fields issued from model results of past period combined with validated observation data using data assimilation to improve their accuracy.

In this paper, only hindcasts and reanalysed modelling outputs are considered.

The MACC-II regional air quality service includes (besides individual models) a multi-model ensemble approach. The ensemble products are currently based upon a median value taken for each grid cell and each time step of the – in principle seven – individual regional chemistry transport model results. The median result is denominated as “the Ensemble model”.

The seven individual regional chemical transport models in MACC-II are:

CHIMERE	http://www.lmd.polytechnique.fr/chimere/
EMEP	http://www.emep.int/index_model.html
EURAD-IM	http://www.eurad.uni-koeln.de/index_e.html
LOTOS-EUROS	http://www.lotos-euros.nl/
MATCH	http://www.smhi.se/sgn0106/if/meteorologi/match.htm
MOCAGE	http://www.cnrm.meteo.fr/gmgec/spip.php?article87
SILAM	http://silam.fmi.fi/

The modelling outputs are hourly air quality concentrations over Europe. Fixed specifications and shared input data by all models are defined in order to limit the spread in the model results. All models use the same anthropogenic emissions dataset (Kuenen et al., 2014), the same meteorological input fields and the same boundary conditions provided by the global model. Each model is run in its own original grid specification (i.e. in different grid resolutions, different grid orientations and different spatial projections), the model outputs are then converted or interpolated into a common regular $0.25^\circ \times 0.25^\circ$ (up to and including 2009), resp. $0.1^\circ \times 0.1^\circ$ (since 2010) grid over the MACC-II European domain. The Ensemble is calculated in $0.1^\circ \times 0.1^\circ$ grid resolution. (Thus, up to and including 2009 the models were interpolated from $0.25^\circ \times 0.25^\circ$ to $0.1^\circ \times 0.1^\circ$.) Each individual modelling team has the freedom to choose its own data assimilation strategy, provided that the results are relevant, reliable and improve significantly the raw simulation results. The validation of data assimilation methods used in MACC-II is performed within its EDA (Air quality data assimilation) subproject.

The outputs of all applied models are both hindcasts and reanalysis (using data assimilation). In the data assimilation, the modelling teams combine atmospheric dispersion models with observational data. The most often used observational data are in-situ AirBase data from background measurement stations (both rural and urban/suburban). Besides that, the EURAD-IM reanalysis model uses also the satellite data. Table 2.3 summarises the grid resolution, the data assimilation methods and the assimilated observational data used by the individual models in MACC-II.

Table 2.3 Grid resolution, data assimilation methods and assimilated observational data used in the individual models in MACC-II

Code	Model	Grid resolution	Data assimilation chain	Assimilated observational data
CHM	CHIMERE	$0.25^\circ \times 0.25^\circ$	Kriging	AirBase in-situ data
EMP	EMEP	$0.25^\circ \times 0.25^\circ$	No operational data assimilation	---
RIU	EURAD-IM	15 km x 15 km	4D-Var	AirBase in-situ data, MOSAIC air borne in-situ measurements, PM ₁₀ SYNAER
KNM	LOTOS-EUROS	$0.25^\circ(\text{lon}) \times 0.125^\circ(\text{lat})$	Ensemble Kalman filter	AirBase in-situ data
SMH	MATCH	$0.5^\circ \times 0.5^\circ$ (to 2009) $0.2^\circ \times 0.2^\circ$ (since 2010)	3D-Var with transform into spectral space	AirBase in-situ data
MFM	MOCAGE	$0.2^\circ \times 0.2^\circ$	3D-Var operational chain	AirBase in-situ data
FMI	SILAM	$0.2^\circ \times 0.2^\circ$	3D-Var operational chain	AirBase in-situ data

The current configuration of the modelling systems is detailed in QA/QC dossiers (MACC, 2013) and available on the MACC-II project website for each model (<http://gmes-atmosphere.eu>). It should be noted that this model documentation is related to ENS runs, i.e. forecast and near-real-time analysis, while in EVA runs, i.e. in hindcasts and reanalysis, differences may occur in comparison with ENS runs, see Rouil et al. (2013). The detailed description for EVA runs is not available. In Table 2.3 and also in Section 3.2 (point B, paragraphs *b* and *e*), the information from dossiers for ENS are given, supplemented with known differences in EVA runs. However, due to lack on EVA documentation we may have overlooked some relevant differences.

Beside hindcast outputs, reanalysis results using different data assimilation methods are produced. At the data assimilation, air quality measurement data are incorporated in a numerical model, i.e. the state vector of the dispersion model is optimized based on these measurement data and used in a next step of the model. This is contrary to the spatial interpolation methods like ETC/ACM mapping (Section 2.1), which combine the measurement data with the resulting model output, see Denby et al. (2005). The individual data assimilation methods used in MACC-II are *3D-Var*, *4D-Var* and *ensemble Kalman filtering* (Table 2.3). The CHIMERE model presently uses a variant of *kriging*, namely the external drift kriging, i.e. a spatial interpolation method similar to the residual kriging as presented in Section 2.1. (Similarly, its output is not used in a next step of the model.) Variational assimilation methods (*3D-Var*, *4D-Var*) are based on the minimization of the cost function, which measures the differences between modelled and measured values. In a *3D-Var* method one time step only is considered. Whereas in a *4D-Var* method the data of both modelling and measurements are distributed in time. (The *4D-Var* approach brings large benefits compared to *3D-Var*, however at a high computational cost.) Sequential assimilation methods, like ensemble Kalman filters, represent the probability density function of the model solution, based on the previous state of the model system and observational data corresponding in time, using the Bayes theorem. Variational methods aim at globally adjusting a model solution to all the observations available over the assimilation period. Whereas sequential methods perform successive analysis in which only observations from some period until the time of analysis are considered. For further information on data assimilation techniques applied in the different MACC-II models, refer to Elbern et al. (2011) and the webpages of individual models.

The ensemble products are currently (i) the median of hindcasts and (ii) the median of reanalysis. The median is used as statistic as it accounts better for skewed concentration distributions than the ensemble mean does although other choices may be adopted in the future following Galmarini et al. (2013). The factual grid resolution of the MACC-II ensemble products should be considered as close to $0.25^\circ \times 0.25^\circ$ (up to and including 2009), resp. to $0.2^\circ \times 0.2^\circ$ (since 2010), as the Ensemble is constructed using the individual models in different original grid resolutions. The factual grid resolution of the Ensemble is related to the original grid resolutions of the individual models used in it.

On a yearly basis, extensive analysis of the performance of the modelling systems is carried out and the capability of the Ensemble model to predict the concentrations is evaluated by the MACC-II regional service (Rouil et al., 2011a, 2011b, 2012a, 2013). This includes a systematic evaluation against a relevant set of dedicated observation data from the European AirBase database (AirBase, 2013).

The evaluation of the MACC-II modelling results for 2010 is presented in Figure 2.2.

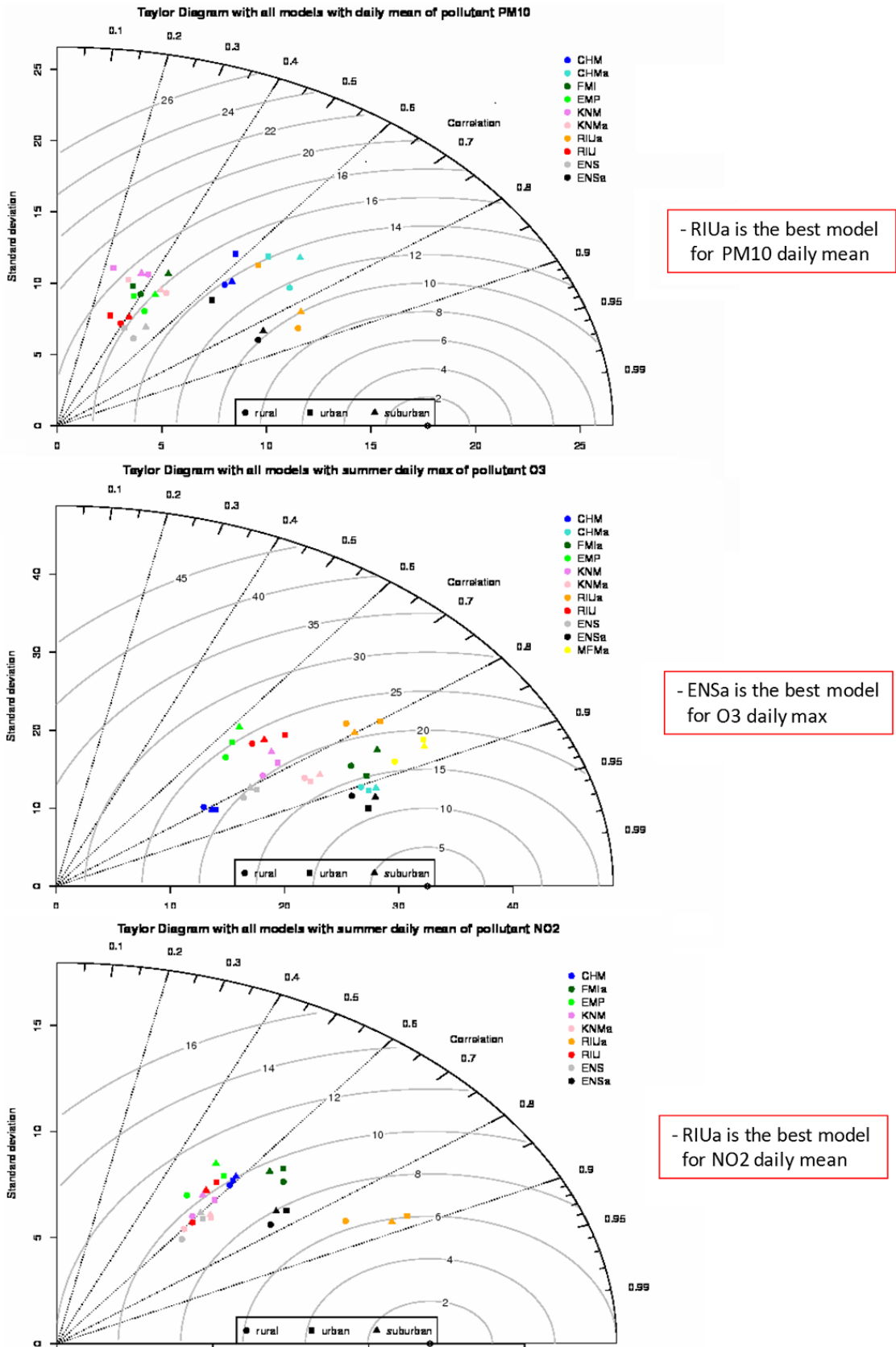


Figure 2.2 Taylor diagrams for all MACC-II models and their Ensemble for daily mean PM₁₀ (top), daily maximum hourly ozone (centre) and daily mean NO₂ (bottom) concentrations, 2010, with and without data assimilation. (See Table 2.3 for model acronyms, 'a' means data assimilated.)

The Figure 2.2 (taken from Rouil et al., 2013, adapted) represents Taylor diagrams for regulatory indicators of air quality: daily mean concentration of PM₁₀ particulates, daily maximum hourly concentration of ozone and daily mean concentration of dioxide nitrogen for 2010. In the figure, statistical results for various model outputs are presented. For the acronyms of individual models, see Table 2.3; MACC-II Ensemble model is labelled as 'ENS'. Data assimilated results correspond to the models noted with an 'a' index, while the hindcast results are not noted by any additional index. It should be noted that in the MACC-II project some models do not participate on a production level each year for hindcast and/or reanalysis calculations and are therefore missing in this Taylor diagram.

Figure 2.2 shows that the best results for PM₁₀ and NO₂ are obtained with EURAD-IM reanalysis (labelled as RIUa), while MACC-II Ensemble reanalysis (labelled as ENSa) gives the best results for ozone. If considered only the hindcasts, the best results for PM₁₀ and NO₂ are given by CHIMERE (labelled as CHM), while LOTOS-EUROS (labelled as KNM) gives the best results for ozone.

Annex 7 provides further information on Taylor diagrams (Taylor, 2001).

2.3 Mapping approach within EC4MACS

The EC4MACS project (<http://www.ec4macs.eu/>) is an EU-LIFE-ENVIRONMENT program, which aims at building a knowledge base for policy making related to air quality and climate change in the European Union. During 2006–2013, EC4MACS (2012) set up an integrated toolbox of relevant models to explore the synergies and interactions between policy objectives related to climate change, air quality and other issues. Among those tools, a methodology based on the calculation of an urban increment has been developed to correct regional model results over urban areas. The downscaling process implemented in EC4MACS allows the definition of a simple correction at the city level, which reflects the contribution of ground-level urban sources, mostly road traffic and residential sources. To set up this approach the CHIMERE model has been run by INERIS with circa 50x50 km² spatial resolution (regional runs) and circa 7x7 km² spatial resolution (high resolution runs) over the whole of Europe for the entire year 2009. This provides useful material to test the benefits of high-resolution modelling data with respect to mapping methodologies.

Such kinds of tests were performed in 2012 in a ETC/ACM study on urban air quality mapping (Rouil, 2012b). A simple kriging approach was implemented to combine surface observation data with EC4MACS high-resolution model outputs. The external drift kriging technique was used, assuming that the concentration at any point of the domain is a local linear function of one or several auxiliary variables plus a spatially correlated residual. Maps of NO₂ and PM₁₀ annual means were produced on several domains centred on the Air Implementation Pilot cities (<http://www.eea.europa.eu/publications/air-implementation-pilot-2013>). Within each domain, kriging was applied to AirBase rural and sub-urban or urban background data, using CHIMERE 7x7 km² fields and, where relevant, population density as an external drift variable. 'Leave-one-out' cross-validation was used as a first check on the consistency of the results.

3 Comparison approach and data used

The main purpose of this study is to test the use of the regional scale MACC-II Ensemble model output (as described in Section 2.2) in the ETC/ACM routine mapping activities (see Section 2.1) as an auxiliary variable, as an alternative to the EMEP model output. Originally, we intended to use MACC-II Ensemble reanalysis result in this comparison, but finally we used MACC-II Ensemble hindcast output (i.e. model product without data assimilation) for reasons given in Section 3.1. Next to this, other model outputs were included in the comparison as well. Additional to the comparison of the use of different model outputs in ETC/ACM mapping, the preliminary comparison of the ETC/ACM mapping results with the MACC-II Ensemble reanalysis model output is also done. The selection of different options for comparison is motivated and described in Section 3.1.

The mapping results are compared for the main health-related indicators of both PM₁₀ and ozone. For PM₁₀ mapping results, the annual mean and 36th highest daily mean are analysed. For O₃ mapping results, the two indicators analysed are the standard SOMO35 and the 26th highest daily maximum 8-hours mean. The data for 2009 and 2010 are used. All the data used in the comparison are presented in Section 3.2.

We evaluate the level of improvement in the mapping results from the performance of the system in a ‘leave-one-out’ cross-validation. This method is based on the use of all stations and one-by-one excluding a station for calculating a resulting map and then this result is evaluated against the actual measurement value at the excluded station. This cross-validation is explained in more detail in Section 3.3 and it is a method regularly used by the ETC/ACM to evaluate the performance of the mapping results. The selected statistics to evaluate the mapping performance are: RMSE, bias, R² and regression parameters (slope and intercept). The methodology used for the comparison of the different mapping performances is described in detail in Section 3.3.

3.1 Selection of different options for comparison

The selection of the specific modelling output data that serves as input in the ETC/ACM mapping methodology involved thorough discussions within the project team to ensure the appropriateness of the inter-comparison. The following options of comparison were initially considered (where DA means that the input dispersion model used data assimilation):

1. ETC/ACM mapping using EMEP model hindcast (resolution circa 50x50 km²)
2. ETC/ACM mapping using MACC-II Ensemble hindcast
(circa 0.25°x0.25° ≈ 20x30 km² in 2009, resp. 0.2°x0.2° ≈ 15x25 km² in 2010)
3. ETC/ACM mapping using MACC-II Ensemble reanalysis
(circa 0.25°x0.25° ≈ 20x30 km² in 2009, resp. 0.2°x0.2° ≈ 15x25 km² in 2010) DA
4. ETC/ACM mapping using CHIMERE-EC4MACS hindcast
(0.875°x0.4375° ≈ 50x50 km²)
5. ETC/ACM mapping using CHIMERE-EC4MACS hindcast
(0.125°x0.0625° ≈ 7x7 km²)
6. ETC/ACM mapping using EURAD-IM model reanalysis (15x15 km²) 4D-Var DA
7. MACC-II Ensemble reanalysis
(circa 0.25°x0.25° ≈ 20x30 km² in 2009, resp. 0.2°x0.2° ≈ 15x25 km² in 2010) DA
8. Air Pilot approach using CHIMERE-EC4MACS (0.125°x0.0625° ≈ 7x7 km²) DA

The motivation of this selection and the final selection process is described below.

The main problem identified during the selection of dispersion models used for comparison was how to avoid a redundancy in the information (i.e. ground-level measurement data) used for data assimilation and validation/evaluation of the performance of the mapping method. Within MACC-II, the reanalysis/data assimilated (DA) products are based on a split into two groups of ground-level observations: those that are used for assimilation and those that are used for validation. Current ETC/ACM mapping method makes use of all available observations for mapping (to achieve high quality of the spatial maps) and employs a leave-one-out approach for validation (i.e. cross-validation). The use of MACC-II reanalysis fields in the ETC/ACM mapping method would lead to locations where an observation might be used twice: once for the model reanalysis and then again for mapping. This was expected to be a problem e.g. in cross-validation as those locations would not be truly independent of information provided by observations. To avoid this problem, it was recommended to use the pure hindcast modelling data instead of reanalysis (or data assimilated) results. Thus, the use of MACC-II Ensemble fields in ETC/ACM mapping is comparable to the use of EMEP background fields in the mapping (options 1 and 2). This allows for a stronger evaluation simply based on the comparison of the use of different dispersion models in the ETC/ACM mapping.

However, we still thought about the use of reanalysed data. One option considered was the pragmatic use of the MACC-II Ensemble reanalysis in the ETC/ACM mapping (option 3), with no regard to the above mentioned problems of double use of some observational data. Nevertheless, in the end we did not examine this method. Another option considered is motivated as follows: Each MACC-II Ensemble member uses its own approach to data assimilation for the production of reanalysis fields/data assimilated results (see Table 2.3). A model that applies the 4D-Var technique to assimilate observations for improving the modelling results is expected to be more beneficial than one using for example 3D-Var. (For brief 3D-Var and 4D-Var description, see Section 2.2.) The 4D-Var technique makes use of the minimization of the cost function of the model code to run the model backward and forward incrementally, bringing the model state forward while incorporating the actual observations. The assimilation process is constrained by the model code. The resulting reanalysis fields can therefore be regarded as physically consistent new model states. As such, the new fields could be considered free of problems with cross-validation and double-usage of surface observations. EURAD-IM (http://www.eurad.uni-koeln.de/index_e.html) is a model which uses the 4D-Var technique in reanalysis, thus its use in ETC/ACM mapping could be interesting (option 6). Nevertheless, for capacity and resource reasons this model was finally not included in the comparison. It is recommended to do this in the future.

The CHIMERE model outputs as used in EC4MACS project were considered for the use in the comparison because they are available for the same year in two different spatial resolutions (as the options 4 and 5). This would enable the evaluation of the influence the use of a higher spatial resolution of the MACC-II Ensemble may have on the performance of the ETC/ACM mapping system.

Next to the comparison of the use of different model outputs in ETC/ACM mapping, also the overall comparison of the ETC/ACM mapping (e.g. options 1 and 2) with the MACC-II Ensemble reanalysis (data assimilated) results (option 7) were considered. For such comparisons with the MACC-II Ensemble reanalysis results, additional work is required, in cooperation with the regional MACC-II service. In order to carry out a proper comparison,

the stations used in data assimilation need to be identified and be consistent with the station data used for the mapping. The harmonisation of the stations used for data assimilation and validation is not straightforward as MACC-II uses a random system to determine the stations for validation every day. Due to constraints in time and resources, the present study does not include a systematic comparison with MACC-II Ensemble reanalysis products. The comparison presented later in this report with the MACC-II Ensemble reanalysis (data assimilated) results is thus only preliminary.

Additionally, the comparison with the output of the Air Pilot approach (see Section 2.3) was also considered (option 8), but it was not executed for capacity and methodological reasons.

As outcome of the discussions, this study involves only hindcast data to avoid comparability problems as described above. The comparison of the performance of the ETC/ACM mapping results has been tested with different dispersion models as input, as follows:

- a) EMEP model hindcast (with circa 50x50 km² grid resolution)
- b) MACC-II Ensemble hindcast (circa 20x30 km² in 2009, resp. 15x25 km² in 2010)
- c) CHIMERE-EC4MACS model hindcast (circa 50x50 km²)
- d) CHIMERE-EC4MACS model hindcast EC4MACS (circa 7x7 km²)

Thus, the options labelled above as 1, 2, 4 and 5 have been mutually compared. This comparison is further presented in Chapter 4.

Next to this, the preliminary comparison of ETC/ACM mapping results (using (i) EMEP and (ii) MACC-II Ensemble hindcast) with the MACC-II Ensemble reanalyses results has been done. In this preliminary comparison, the options labelled 1 and 2 are compared with the option 7. This preliminary comparison is further presented in Section 5.2.

The calculations have been carried out for 2009 because this is the year for which most dispersion model data were available. Additional calculations have been executed for 2010 using the EMEP model and the MACC-II Ensemble hindcast (and reanalysis), with the additional advantage that in 2010 the MACC-II Ensemble (both hindcast and reanalysis) is available in somewhat higher factual resolution of circa 0.2°x0.2°, i.e. about 15x25 km². For pragmatic reasons this report focuses on 2009 and 2010 since not all relevant data for other years is available. However, further simulations for different additional years (with different meteorological situations) should be carried out to assess the robustness of or to confirm the conclusions from this report.

3.2 Data used for the comparison

The input data used in this report are the same as the ones used in De Smet et al. (2012) and Horálek et al. (2013), except for the modelling input data. The primary data used for the ETC/ACM mapping routines are the air quality measurements at the monitoring stations extracted from AirBase database, including geographical coordinates (*latitude, longitude*). All the supplementary data are converted into the EEA reference projection (ETRS89-LAEA5210) and spatially transformed into the reference EEA grid of 10x10 km² resolution. (Most of these data, namely all the model output data are imported into ArcGIS as a point shape file, subsequently converted into a 200x200 m² resolution raster grid, and spatially aggregated into the reference EEA 10x10 km² grid.)

The input data are:

A. Air quality station measurement (point) data for 2009 and 2010

The station monitoring data for the relevant years 2009 and 2010 and for four PM₁₀ and ozone indicators were extracted from the European monitoring database AirBase (Mol et al. 2011, 2012). The following indicators were used: for PM₁₀ the annual average ($\mu\text{g}\cdot\text{m}^{-3}$) and 36th highest daily average value ($\mu\text{g}\cdot\text{m}^{-3}$), both referring to the PM₁₀ limit values set in the EU's AQ Directive (EC, 2008); for ozone the 26th highest daily maximum 8-hour average value ($\mu\text{g}\cdot\text{m}^{-3}$), referring to the target value set in the AQ Directive, and SOMO35 ($\mu\text{g}\cdot\text{m}^{-3}\cdot\text{day}$). SOMO35 is the annual sum of the differences between maximum daily 8-hour concentrations above 70 $\mu\text{g}\cdot\text{m}^{-3}$ (i.e. 35 ppb) and 70 $\mu\text{g}\cdot\text{m}^{-3}$.

Only data from stations classified as background stations (for the rural areas or suburban and urban areas) and with an annual data coverage of at least 75 percent have been used (for details, see Horálek et al., 2013 and De Smet et al., 2012). Table 3.1 shows for both years the number of the measurement stations used in the mapping of the individual pollutants.

Table 3.1 Number of stations used for the individual pollutants for 2009 and 2010

station type	PM ₁₀		ozone	
	2009	2010	2009	2010
rural background	290	329	500	499
urban and suburban background	1101	1108	1021	989

B. Chemical transport model data

a. EMEP model hindcast output (original resolution circa 50x50 km²) for 2009 and 2010

The Unified EMEP model revision rv3.8.1 (for 2009), resp. rv4.0 (for 2010) is used, which is an Eulerian model (Simpson et al., 2003). The model's output covers completely the mapping domain (i.e. the area of the EEA member and cooperating countries within the map extent *Map_1c*, EEA, 2011b). The model is run in its own grid specification in circa 50x50 km² resolution. Emissions for the relevant years were used (Mareckova et al., 2011, 2012) and the model is driven by ECMWF⁽¹⁾ meteorology. EMEP (2011, 2012a) provides details on the EMEP modelling for 2009 and 2010. For details of the data aggregation, see De Smet et al. (2012) and Horálek et al. (2013).

b. MACC-II Ensemble model hindcast output (original resolution 0.1°x0.1°) for 2009 and 2010

The Ensemble model hindcast result is the median of the hindcast results calculated by all MACC-II individual models available per pollutant and year, taken for every time step and grid cell. The median is defined as the value having 50% of individual model outputs with higher values and 50% with lower values. (If the number of the model used is even, the average of the two "middle" model outputs is used.) The hindcast models available for the Ensemble were the following:

¹ European Centre for Medium-Range Weather Forecasts: <http://www.ecmwf.int/>

PM₁₀, 2009: CHIMERE, EMEP, LOTOS-EUROS, MOCAGE, SILAM
PM₁₀, 2010: CHIMERE, EMEP, LOTOS-EUROS, EURAD-IM, SILAM
O₃, 2009: CHIMERE, EMEP, LOTOS-EUROS, MOCAGE, SILAM
O₃, 2010: CHIMERE, EMEP, LOTOS-EUROS, EURAD-IM

The covered domain is $\langle -14.5^\circ/34.5^\circ \rangle \langle 35.2^\circ/69.5^\circ \rangle$, i.e. the mapped area of the EEA member and cooperating countries, without Iceland, northern Norway and southern Cyprus.

Each model is run in its own grid specification, see Table 2.3. Then, the modelling results are converted or interpolated into the required common MACC-II grid resolution, i.e. $0.25^\circ \times 0.25^\circ$ for 2009 and $0.1^\circ \times 0.1^\circ$ for 2010. (The process of this conversion or interpolation is not documented.) For 2009, all the model results were ultimately interpolated from the required $0.25^\circ \times 0.25^\circ$ resolution into the MACC $0.1^\circ \times 0.1^\circ$ grid, using bilinear interpolation. The Ensemble was calculated (as median of the used individual models) in this $0.1^\circ \times 0.1^\circ$ grid resolution, for each grid cell and each time step.

The meteorology used is from the IFS⁽²⁾ reanalysed model of meteorology of ECWMF. Emission used are the MACC/TNO⁽³⁾ gridded emissions ($0.125^\circ \times 0.0625^\circ$, i.e. about 7×7 km²) reported for 2007 (used in all 2009 models) and for 2009, including forest fire emissions (used in all 2010 models). The boundary conditions were taken from MACC-II global data reanalysis, which took it from the model MOZART. The same meteorology, emissions and boundary conditions are used for all the individual models.

c. *CHIMERE-EC4MACS model hindcast output (original resolution $0.875^\circ \times 0.4375^\circ$), 2009*

The model used was CHIMERE in the $0.875^\circ \times 0.4375^\circ$ resolution (i.e. about 50×50 km²) as reported in EC4MACS (2012). The covered domain is $\langle -13.4375^\circ/32.9375^\circ \rangle$, $\langle 34.4063^\circ/62.8438^\circ \rangle$, i.e. the mapped area of the EEA member and cooperating countries, without Iceland, northern and north central Scandinavia and eastern Cyprus. The meteorology used is from the IFS model of ECWMF (i.e. the same as the one used in all the models in MACC-II). The emissions estimates used were those derived within the EC4MACS project, based on TNO emission inventories and proxies and information from the GAINS⁽⁴⁾ project (EC4MACS, 2012).

d. *CHIMERE-EC4MACS model hindcast output (original resolution $0.125^\circ \times 0.0625^\circ$), 2009*

The model used was CHIMERE in the $0.125^\circ \times 0.0625^\circ$ resolution (i.e. about 7×7 km²) as reported in EC4MACS (2012) and in Terrenoire et al. (2013). The covered domain is $\langle -10.4375^\circ/30.4375^\circ \rangle \langle 35.9063^\circ/61.8438^\circ \rangle$, i.e. the mapped area of the EEA member and cooperating countries, without Iceland, northern and central Scandinavia and eastern Cyprus. Emissions and meteorology were the same as under paragraph c.

² The Integrated Forecast System (IFS) is developed and maintained by the European Centre for Medium-Range Weather Forecasts (ECMWF) based in Reading, England.

³ MACC/TNO emissions, see:

http://www.gmes-atmosphere.eu/about/project_structure/input_data/d_emis/

⁴ The Greenhouse Gas and Air Pollution Interactions and Synergies (GAINS)-Model, International Institute for Applied Systems Analysis (IIASA), Austria; <http://gains.iiasa.ac.at/models/>

e. *MACC-II Ensemble reanalysis, using data assimilation (DA) (original resolution 0.1°x0.1°) for 2009 and 2010*

The output of the MACC-II Ensemble reanalysis, based on data assimilation (DA) consists of the median of all available modelling results from the MACC-II models which applied DA. Table 2.3 provides an overview of the data assimilation methods applied in each of the models of the MACC-II Ensemble reanalysis. The data assimilated models available for the Ensemble were the following:

PM₁₀, 2009: CHIMERE, EURAD-IM, LOTOS-EUROS

PM₁₀, 2010: CHIMERE, EURAD-IM, LOTOS-EUROS

O₃, 2009: CHIMERE, EURAD-IM, LOTOS-EUROS, MOCAGE,

O₃, 2009: CHIMERE, EURAD-IM, LOTOS-EUROS, MOCAGE, SILAM

The grid resolution, meteorology and emissions used are the same as for hindcast (paragraph b).

All the model data were temporal aggregated to the same to the same set of indicators as in the case of the air quality observations, i.e. the annual average and the 36th highest daily mean for PM₁₀, and the 26th highest daily maximum 8-hourly mean and SOMO35 for ozone.

Throughout the paper, all models, which are not labelled as hindcast or reanalysis, are hindcast.

C. Altitude (original resolution 30x30 arc-seconds)

The altitude data field (in meters above sea level) is taken from GTOPO30⁽⁵⁾ that covers the European continent. For details, see Horálek et al. (2007).

D. Meteorology parameters (original resolution 0.25°x0.25°) for 2009 and 2010

Wind speed (annual average, in m.s⁻¹) and surface solar radiation (annual average of daily sum, MWs.m⁻²) were used. The daily data were extracted from the Meteorological Archival and Retrieval System (MARS) ERA-interim reanalyses of ECMWF. For details, see Horálek et al. (2007).

E. Population density

Population density (in inhabitants.km⁻², census 2001) for the majority of countries is based on data provided by the European Commissions (EC) Joint Research Centre (JRC). The original resolution is 100x100 m². For countries and regions lacking JRC data, we use ORNL population data in the 1x1 km² resolution. For details, see Horálek et al. (2013).

⁵ GTOPO30 is a global digital elevation model (DEM) with a horizontal grid spacing of 30 arc seconds (approximately 1 kilometre); <https://lta.cr.usgs.gov/GTOPO30>

3.3 Methodology used for the comparison

The basic method used for the comparison of the mapping results is *cross-validation*. The so-called “leave-one-out“ cross-validation method computes the quality of the spatial interpolation for each measurement point from all available information except from the point in question, i.e. it withholds one data point and then makes a prediction at the spatial location of that point. This procedure is repeated for all measurement points in the available set. The predicted and measured values at these points are plotted in the form of a scatter plot. With the help of statistical indicators the quality of the predictions is demonstrated objectively. The advantage of the nature of this cross-validation technique is that it enables evaluation of the quality of the predicted values at locations without measurements, as long as they are within the area covered by the measurements.

The main cross-validation indicators for comparison are *root mean squared error (RMSE)*, *bias* (or *mean predicted error, MPE*), *coefficient of determination (R^2)* and the regression equation parameters *slope* and *intercept*, following from the scatter plot between the predicted (using cross-validation) and the observed concentrations. RMSE can be expressed not only in absolute values, but also in relative terms as a percentage of a mean indicator value for all stations. *RMSE*, *bias* and R^2 are calculated according to equations:

$$RMSE = \sqrt{\frac{1}{N} \sum_{i=1}^N (\hat{Z}(s_i) - Z(s_i))^2}, \quad bias = \frac{1}{N} \sum_{i=1}^N (\hat{Z}(s_i) - Z(s_i)),$$

$$R^2 = \frac{\left(\sum_{i=1}^N (Z(s_i) - \bar{Z})(\hat{Z}(s_i) - \bar{\hat{Z}}) \right)^2}{\sum_{i=1}^N (Z(s_i) - \bar{Z})^2 \cdot \sum_{i=1}^N (\hat{Z}(s_i) - \bar{\hat{Z}})^2} = 1 - \frac{\sum_{i=1}^N (Z(s_i) - \hat{Z}(s_i))^2}{\sum_{i=1}^N (Z(s_i) - \bar{Z})^2}, \quad RMSE[\%] = \frac{RMSE}{\bar{Z}} \cdot 100$$

where $Z(s_i)$ is the measured concentration at the point s_i , with $i = 1, \dots, N$,

N is the number of the measuring points,

$\hat{Z}(s_i)$ is the estimated concentration at point s_i using other information, excluding the actual measured concentration at the point s_i ,

\bar{Z} , $\bar{\hat{Z}}$ is the arithmetic average of $Z(s_1), \dots, Z(s_N)$, resp. $\hat{Z}(s_1), \dots, \hat{Z}(s_N)$.

RMSE should be as small as possible, *bias* should be as close to zero as possible, R^2 should be as close to 1 as possible, slope a should be as close to 1 as possible, and intercept c should be as close to zero as possible (in the regression equation $y = a.x + c$).

Next to the cross-validation, in some cases also the simple *comparison of measured and predicted grid values* was done. In these cases, the similar statistical indicators as in cross-validation are used (i.e. *RMSE*, *bias*, R^2 , *slope* and *intercept*).

Additionally, the indicators of the linear regression models used are compared, namely *RMSE* and *adjusted coefficient of determination* R_{adj}^2 . In this case, R_{adj}^2 is calculated according to:

$$R_{adj}^2 = R^2 - \frac{P}{(N - p - 1)} \cdot (1 - R^2),$$

where R^2 is the coefficient of determination,
 N is the number of the measuring points,
 p is the number of parameters in the regression model with equation $y = a_1.x + a_2.x + \dots + a_p.x + c$.

The comparisons are executed for rural and urban/suburban stations separately. In all comparisons, consistent sets of stations are used for all compared models. Each set consists of all stations within the domain covered by all the compared models. Two different sets of stations are used, see Table 3.2.

Table 3.2 Number of monitoring stations used in comparisons

station type and comparison set		PM ₁₀		ozone	
		2009	2010	2009	2010
rural background	A	288	328	488	497
	B	289	328	498	497
urban and suburban background	A	1067	1092	1018	989
	B	1034	1035	1021	989

Set “A” is used for the comparisons of the hindcast results presented in Chapter 4, Section 5.1, Annex 2 and Annex 5, and set “B” for the comparisons with the reanalysis results presented in Section 5.2 and Annex 6. The differences between the two sets are caused by the following: the comparisons in Section 5.2 with the reanalysis do not include the CHIMERE-EC4MACS models (i.e. the common domain of the compared models is larger); the comparisons do include, however, the final merged ETC/ACM-EMEP maps. (As a consequence, no Turkish stations are used in “B” set, as the ETC/ACM final merged map does not include Turkey, due to the lack of Turkish stations in the rural areas.) In general, the numbers of stations per set used in the comparisons of mapping results using the different models are smaller than the sets of stations used as primary input data in the ETC/ACM mapping method (Table 3.1). That is because only the stations within located the domains of all relevant models are used in the comparisons. Whereas all available stations (Table 3.1) are used in the construction of the ETC/ACM maps.

4 Comparison of mapping results using different model outputs

This chapter examines and compares the performance of the ETC/ACM mapping results using different model outputs, with the aim to conclude on the model that could best be used in the mapping method in the future on a routine basis. For the motivation of the model selection in the comparison, see Section 3.1. The ETC/ACM mapping procedure, a linear regression model followed by kriging of its residuals (Section 2.1), was applied for all examined PM₁₀ and ozone indicators, for the years 2009 and 2010. The results are presented separately for rural and urban background area types.

For 2009, the ETC/ACM mapping procedure was carried out using the four different chemical transport model outputs (as described in Section 3.2) as dependent variables in the residual kriging. The four model outputs are:

- a) EMEP model output (original resolution circa 50x50 km²),
- b) MACC-II Ensemble model output (original factual resolution circa 20x30 km²),
- c) CHIMERE-EC4MACS model output (original resolution circa 50x50 km²),
- d) CHIMERE-EC4MACS model output (original resolution circa 7x7 km²).

For 2010, the mapping procedure was carried out using the available model results:

- a) EMEP model output (original resolution circa 50x50 km²),
- b) MACC-II Ensemble model output (original factual resolution circa 15x25 km²).

All these model outputs are *hindcasts*, i.e. the model results without data assimilation. For completeness, Annex 4 presents maps of all these model outputs, i.e. the inputs into the ETC/ACM mapping procedure. Using these different model outputs, both rural and urban background maps are constructed as described in Section 2.1. The rural maps are applicable for the rural background areas only, while the urban background maps are applicable for the urban background areas only.

The maps in the following sections are all given in the same 10x10 km² spatial resolution and represent the spatial interpolated concentration field with the measured values at their measurement points; the rural background stations in the rural maps and the urban and suburban background stations in the urban background maps. Next to the maps, the cross-validation comparison tables are presented and discussed. Section 4.1 does that for PM₁₀ and Section 4.2 for ozone. Section 4.3 presents the conclusions from this chapter.

We did not analyse the final merged mapping results, i.e. the maps created by combination of rural and urban maps according to the criteria described in Section 2.1, because the conclusions for the final merged maps predominantly depend on the findings for the separate rural and urban background maps (Horálek et al., 2010).

Annex 1 provides tables with statistics of the performance of the mapping method using the different chemical transport models, Annex 2 the related cross-validation scatter plots, and Annex 3 the differences between the ETC/ACM mapping results using the different model outputs.

4.1 PM_{10}

4.1.1 Mapping using EMEP, MACC-II Ensemble and CHIMERE models

PM_{10} , annual average, 2009

Figure 4.1 presents for rural background areas and Figure 4.2 for urban and suburban background areas the 2009 mapping results of the annual mean PM_{10} concentrations derived from the ETC/ACM spatial interpolation method using each of the four chemical transport models. The rural maps are applicable for rural areas only and the urban background maps are applicable for urban areas only.

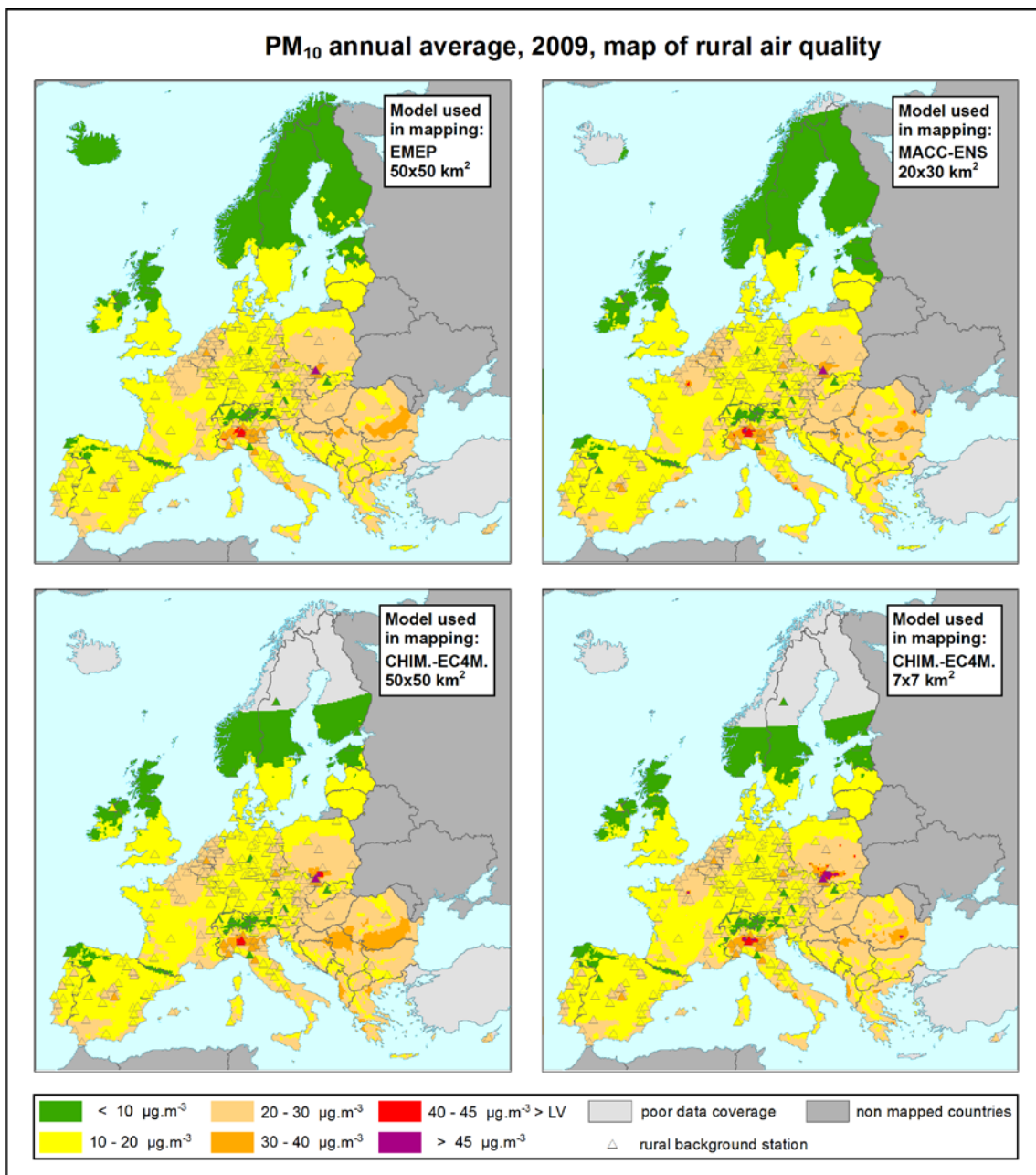


Figure 4.1 PM_{10} annual average for 2009, rural map, ETC/ACM mapping result using EMEP, MACC-II Ensemble, CHIMERE-EC4MACS_50km, and CHIMERE-EC4MACS_7km. *Note: Applicable for rural areas only.*

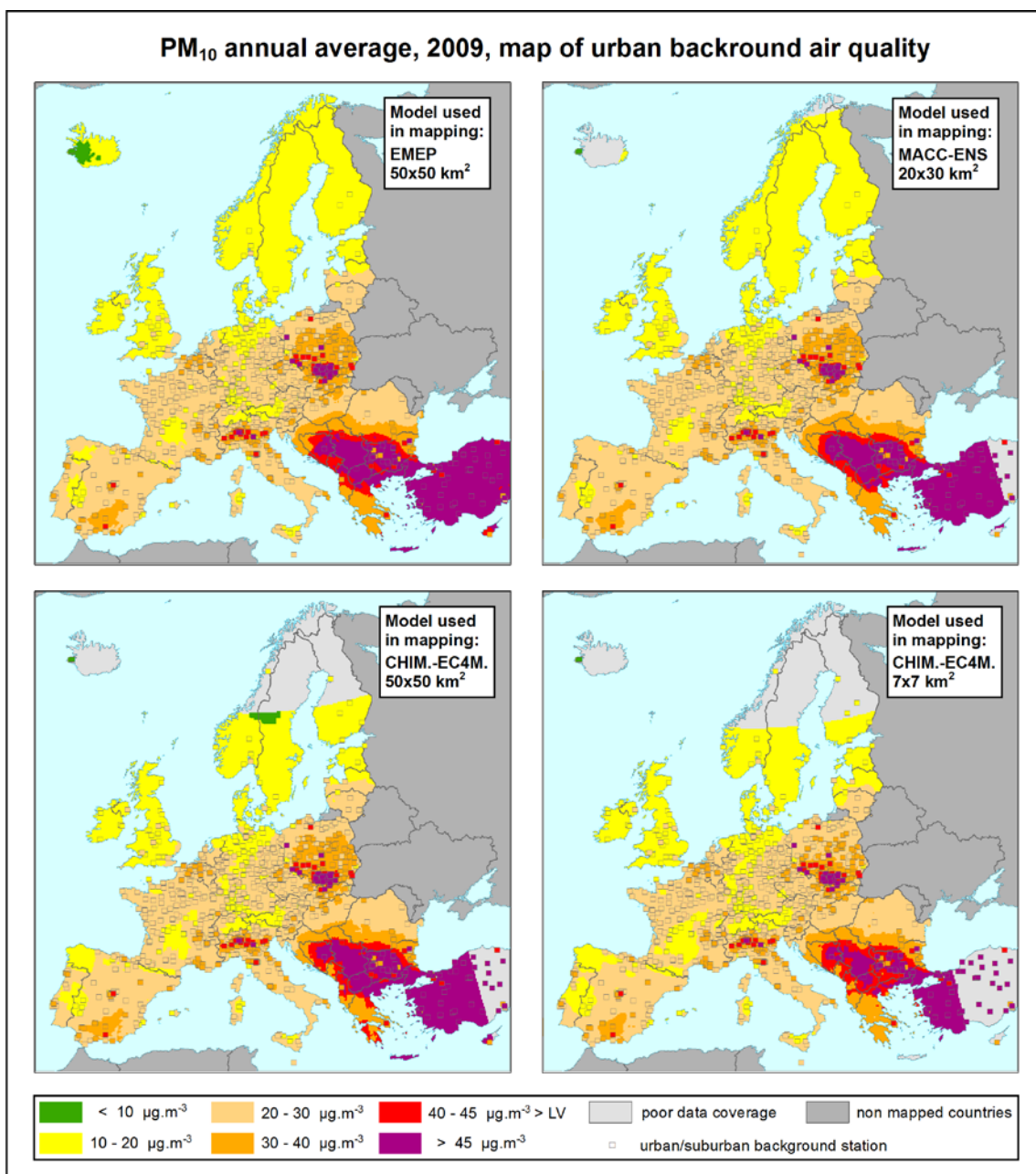


Figure 4.2 PM₁₀ annual average for 2009, urban background map, ETC/ACM mapping result using EMEP, MACC-II Ensemble, CHIMERE-EC4MACS_50km, and CHIMERE-EC4MACS_7km. *Note: Applicable for urban areas only.*

These maps and all others in this report show differences in the coverage of the mapping domain depending on the chemical dispersion model used as input to the mapping. There are data gaps in the northernmost and southernmost areas of Europe (northern Scandinavia, Iceland, Cyprus) for the mapping results for which the MACC-II Ensemble was used. Throughout this report these gaps are observed in all maps where the MACC-II Ensemble has been applied as the MACC-II modelling domain does not cover the whole ETC/ACM mapping domain. For potential future applications, operational use of the MACC-II Ensemble results in the ETC/ACM mapping routines would only be acceptable when the modelling domain is extended to match the ETC/ACM mapping that is used EEA product. There are also significant gaps in the mapping results when using the models taken from the

EC4MACS exercise. In the case of CHIMERE as used in EC4MACS, the missing mapping results affect even a larger area, covering most of Scandinavia. As indicated in Section 3.2, the reason is that the domains of CHIMERE-EC4MACS models are considerably smaller than the MACC-II domain and the domain used for ETC/ACM mapping activities. The domain for the 7x7 km² version of CHIMERE-EC4MACS is even somewhat smaller than the domain for its 50x50 km² version.

Concerning the annual mean PM₁₀ concentration in Figures 4.1 and 4.2, it is interesting to note that the spatial distribution of PM₁₀ is very similar, independently of the choice of chemical transport model used in the ETC/ACM spatial mapping. This is contrary to the different concentration levels of the original model outputs, see Annex 4, Figure A4.1, where the EMEP and the MACC-II Ensemble models give lower results in comparison to both CHIMERE-EC4MACS models. The outputs of the mapping have been fitted to the concentration levels of the station measurements.

The largest remarkable differences observed in the mapping results of annual mean PM₁₀ concentrations are those between Figures 4.1 and 4.2, i.e. between rural and urban background maps. That means that the differences in the maps are primarily driven by observations, i.e. the measurement results. The rural maps are based on rural background stations from the AirBase database, while the urban background maps are based on urban and suburban background stations from the same database.

As an illustration, and for PM₁₀ annual average for 2009 only, Figure 4.3 presents the difference maps showing the differences between ETC/ACM mapping results using EMEP and MACC-II Ensemble model outputs, for rural background and urban background areas separately. Figures A3.1 and A3.2 in Annex 3 provide additional difference maps with the differences between the ETC/ACM mapping results using the EMEP and either one of the CHIMERE-EC4MACS models, and also between ETC/ACM mapping results using the CHIMERE- EC4MACS models in different resolutions.

In the rural background areas, the major differences between the maps using the EMEP and the MACC-II Ensemble models are observed in areas with a low density of measurement stations (Finland, Balkan area). It is interesting to see how the differences between the two model outputs alone (Annex 4, Figure A4.1) relate to the differences of the relevant ETC/ACM mapping results that made use of these model outputs (Figure 4.3). In general, in areas lacking stations (e.g. north-eastern Greece) model differences do have their influence on the mapping results. Contrary to that, model differences in areas with high density of stations (e.g. The Netherlands, north-western Germany) do not have any remarkable influence on the mapping results.

If comparing the maps using the EMEP model with one of both CHIMERE-EC4MACS models, one can see that the major differences (see Annex 3, Figure A3.1) occur in areas with a low density of stations, for example, in the Balkan, and in the case of CHIMERE-EC4MACS in 7x7 km² resolution also in the Silesia region. The differences of the estimated concentration levels in the Silesia region are also observed by just comparing both original CHIMERE-EC4MACS models with each other (Annex 4, Figure A4.1). These differences are related to the different resolutions: a model in a higher resolution estimates better the concentrations in small but highly polluted areas.

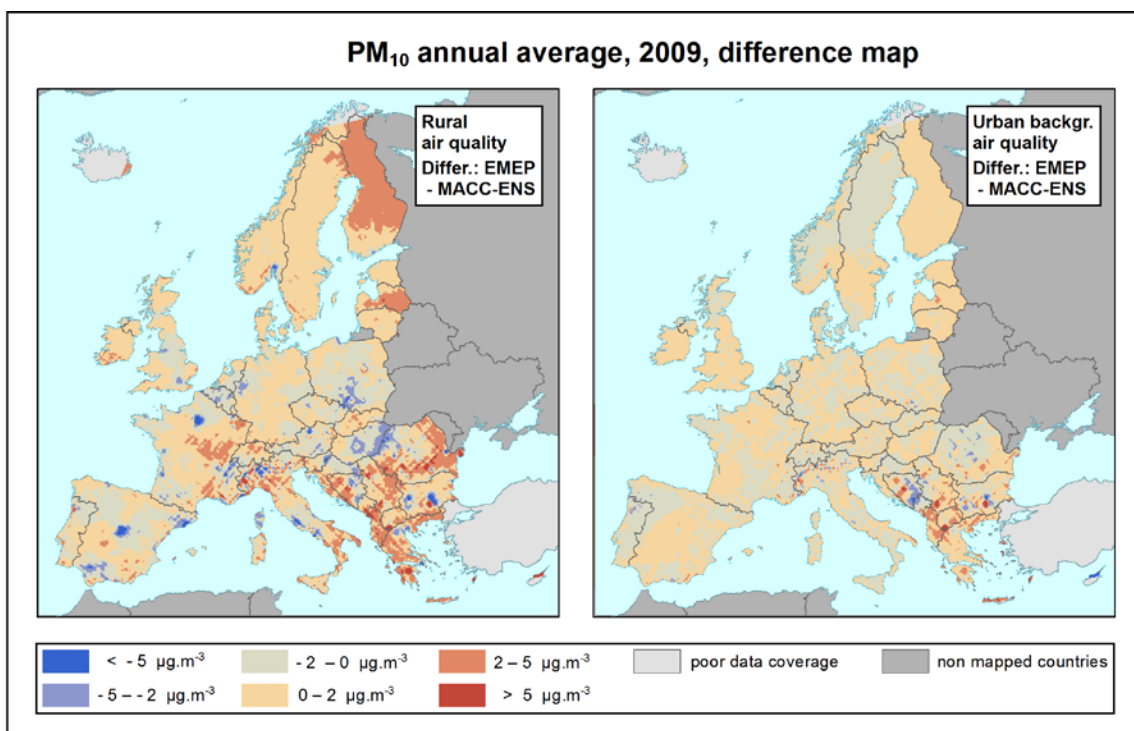


Figure 4.3 **PM₁₀ annual average for 2009, difference of the ETC/ACM mapping results using EMEP and MACC-II Ensemble for rural (left) and urban background (right) maps. Note: Applicable for rural (left), resp. urban (right) areas only.**

For the urban background maps (Figure 4.2), the mapping results using EMEP, MACC-II Ensemble and CHIMERE-EC4MACS in 50x50 km² resolution are very similar. The only exceptions are areas with a low density of stations (Greece, Montenegro) and in the case of CHIMERE-EC4MACS also the Silesia region and Po Valley (Annex 3, Figure A3.2). The main differences occur when one uses CHIMERE-EC4MACS in the 7x7 km² resolution. The most obvious difference in the map created by using this model is its somewhat lower concentration levels compared to the maps using the other models. This is caused by the fact that the CHIMERE-EC4MACS model with its higher grid resolution, underestimates urban concentrations less than the other models with their coarser resolution (Annex 5, Figure A5.2). That leads subsequently to lower concentration levels in the relevant ETC/ACM maps in areas just outside the cities (e.g. in the areas surrounding Paris or London, see Annex 3, Figure A3.2, bottom). However, for such areas the urban map is not applicable as these are considered to be rural. Hence, the evaluation of the real quality of this map on urban areas should be done against actual urban observational data by means of a cross-validation analysis; see Section 4.1.2.

Similar type of results are obtained with the maps using EMEP (50x50 km²), MACC-II Ensemble (circa 20x30 km²) and CHIMERE-EC4MACS in 50x50 km² resolution. These are the chemical transport models with a relative low spatial resolution. This finding is in agreement with an assumption that the mapping results do not significantly vary when input models are used that have a grid resolution in the range of 50x50 km² to 20x20 km² (Denby et al., 2011a). The largest effect was expected when chemical dispersion models would be used with higher spatial resolution in the range of 5x5 km² to 10x10 km², such as the CHIMERE-EC4MACS in 7x7 km² resolution. Our findings are consistent with the findings reported in Cuvelier et al. (2013) that indicate an improvement of the performance of

chemical transport models in background calculations when the spatial resolution scale improves from 20–50 km down to 5–10 km.

PM₁₀, 36th highest daily mean, 2009

Figure 4.4 and 4.5 show the ETC/ACM mapping results using different chemical transport models for PM₁₀ indicator the 36th highest daily mean, for 2009.

The differences between the mapping results using different model outputs for the 36th highest daily mean are presented in Annex 3, Figures A3.3 and A3.4.

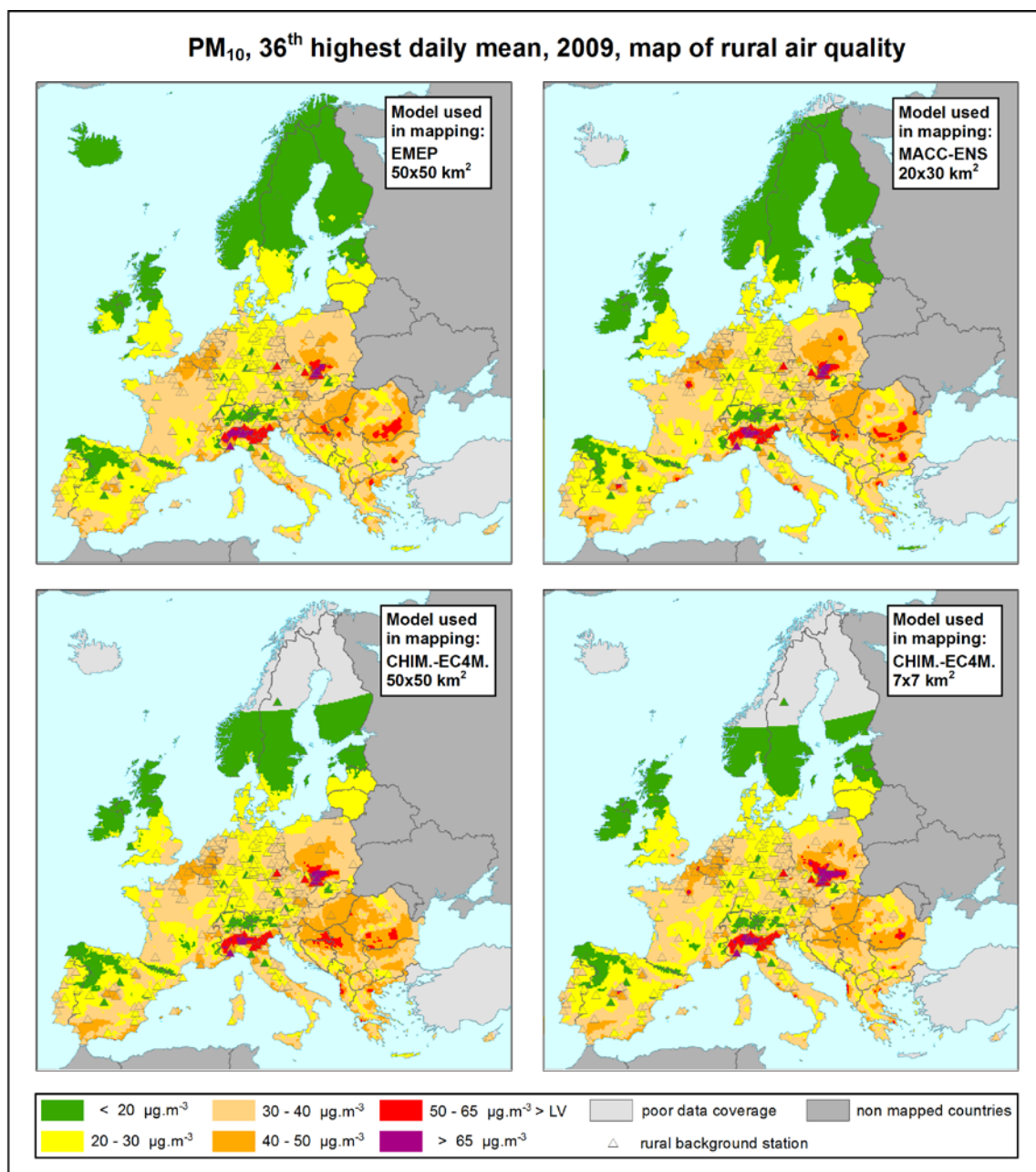


Figure 4.4 PM₁₀ indicator 36th highest daily mean for 2009, rural map, ETC/ACM mapping result using EMEP, MACC-II Ensemble, CHIMERE-EC4MACS_50km, and CHIMERE-EC4MACS_7km as input. *Note: Applicable for rural areas only.*

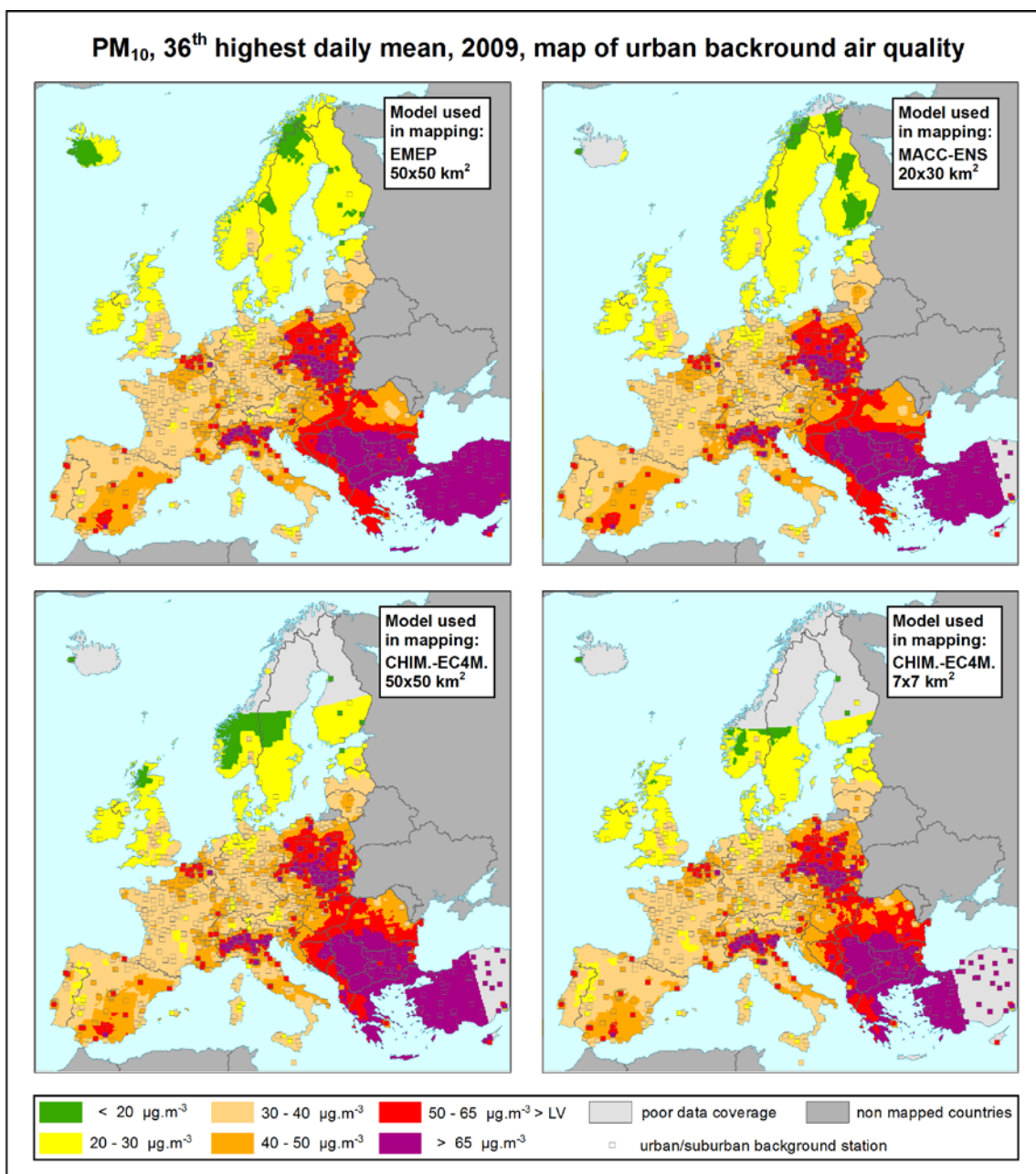


Figure 4.5 PM₁₀ indicator 36th highest daily mean for 2009, urban background map, ETC/ACM mapping result using EMEP, MACC-II Ensemble, CHIMERE-EC4MACS_50km, CHIMERE-EC4MACS_7km. *Note: Applicable for urban areas only.*

The figures show considerable differences between rural and urban background maps. As for the PM₁₀ annual mean, the choice of the chemical transport model, either EMEP, MACC-II Ensemble, or CHIMERE-ETC4MACS models, infers only small differences in the mapping results while differences driven by observations are more significant.

In Annex 4, Figure A4.2 shows the different concentration levels of the individual model outputs. The EMEP and MACC-II Ensemble models give lower results compared to both CHIMERE-EC4MACS models. Irrespective to this, the ETC/ACM spatial interpolation gives similar concentration levels at all models used. The output of the mapping procedure is fitted

to the concentration levels of the station measurements, at both the rural and the urban background concentration data.

We come to similar findings as at the annual average maps: in the rural areas, the major differences are observed in areas with low density of measurement stations (Finland, southern Sweden, Balkan area). In the case of the map using the CHIMERE-EC4MACS in 7x7 km² resolution, it is also in the Silesia region.

In the urban background areas, the mapping results using the EMEP and the MACC-II Ensemble models are very similar. Compared to these maps, the mapping results using CHIMERE-EC4MACS show differences especially in areas with low density of stations (Balkan area, Sweden).

PM₁₀, annual average and 36th highest daily mean, 2010

Figures 4.6 and 4.7 provide ETC/ACM mapping results of PM₁₀ annual mean and Figures 4.8 and 4.9 of the PM₁₀ indicator 36th highest daily mean for 2010. They concern mapping results using the EMEP and the MACC-II Ensemble models only, as for 2010 no CHIMERE-EC4MACS modelling output was available. Annex 3, Figures A3.5 and A3.6 represent the differences between the mapping results using the two model outputs.

In 2010, the choice of the chemical dispersion model has a more significant impact on the results of the mapping than in 2009. This is due to the major differences between the original EMEP and MACC-II Ensemble model outputs (Annex 4, Figures A4.5 and A4.6), especially in the areas of south-eastern Europe and Sicily. These differences in model outputs have their influence on the ETC/ACM mapping results at these areas due to a lack of measurement stations there.

In general, we obtain similar findings in 2010 as for 2009: the mapping results are predominantly driven by the observations. The major differences in the ETC/ACM maps using output of different models as input are in areas where measurement stations are lacking, especially if just the individual model outputs show there the differences.

Figure 4.8 shows such an example for the area of Greece. Here no rural background PM₁₀ station fulfilled the annual data coverage criterion of at least 75% for 2010, i.e. results from observations could not be accounted for. The outputs of EMEP and MACC-II Ensemble models differ a lot in this area (Annex 4, Figure A4.4), i.e. both models show different concentration levels of PM₁₀.

When compared to the long-term average, the variability of meteorological conditions of 2009 and 2010 are not considered extreme for the mapping domain under consideration. In 2010 there were some extreme events: dry and warm summer season in Eastern Europe, accompanied by extended and long-lasting forest fires throughout the summer months, and meteorological inversion situations in winter in some parts of Central and Eastern Europe, both causing elevated PM₁₀ levels in those parts of Europe. The high PM₁₀ levels in south-eastern Iceland were due to the volcanic activity of Eyjafjallajökull.

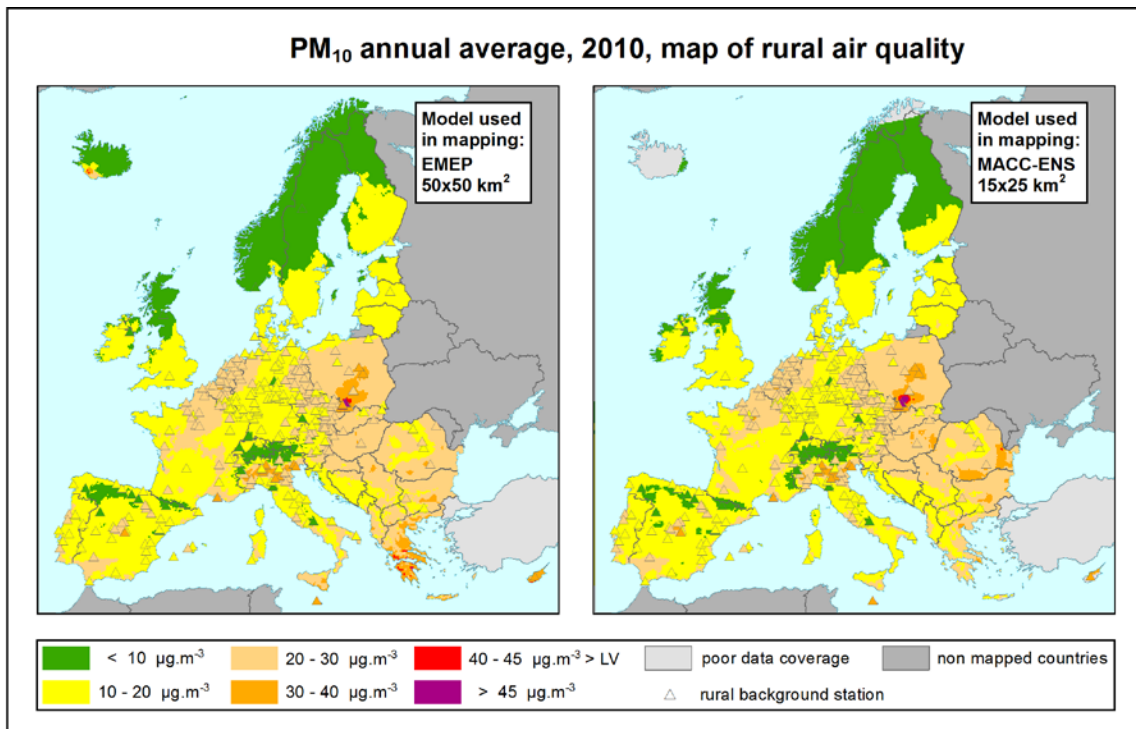


Figure 4.6 PM₁₀ annual average for 2010, rural map, ETC/ACM mapping result using EMEP (left) and MACC-II Ensemble (right). *Note: Applicable for rural areas only.*

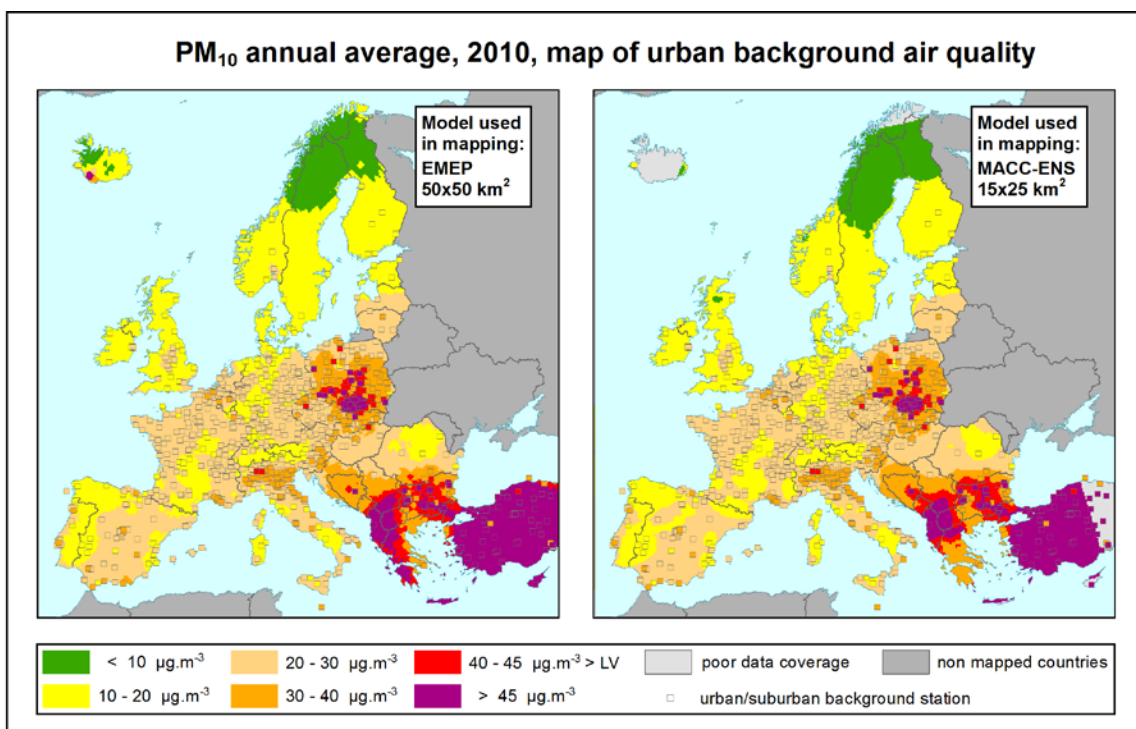


Figure 4.7 PM₁₀ annual average for 2010, urban background map, ETC/ACM mapping result using EMEP (left) and MACC-II Ensemble (right). *Note: Applicable for urban areas only.*

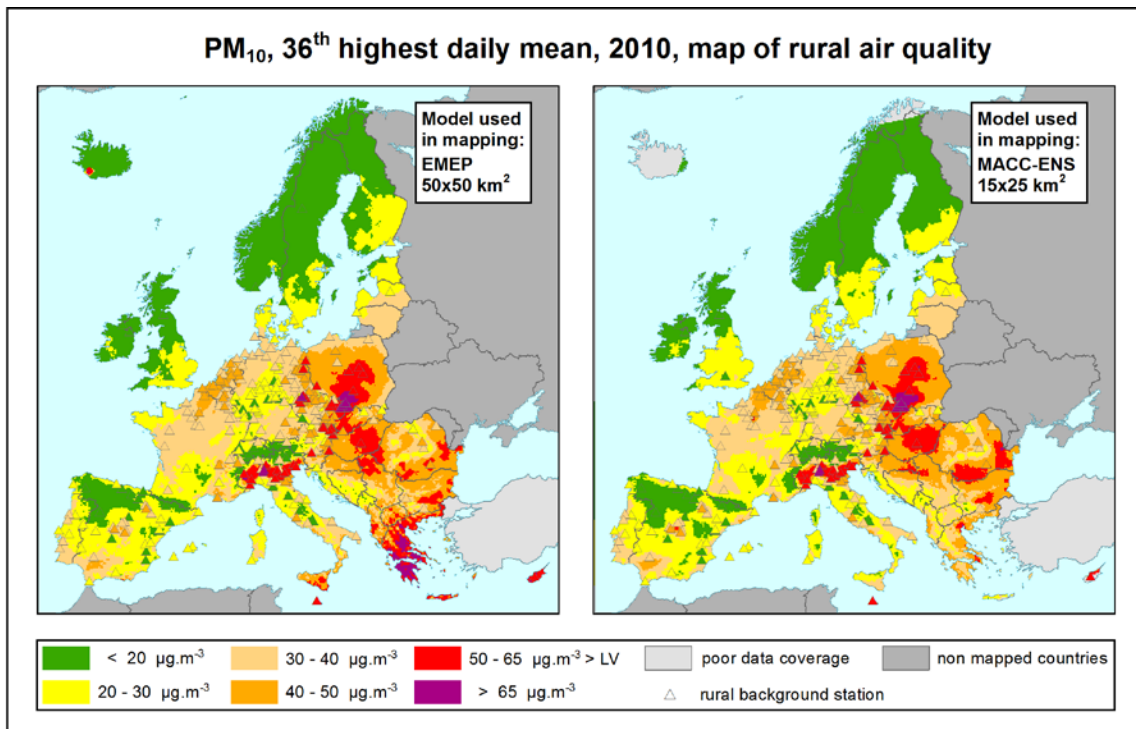


Figure 4.8 PM₁₀ indicator 36th highest daily mean for 2010, rural map, ETC/ACM mapping result using EMEP (left) and MACC-II Ensemble (right). *Note: Applicable for rural areas only.*

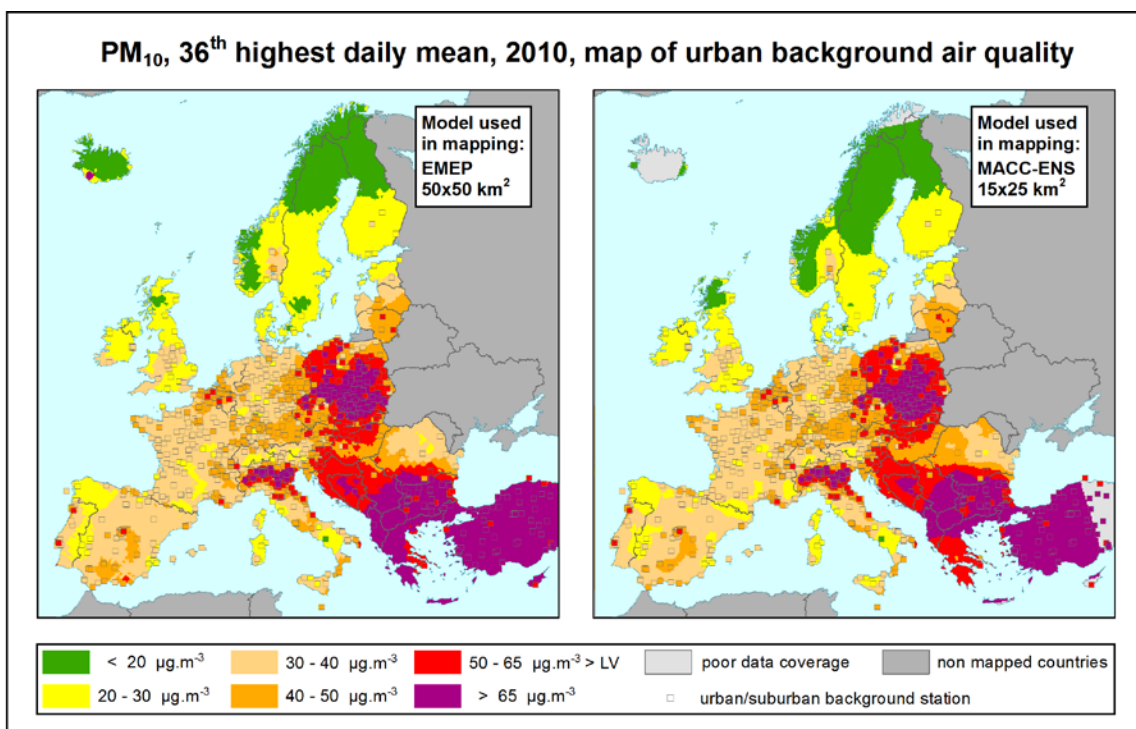


Figure 4.9 PM₁₀ indicator 36th highest daily mean for 2010, urban background map, ETC/ACM mapping result using EMEP (left) and MACC-II Ensemble (right). *Note: Applicable for urban areas only.*

The figures presented in this Section 4.1.1 show that there are indeed some differences in the ETC/ACM mapping results when using different chemical transport models as input. The question is which mapping results are closer to reality (i.e. closer to the measurements). To answer this question a cross-validation analysis has been carried out in Section 4.1.2.

4.1.2 Cross-validation results

In order to establish the accuracy of the maps presented in the previous section, the mapping results were cross-validated against observations according the repetitive ‘leave-one-out’ method as described in Section 3.3. This cross-validation analysis was executed for all the ETC/ACM mapping results obtained using different dispersion model outputs and its results are described in terms of the following statistics: the root mean square error (RMSE), the bias, the coefficient of determination (R^2) and the parameters of the regression equation.

Table 4.1 summarises for 2009 and Table 4.2 for 2010 the performance statistics of the cross-validation for PM_{10} annual mean and 36th highest daily value. The tables highlight the statistics of the chemical transport models that for each indicator provide the best performance (the darker the green marking, the better). Lower RMSE and higher R^2 generally indicate better performance; bias closer to zero is also an indication of better performance. Furthermore, the slope should be as close to 1 as possible and the intercept as close to 0 as possible.

Table 4.1 Comparison of cross-validation indicators for interpolation with the use of different dispersion model outputs – PM_{10} , 2009

model used in ETC/ACM mapping	PM ₁₀ annual average, 2009									
	rural					urban background				
	RMSE	bias	R ²	regr. equation	RMSE	bias	R ²	regr. equation		
EMEP, 50x50	4.70	24.3%	0.16	0.518	y = 0.565x + 8.58	5.81	20.6%	-0.07	0.714	y = 0.700x + 8.37
MACC-ENS, 20x30	4.55	23.5%	0.16	0.554	y = 0.620x + 7.51	5.74	20.4%	-0.09	0.721	y = 0.702x + 8.30
CHIMERE-EC4M., 50x50	4.43	22.9%	0.14	0.568	y = 0.577x + 8.32	5.93	21.1%	-0.08	0.702	y = 0.712x + 8.03
CHIMERE-EC4M., 7x7	4.21	21.8%	0.15	0.613	y = 0.645x + 7.01	6.04	21.5%	-0.06	0.692	y = 0.732x + 7.48
model used in ETC/ACM mapping	PM ₁₀ 36 th highest daily mean, 2009									
	rural					urban background				
	RMSE	bias	R ²	regr. equation	RMSE	bias	R ²	regr. equation		
EMEP, 50x50	7.98	24.1%	0.61	0.553	y = 0.577x + 14.6	11.37	23.7%	-0.03	0.707	y = 0.694x + 14.6
MACC-ENS, 20x30	7.55	22.8%	0.36	0.599	y = 0.637x + 12.4	11.25	23.5%	-0.08	0.713	y = 0.698x + 14.4
CHIMERE-EC4M., 50x50	7.61	23.0%	0.54	0.592	y = 0.603x + 13.7	11.28	23.5%	0.18	0.711	y = 0.716x + 13.8
CHIMERE-EC4M., 7x7	7.00	21.1%	0.55	0.657	y = 0.692x + 10.7	11.69	24.4%	0.25	0.691	y = 0.714x + 14.0

Table 4.2 Comparison of cross-validation indicators for interpolation with the use of different dispersion models outputs – PM₁₀, 2010

model used in ETC/ACM mapping	PM ₁₀ annual average, 2010									
	rural					urban background				
	RMSE	bias	R ²	regr.equation		RMSE	bias	R ²	regr.equation	
EMEP, 50x50	4.51	22.8%	0.16	0.613	y = 0.644x + 7.21	5.96	20.6%	-0.16	0.775	y = 0.771x + 6.48
MACC-ENS, 15x25	4.49	22.7%	0.29	0.620	y = 0.667x + 6.88	5.78	20.0%	-0.16	0.789	y = 0.795x + 5.79

model used in ETC/ACM mapping	PM ₁₀ 36 th highest daily mean, 2010									
	rural					urban background				
	RMSE	bias	R ²	regr. equation		RMSE	bias	R ²	regr. equation	
EMEP, 50x50	8.58	24.3%	0.21	0.641	y = 0.646x + 12.8	11.37	22.4%	-0.34	0.783	y = 0.777x + 10.9
MACC-ENS, 15x25	8.64	24.4%	0.53	0.639	y = 0.663x + 12.4	11.20	22.1%	-0.21	0.787	y = 0.799x + 10.0

In general, the mapping procedure provides lower cross-validation RMSE in absolute values for the annual PM₁₀ average than for 36th highest daily value. This is caused by the higher absolute values in general of the 36th highest daily means. The same reason explains why the RMSE in absolute values for the urban background are higher than for rural mapping: PM₁₀ values are usually higher in urban background areas than in the rural background areas.

Other factors play also a role regarding the actual values of the cross-validation statistics, such as the actual performance of the chemical model results against observations. For instance, in rural background areas, the use of the CHIMERE-EC4MACS model in 7x7 km² resolution gives the best R² results in 2009, both for the 36th highest daily mean and the annual average. It is probably just caused by the best correlation between modelled and measurement data for this model output (Annex 5, Figures A5.1 and A5.3). Another factor influencing the cross-validation statistics is the spatial density of the station network. The high number of urban and suburban background stations probably contributes to higher R² values in the urban background areas than in the rural ones with their less dense rural background station network, although the correlation between modelled and measurement data is better in the rural areas (Annex 5, Figures A5.1 – A5.8). The spatial distribution of the residual fields also has its influence on the cross-validation statistics. Next to this, it should be noted that these statistics are quite sensitive to the occurrence of outliers.

Irrespective the different concentration levels calculated with the individual models in 2009 (Annex 4, Figures A4.1 – A4.2, and Annex 5, Tables A5.1 and A5.2), the cross-validation results of Table 4.1 show quite similar values for the bias for the different models used in the ETC/ACM mapping. Thus, this confirms that the mapping procedure ensures that the resulting maps reflect the concentration levels of the measurement data, at both rural and urban background.

In 2009, in the rural areas the use of the CHIMERE-EC4MACS model in 7x7 km² resolution gives out of the four models the best result, while the use of the EMEP model gives there the weakest result. In the urban background areas, the use of the MACC-II Ensemble gives the best result for most of the cross-validation statistics. Surprisingly, the use of the CHIMERE-EC4MACS model in 7x7 km² resolution gives the weakest results in the sense of RMSE and R², regardless its highest resolution.

In 2010, in the rural areas the use of the MACC-II Ensemble gives slightly better results for the annual average, and slightly worse results for the 36th highest daily mean, than the use of the EMEP model (Table 4.2). In the case of the 36th highest daily mean, the influence of the

outlying station MT00007, which is estimated better by EMEP than by MACC-II Ensemble, plays a role. (If removing this station, the RMSE would be 8.60 for EMEP and 8.57 for MACC-II Ensemble.) In the urban background areas, the use of MACC-II Ensemble gives better results for both PM₁₀ indicators.

The results of the cross-validation indicate the effect the grid resolution has on the mapping results. Table 4.1 includes the results of the cross-validation indicators for 2009 using four different dispersion models with different spatial resolutions. The cross-validation results are presented by showing the ETC/ACM mapping procedure that uses the two chemical transport models of coarser spatial resolution (EMEP and CHIMERE in EC4MACS with ca. 50x50 km²), the MACC-II Ensemble with a factual spatial resolution of about 20x30 km², and the model of finer scale resolution (CHIMERE in EC4MACS with ca. 7x7 km² resolution). Table 4.2 shows for 2010 the cross-validation results of the ETC/ACM mapping using the EMEP model with the same resolution as for 2009, and the MACC-II Ensemble with a higher factual spatial resolution of ca. 15x25 km². The grid resolutions of the individual models used in the ensemble (Section 3.2) influences the output of the MACC-II Ensemble.

In general, the cross-validation statistics for PM₁₀ improve in rural areas when the spatial resolution of the dispersion model used to support the mapping is refined.

In urban background areas, we observe at both years an improvement when using the MACC-II Ensemble, irrespective its resolution, instead the EMEP model. Such improvement is not observed when using the CHIMERE-EC4MACS models in 2009. In urban background areas the performance on the 2009 data of the mapping methodology using the CHIMERE-EC4MACS dispersion models is remarkably different than when using the other two models. The correlation, i.e. the fit of the linear regression equation expressed by R², between modelled and the measurement data is higher for both CHIMERE models (see Annex 5, Figure A5.2 and A5.4), but not the RMSE from cross-validation (Table 4.1). In other words, better correlation between modelled and measurement data does not necessarily lead to better mapping results, as these are influenced by the spatial structure of the regression's residual field.

The PM₁₀ cross-validation results for 2009 in Table 4.1 indicate that in rural areas, the use of the model with the highest resolution (which is CHIMERE-EC4MACS model on 7x7 km²) generally produces the best results. The same conclusion can be drawn for 2010 with the MACC-II Ensemble, circa 15x25 km², Table 4.2), although in rural areas in case of the 36th highest daily mean the use of the EMEP model results in better performance on the most of the cross-validation statistics. In most cases, the use of the MACC-II Ensemble in the mapping gives slightly better results than the use of the EMEP model.

4.2 Ozone

4.2.1 Mapping using EMEP, MACC-II Ensemble and CHIMERE models

Figures 4.10 to 4.13 present ETC/ACM mapping results of ozone indicators using the four different chemical transport models for 2009. Figures 4.14 to 4.17 show the results when using the EMEP model and the MACC-II Ensemble model for 2010. The spatial interpolation maps using these different dispersion models as input are shown for the selected ozone indicators 26th highest daily maximum 8-hourly mean and the sum of ozone daily maximum 8-hourly means over 35 ppb (SOMO35).

The same conclusions can be drawn from the analyses of the ozone indicators as discussed in Section 4.1.1 on the analysis of PM₁₀. The spatial distribution of the ozone indicator mapping results is very similar independent of the chemical dispersion model used as input for the ETC/ACM mapping routines, when the models tested are the EMEP 50x50 km² model and the MACC-II Ensemble for 2009 (circa 20x30 km²) and 2010 (circa 15x25 km²), and CHIMERE-EC4MACS in 50x50 km² and 7x7 km² resolutions for 2009. Differences between rural and urban background maps are more significant than differences caused by the choice of chemical dispersion model. This is because spatial interpolations methods, such as the residual kriging method used at ETC/ACM, are predominantly driven by observations. The mapping results primarily reflect the differences between ozone levels measured at rural background stations and those at urban or suburban background stations. Therefore, the choice of model (EMEP, MACC-II Ensemble or CHIMERE models) has minor effect on the mapping results, regardless the estimated concentration level of the individual chemical transport models.

The original model outputs (see Annex 4, Figures A4.5 to A4.8) estimated by the individual models differ a lot from each other in many cases. Contrary to that, the outputs of the ETC/ACM mapping procedure using these models are quite similar, regardless the individual model used (see the Figures 4.10 – 4.17). Therefore, one can conclude that the output of this ETC/ACM mapping procedure is predominantly fitted to the concentration level of the measurement values, at both rural and urban background areas.

Annex 3, Figures A3.7 to A3.12 present for both the indicators the differences between the ETC/ACM mapping results using different models for 2009 and 2010. The difference maps show the difference between the mapping result using EMEP (as current default model) and another model output, and also between the mapping results using the CHIMERE-EC4MACS models in different resolutions.

Ozone, 26th highest daily maximum 8-hourly mean, 2009

In the year 2009, the major differences for the 26th highest daily maximum 8-hourly mean maps in the rural areas (Figure 4.10 and Annex 3, Figure A3.7) are observed in areas with a low density of measurement stations (Norway, Balkan area, southern Italy, the Alps).

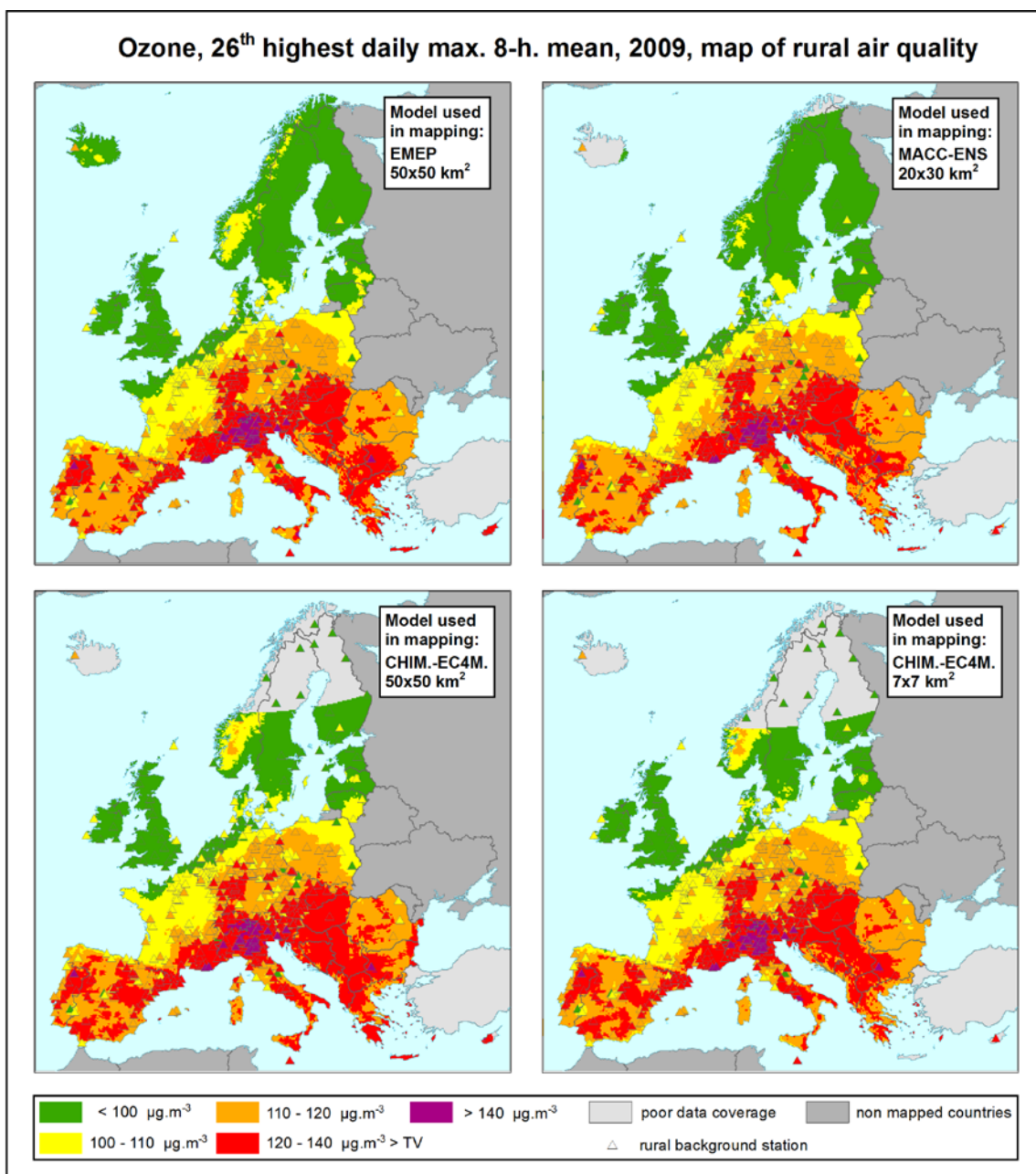


Figure 4.10 Ozone indicator 26th highest daily maximum 8-hourly mean for 2009, rural map, ETC/ACM mapping result using EMEP, MACC-II Ensemble, CHIMERE-EC4MACS_50km, and CHIMERE-EC4MACS_7km.
Note: Applicable for rural areas only.

In the case of the urban background maps (Figure 4.11 and Annex 3, Figure A3.8), the major differences are in Norway, Balkan area, and the Iberian Peninsula, i.e. again in the areas with a low density of the measurement stations.

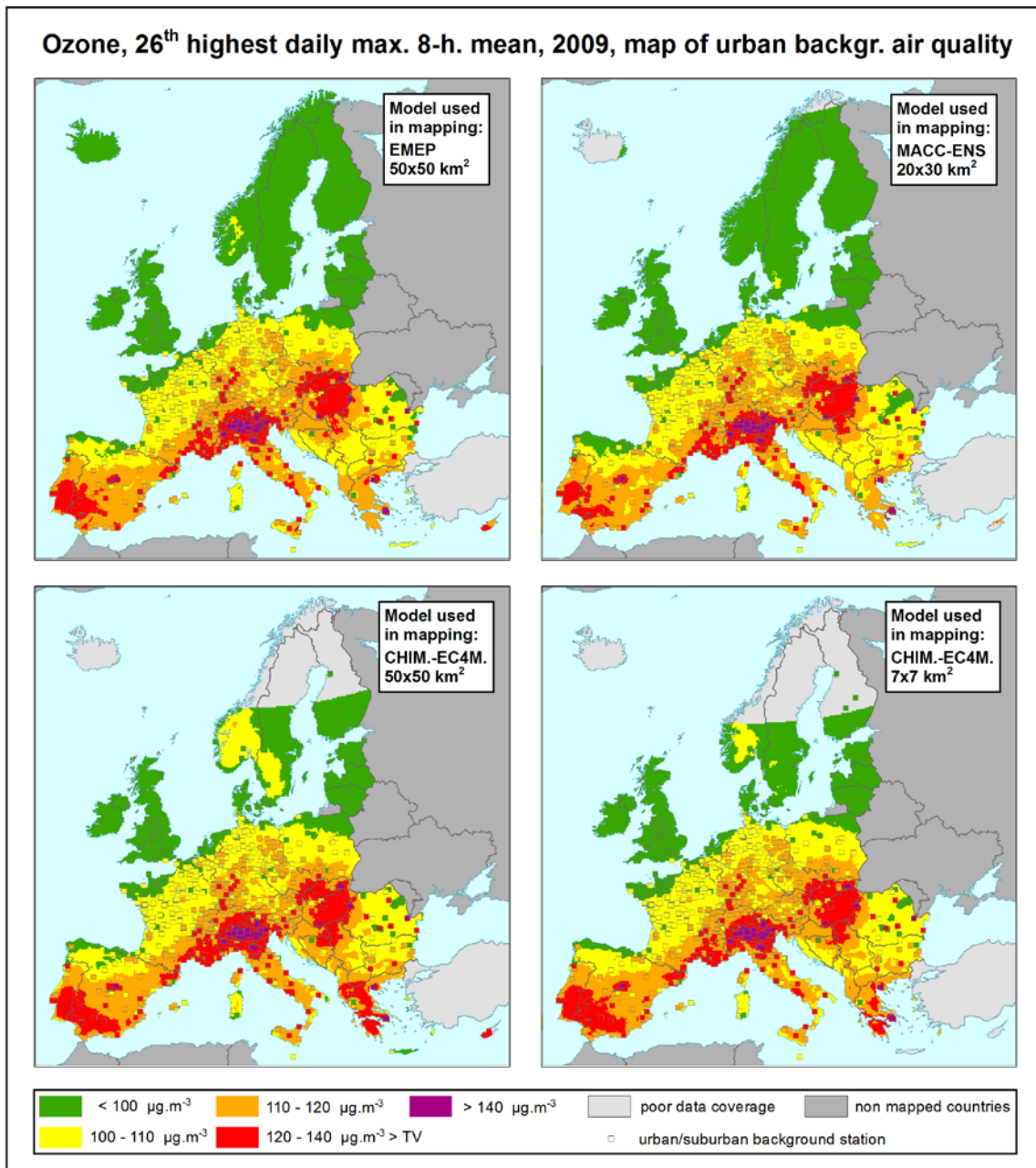


Figure 4.11 Ozone indicator 26th highest daily max. 8-hourly mean for 2009, urban background map, ETC/ACM mapping result using EMEP, MACC-II Ensemble, CHIMERE-EC4MACS_50km, and CHIMERE-EC4MACS_7km.
Note: Applicable for urban areas only.

In both the rural background and the urban background areas, the differences between the maps using the EMEP and the MACC-II Ensemble can be seen in some mountainous areas (the Alps, the Pyrenees, the Romanian Carpathians), see Annex 3, Figures A3.7–A3.8. The reason cannot be the use of the altitude as a supplementary variable in the residual kriging, as this parameter has not been used in the ETC/ACM mapping of the urban background areas (see Table 1.1). Thus, the reason should be in the model outputs that have been used. This is in agreement with the differences of original EMEP and MACC-II Ensemble model outputs in the mountainous areas, see Annex 4, Figure A4.5. The MACC-II Ensemble output shows lower concentrations in mountainous areas than in other areas, while the EMEP model output does not.

Ozone, SOMO35, 2009

In the case of the rural maps of SOMO35 in 2009 (Figure 4.12), the major differences in the rural areas can be seen in Balkan area, which is the area with a lack of rural measurement stations (see Annex 3, Figure A3.9). Other such areas are e.g. the Iberian Peninsula including the Pyrenees, Italy, the Alps, and the Baltic states. Again, these are areas with a low density of the measurement stations.

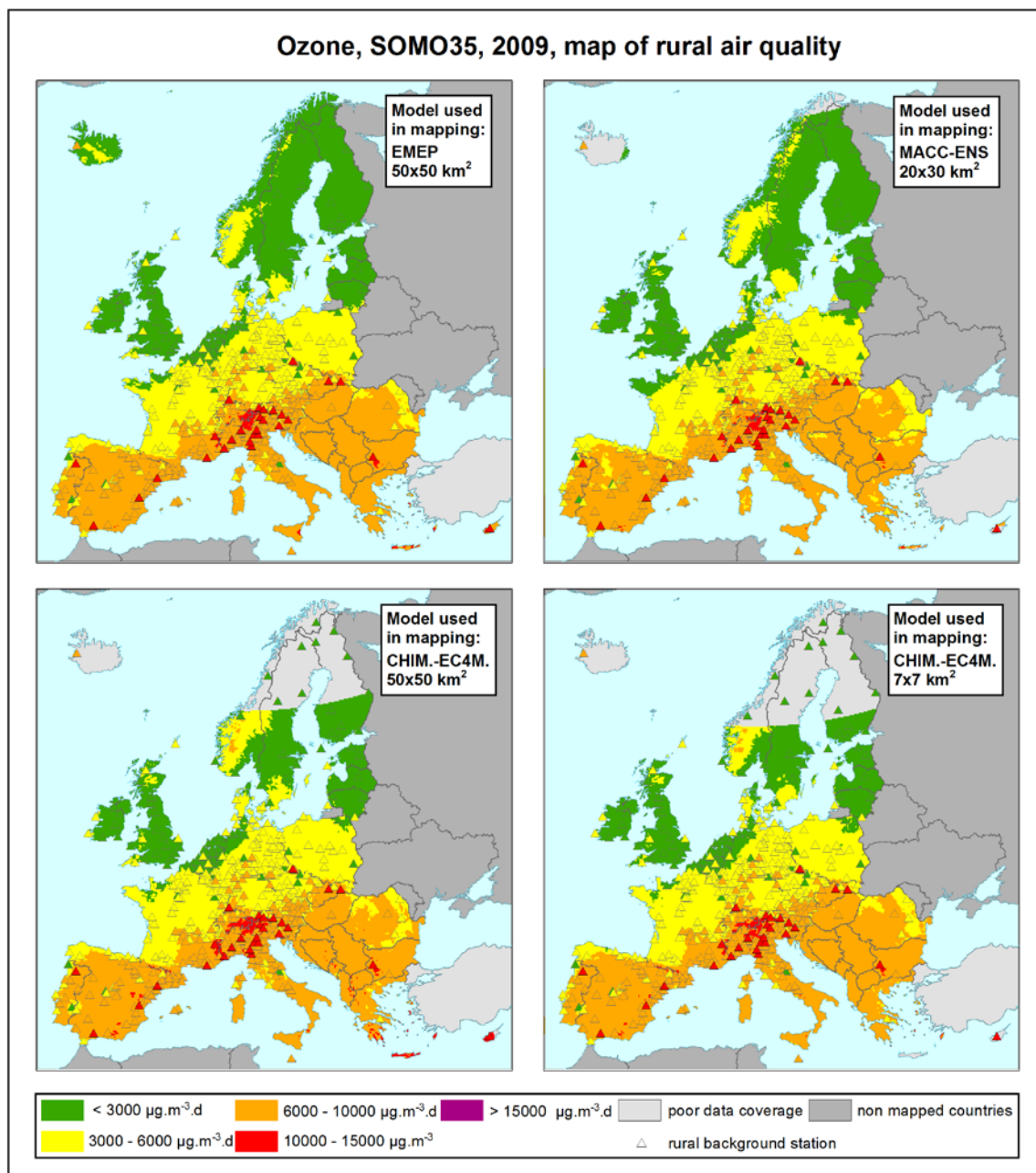


Figure 4.12 Ozone indicator SOMO35 for 2009, rural map, ETC/ACM mapping result using EMEP, MACC-II Ensemble, CHIMERE-EC4MACS_50km, and CHIMERE-EC4MACS_7km. Note: Applicable for rural areas only.

In the case of the urban background maps (see Figure 4.13 and Annex 3, Figure A3.10), the mapping results are very similar at all model cases used. The only exception in all of these maps is southern Greece, and in the case of the map using MACC-II Ensemble also the

mountainous areas, however, these mapping results are only applicable to mountainous cities of which only a limited number exists.

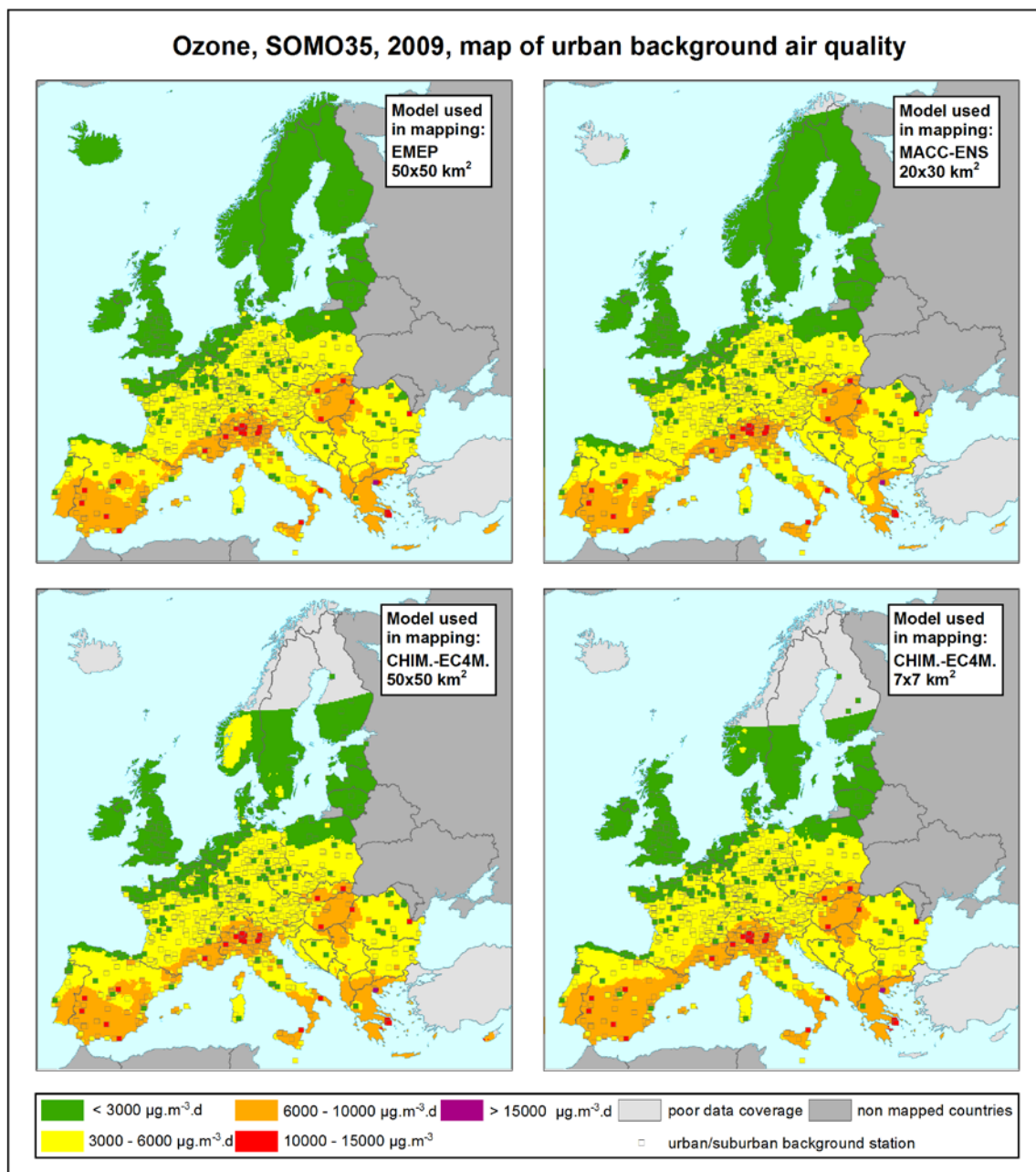


Figure 4.13 Ozone indicator SOMO35 for 2009, urban background map, ETC/ACM mapping result using EMEP, MACC-II Ensemble, CHIMERE-EC4MACS_50km, and CHIMERE-EC4MACS_7km. Note: Applicable for urban areas only.

The impact of spatial resolution of the chemical transport models is less relevant for ozone than it was for PM₁₀ (Section 5.1.1). This is because ozone is typically a background pollutant and its concentration is generally well reproduced by chemical transport models with a regional scale spatial resolution. Annex 5, Figures A5.9 to A5.16 present the performance of the chemical transport models in comparison with ozone observations. The different scatter plots in this annex also demonstrate that in general there is a better ability of

the models to reproduce the observed ozone levels than they do at the observed PM₁₀ levels (Figures A5.1 to A5.8).

Ozone, 26th highest daily maximum 8-hourly mean and SOMO35, 2010

Figures 4.14 and 4.15 present ETC/ACM mapping results of the ozone indicator 26th highest daily maximum 8-hourly mean and Figures 4.16 and 4.17 of the ozone indicator SOMO35 for 2010. Annex 3, Figures A3.11 and A3.12 present the differences between the mapping results using the EMEP and the MACC-II Ensemble model outputs for 2010. No output of CHIMERE-EC4MACS are available for 2010.

The major differences for the 26th highest daily maximum 8-hourly mean in both the rural and the urban background areas (Figures 4.14 and 4.15) are again in the areas with a low density of the measurement stations (e.g. Scandinavia, Balkan area, Iberian Peninsula), including the mountainous areas (the Alps, the Pyrenees, the Romanian Carpathians).

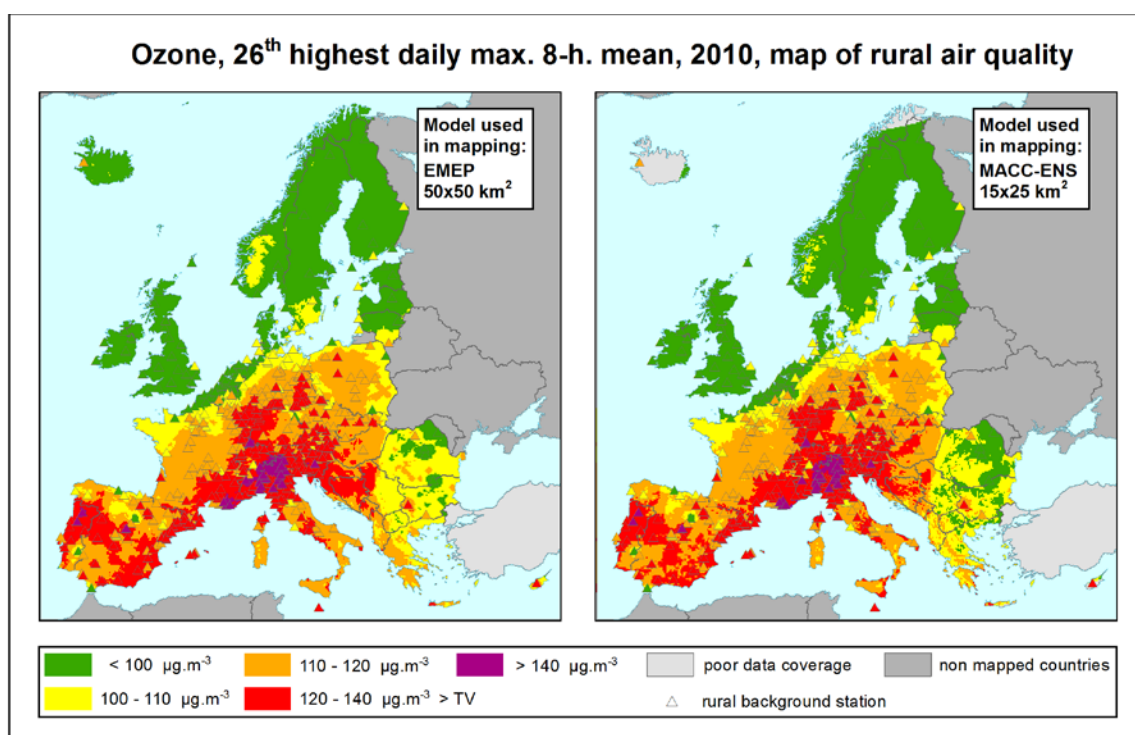


Figure 4.14 Ozone indicator 26th highest daily maximum 8-hourly mean for 2010, rural map, ETC/ACM mapping result using EMEP (left) and MACC-II Ensemble (right). *Note: Applicable for rural areas only.*

In the case of the rural maps of SOMO35 in 2010 (Figure 4.16), the maps are almost the same.

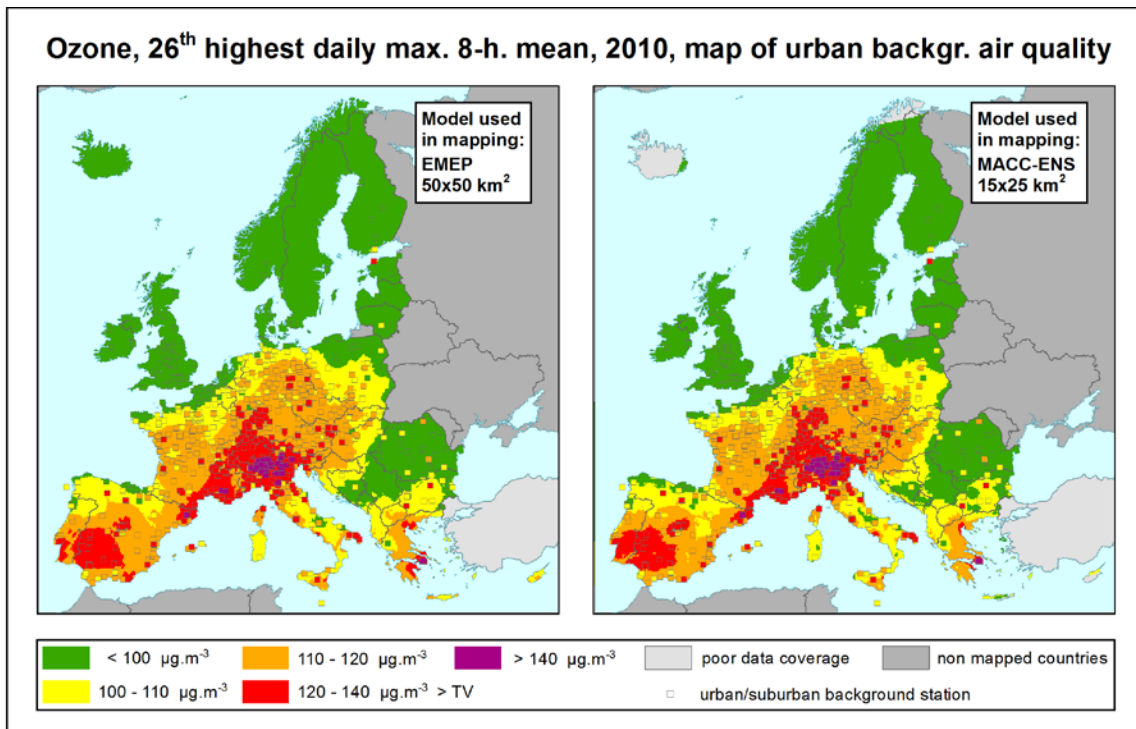


Figure 4.15 Ozone indicator 26th highest daily max. 8-hourly mean for 2010, urban background map, ETC/ACM mapping result using EMEP (left) and MACC-II Ensemble (right). *Note: Applicable for urban areas only.*

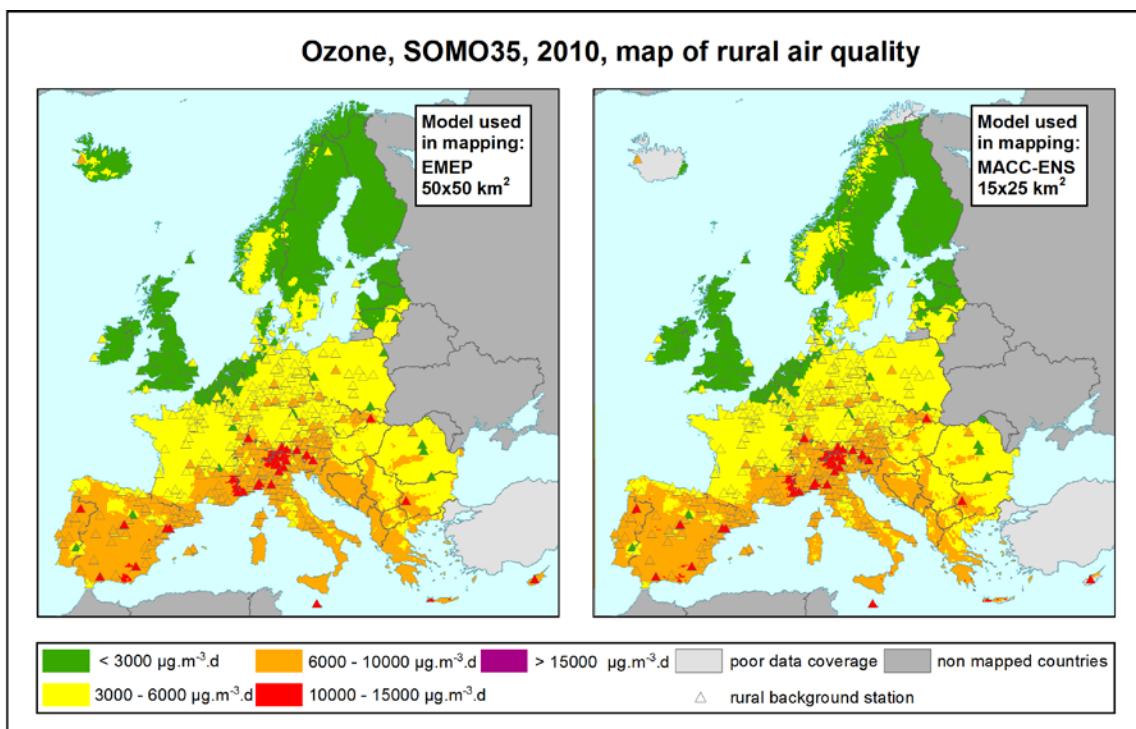


Figure 4.16 Ozone indicator SOMO35 for 2010, rural map, ETC/ACM mapping result using EMEP (left) and MACC-II Ensemble (right). *Note: Applicable for rural areas only.*

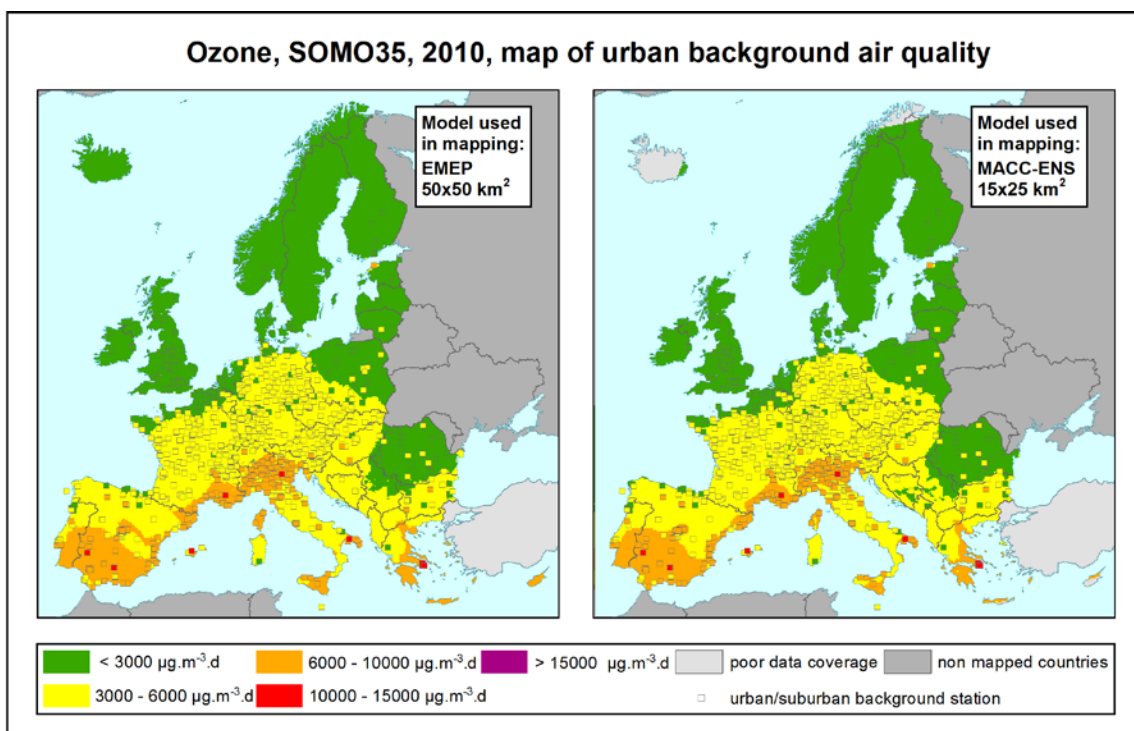


Figure 4.17 Ozone indicator SOMO35 for 2010, urban background map (applicable for urban areas only), using EMEP (left) and MACC-II Ensemble (right). *Note: Applicable for urban areas only.*

In the case of the urban background maps of SOMO35 in 2010 (Figure 4.17), the differences are only found in some limited areas. For the difference maps, see Annex 3, Figure A3.12.

When compared to the long-term average, the variability of meteorological conditions of 2009 and 2010 are not considered extreme for the mapping domain under consideration. The variability of the meteorological conditions for ozone between the year 2009 and 2010 is described briefly by EMEP (2012b, section 2.1), saying that 2010 ozone levels are fairly low compared to the long term average of 2000–2009.

4.2.2 Cross-validation results

A similar cross-validation analysis as for PM₁₀ was executed also for ozone. Tables 4.3 and 4.4 present the statistics for the ETC/ACM mapping performance with all models available, again highlighting the mapping results with better performance (the darker the green, the better).

In 2009, for both ozone indicators and for rural and urban areas, results are the best for the ETC/ACM mapping using MACC-II Ensemble (factual resolution 20x30 km²). The better performance of the mapping that uses the MACC-II Ensemble as chemical transport model is calculated for most statistics, despite the higher resolution of the CHIMERE-EC4MACS 7x7 km² model. Nevertheless, the second best results are given for the mapping procedure using CHIMERE-EC4MACS in 7x7 km² resolution. In 2010 the results for EMEP model (resolution 50x50 km²) are about the same as MACC-II Ensemble (factual resolution 15x25 km²).

The reason of the best results of MACC-II Ensemble (20x30 km²) in 2009 probably lies just in the fact that the best correlation between the results of the linear regression models using MACC-II Ensemble and the measurement data, at both rural and urban areas, for both ozone indicators (see adjusted R² in Annex 1, Table A1.4 and A1.5). An additional reason for the better performance of the mapping with MACC-II Ensemble is that in most cases, the MACC-II Ensemble shows in 2009 the best correlation also for the direct comparison with the measurement data, as illustrated in the scatter plots in Annex 5, Figures A5.9 to A5.12.

Table 4.3 Comparison of cross-validation indicators for interpolation with the use of different dispersion models outputs – Ozone, 2009

model used in ETC/ACM mapping	Ozone, 26 th highest daily 8-hourly maximum, 2009									
	rural					urban background				
	RMSE	bias	R ²	regr.equation		RMSE	bias	R ²	regr.equation	
EMEP, 50x50	8.18	7.11%	0.00	0.685	y = 0.707x + 33.7	9.33	8.41%	0.09	0.642	y = 0.668x + 37.0
MACC-ENS, 20x30	7.84	6.82%	0.02	0.710	y = 0.714x + 33.0	9.08	8.19%	0.12	0.660	y = 0.678x + 35.8
CHIMERE-EC4M., 50x50	8.57	7.45%	0.13	0.656	y = 0.696x + 35.1	9.48	8.55%	0.06	0.631	y = 0.672x + 36.4
CHIMERE-EC4M., 7x7	7.87	6.84%	0.01	0.708	y = 0.728x + 31.3	9.23	8.33%	0.06	0.649	y = 0.671x + 36.5

model used in ETC/ACM mapping	Ozone, SOMO35, 2009									
	rural					urban background				
	RMSE	bias	R ²	regr.equation		RMSE	bias	R ²	regr.equation	
EMEP, 50x50	1617	29.1%	3	0.633	y = 0.638x + 2015	1476	33.1%	-1	0.613	y = 0.619x + 1701
MACC-ENS, 20x30	1567	28.2%	-11	0.655	y = 0.661x + 1876	1456	32.6%	-3	0.624	y = 0.636x + 1623
CHIMERE-EC4M., 50x50	1665	30.0%	16	0.613	y = 0.648x + 1973	1496	33.5%	-7	0.603	y = 0.620x + 1690
CHIMERE-EC4M., 7x7	1626	29.2%	2	0.629	y = 0.646x + 1969	1460	32.7%	-5	0.622	y = 0.628x + 1657

The results for the use of the CHIMERE-EC4MACS in 7x7 km² are quite interesting. The correlations of the CHIMERE-EC4MACS in 7x7 km² in comparison with the measurement data at the station points are worse than the correlations of EMEP 50x50km², whereas one would expect that the higher resolution would lead to a higher correlation with the measurement data. The scatter plots with these results are given in Annex 5, Figures A5.9 – A5.12. The lower R² in these scatter plots expresses a poorer correlation. Nevertheless, the kriging of its residuals give slightly better results than the kriging of the EMEP's ones (higher R² and RMSE for CHIMERE-EC4MACS 7x7 than for EMEP 50x50 in Table 4.3, in most cases). This is probably somehow caused by its higher resolution in comparison with EMEP.

Table 4.4 Comparison of cross-validation indicators for interpolation with the use of different dispersion models outputs – Ozone, 2010

model used in ETC/ACM mapping	Ozone, 26 th highest daily 8-hourly maximum, 2010									
	rural					urban background				
	RMSE	bias	R ²	regr.equation		RMSE	bias	R ²	regr.equation	
EMEP, 50x50	8.87	7.7%	0.17	0.686	y = 0.721x + 32.5	9.13	8.1%	0.04	0.711	y = 0.727x + 30.7
MACC-ENS, 15x25	8.91	7.7%	0.13	0.684	y = 0.727x + 31.8	9.04	8.1%	0.06	0.717	y = 0.734x + 29.8

model used in ETC/ACM mapping	Ozone, SOMO35, 2010									
	rural					urban background				
	RMSE	bias	R ²	regr.equation		RMSE	bias	R ²	regr.equation	
EMEP, 50x50	1582	29.2%	18	0.629	y = 0.651x + 1908	1271	29.5%	6	0.650	y = 0.667x + 1441
MACC-ENS, 15x25	1566	28.9%	15	0.637	y = 0.663x + 1843	1272	29.5%	5	0.650	y = 0.666x + 1445

In 2010, the results for the mapping using EMEP 50x50 km² and MACC-II Ensemble 15x25 km² show very similar performance, with a slightly better performance when using the MACC-II Ensemble. This is likely due to its higher spatial resolution.

Irrespective the different concentration levels calculated with the individual models (see Annex 4, Figures A4.5 – A4.8, and Annex 5, Tables A5.3 and A5.4), the cross-validation results show quite similar values for the bias for the different models used in the ETC/ACM mapping (see Table 4.3 and 4.4). Thus, this confirms that the mapping procedure ensures that the resulting maps reflect the concentration levels of the measurement data, at both rural and urban background.

4.3 Conclusions

The results in this chapter have shown how the performance of the spatial interpolation mapping varies with the use of different chemical dispersion models in different original resolutions.

The mapping results are predominantly driven by the observations. Irrespective to the different concentration levels of the individual models, the ETC/ACM mapping results give similar concentration levels at each of the models used in its mapping procedure.

There is a general improvement in the cross-validation results when using the MACC-II Ensemble model instead of the EMEP model, as Table 4.5 summarises. The improvement of the results appears primarily to be related to the higher spatial resolution of the MACC-II Ensemble model output.

Table 4.5 Summary comparison table of the use of MACC-II Ensemble and EMEP model hindcasts in the ETC/ACM mapping ('+' means better results of MACC-II Ensemble, '-' better results of EMEP, '0' the equal results)

Pollutant and indicator		2009		2010	
		rural	urban background	rural	urban background
PM ₁₀	annual average	+	+	+	+
	36 th highest daily mean	+	+	-	+
Ozone	26 th highest daily 8-h max.	+	+	-	+
	SOMO35	+	+	+	0

The improvement applies to both PM₁₀ and ozone indicators in 2009 and in most cases also in 2010. It should be noted, however, that these improvements by chemical dispersion models are relatively modest and that the most significant improvements in mapping European-wide pollution levels are yet obtained specifically from the use of primarily observational data in spatial interpolation methods.

5 Comparison with model results

5.1 Comparison with hindcast model outputs

The results in Chapter 4 focus on the comparison of the mapping results when different chemical dispersion models are used as dependent variables in the residual kriging. What the results in Chapter 4 does not show is the added value of the ETC/ACM mapping routines with respect to any of the dispersion chemical models used.

In this section we show some of the strengths and capabilities of the ETC/ACM mapping. It presents the comparison of the ETC/ACM mapping results with the *hindcast* dispersion model outputs (i.e. model outputs without data assimilation), using maps and scatter plots with measurement data. Contrary to that, Section 5.2 addresses an initial comparison with the *reanalysis* (i.e. data assimilated) model results. Table 2.2 highlights the difference between hindcast and reanalysis model results. Although the results are shown only for PM₁₀ annual average and ozone indicator SOMO35 for 2009, the conclusions drawn from the comparison are valid for all four indicators and for both years dealt with in this report.

PM₁₀

Figure 5.1 compares the ETC/ACM mapping results (using the EMEP model) at rural and urban background areas with the hindcast results from two chemical transport models (the EMEP model and the MACC-II Ensemble model) for PM₁₀ annual average in 2009. This figure illustrates clearly the refined level of detail in the ETC/ACM map compared to the maps from the modelling results. ETC/ACM mapping results using MACC-II Ensemble hindcast outputs instead are not included in Figure 5.1. However, they show quite similar results (see Figures 4.1 and 4.2, upper right). All maps are presented in a 10x10 km² grid resolution.

Annex 4 presents the maps of the dispersion modelling results for all models and all indicators used in this paper, for both 2009 and 2010. These model results are comparable to the relevant ETC/ACM mapping results presented in Chapter 4.

The maps furthermore demonstrate well at extended parts of the maps the differences in the concentration levels between the results of the ETC/ACM mapping and of the dispersion modelling. The elevated concentrations of the ETC/ACM urban background map in comparison with both dispersion model outputs, is quite natural. One has to realise that from the methodological point of view this ETC/ACM map is applicable for urban areas only. Whereas the model output maps represent both rural and urban areas in a 10x10 km² grid resolution, which means that the urban areas are quite smoothed in the model outputs. However, at the ETC/ACM map representing the rural background areas one observes more elevated concentration levels compared to the maps of both dispersion models as well. This could indicate that at the dispersion modelling results an underestimation applies to both urban and rural background areas, in the case of PM₁₀. By means of scatter plots and statistical indicators one is able to demonstrate how these maps relate to the observations.

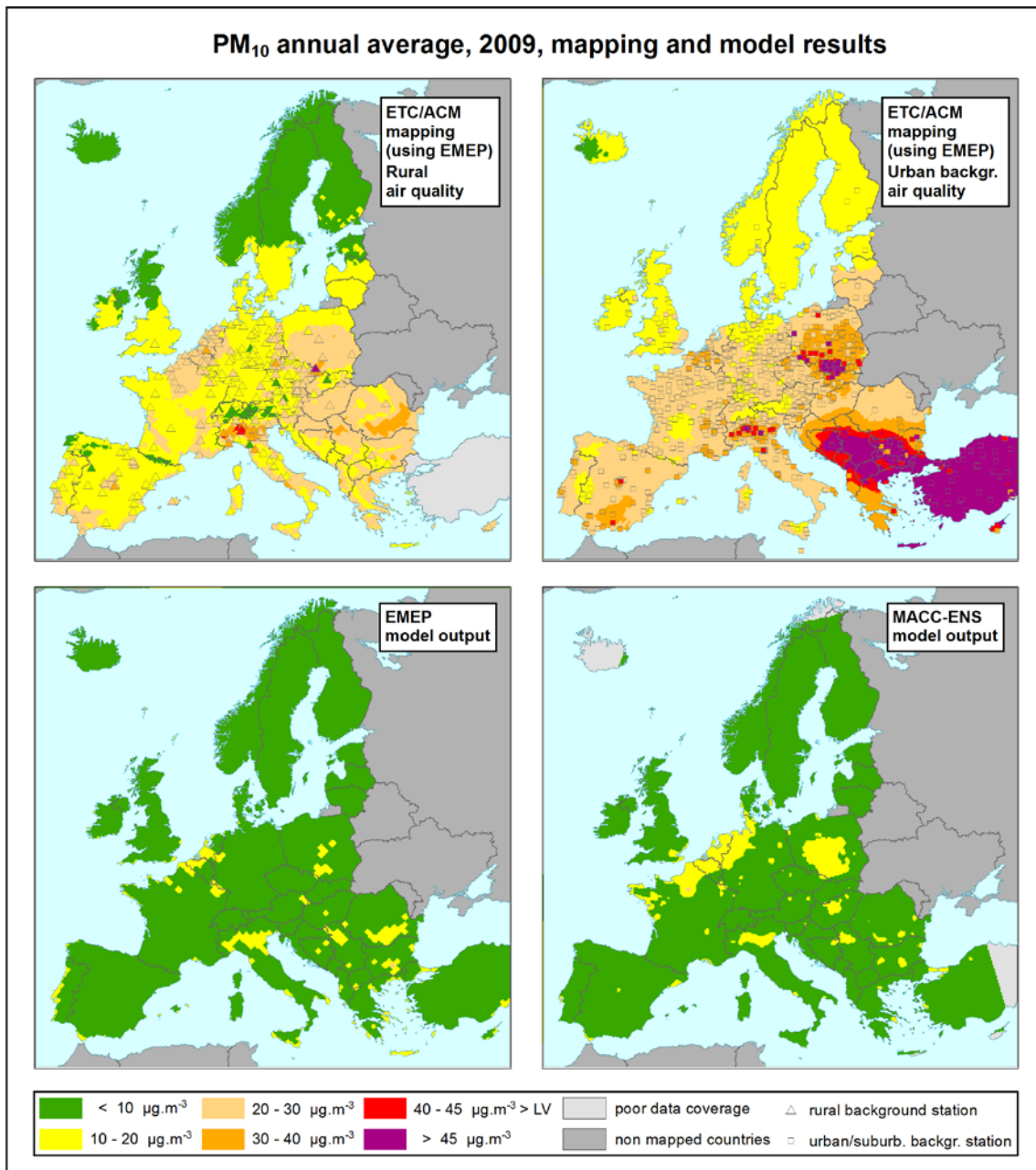


Figure 5.1 Comparison of ETC/ACM mapping results for rural (upper left, *applicable for rural areas only*) and urban background (upper right, *applicable for urban areas only*) air quality with dispersion model hindcast results from EMEP (lower left) and MACC-II Ensemble (ENS) (lower right) models (*applicable to both rural and urban areas*) for PM₁₀ annual average in 2009

The scatter plots for PM₁₀ annual average of the 2009 showing the performance of the ETC/ACM mapping results through leave-one-out cross-validation and the performance of two different chemical transport models (hindcasts of the EMEP model and the MACC-II Ensemble model) against the observations are presented in Figure 5.2 for rural background areas and in Figure 5.3 for urban background areas. The left hand side represents the scatter plots of the ETC/ACM mapping results in cross-validation versus the measured values; the right hand side scatter plots those of the dispersion model outputs versus the observations. The top row scatter plots represent the ETC/ACM mapping results using the EMEP model,

compared to the scatter plots for the EMEP model output. While at the bottom row represents the scatter plots for the ETC/ACM mapping results using MACC-II Ensemble, compared to the scatter plots for the MACC-II Ensemble output.

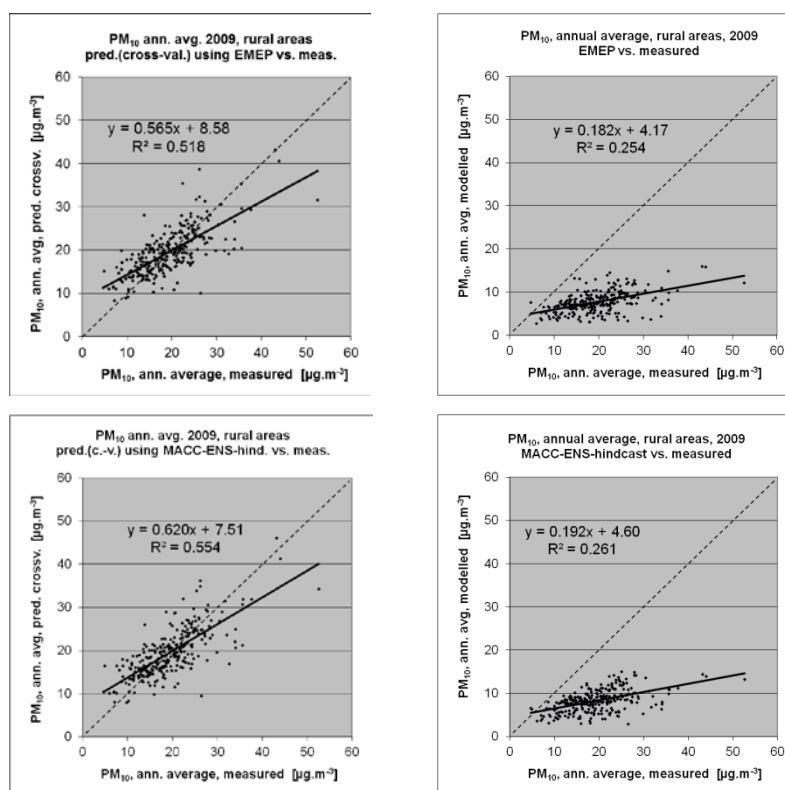


Figure 5.2 Scatter plots showing ETC/ACM mapping results for rural background areas in cross-validation (left) and dispersion model outputs (right) versus rural background observations for PM₁₀ annual average in 2009

The considerable higher R^2 and steeper slopes of the regression equations at the ETC/ACM mapping results, using either the EMEP or the MACC-II Ensemble hindcast model, demonstrate clearly their better performance than the application of the chemical model outputs.

The comparisons for other models (i.e. the CHIMERE-EC4MACS models), other year (i.e. 2010) and other PM₁₀ indicator (i.e. 36th highest daily mean) are not presented here, however, their results are quite similar as one can derive from the relevant scatter plots in Annex 2 and Annex 5.

Annex 5, Tables A5.1 and A5.2 present statistical indicators for different model outputs against the observations. These tables are directly comparable with Tables 4.1 and 4.2. One can see that ETC/ACM mapping gives better results (lower RMSE, bias closer to zero) than any chemical transport model output.

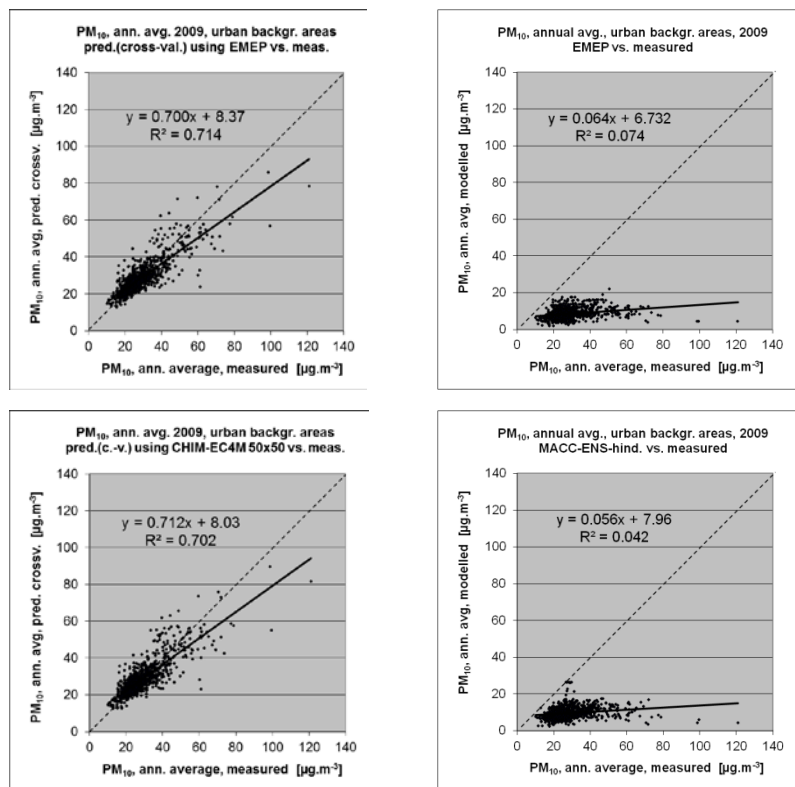


Figure 5.3 Scatter plots showing ETC/ACM mapping results for urban background areas in cross-validation (left) and dispersion model results (right) versus urban/suburban background observations for PM₁₀ annual average in 2009

Ozone

Figure 5.4 compares the ETC/ACM mapping results (using EMEP model) at rural and urban background areas with the results from two chemical transport models (the EMEP and the MACC-II Ensemble hindcasts), for ozone indicator SOMO35 in 2009. The rural and urban ETC/ACM mapping results using MACC-II Ensemble model are not included in this figure, however they provide quite similar mapping results (Figures 4.12 and 4.13, upper right). All the maps are presented in a 10x10 km² grid resolution.

The concentration levels of the chemical transport models and ETC/ACM mapping results differ less at the case of ozone than at the case of PM₁₀ (Figures 5.1 and 5.4). Again, we prepared scatter plots to demonstrate the relation of these maps of the ozone indicator SOMO35 derived from the actual observations.

Figure 5.5 presents the scatter plots for the ozone indicator SOMO35 in 2009 showing the ETC/ACM mapping results through cross-validation and the outputs of the two chemical transport models (hindcasts of the EMEP model and the MACC-II Ensemble model) against the observations for rural background areas. Figure 5.6 shows the same for urban background areas. The scatter plots with their higher R² and steeper slopes at the ETC/ACM mapping results indicate a better performance than the model outputs.

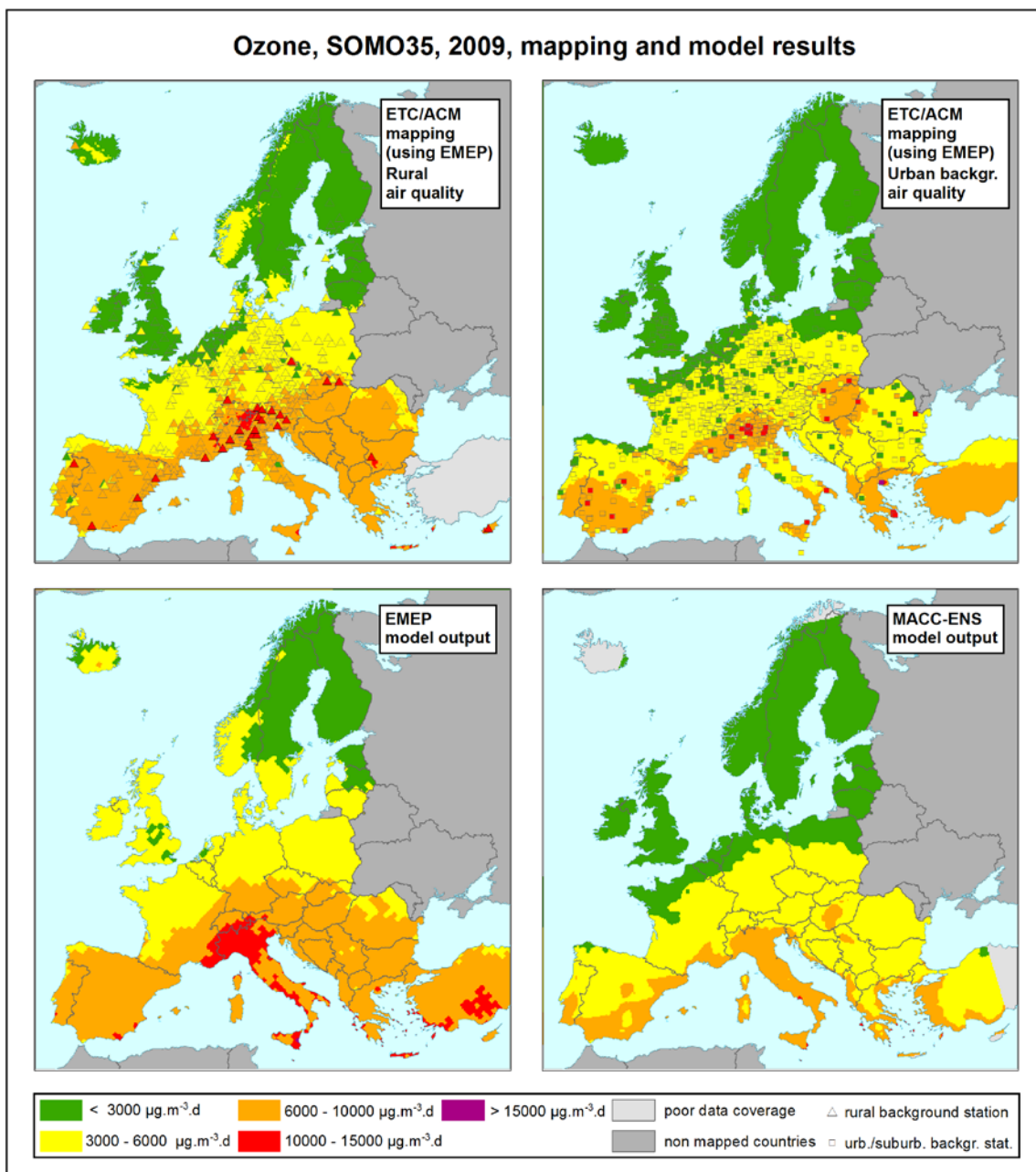


Figure 5.4 Comparison of ETC/ACM mapping results for rural (upper left, *applicable for rural areas only*) and urban background (upper right, *applicable for urban areas only*) air quality with dispersion model hindcast results from EMEP (lower left) and MACC-II Ensemble (lower right) models (*applicable to both rural and urban areas*) for ozone indicator SOMO35 in 2009

The comparisons for other models (i.e. CHIMERE-EC4MACS models), other year (i.e. 2010) and other ozone indicator (i.e. 26th highest daily maximum 8-hourly mean) are not presented here, however, their results are quite similar as one can derive from the relevant scatter plots in Annex 2 and Annex 5.

Annex 5, Tables A5.3 and A5.4 present statistical indicators for different model outputs against the observations. These tables are directly comparable with Tables 4.3 and 4.4. ETC/ACM mapping gives better results (lower RMSE, bias closer to zero) than any model output.

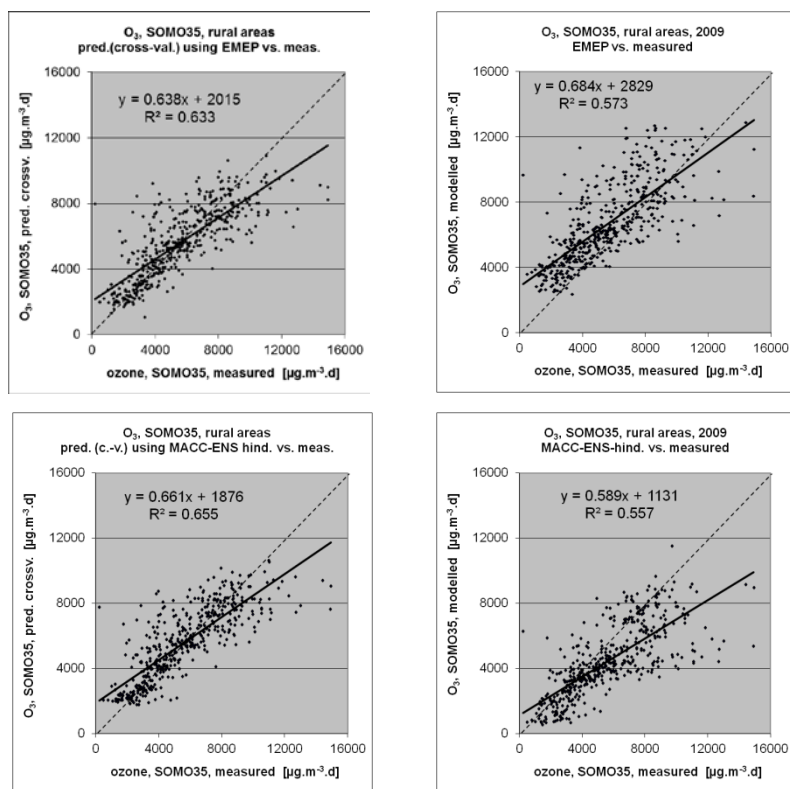


Figure 5.5 Scatter plots showing ETC/ACM mapping results for rural background areas in cross-validation (left) and dispersion model results (right) versus rural background observations for ozone indicator SOMO35 in 2009

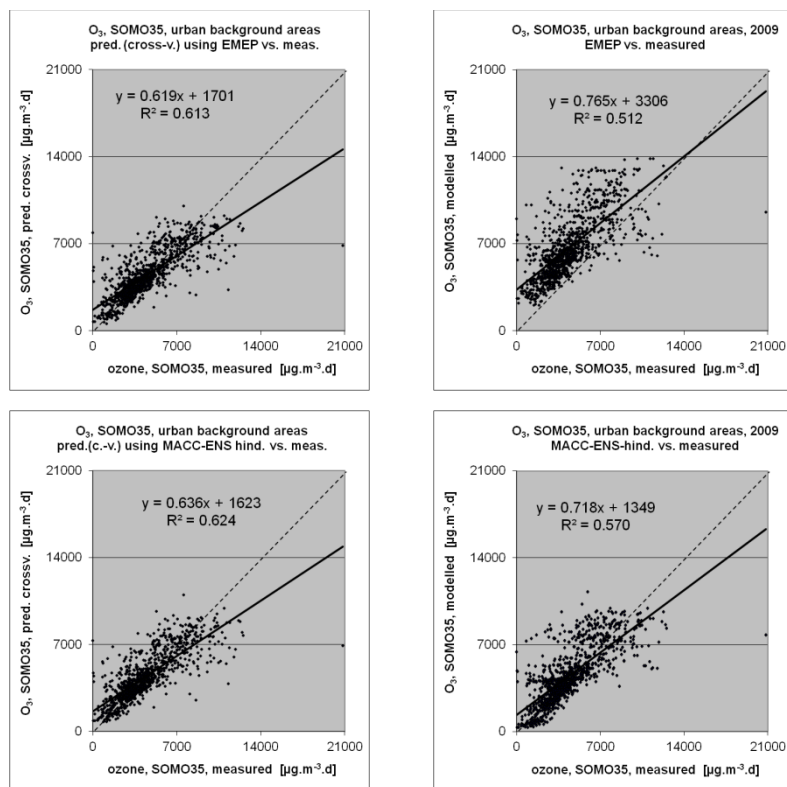


Figure 5.6 Scatter plots showing ETC/ACM mapping results for urban background areas in cross-validation (left) and dispersion model results (right) versus urban/suburban background observations for SOMO35 in 2009

Conclusion

The scatter plots of the ETC/ACM mapping cross-validated results against the observations demonstrate the higher R^2 , compared to those at the scatter plots of the individual model outputs against the observations. Next to this, the ETC/ACM mapping gives lower RMSE and bias closer to zero than any chemical transport model output. In general, one can conclude that the ETC/ACM mapping results are clearly driven by the observations and that their statistics show that they provide a more appropriate description of the spatial distribution of PM_{10} and ozone concentrations over Europe than any of the current state of art chemical dispersion models alone.

The results from ETC/ACM mapping for PM_{10} are significantly better than the modelling results as illustrated in Figures 5.2 and 5.3 because current dispersion models generally underestimate PM_{10} . In the case of ozone and ozone indicators, current dispersion modelling results are of significantly better quality than for PM_{10} . Still, the ETC/ACM mapping provides a better approximation of the observational data, as can be concluded from the scatter plots in Figures 5.5 and 5.6 and from the statistical indicators in Tables 4.3 and 4.4 in comparison with Annex 5, Tables A5.3 and A5.4 (lower RMSE, bias closer to zero).

The better performance of the ETC/ACM mapping results with regard to deterministic modelling is inherent to the use of residual kriging that combines the chemical dispersion model output with observational data.

5.2 Initial comparison with reanalysis model results

In order to secure the comparability of results, only *hindcast* data from MACC-II has been considered in the calculations included in this report so far. The MACC-II Ensemble, however, is also available as a *reanalysis* in a factual resolution of circa $20 \times 30 \text{ km}^2$ for 2009 and circa $15 \times 25 \text{ km}^2$ for 2010. Reanalysis ensemble results are derived from the data assimilated results from available individual dispersion models in MACC-II (see Table 2.3). The use of different data assimilation techniques by the individual models results in a better performance of the reanalysis compared to the hindcast results, see Figure 2.2 and Rouil et al. (2013).

Based on available reanalysis results of the individual MACC-II models, the MACC-II Ensemble reanalysis model is calculated, using the median of the involved reanalysis model results for every time step and grid cell, see Section 3.2. For PM_{10} , the reanalysis model results of EURAD-IM, CHIMERE and LOTOS-EUROS are used for both years. For ozone, the reanalysis model results of EURAD-IM, CHIMERE, LOTOS-EUROS and MOCAGE are used for both years, and for 2010 additionally the reanalysis model results of SILAM.

In this section we try to illustrate of how the ETC/ACM mapping results compare to MACC-II Ensemble reanalysis results. As such, this section presents the maps of MACC-II Ensemble reanalysis results. Next to this, we execute an initial comparison of the ETC/ACM mapping results with the MACC-II Ensemble reanalysis results, using statistical indicators and scatter plots. We compare:

- a) MACC-II Ensemble reanalysis results,
- b) ETC/ACM mapping results, using (i) EMEP and (ii) MACC-II Ensemble hindcast,

Section 5.2.1 deals with PM_{10} and Section 5.2.2 with ozone. Annex 6 provides all related scatter plots.

5.2.1 PM₁₀

Maps

Figures 5.7 and 5.8 show the MACC-II Ensemble reanalysis results for PM₁₀ indicators annual average and 36th highest daily mean, for 2009 and 2010. All the reanalysis results are presented in a 10x10 km² grid resolution (see Section 3.2).

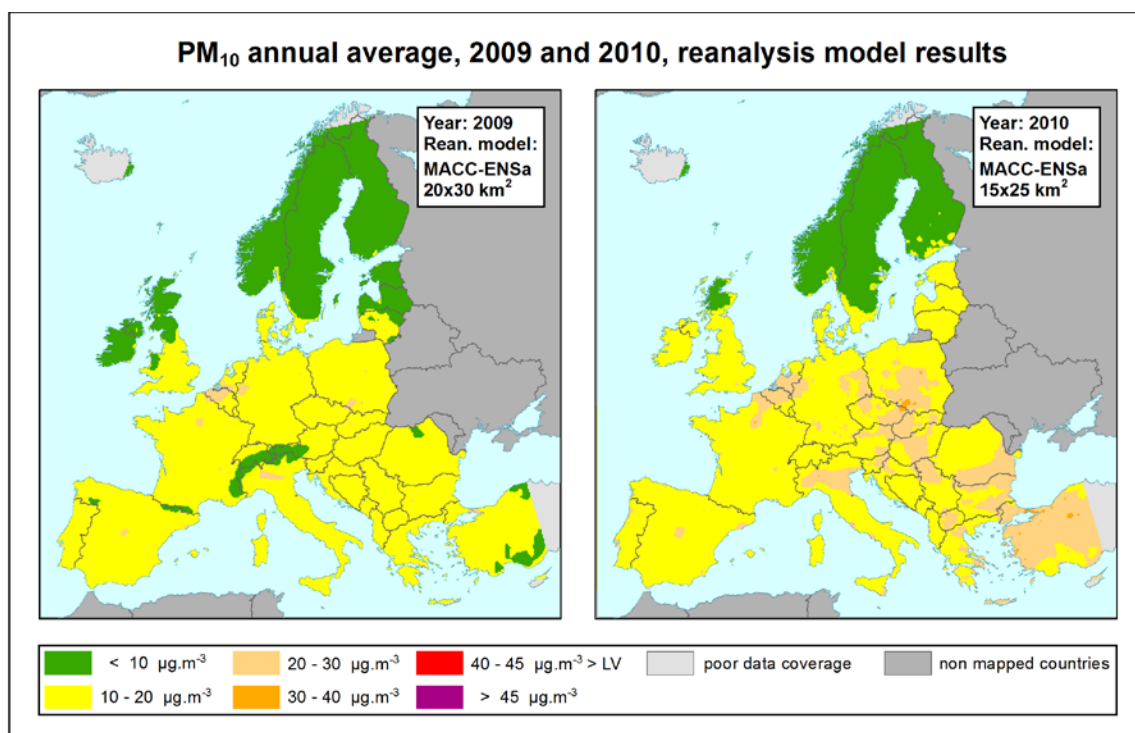


Figure 5.7 PM₁₀ annual average for 2009 (left) and 2010 (right), MACC-II Ensemble reanalysis model results

The concentration level of these results is higher than for MACC-II Ensemble hindcast (i.e. without data assimilation), see Annex 4, Figures A4.1 to A4.4.

It can be stated that the reanalysis results for PM₁₀ provide a reduced level of underestimation – compared to the hindcast results – with respect to observations. This is confirmed by scatter plots that compare the MACC-II Ensemble hindcast output (Annex 5, Figures A5.1 to A5.8, upper right scatter plots) and the MACC-II Ensemble reanalysis results (Annex 6, Figures A6.1 to A6.8, upper left scatter plots) with the measurement data.

Still, compared to the observations the MACC-II Ensemble reanalysis results underestimate PM₁₀ in both 2009 and 2010, see below, Tables 5.1 and 5.2. However, the level of underestimation is smaller in 2010 compared to 2009.

Furthermore, by comparing the MACC-II Ensemble reanalysis maps (Figures 5.7 and 5.8) with the ETC/ACM mapping results (Figures 4.1 – 4.9) one can visually derive that the reanalysis results show lower concentration levels than the ETC/ACM maps.

The relation of these reanalysis results to the observations is shown by means of statistical indicators and scatter plots.

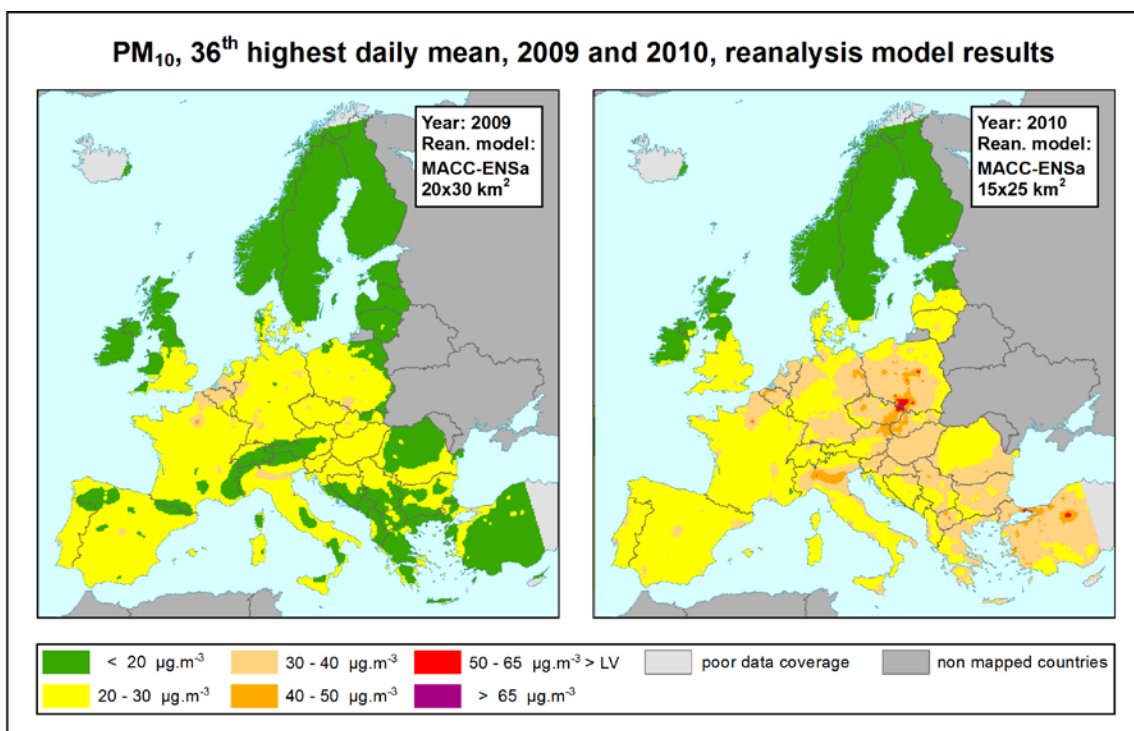


Figure 5.8 PM_{10} indicator 36th highest daily mean for 2009 (left) and 2010 (right), MACC-II Ensemble reanalysis model results

Statistical indicators

The agreement of the MACC-II Ensemble reanalysis results with the measured values has been analysed and compared with the results of the ETC/ACM mapping technique, using either EMEP or MACC-II Ensemble hindcast models, separately for the rural and urban background areas, using scatter plots and statistical indicators (as described in Section 3.3). This comparison is only initial or preliminary: a proper comparison would be based on an exclusive consideration of those stations that were not used in the reanalysis. However, it cannot be easily done, because MACC-II uses a random system to choose the stations to be used for validation every day. Thus, both stations used and not used in the reanalysis are employed in the comparison. Based on this, a following approach for preliminary comparison has been chosen: the scatter plots and statistical indicators of reanalysed data are compared not only with the cross-validated, but also with the non-cross-validated (or simple) scatter plots and indicators of ETC/ACM mapping. One may assume that the results (i.e. scatter plots and statistical indicators), which would actually correspond to the results of the reanalysis, could be found anywhere “in between” the two results (cross-validated and simple) of the ETC/ACM mapping exercise. In fact, the cross-validated scatter plots show the interpolated data against the measurement data that are not used in this interpolation, while the simple scatter plots show the interpolated data against the measurement data used in the interpolation.

In the reanalysis, rural and urban/suburban background stations are handled together. Thus, the reanalysed model result aims to represent both the rural and urban background air quality. Contrary to this, in the ETC/ACM mapping the rural and urban background air quality is estimated separately (at the $10 \times 10 \text{ km}^2$ resolution). The rural and urban background maps are merged together at the $1 \times 1 \text{ km}^2$ resolution, which is considered to capture better the differences between the rural and the urban background areas than when merging at the $10 \times 10 \text{ km}^2$ resolution, see Horálek et al. (2010).

The scatter plots and statistical indicators for the ETC/ACM mapping are compiled primarily for the separate rural and background maps. Additionally and for the mapping procedure using EMEP model only, the scatter plots and indicators for the merged map in 1x1 km² resolution are also prepared. (However, for capacity and computational reasons, only simple non-cross-validated scatter plots and the relevant indicators are prepared.) There are two reasons for this additional exercise: first, these maps represent both the rural and urban air quality and are in this sense directly comparable with the reanalysed model output (although in different resolution). Second, by comparing the scatter plots and the statistical indicators of the merged and the separate rural, resp. urban background maps, one can assess how the urban and rural areas are represented in the merged map. Knowing this, we can assess how the separate ETC/ACM rural and urban background maps compare to the MACC-II Ensemble reanalysis results.

In Tables 5.1 and 5.2 the statistical indicators for PM₁₀ are presented for 2009 and 2010, separately for the rural and the urban background areas. For the rural areas, the map results are related to the measurement data from the rural background stations, while for the urban background areas, the map results are related to the urban and suburban background stations.

Table 5.1 Comparison of statistical indicators for the MACC-II Ensemble reanalysis model and the ETC/ACM interpolation with the use of different dispersion models outputs – PM₁₀, 2009

	PM ₁₀ annual average, 2009							
	rural				urban background			
	RMSE	bias	R ²	regr. equation	RMSE	bias	R ²	regr. equation
MACC-ENS reanalysis	6.7	-4.0	0.43	y = 0.278x + 9.8	13.3	-10.5	0.11	y = 0.115x + 13.3
ETCACM_EMEP separ. (r or ub), c.-v.	4.6	0.4	0.55	y = 0.574x + 8.5	5.0	0.1	0.67	y = 0.682x + 8.6
ETCACM_EMEP separate (r or ub)	3.3	-0.2	0.78	y = 0.679x + 5.9	3.8	-0.2	0.81	y = 0.747x + 6.6
ETCACM_EMEP final merged 1x1 km	3.2	0.3	0.79	y = 0.709x + 5.9	4.4	-0.6	0.75	y = 0.723x + 6.9
ETCACM_MACC-ENS separate, c.-v.	4.5	0.2	0.57	y = 0.628x + 7.3	4.9	0.1	0.67	y = 0.682x + 8.6
ETCACM_MACC-ENS separate	3.0	-0.2	0.81	y = 0.742x + 4.7	3.7	-0.2	0.83	y = 0.754x + 6.4
	PM ₁₀ 36 th highest daily mean, 2009							
	rural				urban background			
	RMSE	bias	R ²	regr. equation	RMSE	bias	R ²	regr. equation
MACC-ENS reanalysis	12.8	-8.1	0.34	y = 0.228x + 17.2	25.6	-19.2	0.03	y = 0.054x + 24.0
ETCACM_EMEP separ. (r or ub), c.-v.	7.9	0.6	0.59	y = 0.593x + 13.8	9.4	0.2	0.70	y = 0.691x + 14.3
ETCACM_EMEP separate (r or ub)	5.4	-0.3	0.81	y = 0.704x + 9.3	7.3	-0.5	0.82	y = 0.748x + 11.0
ETCACM_EMEP final merged 1x1 km	5.2	0.5	0.82	y = 0.729x + 9.3	8.1	-1.1	0.78	y = 0.730x + 11.3
ETCACM_MACC-ENS separate, c.-v.	7.4	0.4	0.61	y = 0.644x + 12.1	9.3	0.2	0.70	y = 0.696x + 14.1
ETCACM_MACC-ENS separate	4.1	-0.3	0.89	y = 0.799x + 6.3	6.8	-0.4	0.85	y = 0.768x + 10.2

In the tables, the statistical indicators (i.e. RMSE, bias, R², parameters of regression equation, see Section 3.3) show the agreement of MACC-II Ensemble reanalysis and ETC/ACM mapping results with the measurement data for rural and urban/suburban background stations separately. For MACC-II Ensemble reanalysis, its results are related to the measurement data in a simple way, without taking into account which stations were used in the reanalysis (see above). For the ETC/ACM maps using either EMEP or MACC-II Ensemble hindcast, on the one hand the cross-validated results and on the other hands the simple non-cross-validated results are related to the measurement data, with rural maps to rural stations data, urban background maps to urban/suburban background stations data and all in the 10x10 km² resolution. Additional to that and for results of the ETC/ACM mapping using EMEP only,

the simple non-cross-validated result of the *final merged* ETC/ACM map in 1x1 km² resolution is related to the measurement data.

The slightly different set of stations used here and in the comparisons of Chapter 4 (see Table 3.2) causes slightly different cross-validation results for ETC/ACM mapping presented here and in Tables 4.1 and 4.2.

Table 5.2 Comparison of statistical indicators for the MACC-II Ensemble reanalysis model and the ETC/ACM interpolation with the use of different dispersion models outputs – PM₁₀, 2010

	PM ₁₀ annual average, 2010							
	rural				urban background			
	RMSE	bias	R ²	regr. equation	RMSE	bias	R ²	regr. equation
MACC-ENS reanalysis	4.6	-1.0	0.68	y = 0.442x + 10.0	10.3	-6.9	0.35	y = 0.259x + 13.1
ETCACM_EMEP separ. (r or ub), c.-v.	4.4	0.2	0.62	y = 0.646x + 7.2	5.1	-0.1	0.70	y = 0.725x + 7.4
ETCACM_EMEP separate (r or ub)	3.3	-0.3	0.80	y = 0.729x + 5.1	3.4	-0.2	0.87	y = 0.813x + 4.8
ETCACM_EMEP final merged 1x1 km	3.2	0.2	0.80	y = 0.755x + 5.0	4.0	-0.6	0.82	y = 0.793x + 5.0
ETCACM_MACC-ENS separate, c.-v.	4.4	0.3	0.62	y = 0.670x + 6.8	5.0	-0.1	0.71	y = 0.727x + 7.3
ETCACM_MACC-ENS separate	2.5	-0.1	0.89	y = 0.815x + 3.5	3.4	-0.2	0.87	y = 0.815x + 4.8
	PM ₁₀ 36 th highest daily mean, 2010							
	rural				urban background			
	RMSE	bias	R ²	regr. equation	RMSE	bias	R ²	regr. equation
MACC-ENS reanalysis	9.8	-3.9	0.70	y = 0.437x + 15.9	21.3	-14.2	0.37	y = 0.246x + 21.6
ETCACM_EMEP separ. (r or ub), c.-v.	8.4	0.2	0.64	y = 0.645x + 12.7	9.7	-0.2	0.75	y = 0.747x + 11.9
ETCACM_EMEP separate (r or ub)	6.0	-0.5	0.84	y = 0.740x + 8.7	6.7	-0.5	0.88	y = 0.819x + 8.1
ETCACM_EMEP final merged 1x1 km	6.0	0.2	0.83	y = 0.760x + 8.6	7.4	-1.1	0.86	y = 0.808x + 8.0
ETCACM_MACC-ENS separate, c.-v.	8.5	0.5	0.64	y = 0.665x + 12.4	9.7	-0.1	0.75	y = 0.761x + 11.3
ETCACM_MACC-ENS separate	4.7	-0.2	0.90	y = 0.814x + 6.3	6.1	-0.4	0.90	y = 0.844x + 7.0

The negative bias (which is given in µg.m⁻³) shows that the MACC-II Ensemble reanalysis is still underestimating the PM₁₀ levels, especially in the case of the urban background areas. This underestimation appears at both the annual average and the 36th highest daily mean. The underestimation is larger in 2009 than in 2010.

The ETC/ACM mapping method, using either the EMEP or the MACC-II Ensemble hindcast modelling results, gives at both the cross-validated and the simple scatter plots better, i.e. lower, RMSEs compared to the one of the MACC-II Ensemble reanalysis at both the annual average and the 36th highest daily mean, for both years.

When comparing the ETC/ACM final merged 1x1 km² map with the separate rural, resp. urban background map, one can analyse how the rural and urban background areas are represented in the final merged map and thus, how the indicators of the separate ETC/ACM rural and urban background maps are comparable to the MACC-II Ensemble reanalysis results. The results for the rural and final merged maps are almost the same, which indicates good representation of the rural areas in the final merged map. In the case of the urban background areas, the agreement is somewhat poorer, but both results (for the urban background and final merged maps) are still of a similar level when compared to the MACC-II Ensemble reanalysis results.

Scatter plots

As summarising illustration the scatter plots for PM₁₀ annual average for 2010 are presented in Figures 5.9 and 5.10. All PM₁₀ scatter plots for the years 2009 and 2010 are included in Annex 6, Figures A6.1 to A6.8.

The scatter plot comparison has been executed on the same set of mapping results as presented in Tables 5.1 and 5.2: the MACC-II Ensemble reanalysis scatter plot (upper left) is comparable to the cross-validated (centre) and simple (right) scatter plot of the ETC/ACM mapping results using either EMEP (top) or MACC-II Ensemble (bottom) model hindcast outputs, and it is comparable to the final merged 1x1 km² ETC/ACM map using EMEP output (lower left). Again, one may assume that the scatter plots, which would actually correspondent to the results of the MACC-II Ensemble reanalysis, could be found somewhere “in between” the cross-validated and the simple scatter plots of the ETC/ACM mapping results. Next to this, the simple scatter plot of the ETC/ACM final merged map (bottom left) can be compared on the one hand with the simple scatter plot of the separate ETC/ACM rural, resp. urban background map (top right), and on the other hand with the scatter plot of the MACC-II Ensemble reanalysis (top left).

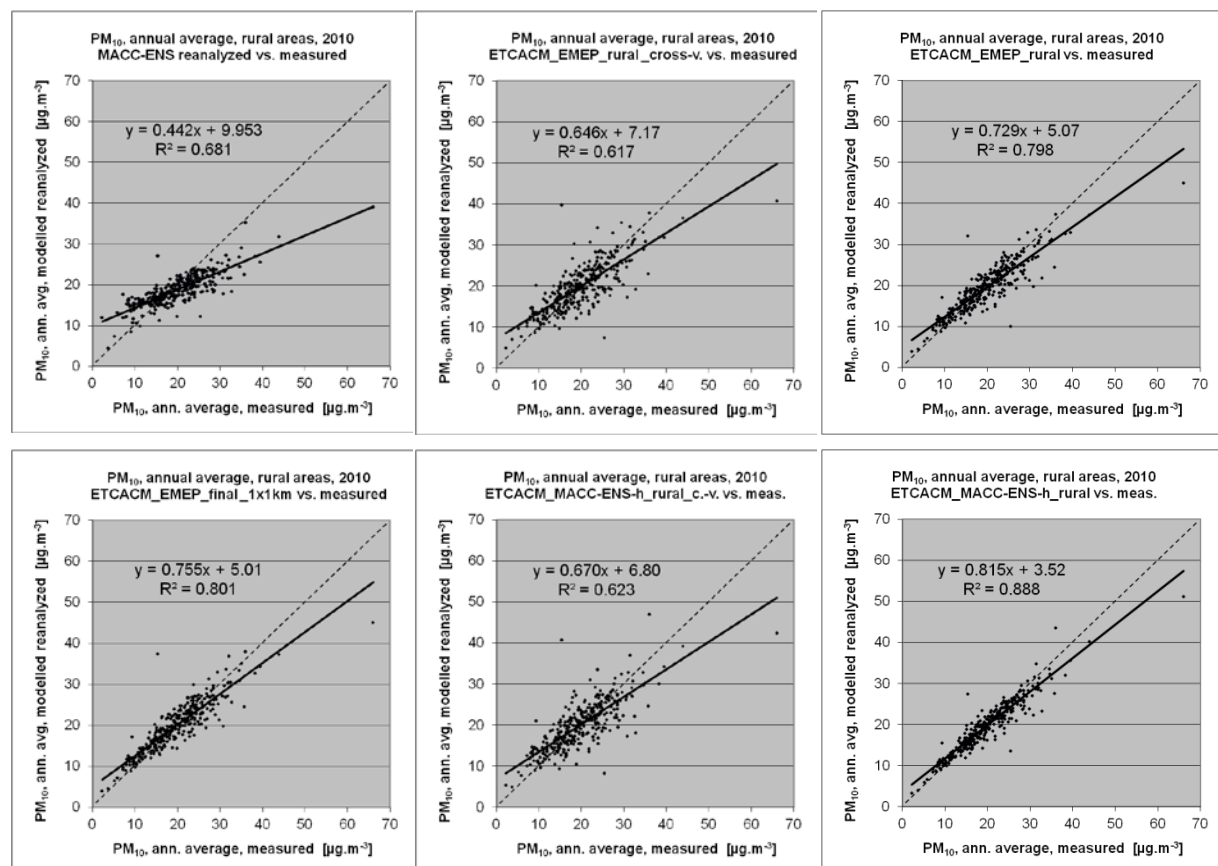


Figure 5.9 Scatter plots showing MACC-II Ensemble reanalysed vs. measurement data (upper left) versus ETC/ACM mapping using EMEP vs. measurement data using cross validation (upper middle) and simple comparison using rural (upper right) and final merged (lower left) map and ETC/ACM mapping using MACC-II Ensemble hindcast vs. measurement data using cross validation (lower middle) and simple comparison (lower right) for PM₁₀ annual average 2010 for rural background areas

In 2009, the MACC-II Ensemble reanalysis model does not reach the level of accuracy of the ETC/ACM mapping results, in the sense of R^2 (see Annex 6, Figures A6.1 to A6.4). The performance of the MACC-II Ensemble reanalysis improves considerably at the 2010 data (see Annex 6, Figures A6.5 to A6.8) in comparison with 2009 data. Part of the reason may be the application of a higher resolution of the MACC-II Ensemble, leading to an improvement of the factual output resolution from circa 20x30 km² to circa 15x25 km². Besides, it is expected that the maturity of the data assimilation schemes in the models used in MACC-II evolve over time, such that results from more recent years have improved compared to earlier calculations. In 2010, for rural areas, the MACC-II reanalysis result is quite comparable to the ETC/ACM mapping results in the sense of R^2 as one can derive from Figure 5.9, where R^2 for MACC-II Ensemble reanalysis result is in between the R^2 for the simple and cross-validated scatter plots of the ETC/ACM mapping. At the urban background areas this is not the case (Figure 5.10). However, the MACC-II Ensemble reanalysis results still underestimate reality as can be concluded from the low values of the slopes in the regression equations in Figures 5.9 and 5.10, and especially from the negative values of the bias as stated earlier at Table 5.2.

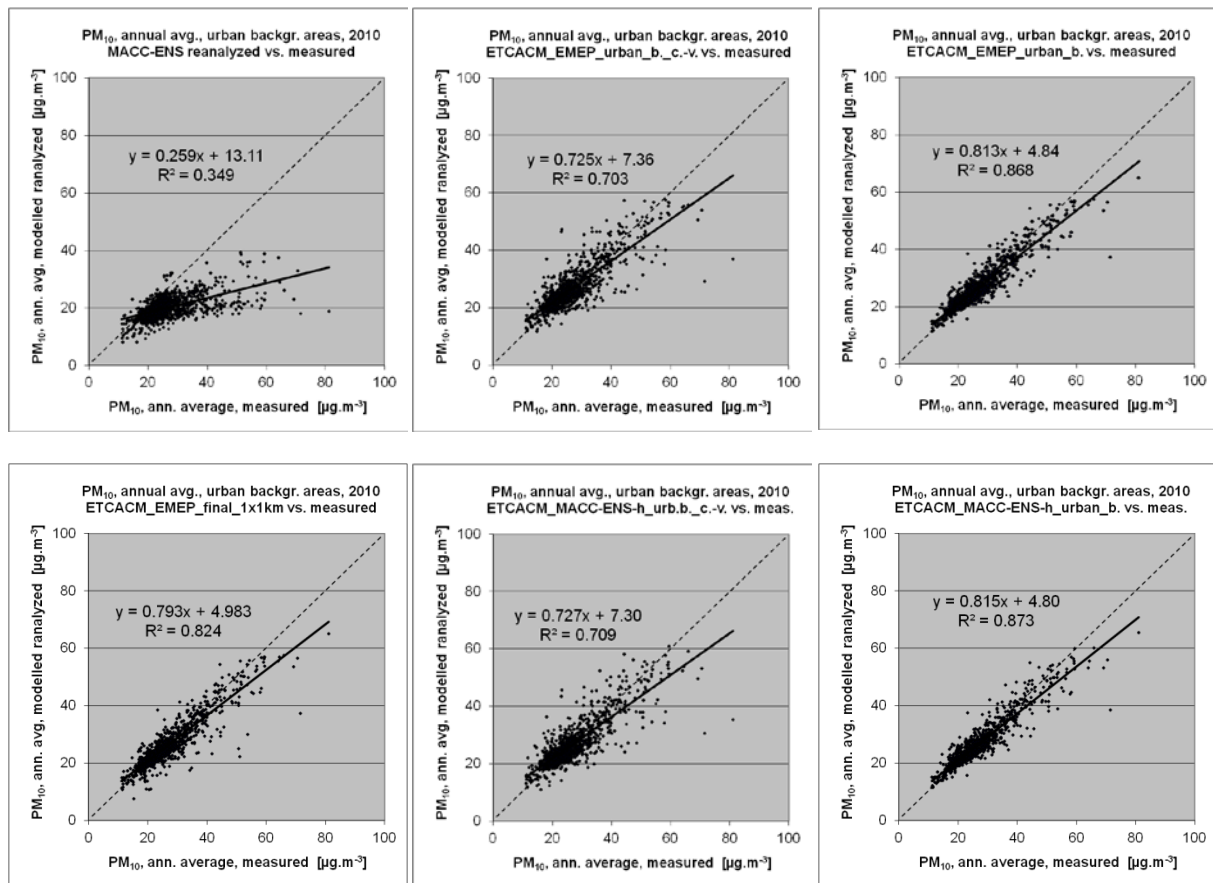


Figure 5.10 Scatter plots showing MACC-II Ensemble reanalysed vs. measurement data (upper left) versus ETC/ACM mapping using EMEP vs. measurement data using cross validation (upper middle) and simple comparison using urban background (upper right) and final merged (lower left) map and ETC/ACM mapping using MACC-II Ensemble hindcast vs. measurement data using cross validation (lower middle) and simple comparison (lower right) for PM₁₀ annual average 2010 for urban background area

Conclusion

In general, the ETC/ACM mapping gives better results than the MACC-II Ensemble reanalysis (lower RMSE, bias closer to zero). This is probably due to the nature of the reanalysis: most of the data assimilation methods require an unbiased model for effective use, however all models of PM₁₀ underestimate its concentration level and therefore reanalysis results for PM₁₀ are worse than what can be obtained using residual kriging approaches (Denby et al., 2008).

5.2.2 Ozone

Maps

A similar analysis as for PM₁₀, was done for ozone. In Figures 5.11 and 5.12 the results of MACC-II Ensemble reanalysis are presented for 2009 and 2010. All the results are presented in a 10x10 km² grid resolution.

Obvious are the lower concentration levels in the mountainous areas (e.g. Alps), compared to the results as calculated with the ETC/ACM mapping method using either the EMEP model or the MACC-II Ensemble hindcast (26th highest max 8-hr daily resp. SOMO35: upper rows of Figures 4.10 – 4.11, resp. Figures 4.12 – 4.13 for 2009; Figures 4.14 – 4.15, resp. Figures 4.16 – 4.17 for 2010). It should be noted that the ETC/ACM mapping involve next to the chemical transport modelling results also altitude as additional supplementary data (see Annex 1, Tables A1.4 to A1.6). Measurement data show in general increased ozone concentrations in higher located areas.

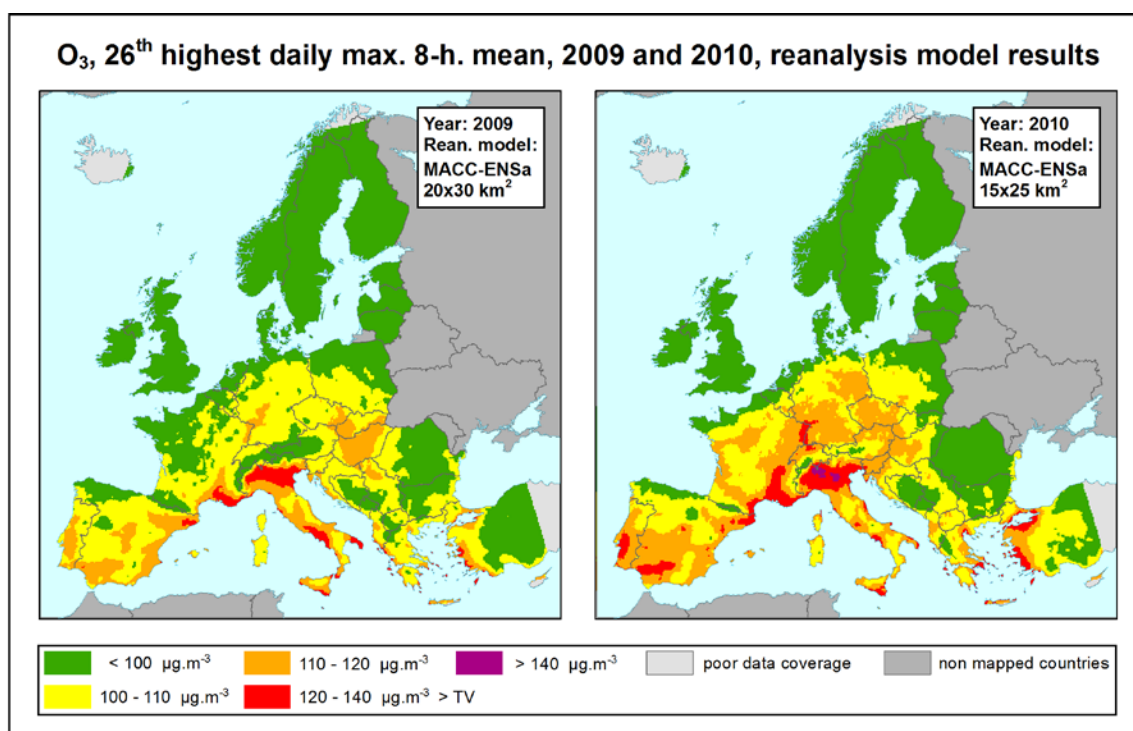


Figure 5.11 Ozone indicator 26th highest daily max. 8-hourly mean for 2009 (left) and 2010 (right), MACC-II Ensemble reanalysis model results

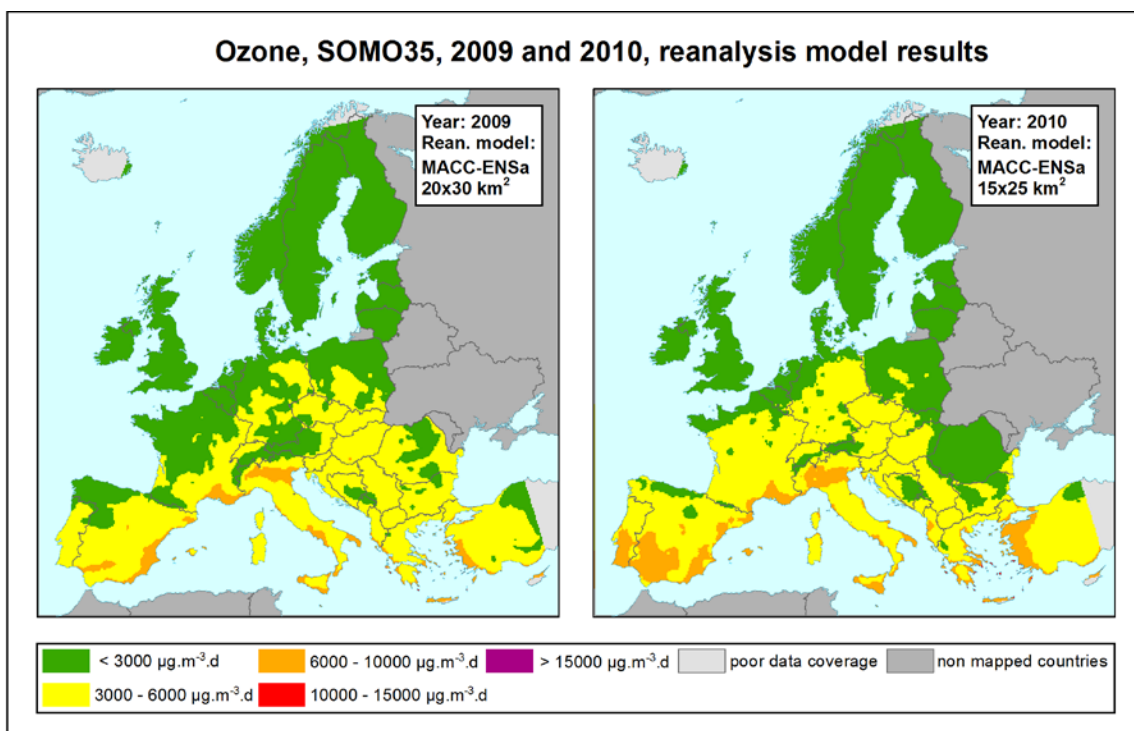


Figure 5.12 Ozone indicator SOMO35 for 2009 (left) and 2010 (right), MACC-II Ensemble reanalysis model results

Statistical indicators

In Tables 5.3 and 5.4, the statistical indicators for ozone are presented for 2009 and 2010. For the rural areas, the maps are related to the measurement data from the rural background stations, while for the urban background areas, the maps are related to the measurement data from the urban and suburban background stations. The same comparisons as for PM_{10} are presented.

The bias shows that the MACC-II Ensemble reanalysis underestimates the concentration levels. However, the level of underestimation is smaller than in the case of PM_{10} . Contrary to PM_{10} , the underestimation is larger at the rural than at the urban background air quality results. This is in agreement with the character of ozone air quality, i.e. its higher concentration levels in rural than in urban areas. This underestimation appears at both the 26th highest daily 8-hourly maximum and the SOMO35, both in 2009 and 2010. The level of the underestimation is smaller in 2010 than in 2009, but the improvement is not as large as in the case of PM_{10} .

Applying either EMEP or MACC-II Ensemble hindcast modelling output in the ETC/ACM mapping procedure, its results give at both the cross-validated and the simple scatter plots better RMSE compared to the one of the MACC-II Ensemble reanalysis in the rural areas and in 2009 also in the urban background areas. At the urban background areas in 2010, the MACC-II Ensemble reanalysis results give comparable RMSE to the ETC/ACM mapping results (i.e. lying in between their RMSE for cross-validation and simple validation).

The bias for MACC-II Ensemble reanalysis is worse compared to the ETC/ACM mapping at both the rural areas and urban background areas, for both years.

Table 5.3 Comparison of statistical indicators for the MACC-II Ensemble reanalysis model and the ETC/ACM interpolation with the use of different dispersion models outputs – ozone, 2009

	Ozone, 26 th highest daily 8-hourly maximum, 2009							
	rural				urban background			
	RMSE	bias	R ²	regr. equation	RMSE	bias	R ²	regr. equation
MACC-ENS reanalysis	14.5	-11.1	0.59	y = 0.590x + 35.8	11.3	-6.1	0.63	y = 0.595x + 38.8
ETCACM_EMEP separ. (r or ub), c.-v.	8.2	0.0	0.69	y = 0.722x + 31.9	9.3	0.1	0.64	y = 0.669x + 36.7
ETCACM_EMEP separate (r or ub)	6.0	-0.1	0.83	y = 0.793x + 23.6	6.6	0.1	0.83	y = 0.762x + 26.5
ETCACM_EMEP final merged 1x1 km	6.4	-0.8	0.82	y = 0.765x + 26.1	7.4	0.4	0.78	y = 0.741x + 29.2
ETCACM_MACC-ENS separate, c.-v.	7.8	0.0	0.73	y = 0.729x + 31.0	9.1	0.1	0.66	y = 0.680x + 35.5
ETCACM_MACC-ENS separate	6.7	0.0	0.79	y = 0.765x + 26.9	6.7	0.1	0.82	y = 0.767x + 25.9

	Ozone, SOMO35, 2009							
	rural				urban background			
	RMSE	bias	R ²	regr. equation	RMSE	bias	R ²	regr. equation
MACC-ENS reanalysis	2854	-2088	0.48	y = 0.418x + 1104	1749	-940	0.62	y = 0.548x + 1073
ETCACM_EMEP separ. (r or ub), c.-v.	1610	5	0.64	y = 0.655x + 1899	1475	-1	0.62	y = 0.621x + 1688
ETCACM_EMEP separate (r or ub)	1364	-2	0.74	y = 0.708x + 1601	1215	-3	0.74	y = 0.687x + 1393
ETCACM_EMEP final merged 1x1 km	1360	-195	0.75	y = 0.695x + 1477	1309	103	0.70	y = 0.688x + 1492
ETCACM_MACC-ENS separate, c.-v.	1551	-14	0.67	y = 0.673x + 1784	1454	-3	0.63	y = 0.637x + 1613
ETCACM_MACC-ENS separate	1468	-11	0.70	y = 0.690x + 1689	1167	2	0.76	y = 0.710x + 1293

Table 5.4 Comparison of statistical indicators for the MACC-II Ensemble reanalysis model and the ETC/ACM interpolation with the use of different dispersion models outputs – ozone, 2010

	Ozone, 26 th highest daily 8-hourly maximum, 2010							
	rural				urban background			
	RMSE	bias	R ²	regr. equation	RMSE	bias	R ²	regr. equation
MACC-ENS reanalysis	11.4	-7.5	0.71	y = 0.691x + 28.3	8.4	-3.1	0.79	y = 0.745x + 25.5
ETCACM_EMEP separ. (r or ub), c.-v.	8.9	0.2	0.69	y = 0.721x + 32.5	9.1	0.0	0.71	y = 0.727x + 30.7
ETCACM_EMEP separate (r or ub)	3.7	0.0	0.95	y = 0.887x + 13.2	7.3	0.0	0.82	y = 0.783x + 24.4
ETCACM_EMEP final merged 1x1 km	5.1	-0.2	0.90	y = 0.846x + 17.6	7.8	0.5	0.79	y = 0.772x + 26.1
ETCACM_MACC-ENS separate, c.-v.	8.9	0.1	0.68	y = 0.727x + 31.8	9.1	0.0	0.71	y = 0.734x + 30.0
ETCACM_MACC-ENS separate	3.9	0.0	0.94	y = 0.883x + 13.6	7.1	0.1	0.83	y = 0.794x + 23.2

	Ozone, SOMO35, 2010							
	rural				urban background			
	RMSE	bias	R ²	regr. equation	RMSE	bias	R ²	regr. equation
MACC-ENS reanalysis	2432	-1639	0.53	y = 0.474x + 1211	1194	-570	0.77	y = 0.708x + 688
ETCACM_EMEP separ. (r or ub), c.-v.	1582	18	0.63	y = 0.652x + 1906	1271	6	0.65	y = 0.667x + 1441
ETCACM_EMEP separate (r or ub)	987	9	0.86	y = 0.786x + 1170	1023	5	0.78	y = 0.733x + 1158
ETCACM_EMEP final merged 1x1 km	1069	-133	0.84	y = 0.757x + 1183	1148	112	0.72	y = 0.734x + 1259
ETCACM_MACC-ENS separate, c.-v.	1566	15	0.64	y = 0.663x + 1843	1272	5	0.65	y = 0.666x + 1445
ETCACM_MACC-ENS separate	902	7	0.89	y = 0.809x + 1041	1035	6	0.77	y = 0.729x + 1174

For the MACC-II Ensemble reanalysis, the agreement with the measurement data is better in the case of the urban background areas (lower RMSE, lower bias and higher R²) than in the case of the rural areas. This is probably caused by the fact that in the reanalysis, both rural and urban/suburban background stations are handled together, while the number of the urban/suburban stations is double so high as the number of the rural background stations.

By comparing the ETC/ACM final merged map at the resolution of 1x1 km² with the separate rural, resp. urban map one can see how the rural and urban background areas are represented in the final merged map. The results for the rural and final merged maps are quite similar, which indicates good representation of the rural areas in the final merged map. In the case of the urban background areas, the agreement is somewhat poorer, but both results (for the urban background and final merged maps) are still of a similar level when compared to the MACC-II Ensemble reanalysis results.

Scatter plots

The scatter plots for ozone indicator SOMO35 for 2010 are presented in Figures 5.13 and 5.14. Annex 6, Figures A6.9 to A6.16 provide all ozone scatter plots of the years 2009 and 2010.

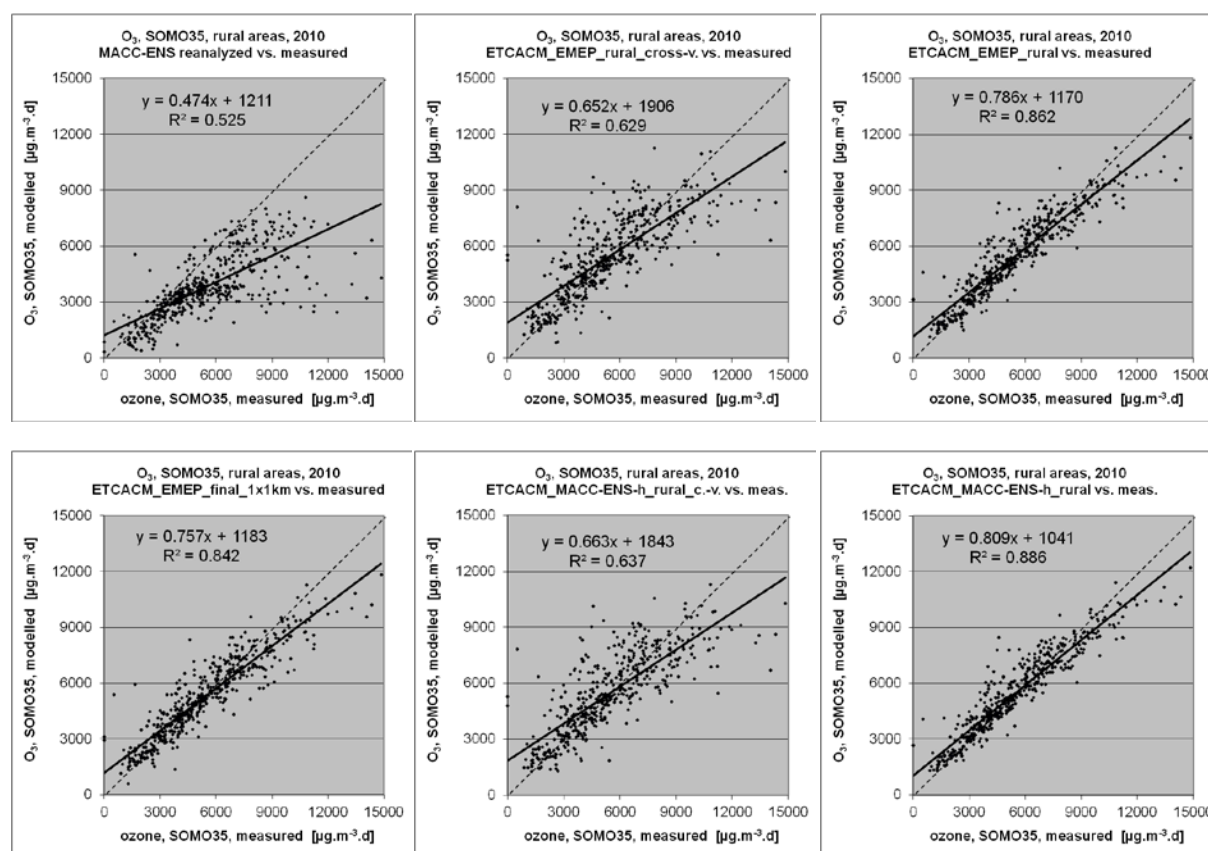


Figure 5.13 Scatter plots showing MACC-II Ensemble reanalysed vs. measurement data (upper left) versus ETC/ACM mapping using EMEP vs. measurement data using cross validation (upper middle) and simple comparison using rural (upper right) and final merged (lower left) map and ETC/ACM mapping using MACC-II Ensemble hindcast vs. measurement data using cross validation (lower middle) and simple comparison (lower right) for ozone indicator SOMO35 for 2010 for rural background areas

In 2009, the reanalysis model does not reach the level of accuracy of the ETC/ACM mapping results, in the sense of R^2 (see Annex 6, Figures A6.9 to A6.12). The performance of the

MACC-II Ensemble reanalysis improves at the 2010 data (see Annex 6, Figures A6.13 to A6.16) in comparison with 2009 data.

In 2010, the ETC/ACM mapping results show better R^2 than the MACC-II reanalysis results in the rural areas (Figure 5.13), while in the urban background areas (Figure 5.14) these results are quite similar, where R^2 for MACC-II Ensemble reanalysis result is in between the R^2 for the simple and cross-validated scatter plots of ETC/ACM mapping. However, the MACC-II Ensemble reanalysis results still underestimate reality, in both rural and urban background areas as can be concluded from quite low values of the slopes and the intercepts in the regression equations in Figures 5.13 and 5.14, and especially from the negative values of the bias as stated earlier at Table 5.4.

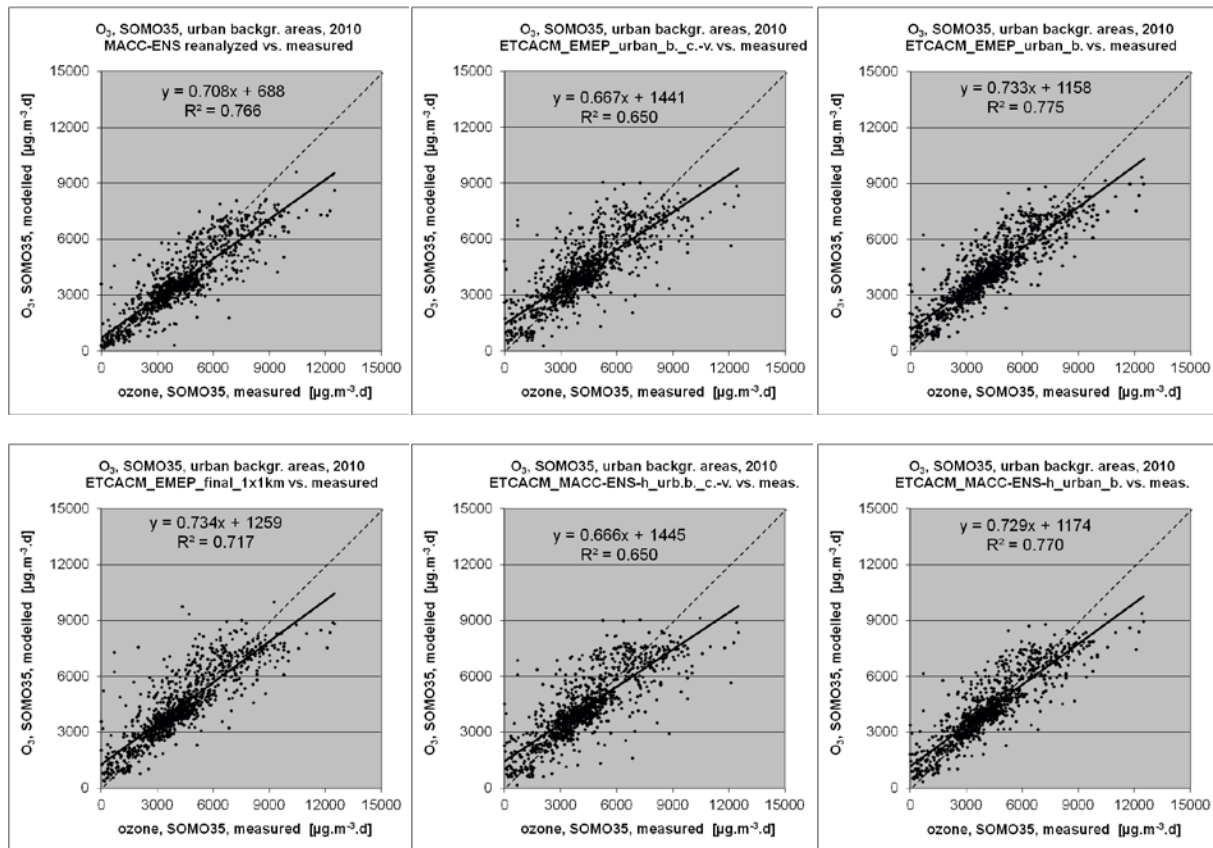


Figure 5.14 Scatter plots showing MACC-II Ensemble reanalysed vs. measurement data (upper left) versus ETC/ACM mapping using EMEP vs. measurement data using cross validation (upper middle) and simple comparison using urban background (upper right) and final merged (lower left) map and ETC/ACM mapping using MACC-II Ensemble hindcast vs. measurement data using cross validation (lower middle) and simple comparison (lower right) for ozone indicator SOMO35 for 2010 for urban background areas

Conclusion

In general, the ETC/ACM mapping gives better results than the MACC-II Ensemble reanalysis (lower RMSE, bias closer to zero), although the difference is not as prominent as in the case of PM_{10} at Section 5.2.1.

6 Recommendations

The main purpose of this report was to identify whether the use of the MACC-II ensemble model products could improve the results obtained from the current ETC/ACM mapping methodology that so far uses EMEP 50x50 km² modelling output as supplementary data source. An additional and related task is to provide recommendations for the future operational use of spatial interpolation techniques at EEA through its ETC/ACM.

The identified improvement of the performance of the ETC/ACM mapping results when using the MACC-II Ensemble model is a necessary condition to consider a possible change in the routine mapping operations. However, in order to recommend a possible change for future operational mapping routines at EEA, further evaluation is required.

In this chapter, we evaluate the capabilities for further use of the MACC-II Ensemble model in ETC/ACM mapping routines. In the following, a list of general requirements concerning the capabilities dispersion models should have in order to be useful for the ETC/ACM mapping activities is presented. The requirements are evaluated for the EMEP model, which is currently used in the operational ETC/ACM mapping routines, and for the MACC-II Ensemble model, as a possible candidate for future operational use. Subsequently, specific requirements for the MACC-II Ensemble dataset are listed. These specific requirements need to be fulfilled in order to consider the use of the MACC-II Ensemble model operationally for the routine ETC/ACM mapping. Finally, a series of recommendations are provided on how ETC/ACM mapping work may be evolving in future years.

6.1 *General requirements for models used in ETC/ACM mapping*

In order to be used regularly within the ETC/ACM mapping routines a series of general requirements need to be fulfilled by the chemical transport models used as input to the system.

The most important additional requirement is the **long-term sustainability** of the modelled data. Since the mapping activities at ETC/ACM support EEA assessments on the status of air quality in Europe, the modelling input data needs to be regularly available and of sound quality. ETC/ACM mapping has relied up to now on EMEP modelling data, provided under the UNECE Convention of Long-range Transboundary Air Pollution (CLRTAP). The long-term sustainability of the UNECE program has guaranteed the availability of the modelling results as well as a product evolution to maintain its soundness and accuracy. On the other hand, the MACC-II ensemble products relate to the pre-operational phase of the future Copernicus Atmospheric Services. The long-term availability of the MACC-II products and their product evolution is linked to the long-term sustainability of the Copernicus programme. The long-term funding of the Copernicus Programme is established by the Copernicus Regulation that was approved by the Commission on 12 July 2013 and has been submitted to the Parliament, where it has been adopted on 12 March 2014, and to the European Council. Thus, in terms of long-term sustainability the two choices are considered to be comparable and notably superior to any individual modelling choice supported via national and/or research funding.

The next requirement is with respect to the **robustness** of the modelled results and their proven **accuracy**. The EMEP model has a long-term record of documented accuracy, with regular reports on the performance of the Unified EMEP model available for the least 10 years. The robustness of the EMEP model is related to its documented accuracy over many different regions in Europe and for different meteorological conditions. The EMEP model is one of the seven models presently included in the MACC-II Ensemble (although in the simplified ‘MACC’ version, not in the ‘research’ version, see model dossiers, MACC, 2013). The superiority of the performance of a model ensemble for air quality purposes with respect to any of its individual model components is widely supposed in the scientific literature (see for example Galmarini et al, 2013; Vautard et al, 2009; Galmarini et al, 2004). However, tests in Rouil (2011a, 2011b, 2012a, 2013) that are based on MACC-II Ensemble *reanalysis* provide best results for ozone, but not for PM₁₀ (see Figure 2.2). Furthermore, when MACC-II Ensemble *hindcasts* are considered, their test results show in Figure 2.2 not to be the best at both PM₁₀ and ozone. In addition, our comparison results in Chapter 5 do not support that ‘superiority’ when at the hindcasts as for PM₁₀ at urban areas the EMEP model seems to perform slightly better than MACC-II Ensemble, however, both do perform at that case rather poor in general. A further aspect of robustness concerns the vulnerability of the system itself. The ensemble approach adopted in MACC-II provides additional robustness to the results of the system. This is because the ensemble relies on a number of models and individual problems or failures with one component of the system do not affect the availability of the ensemble results. In the case of the EMEP model, the use of an individual model allows for certain degree of vulnerability in case of unexpected problems in the production of the results.

ETC/ACM mapping requires **methodologically consistency** of the chemical transport model used in the mapping method. The main purpose of the use of dispersion modelled results in ETC/ACM mapping routine is to provide additional consistent and reliable support in ‘grasping’ the complex information of the spatial distribution of air quality across the whole area, with no regard to the actual level of the concentrations. Thus, a consistency of modelled results across the whole mapping domain is needed. EMEP model provides consistent results for the whole mapping domain, whereas in the MACC-II Ensemble the concentration values in different grid cells and different time steps are estimated by different models.

The **availability** of the results is an essential requirement for their use in ETC/ACM mapping routines. Both the EMEP and the MACC-II modelling results are open and freely available. Regular updates are available every year for data corresponding to two years prior, both for EMEP and for the MACC-II Ensemble model results. The reason for the two years delay is the availability of updated emission and validated observation data. The MACC-II consortium is presently considering the introduction of an interim reanalysis report based on available non-validated data one year arrear. This is because the MACC-II Ensemble relies on up-to-date observational data for their analyses in an operational manner and thus it can allow for an additional interim report with up-to-date non-validated data. If such an interim report becomes a reality, the MACC-II Ensemble will have a considerable advantage with respect to the research version of EMEP in terms of the timeliness of the data.

The **spatial resolution** of the model data is of relevance for the mapping activities at urban background level when the model resolution is finer than 10x10 km². Differences between the EMEP model resolution at 50x50 km² and the MACC-II Ensemble with 20x30 km² or 15x25 km² do not significantly affect the spatial interpolation results for rural and urban background mapping. However, the fact that the MACC-II Ensemble has adopted a 0.1°x0.1°

(i.e. circa 10x10 km²) as target spatial resolution will imply in the future a relevant improvement with respect to background mapping results, after this resolution is adopted by the entire set of individual models taking part in the ensemble. It can be argued that since the EMEP model is one of the MACC-II Ensemble components, results from the EMEP model may also be available at the same spatial resolution. The main difference will then be the corresponding validation of the results as the EMEP validation focus would possibly remain on the program's main focus: the regional scale.

Both the EMEP model and the MACC-II Ensemble evolve in time. New model and ensemble versions are expected regularly as part of the program or project/service driven product updates and evolution. In such evolution framework it is important to have established **model validation and documentation routines**. Both programs have mature routines to this regard, as corresponds to well-established operational services with many years of experience on numerical forecasting. In this respect, the two systems are very comparable as a consequence of their common origin in meteorological services. However, MACC-II products of its EVA subproject (i.e. hindcasts and reanalysis) are presently poorly documented. It is recommended to improve their documentation.

A summary of the evaluation of the general requirements to the models used in the ETC/ACM mapping routines is given in Table 6.1 for EMEP and the MACC-II Ensemble.

Table 6.1. General model requirements: overview comparison of the capabilities of the EMEP model versus the MACC-II Ensemble model

Model requirements	EMEP	MACC-II Ensemble
Sustainability	Long-term UNECE	Long-term Copernicus
Robustness	10 years' experience with Unified model	Ensemble approach
Accuracy	State of art chemical transport model	Similar level of performance as EMEP Better accuracy supposed in future due to higher spatial resolution
Methodological consistency	All the grid cells and the time steps calculated by the same methodology for the same grid.	Grid cell estimates originating from different models, each based on different time steps and on a different grid.
Timeliness Availability	Every year, two years arrears Y-2	Every year, two years arrears Y-2
Spatial resolution	50x50 km ²	15x25 km ² 10x10 km ² in the future
Model validation	Yearly evaluation reports + daily evaluation of forecasts as part of MACC-II	Yearly evaluation reports, daily evaluation of forecasts
Documentation	Scientific reviews, project and model documentation, scientific articles	Project and model documentation, scientific articles

There is an additional feature in the case of the MACC-II Ensemble *reanalysis* that differs from the EMEP model, the use of data assimilation techniques. However, the consequences or possible improvements of the use of data assimilation for the ETC/ACM mapping activities have not been evaluated in this report and it is not easy to determine at present how such feature may turn advantageous for mapping assessments.

The discussion above indicates that if the MACC-II Ensemble model is able to implement its intended, and in Section 6.2 suggested, improvements on the set of requirements, then it is preferable to the EMEP model with respect to robustness, accuracy and because of the use of finer spatial resolution. The EMEP model is preferable with regard to methodological consistency. The two model choices are similar in terms of long-term sustainability, validation routines, availability and documentation.

6.2 Specific requirements for MACC-II products

The use of the MACC-II ensemble products in this feasibility study has helped to identify a number of specific requirements to be addressed before any MACC-II product, either ensemble or individual model output, can be considered for operational use in ETC/ACM mapping routines. The essential requirements are:

1) Extension of the model domain

The northernmost and southernmost part of Europe is not yet included in the MACC-II modelling domain. The model domain needs to be extended to secure data availability for the purpose of ETC/ACM mapping routines.

2) Hindcast results as standard MACC-II products

Standard products from the regional MACC-II air quality service include 72h forecasts, daily analysed maps and yearly reanalyses using data assimilated results. The hindcast products used in this report are not included as standard products from MACC-II. These should be included as standard products to be readily available for users such as the EEA – ETC/ACM. It is suggested to use hindcast products for the purpose of spatial interpolation activities at ETC/ACM in order to avoid the problems with the double usage of the measurement data (once for reanalysis and then again for mapping). Alternatively, common methods used by all models in the ensemble for the identification of observational data to be used in data assimilation and data validation should be adopted.

Other requirements are:

3) Interim annual model data for Y-1

The planned interim delivery of Y-1 (hindcast and reanalysis) air pollution model data from the MACC-II regional team would be very valuable for the mapping assessments at ETC/ACM because it would allow the elaboration of timely reports half a year in advance from existing routines. The ETC/ACM mapping calculations could then start immediately after release of the annual update of the AirBase database. The ETC/ACM will therefore appreciate an official confirmation of the availability of these Y-1 modelling products (hindcast and reanalysis) from MACC-II.

4) Extension of observational basis

The MACC-II reanalysis products do not use all available AirBase observations, especially over Eastern Europe. As a consequence, one may presume that differences between modelled results and the mapping products are larger over areas in which the MACC-II reanalysis models use relative fewer observations than is available in AirBase. To enhance the quality of the reanalysis results it would be desirable that the MACC-II products make more extensive use of the available stations included in AirBase. It is recognized that activities to secure the use of all AirBase stations in MACC-II are underway and that the successful completion of such work could be beneficial also for the ETC/ACM mapping assessment work.

6.3 Recommendations for future ETC/ACM mapping assessments

The work reported in Chapter 4 shows that there is a general, although small, improvement in the ETC/ACM mapping results when using the MACC-II Ensemble model instead of the EMEP model as background dependent variable in the spatial interpolation calculations. Further, the evaluation of the general requirements for mapping assessments at ETC/ACM indicate that a change of chemical transport model could be beneficial in terms of robustness. Additional benefits are also expected in terms of accuracy of modelling results because of the future use of a higher spatial resolution in the MACC-II Ensemble (10x10 km²). The EMEP model is preferable with regard to methodological consistency. The EMEP model and the MACC-II Ensemble model are similar in terms of long-term sustainability, validation routines, documentation and timeliness. The conclusion from this analysis is that the ETC/ACM could consider adopting the MACC-II Ensemble model for the routine production of spatial mapping assessments.

However, the present feasibility study has also identified two essential and two other specific requirements to MACC-II (Section 6.2) that need to be in place before the ETC/ACM could routinely adopt any MACC-II product as model input for their spatial interpolation routines. Therefore, the ETC/ACM recommends to initiate a dialog with the MACC-II consortium in order to arrange and secure the required extension of the model domain, to arrange the routine access to annual hindcast results as standard products of MACC-II, to urge for reaching a systematic availability of Y-1 interim model results, and to recommend the extension of the observational basis.

In the meantime, it is recommended that testing the capabilities of the MACC-II products for ETC/ACM spatial interpolated mapping assessments should continue, either within MACC-II or within the ETC/ACM itself. In the first place, it is recommended to carry out further robustness tests of the use of the MACC-II Ensemble modelling results for different meteorological years since the present study was limited only to 2009 and 2010. The capability of the MACC-II Ensemble to improve the quality of the ETC/ACM mapping results needs to be assessed and confirmed for different years. It is also recommended to further investigate the capabilities of the MACC-II reanalysed results. An important prerequisite is that the MACC-II project needs to improve its documentation on the point of procedural and methodological steps within the preparation of MACC-II hindcast and reanalysis products, to allow a refined and confident statistical analysis and assessments of these products in the ETC/ACM mapping and other applications.

The present study has not considered the capabilities of data assimilated modelling results in the MACC-II for spatial mapping activities, since only hindcast products were analysed. An initial comparison presented here in Section 5.2 has shown the superiority of the ETC/ACM mapping with respect to MACC-II Ensemble data assimilated fields in cross-validation and validation results. However, the capabilities of the data assimilated results have not been fully assessed in this manner. It is strongly recommended to investigate possible ways to evaluate how the use of data assimilation techniques can strengthen the ETC/ACM mapping results and contribute to the study of uncertainties. In particular, it is recommended to further examine the use of 4D-Var data assimilated model for possible improvement of ETC/ACM mapping, for instance through the use of EURAD-IM (as a MACC-II product) as a representative of 4D-Var data assimilation technique. The additional reason for the examining of the EURAD-IM reanalysis results is that it provides the best results for PM₁₀ (Figure 2.2).

Furthermore, it would be of interest to evaluate how the use of satellite column observations could contribute to constrain the data assimilated fields in the vertical, providing an additional dimension to the evaluation of the existing 2D spatial interpolated fields. It would also be relevant for applications at national level to further evaluate the current ETC/ACM analysis of the probability of limit value exceedance. The current approach is only related to the spatial variability of air pollution levels, while other approaches considering also the temporal variability of the concentrations such as presented in Schneider et al. (2011) may be worth investigating.

7 Summary and Conclusions

Air quality mapping assessments at ETC/ACM are intended to provide reliable information on the status of air pollution in Europe. They do so by combining the best available information from observations and models through the use of spatial interpolation methods. The annual air quality mapping activities at ETC/ACM provide information of European rural and urban background air quality levels. This information is used, for example, for calculation of population exposure and health impacts estimates. It is also expected to support national environmental authorities in their evaluation of the contribution by long-range transported contributions to their pollution levels. It is also useful to establish the rural and urban background levels when carrying out studies on population exposure to air pollution. Current ETC/ACM mapping activities provide a unified methodology to estimate background pollution levels in the whole Europe and offer information on the probability of exceedance of limit or target values in different European areas with a spatial resolution of 10x10 km².

The quality of these mapping assessments relies primarily on the quality of the input data used, namely the quality of the observations being the primary data source, with support of chemical transport models and auxiliary information introduced in the spatial interpolation method. This report shows the potential capabilities of using MACC-II Ensemble model as input data to ETC/ACM mapping activities.

The current spatial interpolation method used at ETC/ACM is residual kriging. This is a linear regression method followed by kriging of its residuals. The linear regression currently uses AirBase measurement data as a dependent variable, while results from the EMEP chemical transport model and supplementary data such as altitude and meteorology are introduced as independent variables. The mapping is carried out separately for rural and urban background areas. The rural map is based on rural background stations from the AirBase database while the urban background map is based on urban and suburban background stations from the same database. The main difference between the rural and the urban background maps is therefore primarily determined by the classification of observation stations. It is a well-established fact that residual kriging results are largely driven by observations. Still, the choice of chemical dispersion model and the accuracy of its results, as well as the choices of auxiliary variables also have an impact in the spatial interpolated results.

This study compares the results provided by the ETC/ACM spatial interpolation methodology when using hindcast output from the EMEP and the MACC-II Ensemble models for two different years, 2009 and 2010. However, since the MACC-II ensemble products were available with two different spatial resolutions in 2009 and 2010, it was decided to include a third model in the comparison to evaluate better the effect of grid resolution of the dispersion model on ETC/ACM mapping results, namely the CHIMERE model as used in the EC4MACS project. The CHIMERE model has the advantage of having available results for two different spatial resolutions for the same year, 2009. In this way, the present study investigates the effect of spatial resolution in the results. The current ETC/ACM residual kriging methodology has thus been applied with a) the EMEP chemical transport model, b) the MACC-II Ensemble model, and c) the CHIMERE model as used in the EC4MACS project, in two different spatial resolutions.

The study has been carried out for the main indicators of PM₁₀ and ozone. For PM₁₀, mapping results for annual mean and 36th highest daily mean have been analysed. For ozone, mapping results have been analysed for the standard SOMO35 and the 26th highest daily maximum 8-hours mean. Different findings and conclusions can be summarized, as follows.

Conclusions concerning hindcast products

The mapping results are predominantly driven by the observations. Irrespective to the different concentration levels of the individual models, the ETC/ACM mapping results give similar concentration levels at each of the models used in the mapping procedure.

The performance of the spatial interpolation routines partially varies with the choice of chemical dispersion model. There is a general improvement in the cross-validation results when using the MACC-II Ensemble model instead of the EMEP model (Table 7.1 = Table 4.5).

Table 7.1 Summary comparison table of the use of MACC-II Ensemble and EMEP model outputs in the ETC/ACM mapping ('+' means better results of MACC-II Ensemble, '-' better results of EMEP, '0' the equal results)

Pollutant and indicator		2009		2010	
		rural	urban background	rural	urban background
PM ₁₀	annual average	+	+	+	+
	36 th highest daily mean	+	+	-	+
Ozone	26 th highest daily 8-h max.	+	+	-	+
	SOMO35	+	+	+	0

The improvement applies to both PM₁₀ and ozone indicators in 2009 and in most cases also in 2010. The improvement of the results appears to be primarily related to the higher spatial resolution of the MACC-II Ensemble. It should be noted, however, that these improvements by the different chemical dispersion model used are relatively modest. The most significant driver in the mapping of European pollution levels is the use of spatial interpolation methods that combines observational data as primary data source, with relevant information from chemical transport models and other supplementary data, such as altitude and meteorology as secondary data sources. The major differences in the ETC/ACM maps using output of different models as input are in those areas where measurement stations are lacking, especially if just the individual model outputs show there similar differences.

Additionally, the report shows the added value of the ETC/ACM mapping routines with respect to any of the chemical transport models used. The ETC/ACM mapping results are clearly driven by the observations and their statistics show that they provide a more appropriate description of the spatial distribution of PM₁₀ and ozone concentrations over Europe than any of the current state of art chemical dispersion models alone.

The analysis of the ETC/ACM mapping results shows that increasing the spatial resolution of the chemical dispersion model from 25-50 km down to 5-10 km has a significant effect in the quality of the results in the case of PM₁₀. The 50x50 km² resolution seems to be appropriate for regional scale dispersion transport calculations and the mapping results do not

significantly vary when the input model used have a resolution in the range between 50x50 km² and 25x25 km². These results are consistent with previous work from Denby et al (2011a). However, the higher spatial resolution outputs in 7x7 km² improve the rural background results from ETC/ACM mapping calculations. These results are consistent with the findings reported in Cuvelier et al. (2013) who report an improvement of the performance of chemical transport models in background calculations when the spatial resolution scale improves from 20-50 km down to 5-10 km.

This work shows that there is a general, although small, improvement in the ETC/ACM mapping results when using the MACC-II Ensemble model hindcast instead of the EMEP model as background dependent variable in the spatial interpolation calculations. Further, the evaluation of the general requirements for mapping assessments at ETC/ACM indicate that a change of chemical dispersion model could be beneficial in terms of robustness. Additional benefits are also expected in terms of accuracy of modelling results because of the future use of higher spatial resolution in the MACC-II Ensemble (10x10 km²). The EMEP model is preferable with regard to methodological consistency. The EMEP model and the MACC-II Ensemble model are similar in terms of long-term sustainability, validation routines, documentation and timeliness. The conclusion from this analysis is that the ETC/ACM could consider adopting the MACC-II Ensemble model for the routine production of spatial mapping assessments.

However, the present feasibility study has also identified two essential and two other specific requirements to MACC-II (Section 6.2) that need to be in place before the ETC/ACM could routinely adopt any MACC-II product as model input for their spatial interpolation routines. It is recommended to initiate a dialog with the MACC-II consortium in order to arrange and secure the required extension of the model domain, to arrange the routine access to hindcast results as standard products of MACC-II, to urge for reaching a systematic availability of the Y-1 interim model results, and to recommend the extension of the observational basis.

In the meantime, it is recommended that testing the capabilities of the MACC-II products for ETC/ACM spatial interpolated mapping assessments should continue, either within MACC-II or within the ETC/ACM itself. In the first place, it is recommended to carry out further robustness tests of the use of the MACC-II Ensemble model for different meteorological years since the present study was limited only to 2009 and 2010. The capability of the MACC-II Ensemble to improve the quality of the ETC/ACM mapping results needs to be assessed and confirmed for different years. It is also recommended to further investigate the capabilities of the MACC-II reanalysed results. An important prerequisite is that the MACC-II project needs to improve its documentation on the point of procedural and methodological steps within the preparation of MACC-II hindcast and reanalysis products.

Conclusions concerning reanalysis products

The present study has not considered the capabilities of data assimilated reanalysis model results in MACC-II for ETC/ACM spatial mapping, only hindcast products were analysed.

The initial comparison of ETC/ACM mapping and MACC-II Ensemble reanalysis results has shown the superiority of the spatial interpolation methods with respect to data assimilated fields: The ETC/ACM mapping gives better results than the MACC-II Ensemble reanalysis for both PM₁₀ and ozone (lower RMSE, bias closer to zero). The difference is more prominent in the case of PM₁₀. This is probably due to the nature of the reanalysis: most of the data assimilation methods require an unbiased model for effective use, however all

models of PM_{10} underestimate its concentration level and therefore reanalysis results for PM_{10} are worse than what can be obtained using residual kriging approaches.

However, the capabilities of the data assimilated results have not been fully assessed. It is strongly recommended to investigate possible ways to evaluate how the use of data assimilation techniques can strengthen the ETC/ACM mapping results and contribute to the study of uncertainties. In particular, it is recommended to further examine the use of 4D-Var data assimilated model for possible improvement of ETC/ACM mapping, for instance through the use of EURAD-IM (as a MACC-II product) as a representative of 4D-Var data assimilation technique.

References

- AirBase (2013). European air quality database. <http://airbase.eionet.europa.eu>
- Cressie N (1993). Statistics for spatial data. Wiley series, New York.
- Cuvelier C, Thunis P, Karam D, Schaap M, Hendriks C, Kranenburg R, Fagerli H, Nyiri A, Simpson D, Wind P, Schulz M, Bessagnet B, Colette A, Terrenoire E, Rouil L, Stern R, Graff A, Baldasano JM, Pay MT (2013). ScaleDep: Performance of European chemistry-transport models as function of horizontal spatial resolution. MSC-W Technical Report 1/2013, EMEP, Norway.
- Denby B, Horálek J, Walker SE, Eben K, Fiala J (2005). Interpolation and assimilation methods for European scale air quality assessment and mapping. Part I: Review and recommendations. ETC/ACC Technical paper 2005/7.
acm.eionet.europa.eu/reports/ETCACC_TechPaper_2005_7_spatial_AQ_interpol_Part_I
- Denby B, Schaap M, Segers A, Builtjes P, Horálek J (2008). Comparison of two data assimilation methods for assessing PM₁₀ exceedances on the European scale. *Atmospheric Environment* 42, pp. 7122–7134.
- Denby B, Cassiani M, de Smet P, de Leeuw F, Horálek J (2011). Sub-grid variability and its impact on European wide air quality exposure assessment. *Atmospheric Environment* 45, pp. 4220–4229.
- Denby B, Horálek J, de Smet P, de Leeuw F (2011c). Mapping annual mean PM_{2.5} concentrations in Europe: application of pseudo PM_{2.5} station data. ETC/ACM Technical Paper 2011/5.
http://acm.eionet.europa.eu/reports/ETCACM_TP_2011_5_spatialPM2.5mapping
- De Smet P, Horálek J, Coňková M, Kurfürst P, de Leeuw F, Denby B (2011). European air quality maps of ozone and PM₁₀ for 2008 and their uncertainty analysis. ETC/ACC Technical Paper 2010/10.
http://acm.eionet.europa.eu/reports/ETCACC_TP_2010_10_spatAQmaps_2008
- De Smet P, Horálek J, Schreiberová M, Kurfürst P, de Leeuw F (2012). European air quality maps of ozone and PM₁₀ for 2009 and their uncertainty analysis. ETC/ACM Technical Paper 2011/11.
http://acm.eionet.europa.eu/reports/ETCACM_TP_2011_11_spatAQmaps_2009
- EC (2008). Directive 2008/50/EC of the European Parliament and of the Council on ambient air quality and cleaner air for Europe. Official Journal L 152(11.6.2008): 1-44.
<http://eur-lex.europa.eu/LexUriServ/LexUriServ.do?uri=OJ:L:2008:152:0001:0044:EN:PDF>
- ECMWF. Meteorological Archival and Retrieval System (MARS). <http://www.ecmwf.int/>
- EC4MACS (2012). The GAINS integrated assessment model, EC4MACS report, March 2012.
http://www.ec4macs.eu/content/report/EC4MACS_Publications/MR_Final%20in%20pdf/GAINS_Methodologies_Final.pdf
- EEA (2009). Spatial assessment of PM₁₀ and ozone concentrations in Europe (2005). EEA Technical report No 1/2009.
http://acm.eionet.europa.eu/reports/EEA_TR_1_2009_Spatial_AQ_assessment_2005
- EEA (2011a). The application of models under the European Union's Air Quality Directive: A technical reference guide. EEA Technical report No 10/2011.
http://acm.eionet.europa.eu/reports/EEA_TP_10_2011_fairmode_tech_ref_guide
- EEA (2011b). Guide for EEA map layout. EEA operational guidelines. August 2011, version 4. www.eionet.europa.eu/gis/docs/GISguide_v4_EEA_Layout_for_map_production.pdf

- Elbern H, Peuch VH, Friese E, Rouil L, Beekmann M, Foret G, Eskes H, Gauss M, Valdebenito A, Robertson L, Cariolle D, Jaumouillé E, Massart S, Piacentini A (2011). European environmental data assimilation documentation and user instruction. <http://www.gmes-atmosphere.eu/documents/deliverables/r-eda/>
- EMEP (2011). Transboundary acidification, eutrophication and ground level ozone in Europe in 2009. EMEP Status Report 1/2011. http://emep.int/publ/reports/2011/status_report_1_2011.pdf
- EMEP (2012a). Transboundary acidification, eutrophication and ground level ozone in Europe in 2010. EMEP Status Report 1/2012. http://emep.int/publ/reports/2012/status_report_1_2012.pdf
- EMEP (2012b). EMEP/MS-CW model performance for acidifying and eutrophying components and photo-oxidants in 2010. Supplementary material to EMEP Status Report 1/2012. http://emep.int/publ/reports/2012/sup_status_report_1_2012.pdf
- Galmarini S, Bianconi R, Addis R, Andronopoulos S, Astrup P, Bartzis JC, Bellasio R, Buckley R, Champion H, Chino M, D'Amours R, Davakis R, Eleveld H, Glaab H, Manning A, Mikkelsen T, Pechinger U, Polreich E, Prodanova M, Slaper H, Syrakov D, Terada H, Van der Auwera L (2004). Ensemble dispersion forecasting – part II: application and evaluation. *Atmospheric Environment*, 38, pp. 4619–4632.
- Galmarini S, Kioutsioukis I, Solazzo E (2013). E pluribus unum: ensemble air quality predictions. *Atmospheric Chemistry and Physics* 13, pp 7153–7182. doi:10.5194/acp-13-7153-2013.
- Horálek J, Denby B, de Smet P, de Leeuw F, Kurfürst P, Swart R, van Noije T (2007). Spatial mapping of air quality for European scale assessment. ETC/ACC Technical paper 2006/6. http://acm.eionet.europa.eu/reports/ETCACC_TechPaper_2006_6_Spat_AQ
- Horálek J, de Smet P, de Leeuw F, Denby B, Kurfürst P, Swart R, (2008). European air quality maps including uncertainty analysis. ETC/ACC Technical paper 2007/7. http://acm.eionet.europa.eu/reports/ETCACC_TP_2007_7_spatAQmaps_ann_interpol
- Horálek J, de Smet P, de Leeuw FA, Coňková M, Denby B, Kurfürst P (2010). Methodological improvements on interpolating European air quality maps. ETC/ACC Technical Paper 2009/16. http://acm.eionet.europa.eu/reports/ETCACC_TP_2009_16_Improv_SpatAQmapping
- Horálek J, de Smet P, Corbet L, de Leeuw FA, Kurfürst P (2013). European air quality maps of PM and ozone for 2010 and their uncertainties. ETC/ACC Technical paper 2012/12. http://acm.eionet.europa.eu/reports/ETCACM_TP_2012_12_spatAQmaps_2010
- Kuenen JJP, Visschedijk AJH, Jozwicka M, van der Gon HACD (2014). TNO-MACC_II emission inventory: a multi-year (2003–2009) consistent high-resolution European emission inventory for air quality modelling. *Atmospheric Chemistry and Physics Discuss.*, 14, 5837–5869, doi: 10.5194/acpd-14-5837-2014. www.atmos-chem-phys-discuss.net/14/5837/2014/
- MACC (2013). QAQC dossiers. <http://www.gmes-atmosphere.eu/documents/deliverables/r-ens/>
- Mareckova K, Wankmüller R, Pazdernik K, Purzner M, Zechmeister A, Joebstl R, Adams M (2011). Inventory Review 2011. Review of emission data reported under the LRTAP Convention and NEC Directive. Stage 1 and 2 Review. Technical Report CEIP 1/2011. http://www.ceip.at/fileadmin/inhalte/emep/pdf/2011/InventoryReport2011_forWeb.pdf
- Mareckova K, Wankmüller R, Whiting R, Pinteris M (2012). Inventory Review 2012. Review of emission data reported under the LRTAP Convention and NEC Directive. Stage 1 and 2 Review. EEA/CEIP Technical Report. http://www.ceip.at/fileadmin/inhalte/emep/pdf/2012/InventoryReport2012_forWeb.pdf

- Mol W, van Hooydonk P (2011). European exchange of monitoring information and state of the air quality in 2009, ETC/ACM Technical Paper 2011/1.
http://acm.eionet.europa.eu/reports/ETCACM_TP_2011_1_EoI_AQ_meta_info2009
- Mol W, van Hooydonk P (2012). European exchange of monitoring information and state of the air quality in 2010, ETC/ACM Technical Paper 2012/1.
http://acm.eionet.europa.eu/reports/ETCACM_TP_2012_1_EoI_AQ_meta_info2010
- Rouïl L, Massart S, Beekman M, Foret G, Sofiev M, Vira J, Eskes H, Meleux F, Ung A, Peuch VH, Aldebenito A, Gauss M, Elbern H, Friese E, Strunk A, Robertson L, Schaap M, Timmermans R, Curier L (2011a). Assessment Report: Air quality in Europe in 2007. & Evaluation Report of the Air quality assessments in Europe for 2007.
<http://www.gmes-atmosphere.eu/documents/deliverables/r-eva/>
- Rouïl L, Massart S, Beekman M, Foret G, Sofiev M, Vira J, Eskes H, Meleux F, Ung A, Peuch VH, Aldebenito A, Gauss M, Elbern H, Friese E, Strunk A, Robertson L, Schaap M, Timmermans R, Curier L (2011b). Assessment Report: Air quality in Europe in 2008. & Evaluation Report of the Air quality assessments in Europe for 2008.
<http://www.gmes-atmosphere.eu/documents/deliverables/r-eva/>
- Rouïl L, Massart S, Beekman M, Foret G, Sofiev M, Vira J, Eskes H, Meleux F, Ung A, Peuch VH, Marécal V, Aldebenito A, Gauss M, Elbern H, Friese E, Strunk A, Robertson L, Schaap M, Timmermans R, Curier L (2012a). Assessment Report: Air quality in Europe in 2009.
<http://www.gmes-atmosphere.eu/documents/deliverables/r-eva/>
- Rouïl L (2012b). Urban Air quality mapping: new methodologies based on the GMES/COPERNICUS services. ETC/ACM Technical paper 2012/5.
acm.eionet.europa.eu/reports/ETCACM_TP_2012_5_urbanAQmapping_meth_GMES
- Rouïl L, Emili E, Beekman M, Foret G, Sofiev M, Vira J, Eskes H, Meleux F, Ung A, Marécal V, Aldebenito A, Carlin-Benedictow A, Elbern H, Friese E, Strunk A, Robertson L, Segers A (2013). Assessment Report: Air quality in Europe in 2010. & Evaluation Report of the Air quality assessments in Europe for 2010.
<http://gmes-atmosphere.eu/documents/maccii/deliverables/eva/>
- Schneider P, Tønnesen D, Denby B (2011). Update of background concentrations over Norway. Norwegian Institute for Air Research, Report OR 68/2011, Kjeller, Norway.
- Schneider P, Tarrasón L, Guerreiro C, (2012). The potential of GMES satellite data for mapping nitrogen dioxide at the European scale, ETC/ACM Technical Paper 2012/9.
acm.eionet.europa.eu/reports/ETCACM_TP_2012_9_GMESsatdata_NOx_Euromap
- Simpson D, Fagerli H, Jonson JE, Tsyro S, Wind P, Tuovinen J-P (2003). Transboundary acidification, eutrophication and ground level ozone in Europe: Unified EMEP model description, EMEP Report 1/2003. Norwegian Meteorological Institute, Oslo, Norway.
http://www.emep.int/publ/reports/2003/emep_report_1_part1_2003.pdf
- Taylor KE (2001) Summarizing multiple aspects of model performance in a single diagram. *Journal of Geophysical Research: Atmospheres*, 106, pp. 7183–7192 (also see PCMDI Report 55, <http://www-pcmdi.llnl.gov/publications/ab55.html>)
- Terrenoire E, Bessagnet B, Rouïl L, Tognet F, Pirovano G, Létinois L, Colette A, Thunis P, Amann M, Menut L.(2013). High resolution air quality simulation over Europe with the chemistry transport model CHIMERE. *Geosci. Model Dev. Discuss.*, 6, pp. 4137–4187.
<http://www.geosci-model-dev-discuss.net/6/4137/2013/gmdd-6-4137-2013.pdf>
- Vautard R, Schaap M, Bergstrom R, Bessagnet B, Brandt J, Builtjes PJH, Christensen JH, Cuvelier C, Foltescu V, Graff A, Kerschbaumer A, Krol M, Roberts P, Rouïl L, Stern R, Tarrason L, Thunis P, Vignati E, Wind P (2009). Skill and uncertainty of a regional air quality model ensemble. *Atmospheric Environment* 43, 31, pp. 4822–4832. doi:10.1016/j.atmosenv.2008.09.083.

Annex 1. Parameters used in ETC/ACM spatial interpolation method

ETC/ACM mapping method, i.e. the linear regression model followed by the kriging of its residuals is described in Section 2.1. Its results using different models (*hindcasts*, not reanalysis) as supplementary data are mutually compared in Chapter 4, while Chapter 5 presents the comparison of its results against both hindcast and reanalysis model outputs.

This annex contains the *parameters* used for the ETC/ACM spatial interpolation method to derive different spatial maps presented throughout the report.

Tables A1.1 – A1.6 present the estimated parameters of the linear regression models (c , a_1 , a_2, \dots) and of the ordinary kriging (*nugget*, *sill*, *range* of the variogram) that is used as a model of spatial autocorrelation to infer optimal estimates of a variable at a given set of locations.

All tables include the statistical indicators of both the regression and the kriging. The adjusted R^2 and standard error are indicators for the fit of the regression relationship, where the adjusted R^2 should be as close to 1 as possible and the standard error should be as small as possible. RMSE is the cross-validation indicator, showing the quality of the resulting map, it should be as small as possible. For the map calculations, all the stations available are used, see Table 3.1. RMSE is calculated using “A” set of the stations, see Table 3.2, for comparable reasons.

In the case of PM_{10} , the linear regression is applied for the logarithmically transformed data of both measured and modelled PM_{10} values. Thus, standard error and variogram parameters refer to these transformed data, whereas RMSE refers to the interpolation after the back-transformation.

Tables A1.1 – A1.3 present the parameters of the ETC/ACM mapping method used for the construction of the maps of PM_{10} indicators, separately for the rural and urban background areas, using different chemical transport model outputs as supplementary data source. For the list of the individual models used, see the introduction of Chapter 4.

When comparing the regression results for the rural background and urban background areas, it can be seen that better results are given for the rural areas in the case of PM_{10} (both for regression and for final interpolation). The more complex character of the urban air quality for this pollutant causes this probably.

In the urban areas, both versions of the CHIMERE-EC4MACS model show better correlation with the measured data than EMEP and MACC-II Ensemble in 2009. This is also true for the data without the logarithmical transformation, see Annex 5, Figures A5.2 and A5.4. Nevertheless, this better regression relation does not lead to better results of the interpolation: RMSE of the two other models is lower in most of the cases. This is probably caused by a better spatial structure of the residual field in the case of the EMEP and MACC-II Ensemble in the urban areas. This assumption is confirmed by the high value of nugget/sill ratio of the residual field in the case of CHIMERE-EC4MACS, which indicates the weak spatial correlation of this field.

Table A1.1 Parameters of the linear regression models and of the ordinary kriging variograms – and their statistics – of PM₁₀ annual average maps for 2009

linear regr. model + ord. kriging on its residuals	PM ₁₀ , annual average, 2009							
	EMEP		MACC-II Ensemble		CHIMERE-EC4M. 50x50		CHIMERE-EC4M. 7x7	
	rural	urban	rural	urban	rural	urban	rural	urban
	coeff.	coeff.	coeff.	coeff.	coeff.	coeff.	coeff.	coeff.
c (constant)	2.22	2.74	1.68	2.85	0.39	0.30	0.10	1.22
a1 (log. model outp. 2009)	0.534	0.262	0.705	0.199	0.957	1.062	0.971	0.684
a2 (altitude GTOPO)	-0.00032		-0.00023		-0.00043		-0.00030	
a3 (wind speed 2009)	-0.157		-0.174		-0.056		-0.027	
a4 (s. solar rad. 2009)	0.026		0.041		0.022		0.024	
adjusted R²	0.38	0.06	0.46	0.04	0.41	0.39	0.46	0.36
stand. error [µg.m⁻³]	0.30	0.35	0.28	0.34	0.28	0.27	0.27	0.26
range [km]	580	460	350	450	580	380	580	400
nugget	0.039	0.019	0.032	0.018	0.040	0.015	0.037	0.015
sill	0.093	0.061	0.079	0.062	0.083	0.046	0.076	0.046
RMSE [µg.m⁻³]	4.70	5.81	4.55	5.74	4.43	5.93	4.21	6.04

Table A1.2 Parameters of the linear regression models and of the ordinary kriging variograms – and their statistics – of the maps of PM₁₀ indicator 36th highest daily mean for 2009

linear regr. model + ord. kriging on its residuals	PM ₁₀ , 36 th highest daily mean, 2009							
	EMEP		MACC-II Ensemble		CHIMERE-EC4M. 50x50		CHIMERE-EC4M. 7x7	
	rural	urban	rural	urban	rural	urban	rural	urban
	coeff.	coeff.	coeff.	coeff.	coeff.	coeff.	coeff.	coeff.
c (constant)	2.22	3.02	1.69	3.23	0.89	0.69	0.48	1.57
a1 (log. model outp. 2009)	0.571	0.287	0.763	0.212	0.877	0.949	0.930	0.638
a2 (altitude GTOPO)	-0.00027		-0.00020		-0.00040		-0.00026	
a3 (wind speed 2009)	-0.145		-0.172		-0.073		-0.038	
a4 (s. solar rad. 2009)	0.027		0.038		0.011		0.010	
adjusted R²	0.40	0.06	0.48	0.03	0.42	0.30	0.49	0.34
stand. error [µg.m⁻³]	0.28	0.38	0.26	0.37	0.27	0.31	0.25	0.28
range [km]	230	330	180	330	180	140	180	90
nugget	0.033	0.022	0.024	0.021	0.023	0.019	0.022	0.020
sill	0.073	0.070	0.068	0.073	0.068	0.050	0.058	0.049
RMSE [µg.m⁻³]	7.98	11.37	7.55	11.25	7.61	11.28	7.00	11.69

Table A1.3 Parameters of the linear regression models and of the ordinary kriging variograms – and their statistics – of the maps of PM₁₀ indicators annual average (left) and 36th highest daily mean (right) for 2010

linear regr. model + ord. kriging on its residuals	PM ₁₀ , annual average, 2010				PM ₁₀ , 36 th highest daily mean, 2010			
	EMEP		MACC-II Ensemble		EMEP		MACC-II Ensemble	
	rural	urban	rural	urban	rural	urban	rural	urban
	coeff.	coeff.	coeff.	coeff.	coeff.	coeff.	coeff.	coeff.
c (constant)	2.02	1.59	1.11	1.46	2.47	1.97	1.25	1.47
a1 (log. model output 2010)	0.585	0.659	0.833	0.702	0.536	0.585	0.915	0.753
a2 (altitude GTOPO)	-0.00045		-0.00039		-0.00045		-0.00033	
a3 (wind speed 2010)	-0.107		-0.096		-0.128		-0.126	
a4 (s. solar rad. 2010)	n. sign.		0.018		n. sign.		n. sign.	
adjusted R²	0.44	0.38	0.48	0.21	0.39	0.34	0.45	0.19
stand. error [µg.m⁻³]	0.30	0.29	0.29	0.32	0.32	0.32	0.30	0.35
range [km]	630	620	200	480	630	620	200	340
nugget	0.032	0.013	0.025	0.012	0.028	0.010	0.025	0.012
sill	0.095	0.064	0.076	0.059	0.108	0.082	0.083	0.071
RMSE [µg.m⁻³]	4.51	5.96	4.49	5.78	8.58	11.37	8.64	11.20

For 2010, the EMEP model shows better correlation with the measured data than the MACC-II Ensemble (and also than the EMEP model for 2009) for PM₁₀ in the urban areas. Again, this is also true for the data without the logarithmical transformation, see Annex 5, Figure A5.6 and A5.8. And also in this case the better correlation does not lead to the better interpolation – RMSE is better in the case of the MACC-II Ensemble, for both PM₁₀ indicators.

For the rural areas, the multiple linear regression using the EMEP model shows the weakest correlation in all cases (i.e. at both 2009 and 2010 and both PM₁₀ indicators). In 2009, the best regression results are given by CHIMERE-EC4MACS in the 7x7 km² resolution application. This highest correlation leads in this case also to the best final map, i.e. with the lowest RMSE (4.2 for annual average, Table A1.1; 7.0 for 36th highest daily mean, Table A1.2).

Different values of regression coefficient *a1* (which is related to the individual models) are caused in general by two distinct reasons: (i) the different concentration level of the models, and (ii) the different weight of the models in the multiple linear regressions. A more detailed view on the individual models and their performances is given in Annex 5, in which the comparison of the models with the measured data is presented. This comparison provides information on both the concentration level of the models (showing under- or over-estimation of the model) and the level of the correlation.

Tables A1.4 – A1.6 present the parameters of the ETC/ACM mapping method for ozone.

Table A1.4 Parameters of the linear regression models and of the ordinary kriging variograms – and their statistics – of the maps of ozone indicator 26th highest daily 8-hourly maximum for 2009

linear regr. model + ord. kriging on its residuals	ozone, 26 th highest daily 8-hourly maximum, 2009							
	EMEP		MACC-II Ensemble		CHIMERE-EC4M. 50x50		CHIMERE-EC4M. 7x7	
	rural	urban	rural	urban	rural	urban	rural	urban
	coeff.	coeff.	coeff.	coeff.	coeff.	coeff.	coeff.	coeff.
c (constant)	12.0	43.1	26.1	48.8	-17.1	40.8	12.3	52.3
a1 (model output 2010)	0.822	0.615	0.822	0.695	1.277	0.924	0.925	0.603
a2 (altitude GTOPO)	0.0068		0.0084		0.0095		0.0099	
a3 (wind speed 2010)		-3.80		-3.21		-6.73		-4.12
a4 (s. solar rad. 2010)	0.467	0.796	n. sign.	n. sign.	n. sign.	n. sign.	n. sign.	0.730
adjusted R²	0.59	0.54	0.67	0.58	0.41	0.45	0.56	0.53
stand. error [µg.m⁻³]	9.45	10.52	8.47	10.05	11.23	11.52	9.66	10.72
range [km]	300	60	400	60	220	60	220	60
nugget	45	45	52	50	55	50	35	45
sill	86	76	69	73	104	96	83	80
RMSE [µg.m⁻³]	8.18	9.33	7.84	9.08	8.57	9.48	7.87	9.23

Table A1.5 Parameters of the linear regression models and of the ordinary kriging variograms – and their statistics – of the maps of ozone indicator SOMO35 for 2009

linear regr. model + ord. kriging on its residuals	ozone, SOMO35, 2009							
	EMEP		MACC-II Ensemble		CHIMERE-EC4M. 50x50		CHIMERE-EC4M. 7x7	
	rural	urban	rural	urban	rural	urban	rural	urban
	coeff.	coeff.	coeff.	coeff.	coeff.	coeff.	coeff.	coeff.
c (constant)	-991	-602	927	1803	473	3847	34	567
a1 (model output 2010)	0.657	0.515	0.867	0.747	0.943	0.764	0.905	0.575
a2 (altitude GTOPO)	1.158		2.030		2.456		1.812	
a3 (wind speed 2010)		-226.7		-212.4		-801.1		-406.1
a4 (s. solar rad. 2010)	155.8	207.9	n. sign.	n. sign.	n. sign.	n. sign.	n. sign.	210.5
adjusted R²	0.60	0.53	0.66	0.58	0.50	0.49	0.57	0.53
stand. error [$\mu\text{g}\cdot\text{m}^{-3}$]	1701	1630	1559	1547	1910	1697	1746	1633
range [km]	290	190	420	190	220	190	270	190
nugget	2.3.E+06	1.3E+06	2.3.E+06	1.2E+06	2.3.E+06	1.3E+06	2.3.E+06	1.3E+06
sill	2.9.E+06	1.7E+06	2.4.E+06	1.7E+06	3.3.E+06	1.9E+06	2.9.E+06	1.8E+06
RMSE [$\mu\text{g}\cdot\text{m}^{-3}$]	1617	1476	1567	1456	1665	1496	1626	1460

Surface solar radiation, expressed by its regression coefficient $a4$, is a statistically non-significant variable in some regression relations, thus it is not used in these cases.

Table A1.6 Parameters of the linear regression models and of the ordinary kriging variograms – and their statistics – of the maps of ozone indicators 26th highest daily 8-hourly maximum (left) and SOMO35 (right) for 2010

linear regr. model + OK on its residuals	O ₃ , 26 th high. daily 8-h maximum, 2010				ozone, SOMO35, 2010			
	EMEP		MACC-II Ensemble		EMEP		MACC-II Ensemble	
	rural	urban	rural	urban	rural	urban	rural	urban
	coeff.	coeff.	coeff.	coeff.	coeff.	coeff.	coeff.	coeff.
c (constant)	9.8	31.4	16.2	47.84	-2163	-1912	-36	1241
a1 (model output 2010)	0.791	0.680	0.954	0.794	0.456	0.434	0.804	0.598
a2 (altitude GTOPO)	0.0068		0.0133		1.482		2.782	
a3 (wind speed 2010)		-2.826		-4.678		-18.6		-375.8
a4 (s. solar rad. 2010)	0.993	0.859	n.sign.	n.sign.	359.3	288.4	175.0	213.9
adjusted R²	0.56	0.51	0.59	0.51	0.59	0.54	0.61	0.52
stand. error [$\mu\text{g}\cdot\text{m}^{-3}$]	10.42	11.86	10.09	11.89	1660	1459	1619	1481
range [km]	100	260	100	120	100	250	100	250
nugget	30	60	30	63	1.5E+06	9.0E+05	1.3E+06	1.0E+06
sill	95	96	89	100	2.6E+06	1.4E+06	2.5E+06	1.5E+06
RMSE [$\mu\text{g}\cdot\text{m}^{-3}$]	8.87	9.13	8.91	9.04	1582	1271	1566	1272

In the case of ozone, generally better correlation is observed at the rural areas than at the urban areas. However, the standard error is higher there in the case of SOMO35, due to the higher ozone concentration level in these rural areas.

For 2009, the best regression results are given by the MACC-II Ensemble at both rural and urban background areas. The same is also true for the final interpolation results.

In the year 2010, the model output generated by MACC-II Ensemble and by EMEP show similar level of performance in the linear regression model and in the ETC/ACM mapping results, both at rural and urban background areas.

Annex 2. Cross-validation scatter plots

Chapter 4 presents the comparison of ETC/ACM mapping results using different models (hindcasts, not reanalysis). Sections 4.1.2 and 4.1.4 present the statistics of the cross-validation results of this comparison. In addition to that, this annex presents the relating cross-validation scatter plots.

The EMEP 50x50 km² products are used by default in the ETC/ACM mapping method so far. For testing the improvement that other models could provide in the mapping results, we introduced in the comparison of the model performances the MACC-II Ensemble products. Furthermore, we included a third model in the comparison, namely the CHIMERE model as used in the EC4MACS project, because it has the advantage of having results available at two different spatial resolutions for the same year, 2009. The model outputs used in the ETC/ACM mapping are:

2009: EMEP model output (original resolution circa 50x50 km²),
MACC-II Ensemble model output (original factual resolution circa 20x30 km²),
CHIMERE-EC4MACS model output (original resolution circa 50x50 km²),
CHIMERE-EC4MACS model output (original resolution circa 7x7 km²),

2010: EMEP model output (original resolution circa 50x50 km²),
MACC-II Ensemble model output (original factual resolution circa 15x25 km²).

All the ETC/ACM mapping results are constructed in the same 10x10 km² spatial resolution.

For the rural areas, rural maps and measured data of rural background stations are used, and for the urban background areas, urban background maps and measured data of urban and suburban background stations are used. The mapping results are cross-validated against observations according the repetitive 'leave-one-out' method as described in Section 3.3.

Figures A2.1 to A2.8 show the cross-validation scatter plots of the ETC/ACM mapping results using different models against the measurement data for PM₁₀, and Figures A2.9 to A2.16 show the scatter plots for ozone.

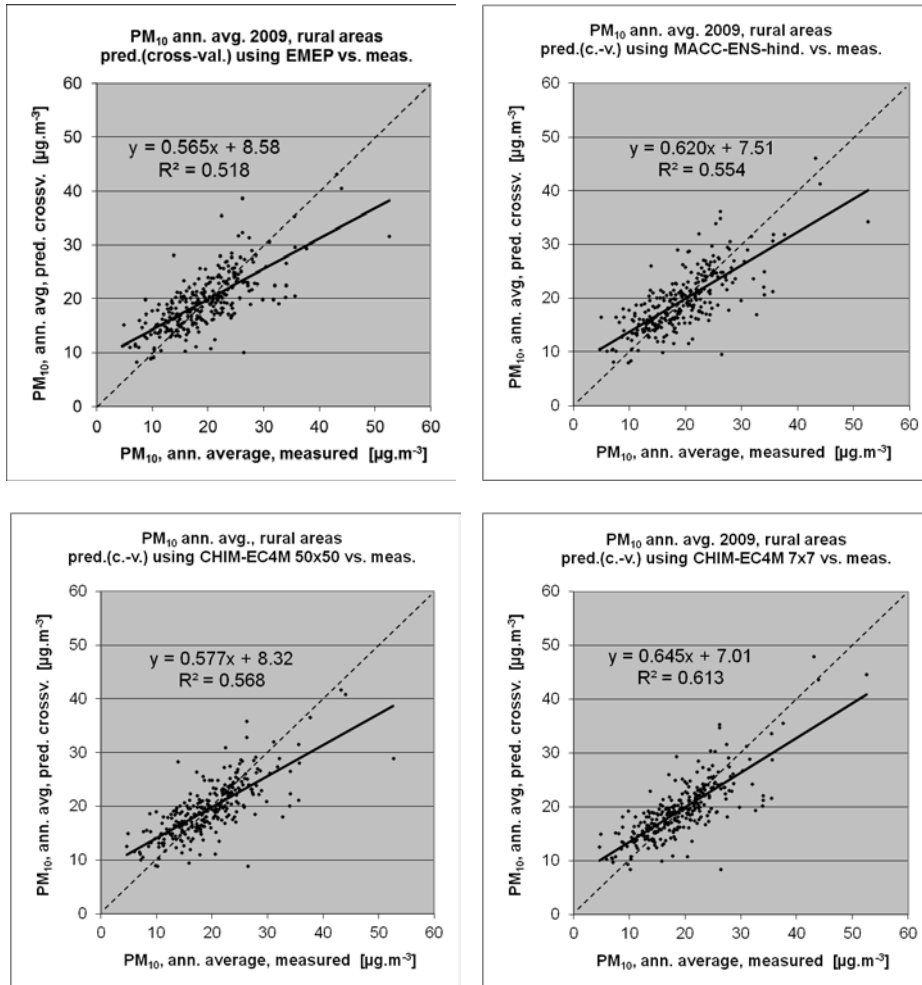


Figure A2.1 Cross-validation scatter plots showing ETC/ACM mapping results using EMEP (upper left), MACC-II Ensemble (upper right), CHIMERE-EC4MACS_50km (lower left) and CHIMERE-EC4MACS_7km (lower right) model outputs for PM₁₀ annual average 2009, rural areas

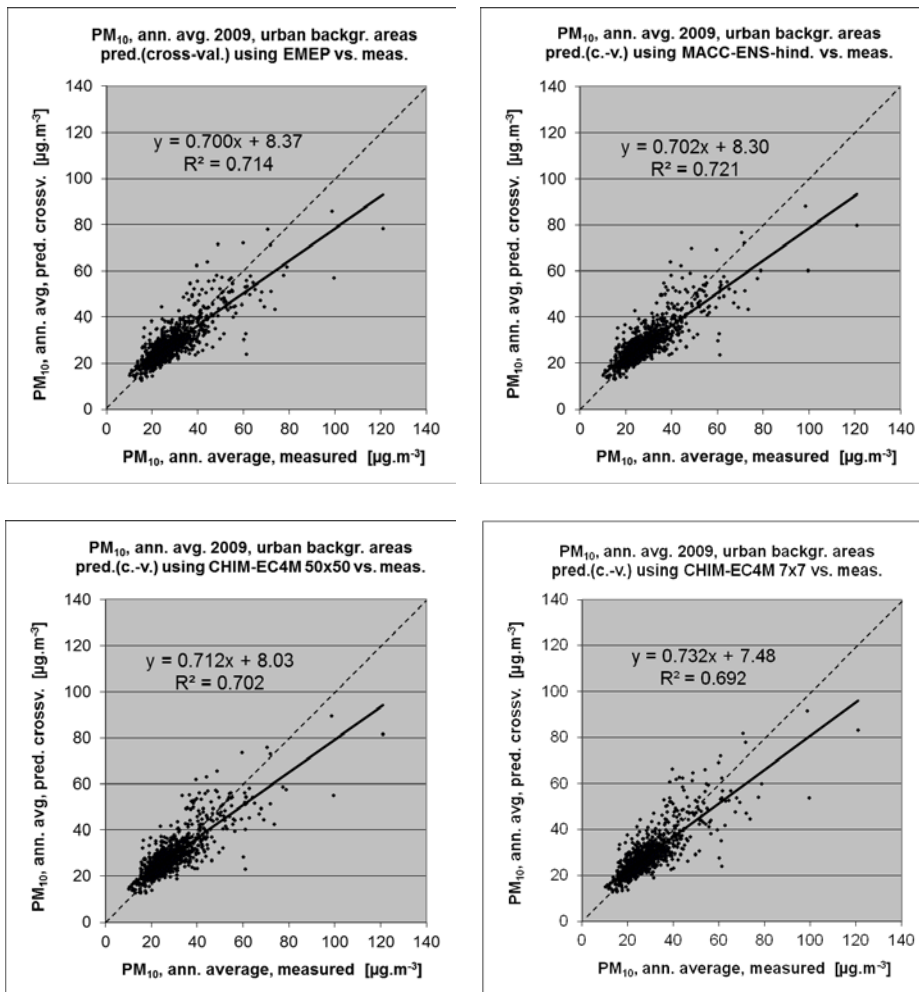


Figure A2.2 Cross-validation scatter plots showing ETC/ACM mapping results using EMEP (upper left), MACC-II Ensemble (upper right), CHIMERE-EC4MACS_50km (lower left) and CHIMERE-EC4MACS_7km (lower right) model outputs for PM₁₀ annual average 2009, urban background areas

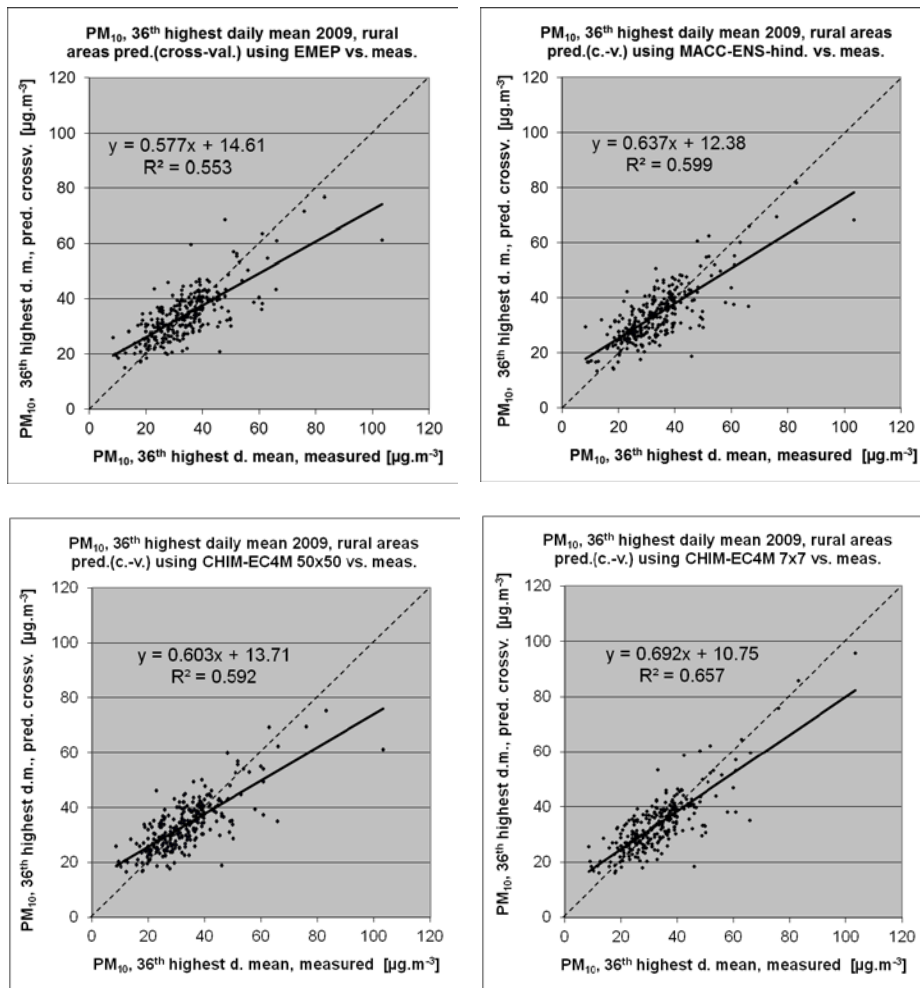


Figure A2.3 Cross-validation scatter plots showing ETC/ACM mapping results using EMEP (upper left), MACC-II Ensemble (upper right), CHIMERE-EC4MACS_50km (lower left) and CHIMERE-EC4MACS_7km (lower right) model outputs for PM₁₀ indicator 36th highest daily mean for 2009, rural areas

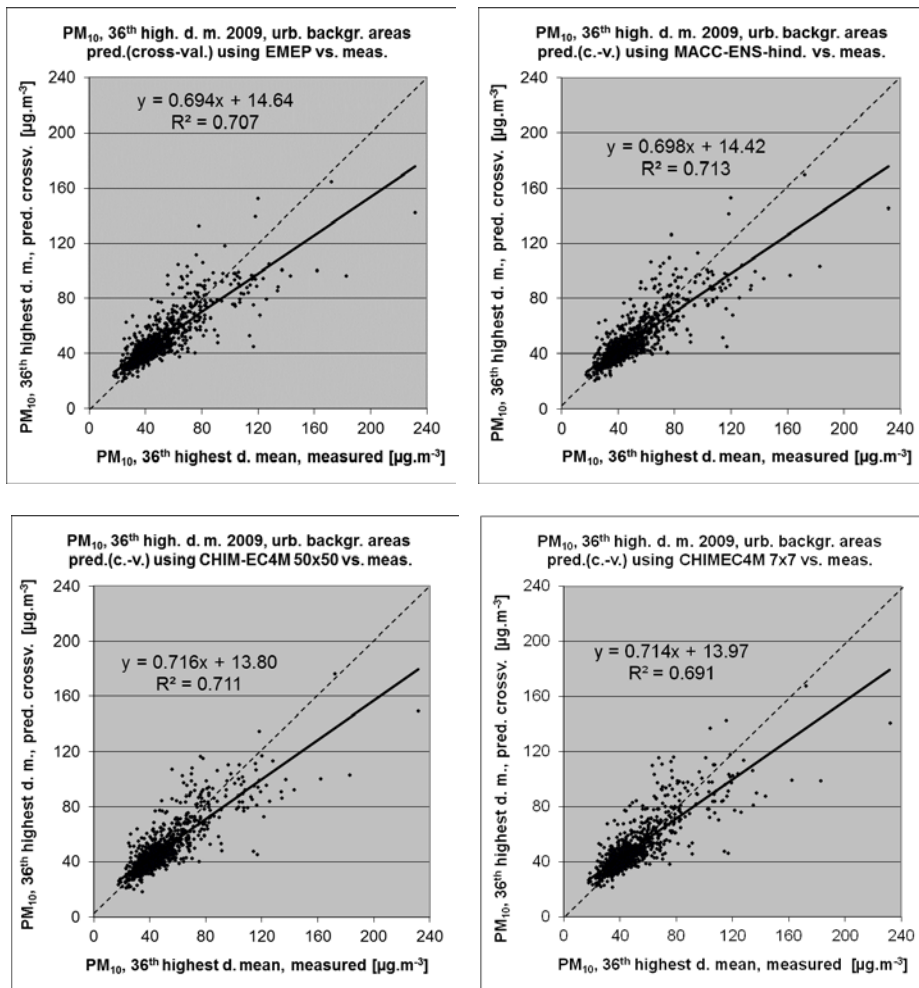


Figure A2.4 Cross-validation scatter plots showing ETC/ACM mapping results using EMEP (upper left), MACC-II Ensemble (upper right), CHIMERE-EC4MACS_50km (lower left) and CHIMERE-EC4MACS_7km (lower right) model outputs for PM₁₀ indicator 36th highest daily mean for 2009, urban background areas

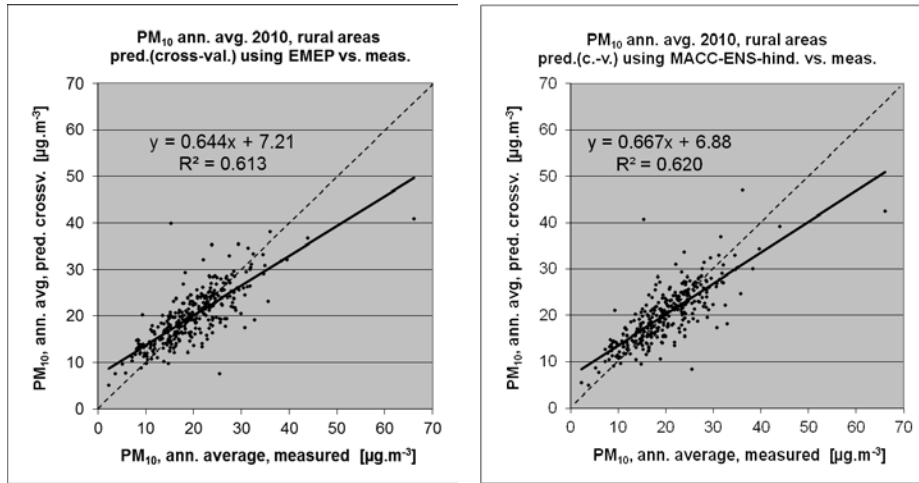


Figure A2.5 Cross-validation scatter plots showing ETC/ACM mapping results using EMEP (left) and MACC-II Ensemble (right) model outputs for PM₁₀ annual average 2010, rural areas

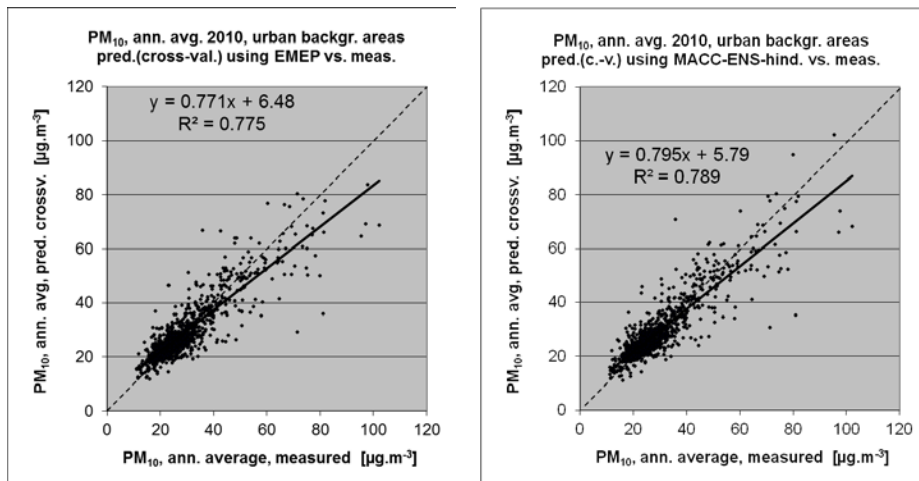


Figure A2.6 Cross-validation scatter plots showing ETC/ACM mapping results using EMEP (left) and MACC-II Ensemble (right) model outputs for PM₁₀ annual average 2010, urban background areas

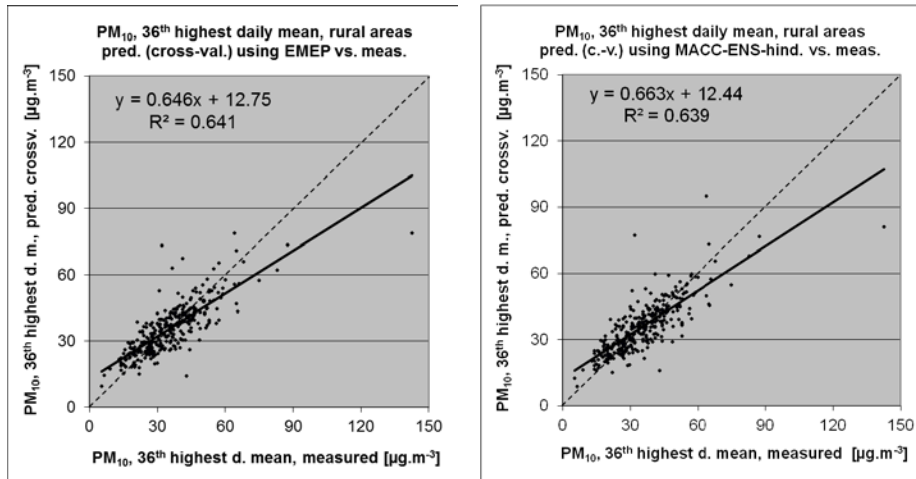


Figure A2.7 Cross-validation scatter plots showing ETC/ACM mapping results using EMEP (left) and MACC-II Ensemble (right) model outputs for PM₁₀ indicator 36th highest daily mean for 2010, rural areas

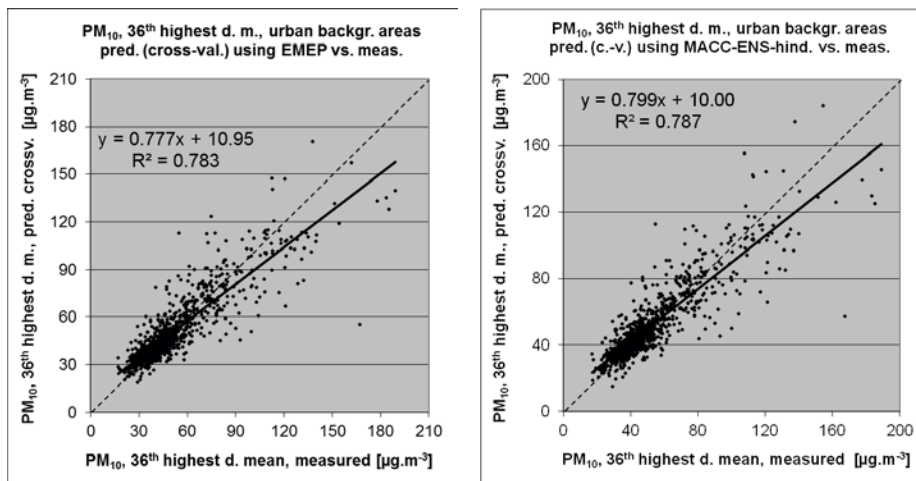


Figure A2.8 Cross-validation scatter plots showing ETC/ACM mapping results using EMEP (left) and MACC-II Ensemble (right) model outputs for PM₁₀ indicator 36th highest daily mean for 2010, urban background areas

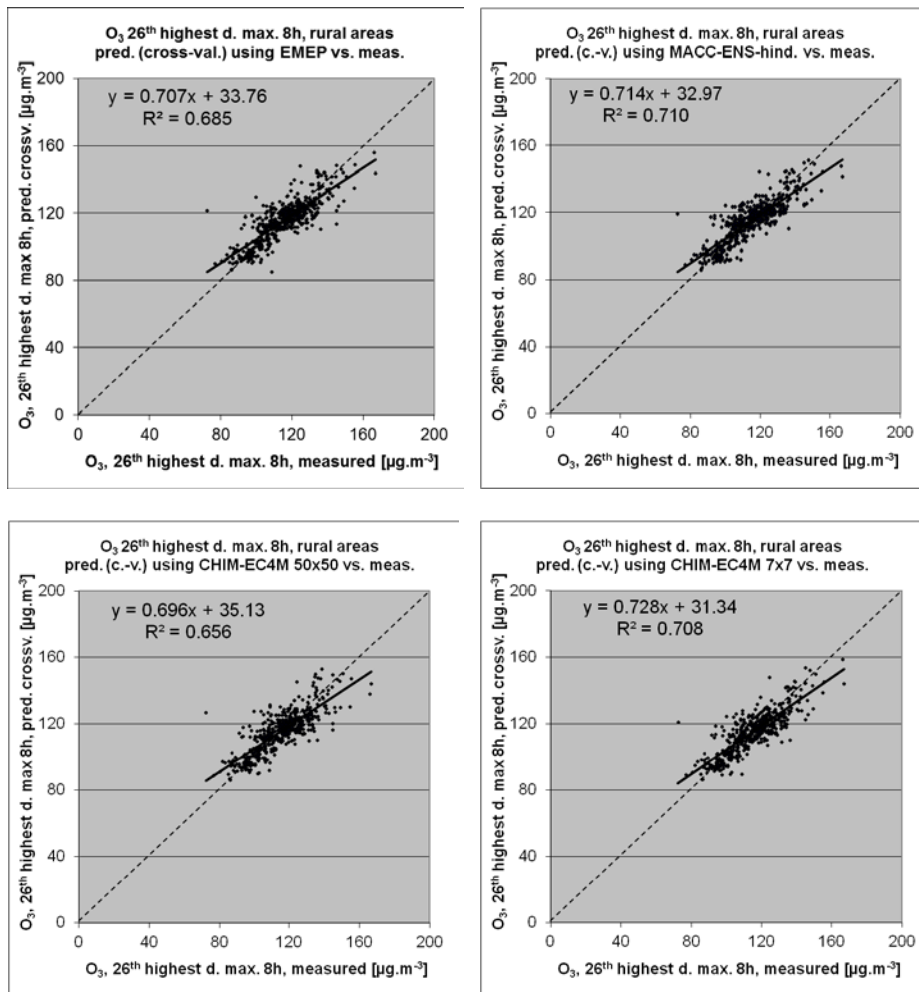


Figure A2.9 Cross-validation scatter plots showing ETC/ACM mapping results using EMEP (upper left), MACC-II Ensemble (upper right), CHIMERE-EC4MACS_50km (lower left) and CHIMERE-EC4MACS_7km (lower right) model outputs for ozone indicator 26th highest daily max. 8-hourly mean for 2009, rural areas

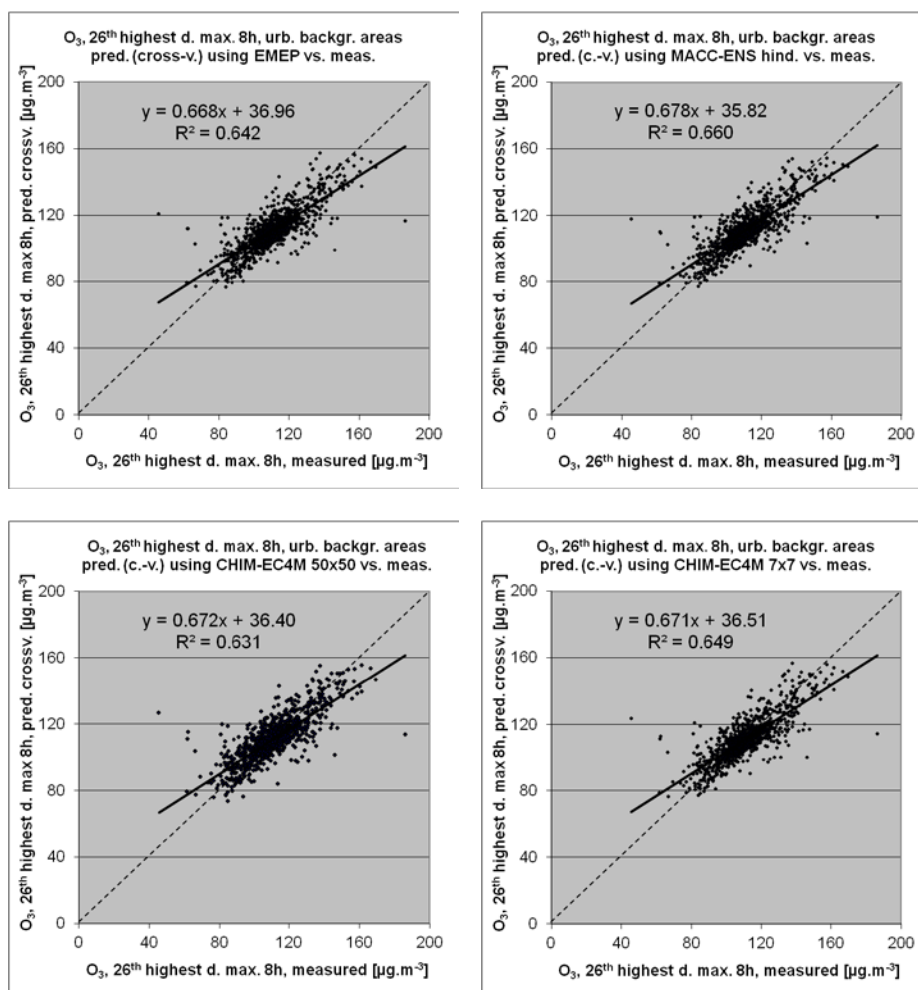


Figure A2.10 Cross-validation scatter plots showing ETC/ACM mapping results using EMEP (upper left), MACC-II Ensemble (upper right), CHIMERE-EC4MACS_50km (lower left) and CHIMERE-EC4MACS_7km (lower right) model outputs for ozone indicator 26th highest daily max. 8-hourly mean for 2009, urban background areas

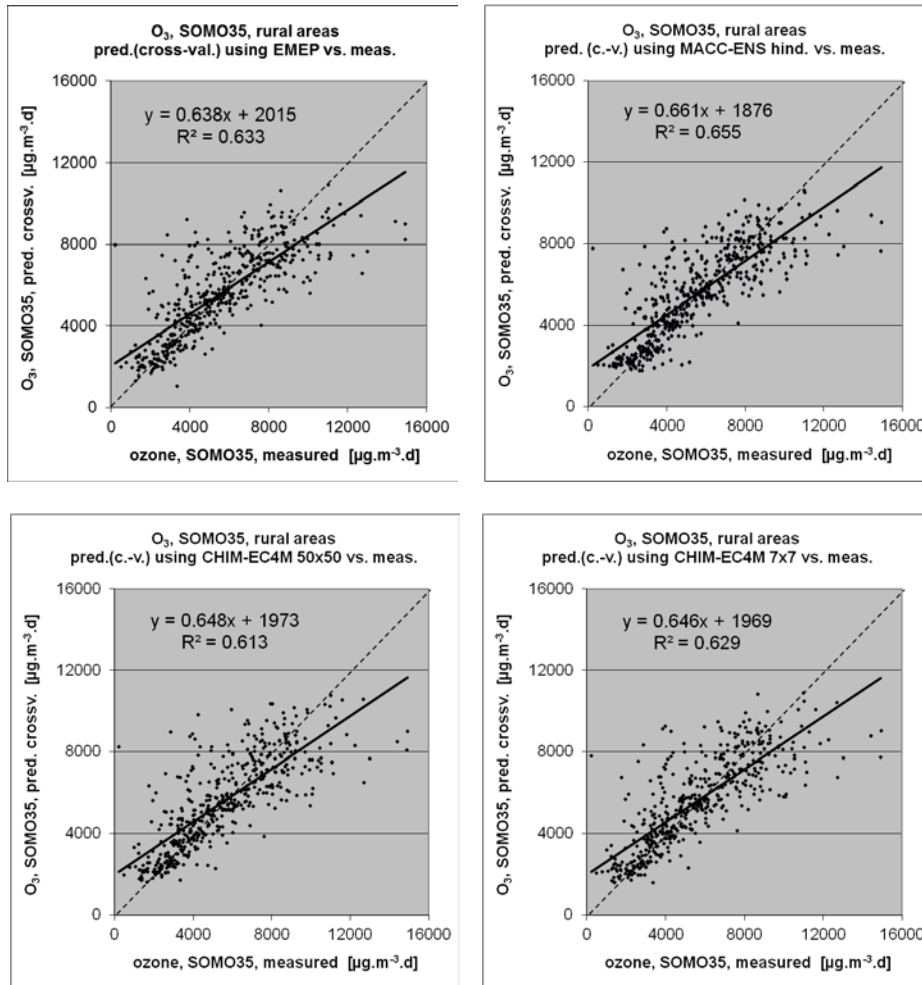


Figure A2.11 Cross-validation scatter plots showing ETC/ACM mapping results using EMEP (upper left), MACC-II Ensemble (upper right), CHIMERE-EC4MACS_50km (lower left) and CHIMERE-EC4MACS_7km (lower right) model outputs for ozone indicator SOMO35 for 2009, rural areas

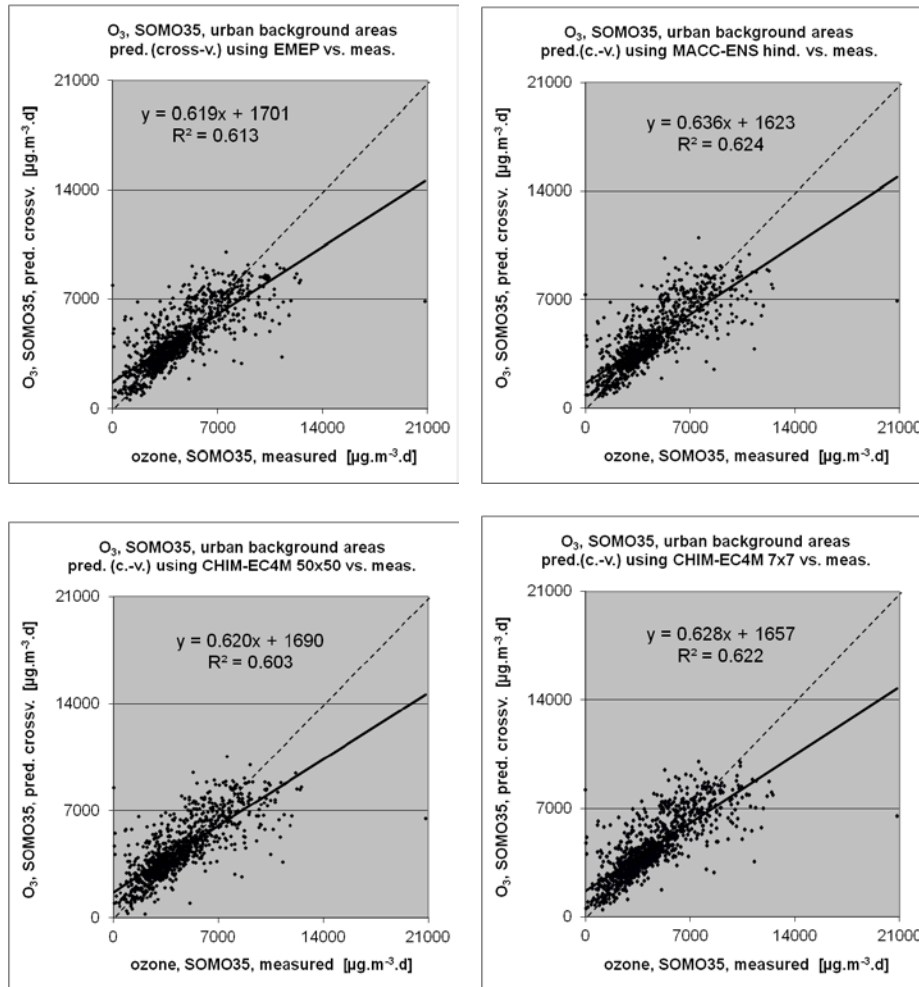


Figure A2.12 Cross-validation scatter plots showing ETC/ACM mapping results using EMEP (upper left), MACC-II Ensemble (upper right), CHIMERE-EC4MACS_50km (lower left) and CHIMERE-EC4MACS_7km (lower right) model outputs for ozone indicator SOMO35 for 2009, urban background areas

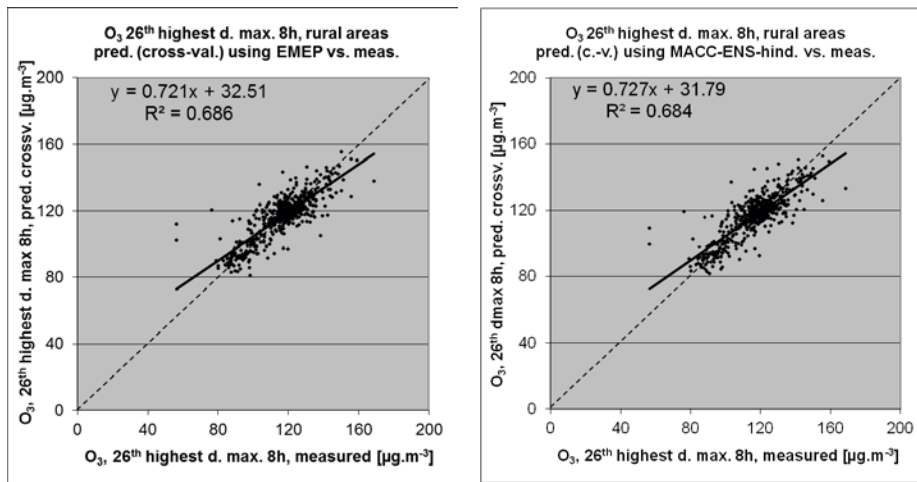


Figure A2.13 Cross-validation scatter plots showing ETC/ACM mapping results using EMEP (left) and MACC-II Ensemble (right) model outputs for ozone indicator 26th highest daily max. 8-hourly mean for 2010, rural areas

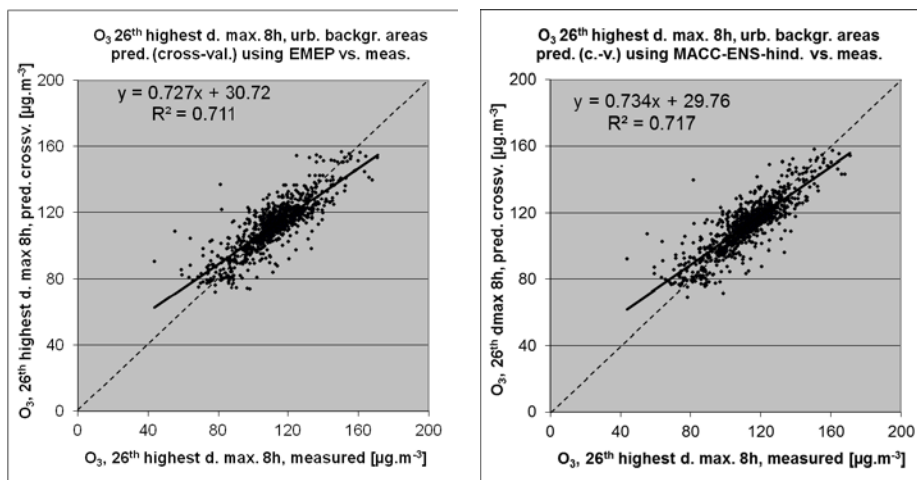


Figure A2.14 Cross-validation scatter plots showing ETC/ACM mapping results using EMEP (left) and MACC-II Ensemble (right) model outputs for ozone indicator 26th highest daily max. 8-hourly mean for 2010, urban background areas

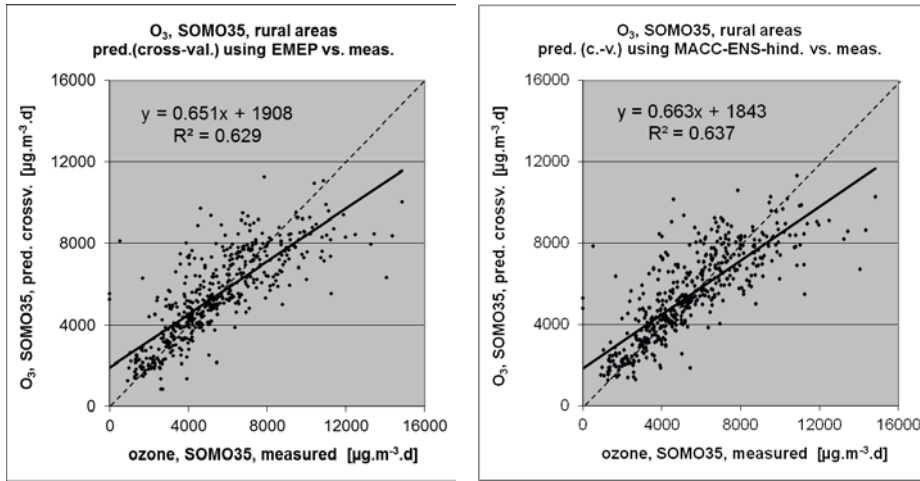


Figure A2.15 Cross-validation scatter plots showing ETC/ACM mapping results using EMEP (left) and MACC-II Ensemble (right) model outputs for ozone indicator SOMO35 for 2010, rural areas

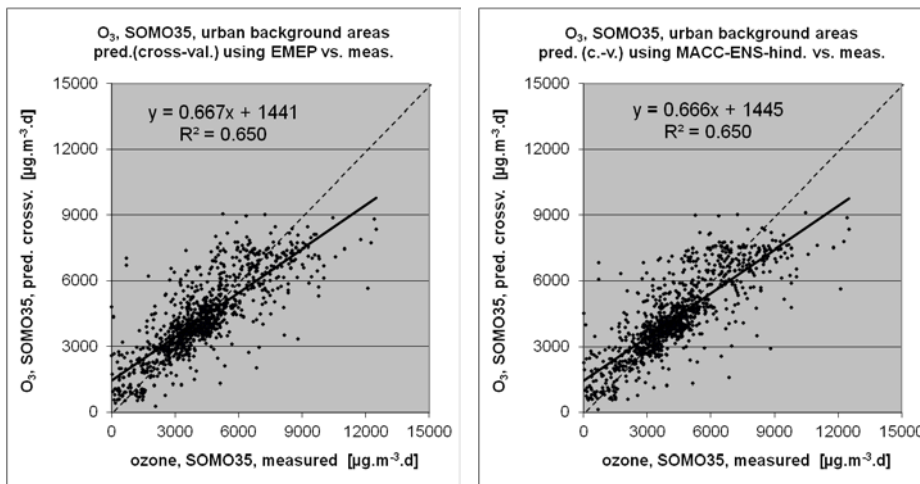


Figure A2.16 Cross-validation scatter plots showing ETC/ACM mapping results using EMEP (left) and MACC-II Ensemble (right) model outputs for ozone indicator SOMO35 for 2010, urban background areas

Annex 3. Maps of differences

Chapter 4 presents the ETC/ACM mapping results using different model hindcast outputs. This Annex 3 shows the maps of differences between the ETC/ACM mapping results using as current default the EMEP model output and using the other model outputs involved in the comparison. Additionally, the maps of differences between the ETC/ACM mapping results using CHIMERE-EC4MACS models in different resolutions are presented. Figures A3.1 to A3.6 show the maps for PM₁₀ and Figures A3.7 to A3.12 show the maps for ozone.

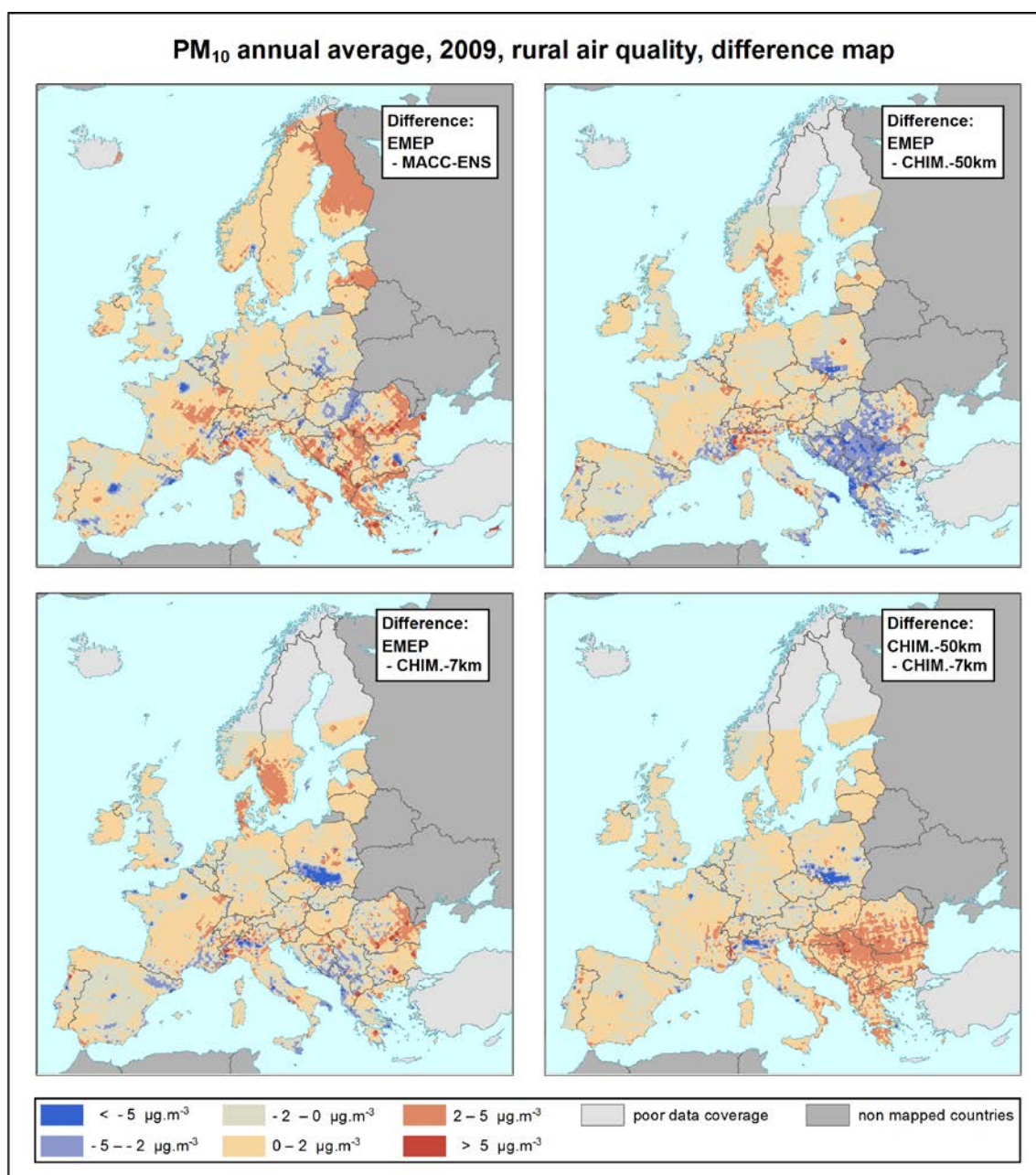


Figure A3.1 PM₁₀ annual average for 2009, rural air quality, difference of the ETC/ACM mapping results using EMEP and MACC-II Ensemble (upper left), EMEP and CHIMERE-EC4MACS_50km (upper right), EMEP and CHIMERE-EC4MACS_7km (lower left) and CHIMERE-EC4MACS_50km and CHIMERE-EC4M._7km (lower right). *Note: Applicable for rural areas only.*

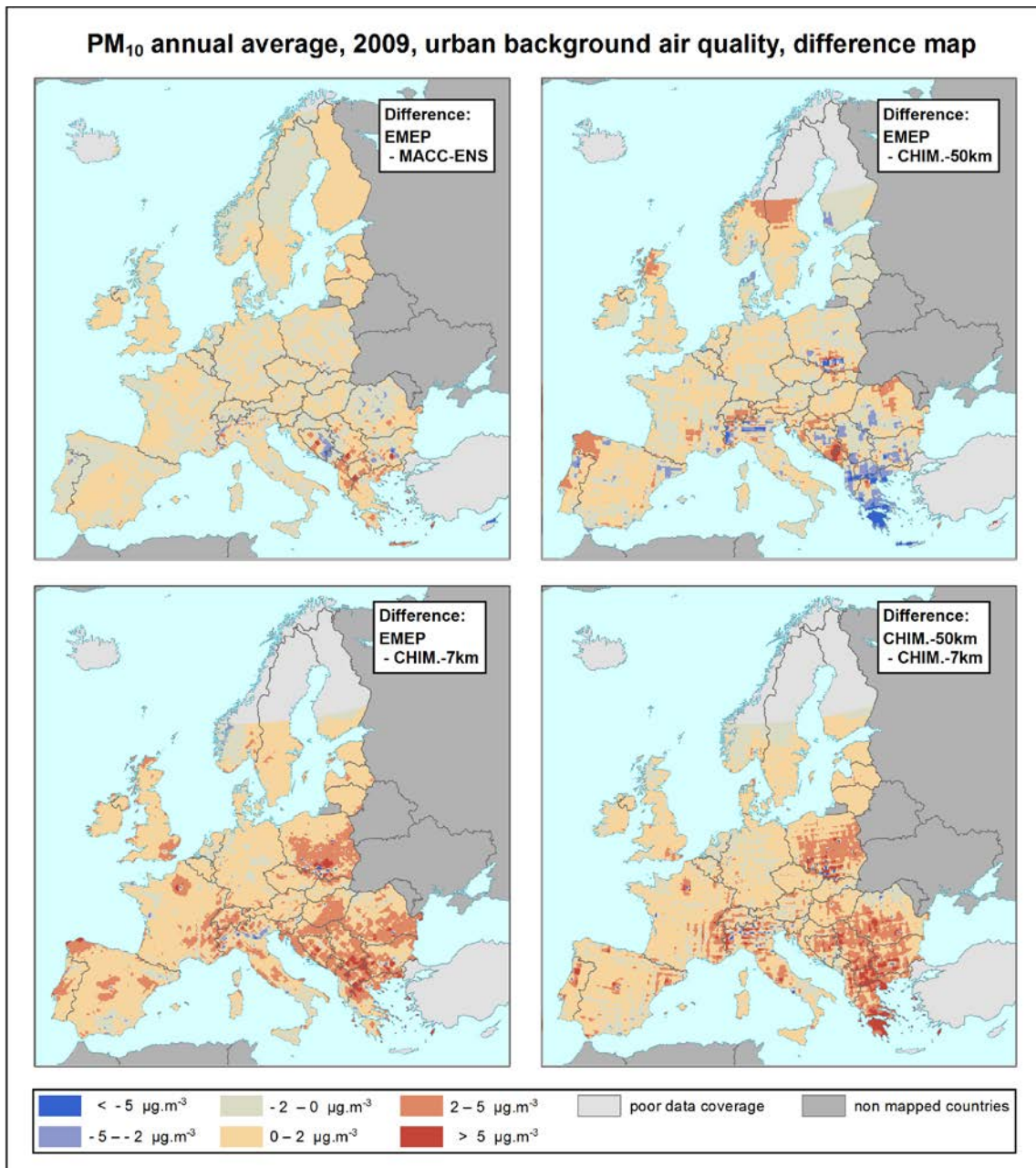


Figure A3.2 PM₁₀ annual average for 2009, urban background air quality, difference of the ETC/ACM mapping results using EMEP and MACC-II Ensemble (upper left), EMEP and CHIMERE-EC4MACS_50km (upper right), EMEP and CHIMERE-EC4MACS_7km (lower left) and CHIMERE-EC4MACS_50km and CHIMERE-EC4MACS_7km (lower right). *Note: Applicable for urban areas only.*

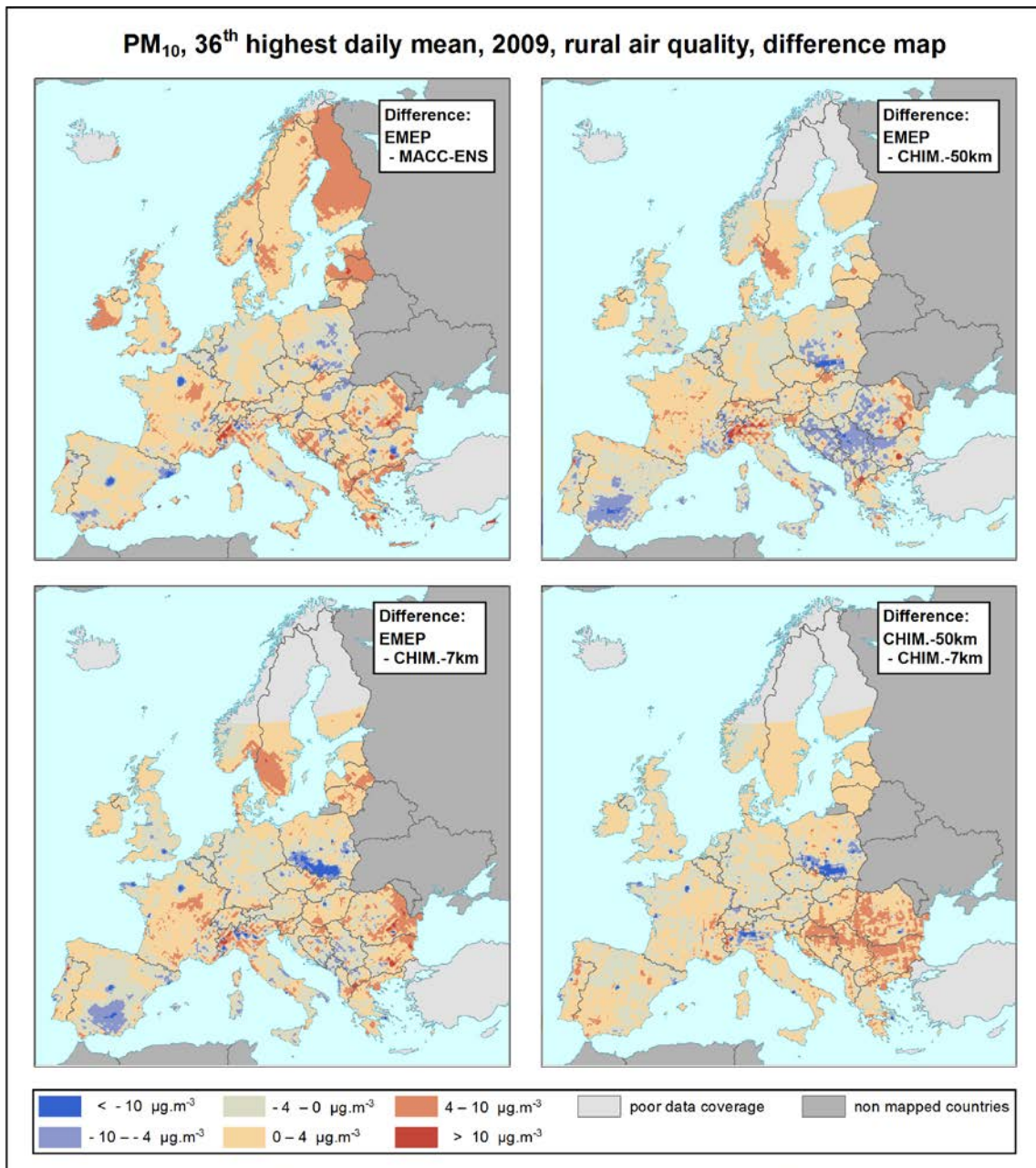


Figure A3.3 PM₁₀ indicator 36th highest daily mean for 2009, rural air quality, difference of the ETC/ACM mapping results using EMEP and MACC-II Ensemble (upper left), EMEP and CHIMERE-EC4MACS_50km (upper right), EMEP and CHIMERE-EC4MACS_7km (lower left) and CHIMERE-EC4MACS_50km and CHIMERE-EC4MACS_7km (lower right). *Note: Applicable for rural areas only.*

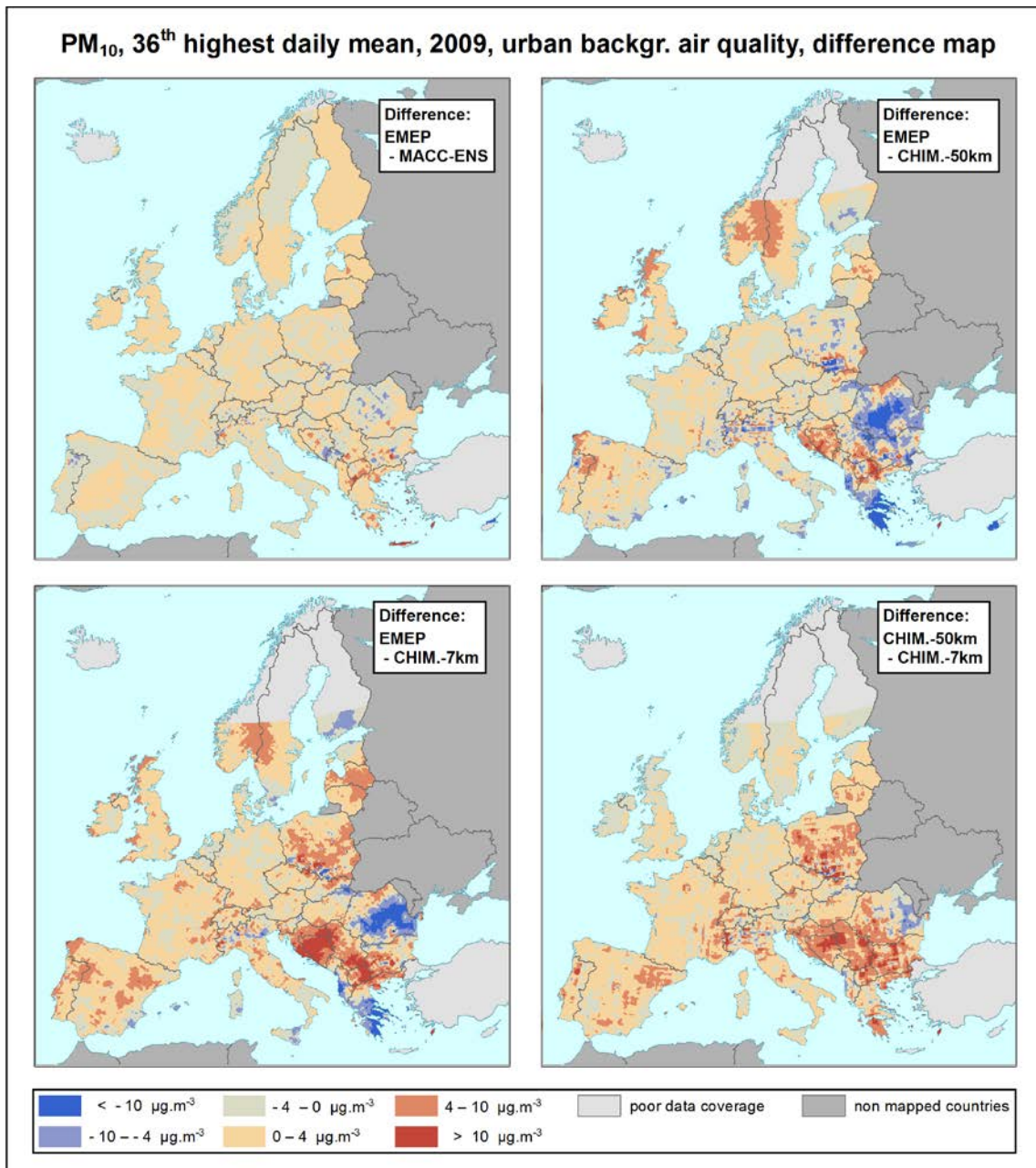


Figure A3.4 PM₁₀ indicator 36th highest daily mean for 2009, urban background air quality, difference of the ETC/ACM mapping results using EMEP and MACC-II Ensemble (upper left), EMEP and CHIMERE-EC4MACS_50km (upper right), EMEP and CHIMERE-EC4MACS_7km (lower left) and CHIMERE-EC4MACS_50km and CHIMERE-EC4MACS_7km (lower right). *Note: Applicable for urban areas only.*

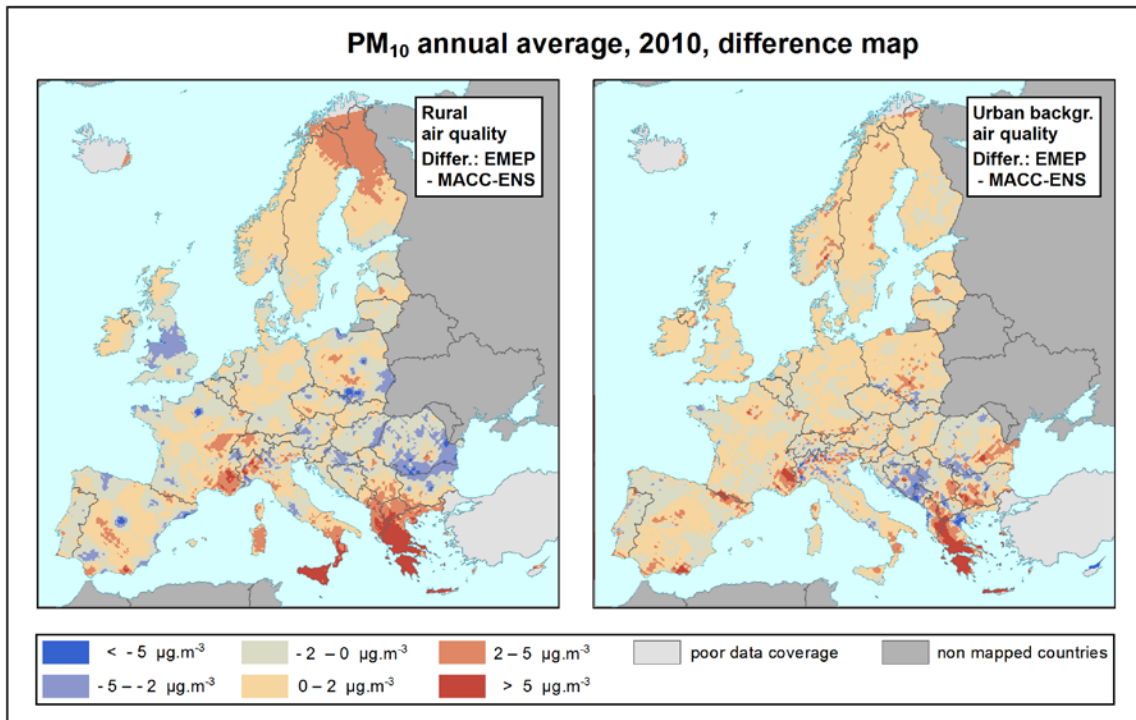


Figure A3.5 PM₁₀ annual average for 2010, difference of the ETC/ACM mapping results using EMEP and MACC-II Ensemble for rural (left) and urban background (right) maps. *Note: Applicable for rural (left), resp. urban (right) areas only.*

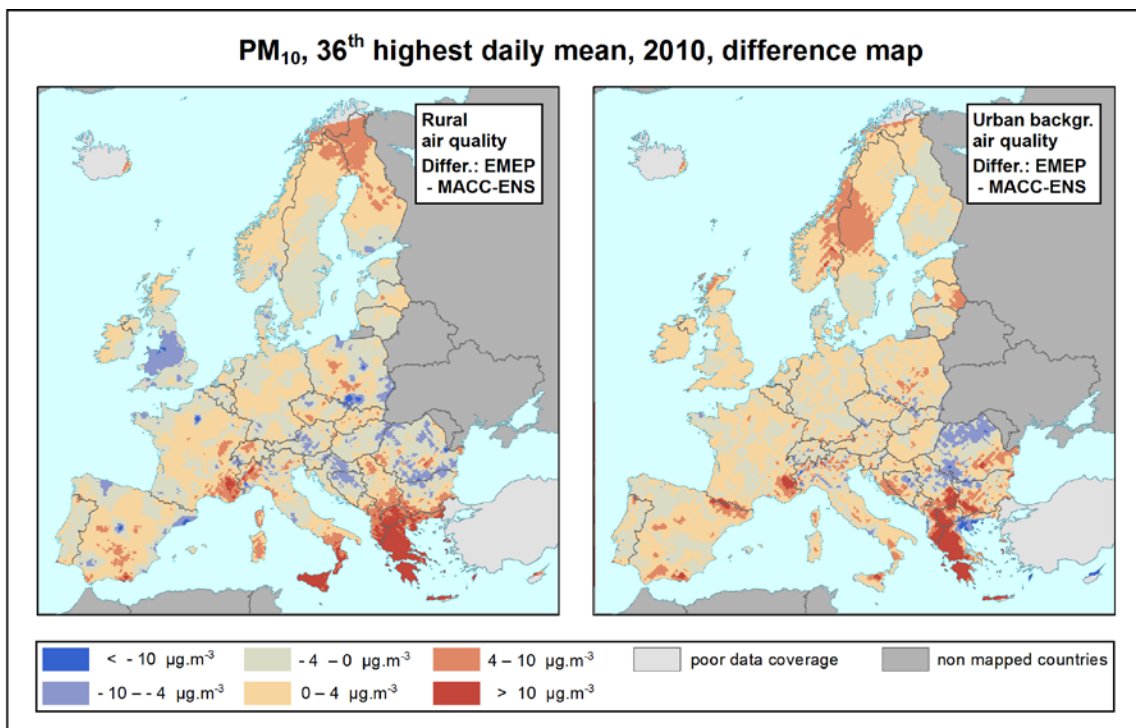


Figure A3.6 PM₁₀ indicator 36th highest daily mean for 2010, difference of the ETC/ACM mapping results using EMEP and MACC-II Ensemble for rural (left) and urban background (right) maps. *Note: Applicable for rural (left), resp. urban (right) areas only.*

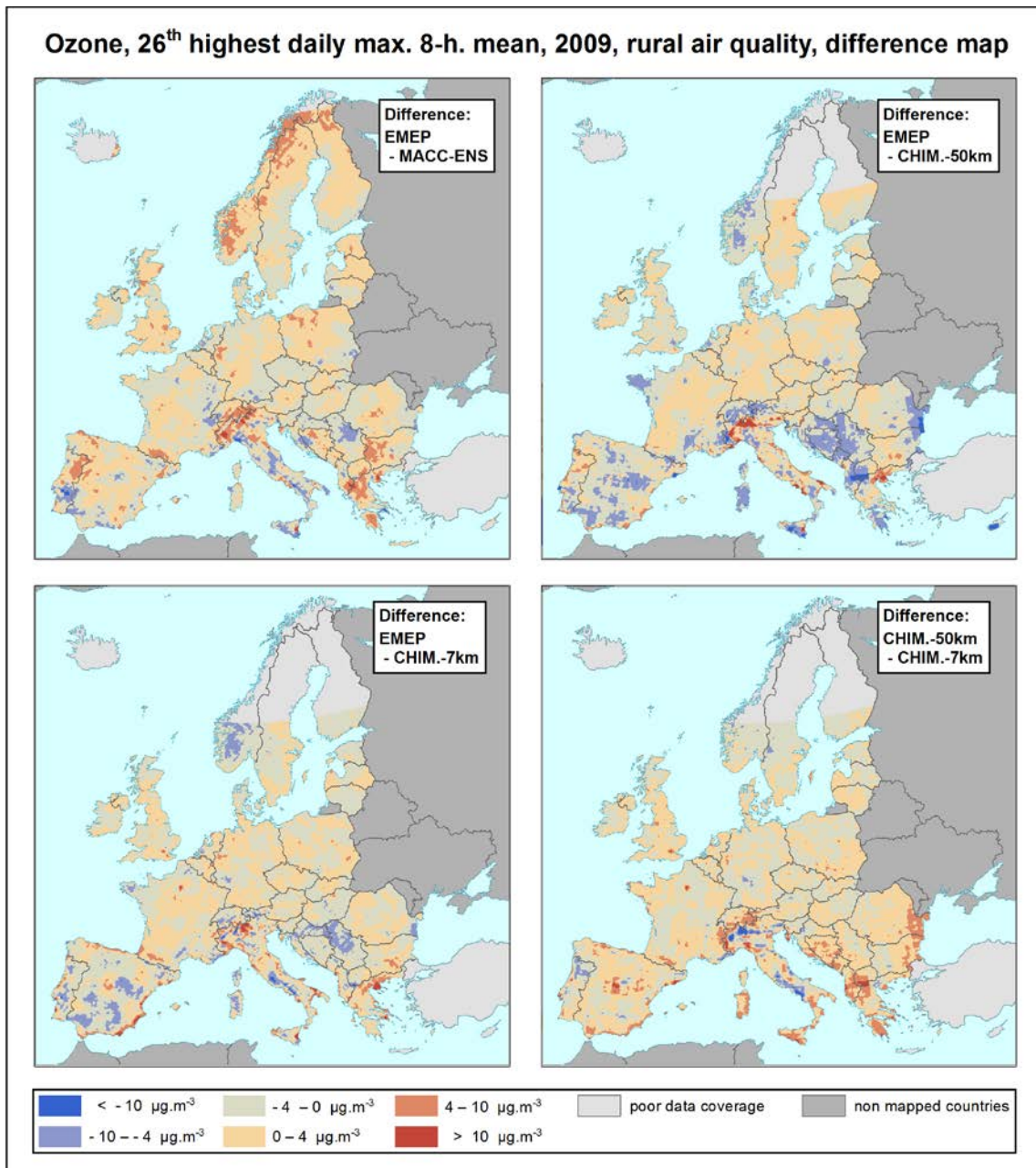


Figure A3.7 Ozone indicator 26th highest daily maximum 8-hourly mean for 2009, rural air quality, difference of the ETC/ACM mapping results using EMEP and MACC-II Ensemble (upper left), EMEP and CHIMERE-EC4MACS_50km (upper right), EMEP and CHIMERE-EC4MACS_7km (lower left) and CHIMERE-EC4MACS_50km and CHIMERE-EC4MACS_7km (lower right). *Note: Applicable for rural areas only.*

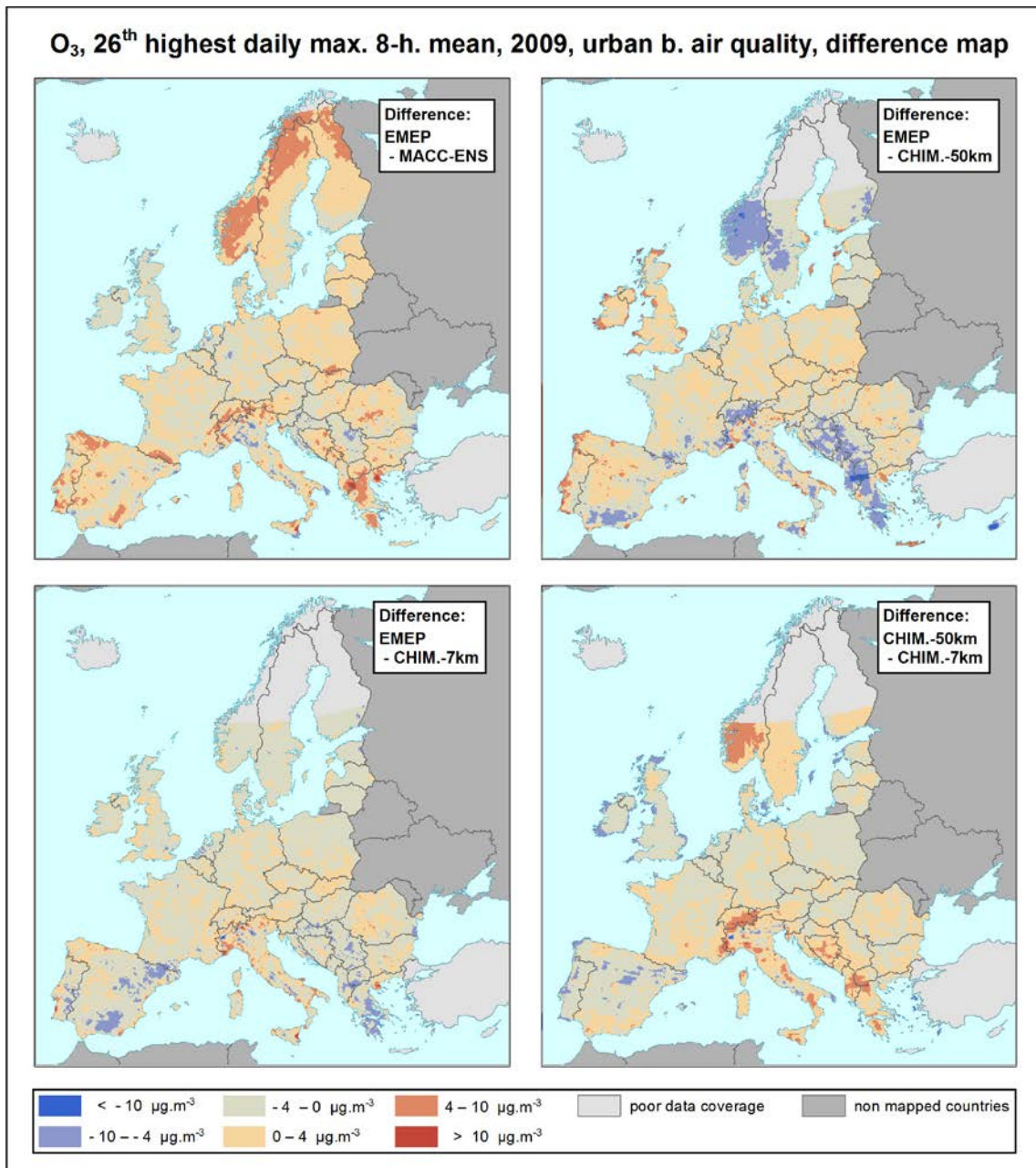


Figure A3.8 Ozone indicator 26th highest daily maximum 8-hourly mean for 2009, urban background air quality, difference of the ETC/ACM mapping results using EMEP and MACC-II Ensemble (upper left), EMEP and CHIMERE-EC4MACS_50km (upper right), EMEP and CHIMERE-EC4MACS_7km (lower left) and CHIMERE-EC4MACS_50km and CHIMERE-EC4MACS_7km (lower right). *Note: Applicable for urban areas only.*

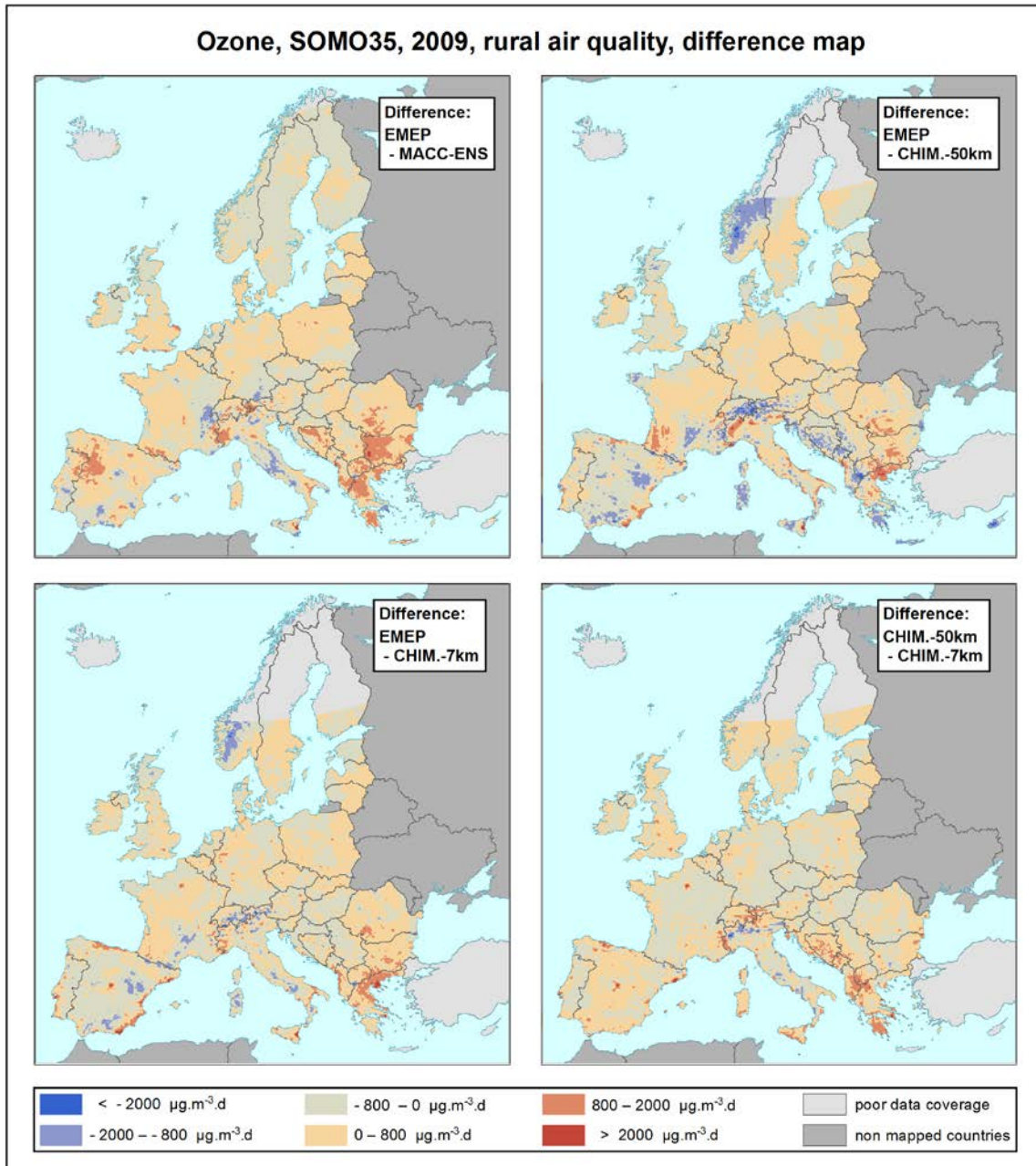


Figure A3.9 Ozone indicator SOMO35 for 2009, rural air quality, difference of the ETC/ACM mapping results using EMEP and MACC-II Ensemble (upper left), EMEP and CHIMERE-EC4MACS_50km (upper right), EMEP and CHIMERE-EC4MCS_7km (lower left) and CHIMERE-EC4MACS_50km and CHIMERE-EC4MACS_7km (lower right). *Note: Applicable for rural areas only.*

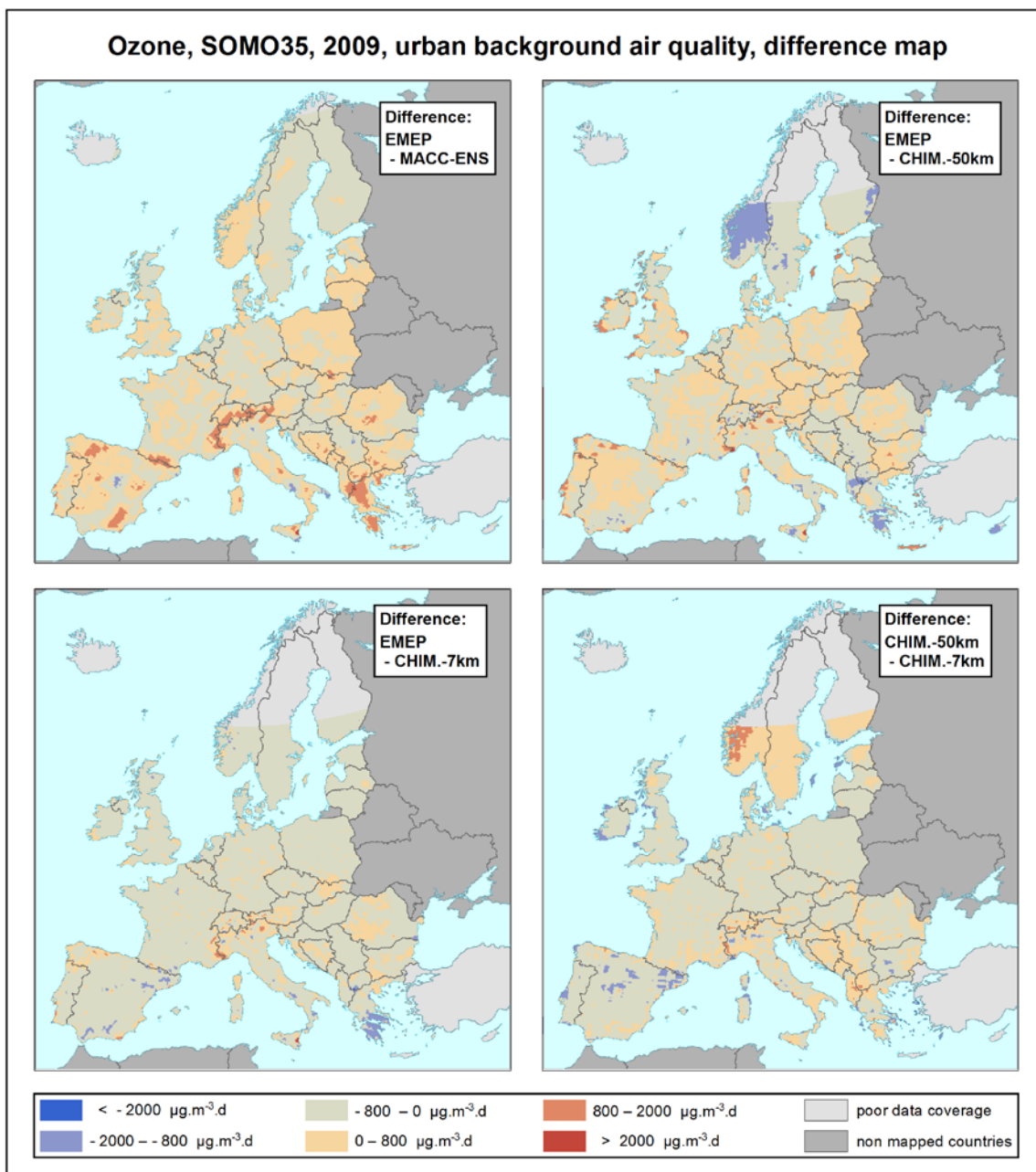


Figure A3.10 Ozone indicator SOMO35 for 2009, urban background air quality, difference of the ETC/ACM mapping results using EMEP and MACC-II Ensemble (upper left), EMEP and CHIMERE-EC4MACS_50km (upper right), EMEP and CHIMERE-EC4MACS_7km (lower left) and CHIMERE-EC4MACS_50km and CHIMERE-EC4MACS_7km (lower right). *Note: Applicable for urban areas only.*

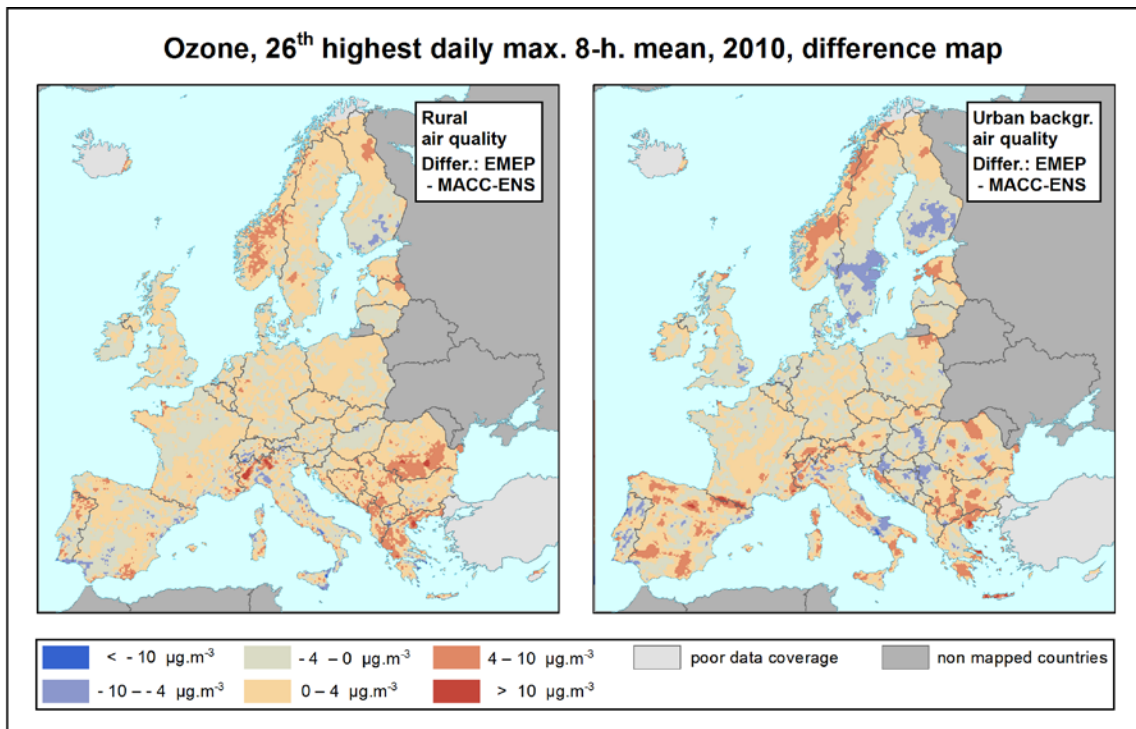


Figure A3.11 Ozone indicator 26th highest daily maximum 8-hourly mean for 2010, difference of the ETC/ACM mapping results using EMEP and MACC-II Ensemble for rural (left) and urban background (right) maps.
Note: Applicable for rural (left), resp. urban (right) areas only.

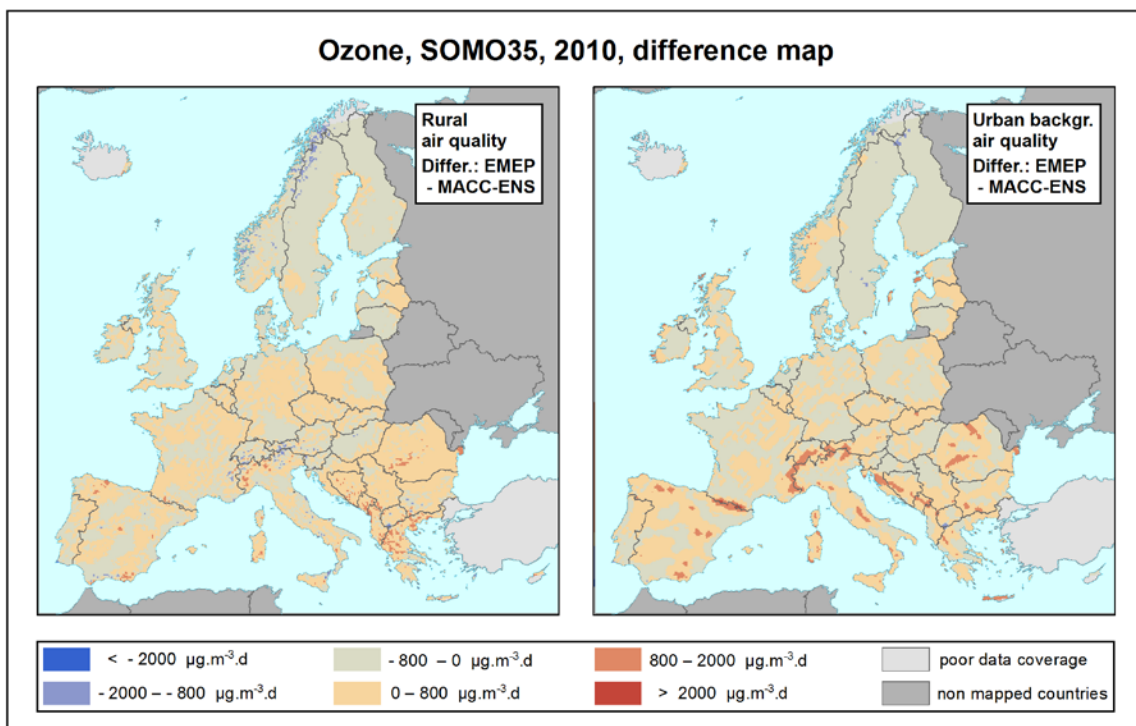


Figure A3.12 Ozone indicator SOMO35 for 2010, difference of the ETC/ACM mapping results using EMEP and MACC-II Ensemble for rural (left) and urban background (right) maps. *Note: Applicable for rural (left), resp. urban (right) areas only.*

Annex 4. Outputs of chemical transport models

In the paper, the outputs of the chemical transport models are used (see Section 3.2). Chapter 4 shows the ETC/ACM mapping results using different model outputs, while Section 5.1 compares the model outputs with the ETC/ACM maps. In both Chapter 4 and Section 5.1, the hindcasts (i.e. model outputs without any data assimilation) are used. This annex presents the *hindcast* outputs of several chemical transport models, that served as supplementary input in the ETC/ACM mapping method as dealt with in Chapter 4 and Section 5.1. (For the *reanalysis*, i.e. data assimilated model results, see Section 5.2, Figures 5.7, 5.8, 5.11 and 5.12.) Figures A4.1 to A4.4 show the model outputs for PM₁₀ and Figures A4.5 to A4.8 show it for ozone.

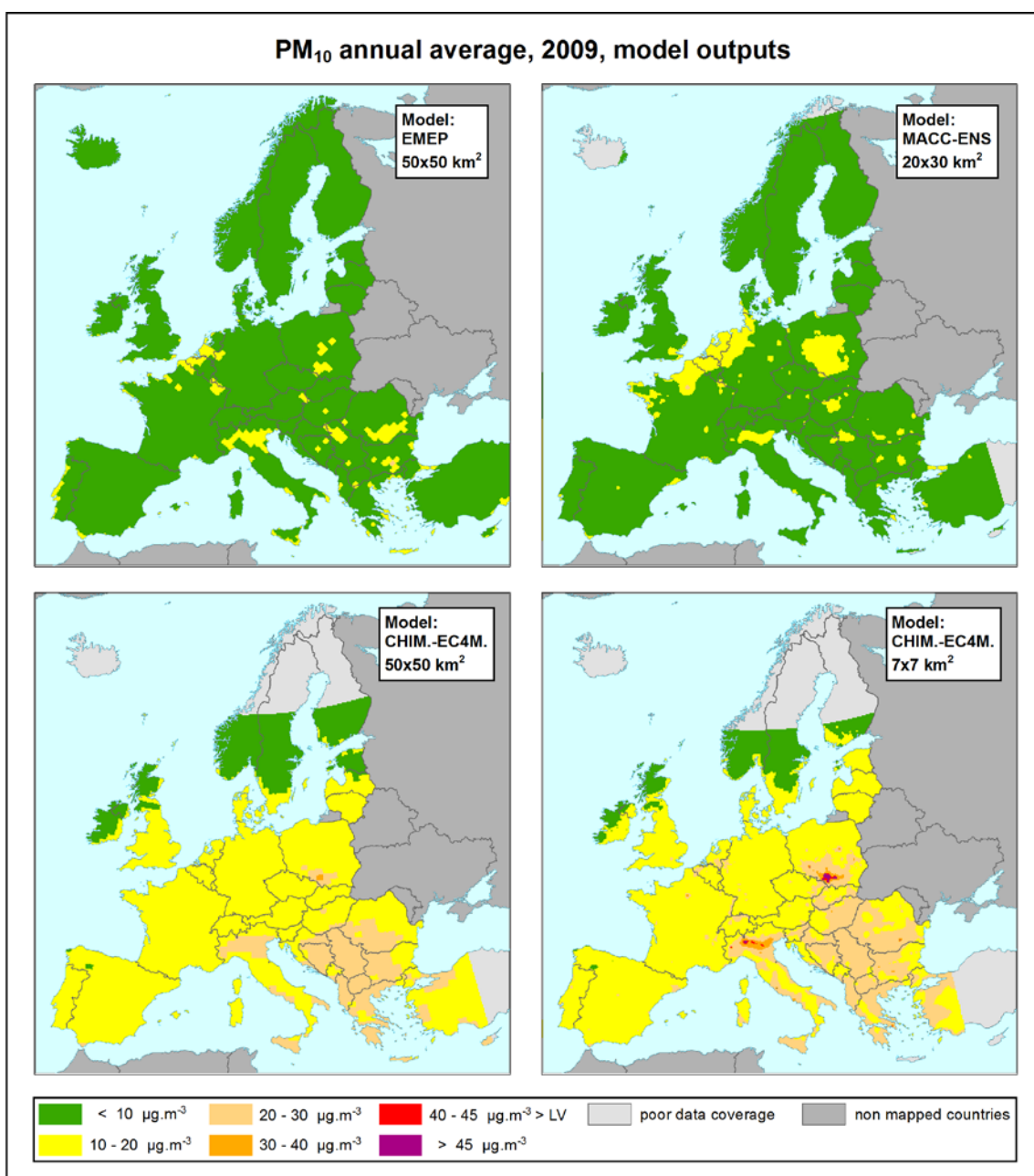


Figure A4.1 PM₁₀ annual average for 2009, model outputs for EMEP (upper left), MACC-II Ensemble (upper right), CHIMERE-EC4MACS_50km (lower left) and CHIMERE-EC4MACS_7km (lower right)

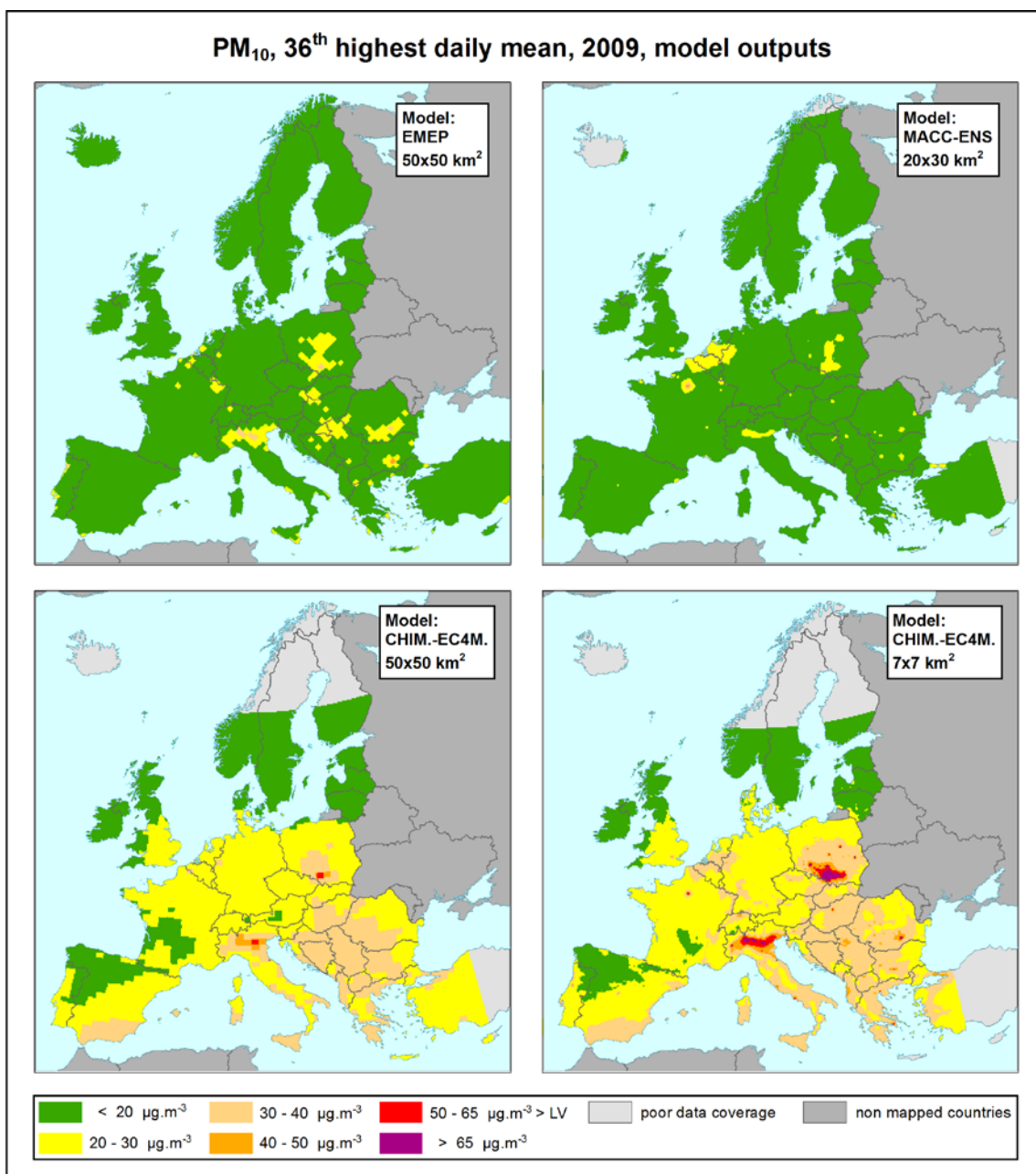


Figure A4.2 PM₁₀ indicator 36th highest daily mean for 2009, model outputs for EMEP (upper left), MACC-II Ensemble (upper right), CHIMERE-EC4MACS_50km (lower left) and CHIMERE-EC4MACS_7km (lower right)

It should be noted that each modelling output is converted into one and the same spatial resolution of a 10x10 km² grid, independently of their original modelling output (see Section 3.2).

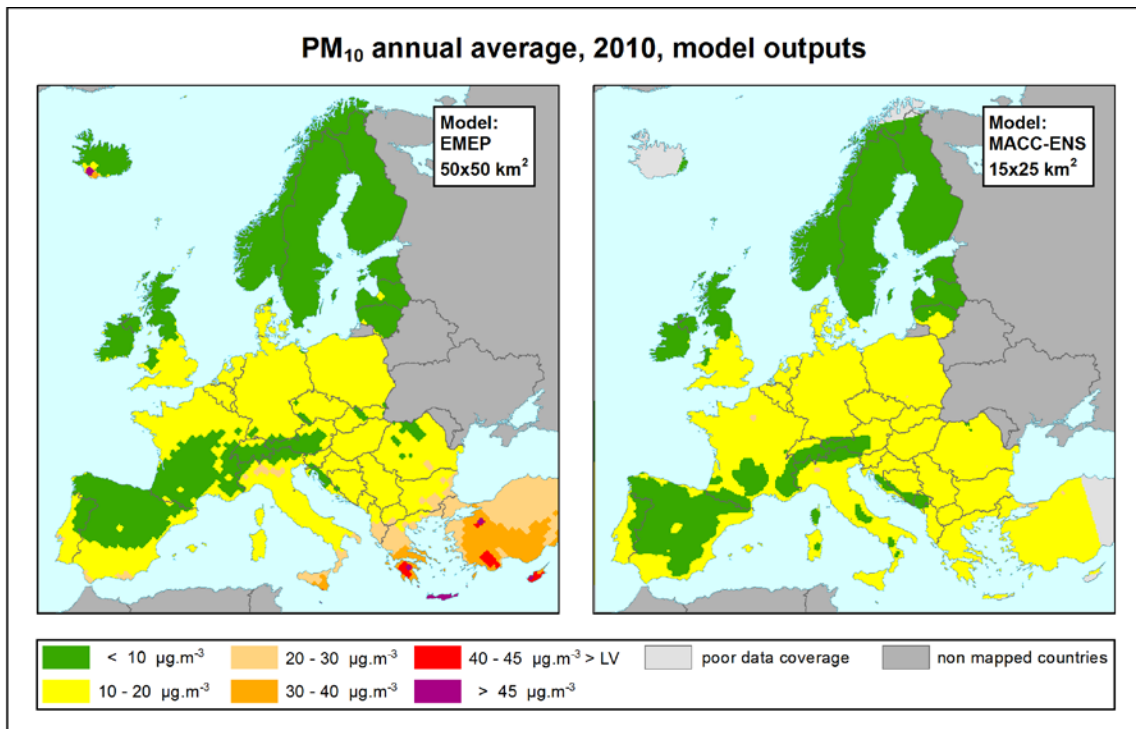


Figure A4.3 PM₁₀ annual average for 2010, model outputs for EMEP (left) and MACC-II Ensemble (right)

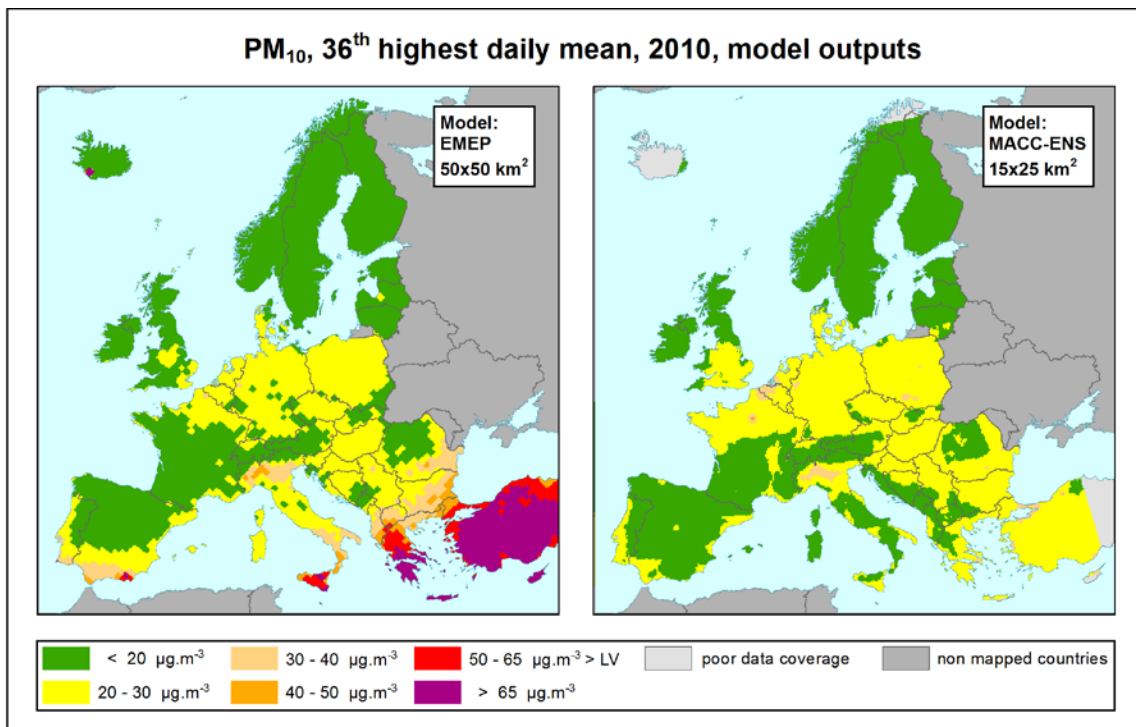


Figure A4.4 PM₁₀ indicator 36th highest daily mean for 2010, model outputs for EMEP (left) and MACC-II Ensemble (right)

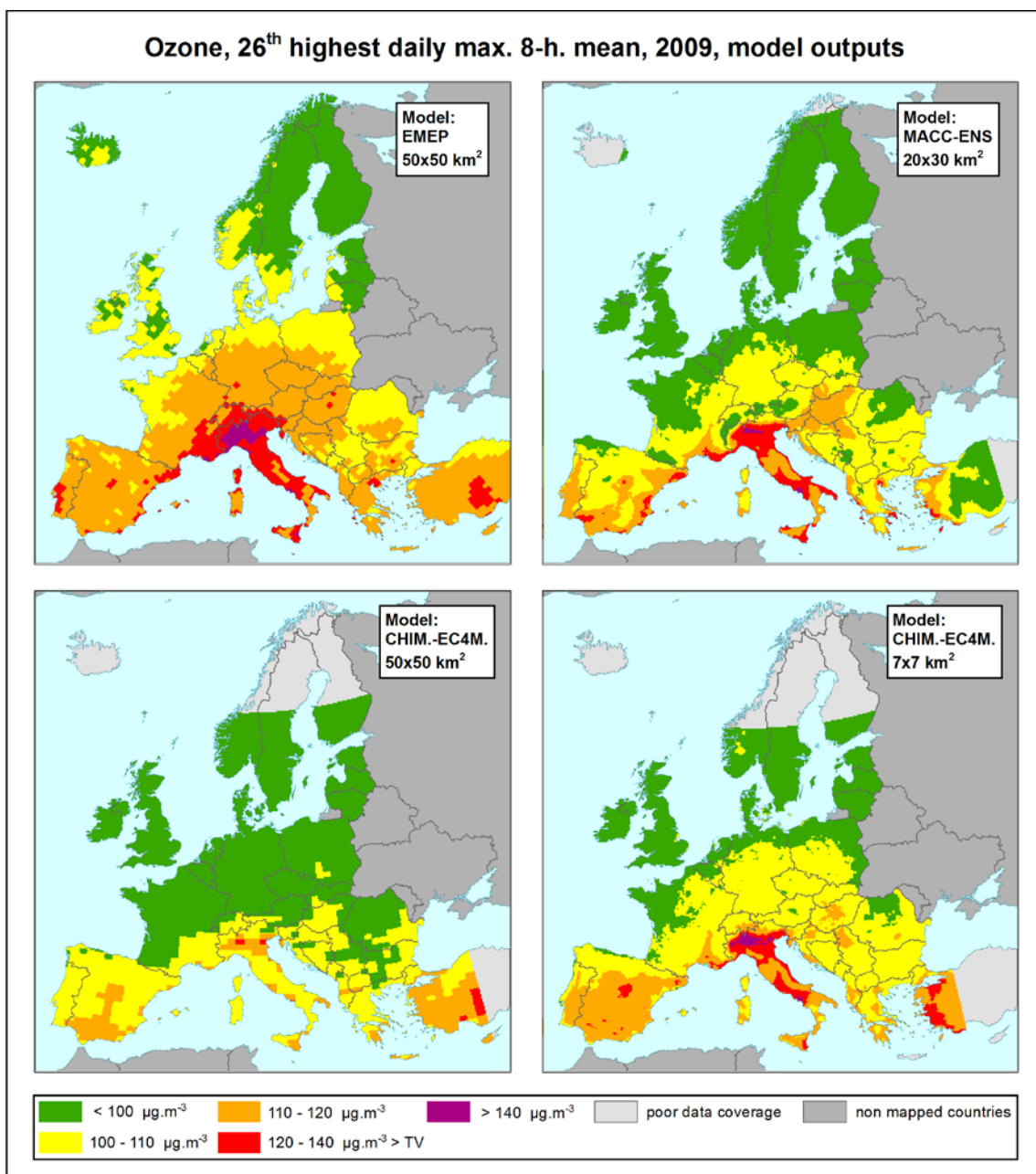


Figure A4.5 Ozone indicator 26th highest daily max. 8-hourly mean for 2009, model outputs for EMEP (upper left), MACC-II Ensemble (upper right), CHIMERE-EC4MACS_50km (lower left) and CHIMERE-EC4MACS_7km (lower right)

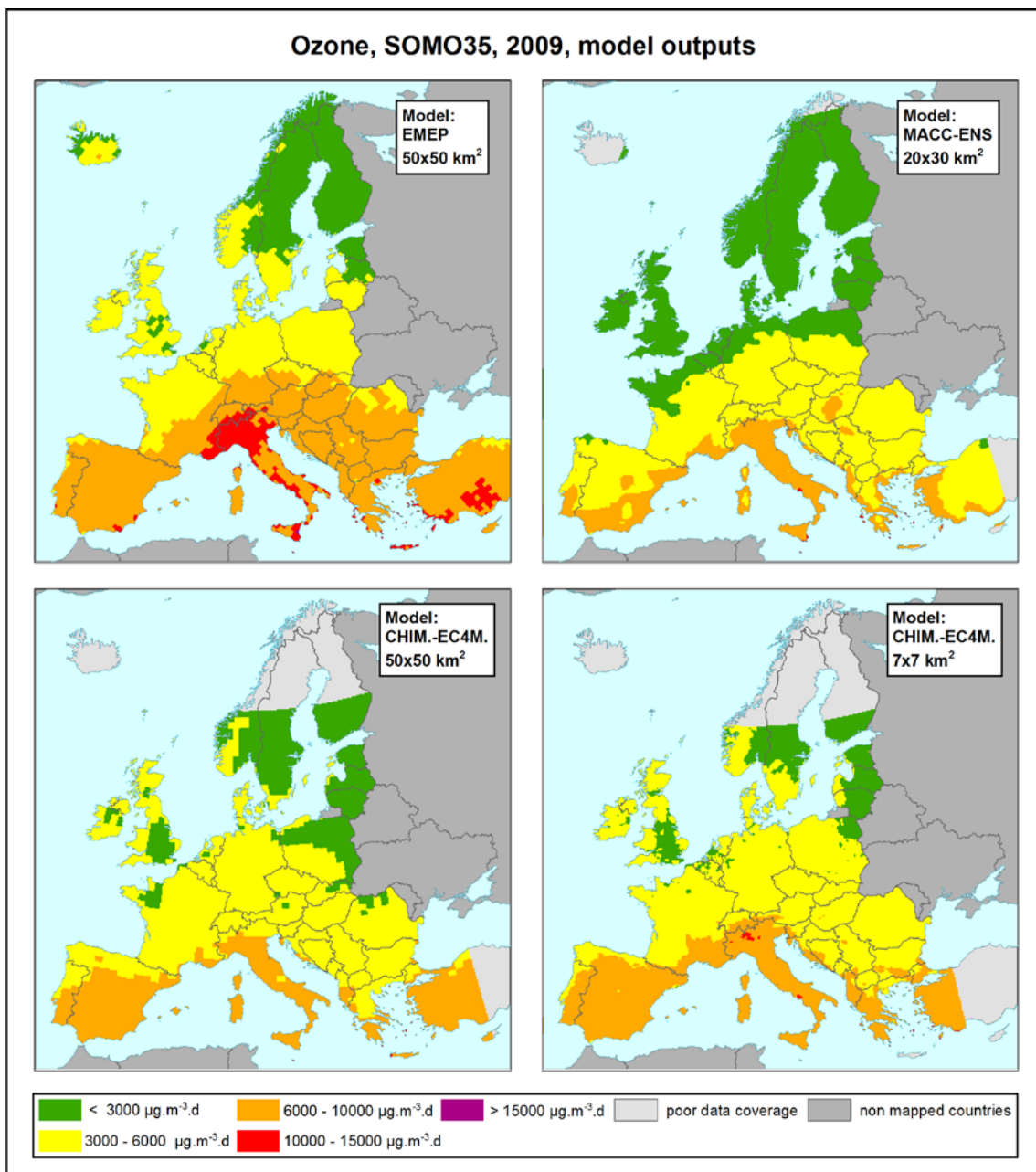


Figure A4.6 Ozone indicator SOMO35 for 2009, model outputs for EMEP (upper left), MACC-II Ensemble (upper right), CHIMERE-EC4MACS_50km (lower left) and CHIMERE-EC4MACS_7km (lower right).

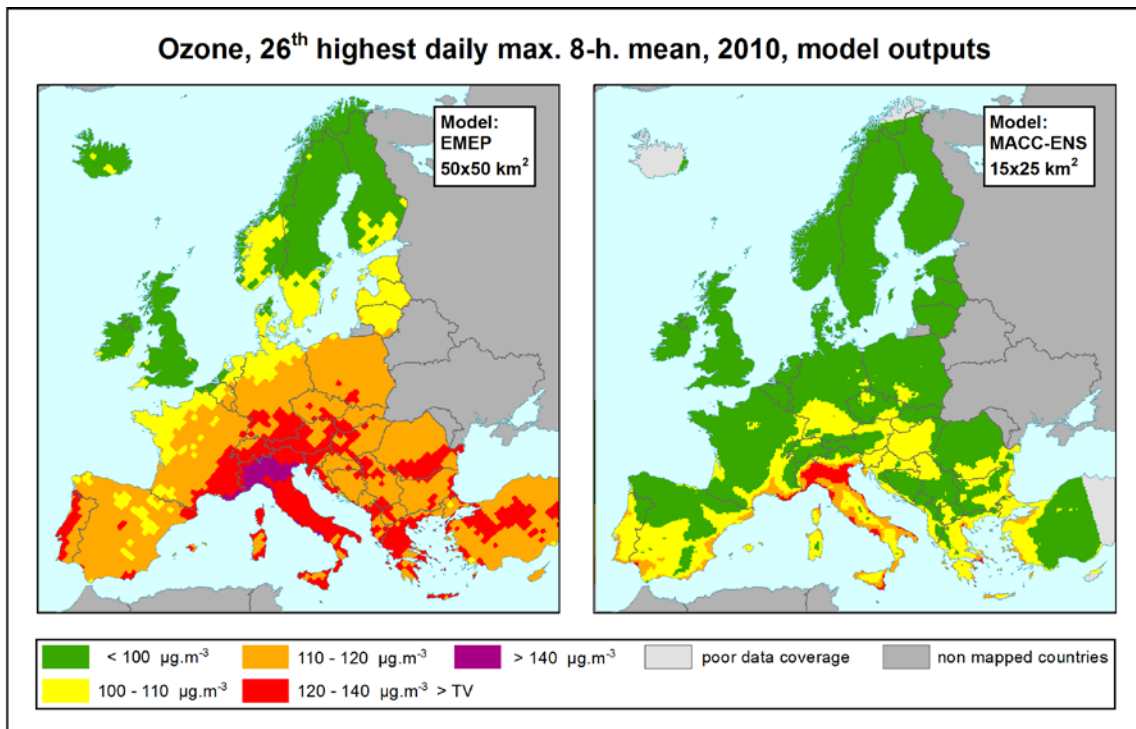


Figure A4.7 Ozone indicator 26th highest daily max. 8-hourly mean for 2010, model outputs for EMEP (left) and MACC-II Ensemble (right).

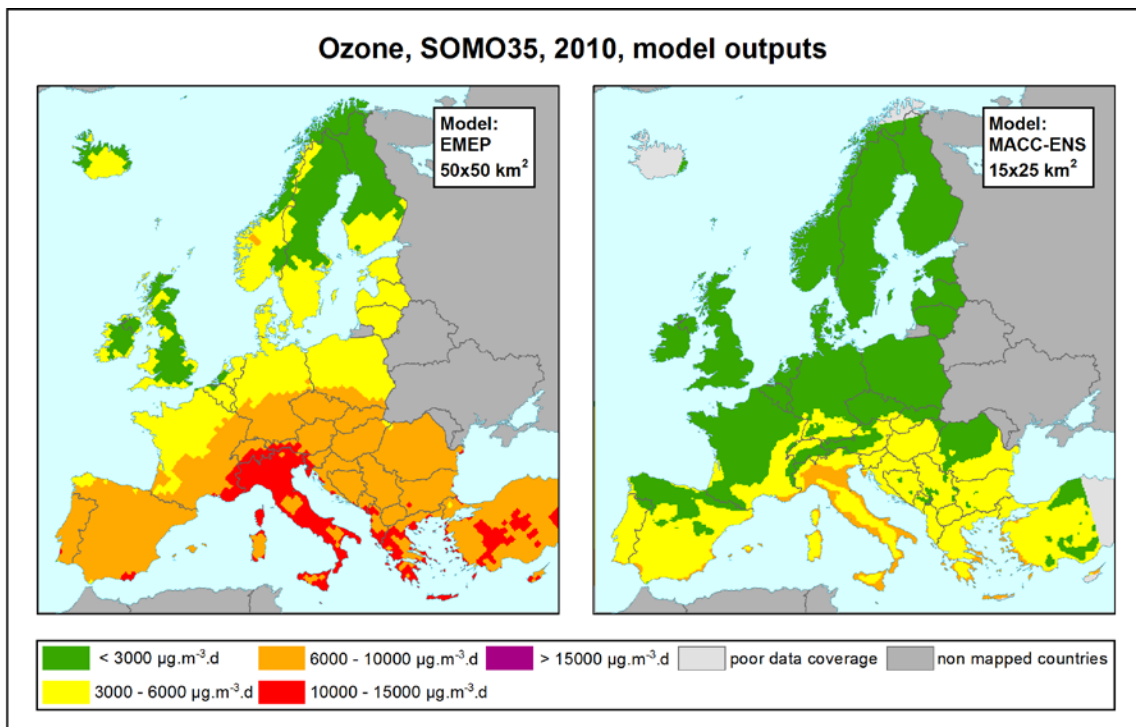


Figure A4.8 Ozone indicator SOMO35 for 2010, model outputs for EMEP (top) and MACC-II Ensemble (right).

Annex 5. Scatter plots and statistical indicators of modelled vs. measurement data

This annex contains scatter plots and statistical indicators showing the model performance results from the four chemical transport models in comparison with the measured data. The four models are compared separately for the rural background and urban/suburban background measurement data. These four chemical transport models are comparatively applied in the ETC/ACM mapping procedure to investigate their specific contribution to the resulting map quality (Chapter 4). The outputs of these models are presented in Chapter 4.

To guarantee comparability between the different models tested against the measurement data, each modelling output is converted into one and the same spatial resolution of a 10x10 km² grid, independently of their original modelling output (see Section 3.2). A common domain has been considered in the scatter plot comparison, namely the smaller model domain. This secures that only the data from measurement stations, which are covered by all the models are taken into account (see Section 3.3).

The statistical indicators for PM₁₀ are presented in Tables A5.1 and A5.2 and the scatter plots in Figures A5.1 to A5.8. Tables A5.3 and A5.4 present the statistical indicators for ozone and Figures A5.9 to A5.16 shows the scatter plots for the same pollutant.

A direct comparison of the model outputs for the years 2009 and 2010 against AirBase station data shows consistent differences between two years for both models. The major differences occur for EMEP, in the case of PM₁₀. The R² for the PM₁₀ annual average at rural stations (Figures A5.1, top left, and A5.5, left) decreases with just 0.05 from 0.27 in 2009 to 0.22 in 2010. For the urban background stations at PM₁₀ annual averages (Figures A5.2, top left, and A5.6, left) the R² increased from 0.03 in 2009 to 0.37 in 2010. A comparable behaviour is found at the 36th highest daily mean. The EMEP modelled the 36th highest daily mean output gave when comparing with rural background stations a R² of 0.30 in 2009 (Figure A5.3, top left) and R² of 0.17 in 2010 (Figure A5.7, left). This is not within the same order of magnitude to the change observed at the rural background annual averages, but at least in identical direction. For urban background stations a low R² of 0.03 in 2009 (Figure A5.4, top left) and considerably increased R² of 0.34 in 2010 (Figure A5.8, left) is found.

The significant changes in model performance at urban stations found for the EMEP model between 2009 and 2010 for both the PM₁₀ annual averages and the 36th highest daily mean were briefly discussed with EMEP research scientists. They indicated that significant changes had been made to the aerosol component of the model between 2009 and 2010. In 2010 processes leading to the formation of secondary organic aerosols (SOAs) were introduced, and further increased the sulphate formation as a consequence of a change in cloud water pH. Further investigations will be necessary to clarify why this appears to primarily affect the urban sites as the current results indicate.

In the case of ozone, the results for EMEP show different bias for different years, see Tables A5.3 and A5.4. The reason probably lies also in the improvements of the EMEP model.

The changes of performance of MACC-II Ensemble model between 2009 and 2010 are probably mainly caused by the different set of the individual models included in the ensemble, see Section 3.2, point B, paragraph *b*.

Table A5.1 Statistical indicators for different chemical transport models outputs against measurement data – PM₁₀, 2009

chemical transport model	PM ₁₀ annual average, 2009							
	rural				urban background			
	RMSE	bias	R ²	regr. equation	RMSE	bias	R ²	regr. equation
EMEP, 50x50	13.05	-11.63	0.254	y = 0.182x + 4.17	22.12	-19.50	0.074	y = 0.067x + 6.73
MACC-ENS, 20x30	12.49	-11.02	0.261	y = 0.192x + 4.60	21.36	-18.51	0.042	y = 0.056x + 7.96
CHIMERE-EC4M., 50x50	6.45	-3.67	0.348	y = 0.258x + 10.67	14.48	-11.13	0.332	y = 0.190x + 11.65
CHIMERE-EC4M., 7x7	5.36	-2.12	0.474	y = 0.414x + 9.21	12.19	-7.01	0.224	y = 0.348x + 11.32
chemical transport model	PM ₁₀ 36 th highest value, 2009							
	rural				urban background			
	RMSE	bias	R ²	regr. equation	RMSE	bias	R ²	regr. equation
EMEP, 50x50	20.44	-17.75	0.296	y = 0.211x + 8.37	36.87	-30.92	0.089	y = 0.073x + 13.53
MACC-ENS, 20x30	21.26	-18.52	0.254	y = 0.173x + 8.84	37.43	-31.25	0.040	y = 0.050x + 14.29
CHIMERE-EC4M., 50x50	12.31	-7.15	0.353	y = 0.259x + 17.02	27.70	-20.54	0.268	y = 0.151x + 20.17
CHIMERE-EC4M., 7x7	9.65	-4.92	0.527	y = 0.444x + 13.45	23.86	-12.70	0.199	y = 0.357x + 18.16

Table A5.2 Statistical indicators for different chemical transport models outputs against measurement data – PM₁₀, 2010

chemical transport model	PM ₁₀ annual average, 2010							
	rural				urban background			
	RMSE	bias	R ²	regr.equation	RMSE	bias	R ²	regr.equation
EMEP, 50x50	10.00	-7.70	0.223	y = 0.242x + 7.30	18.64	-13.31	0.369	y = 0.260x + 6.48
MACC-ENS, 15x25	9.34	-7.15	0.347	y = 0.223x + 8.26	18.27	-14.00	0.145	y = 0.098x + 11.14
chemical transport model	PM ₁₀ 36 th highest value, 2010							
	rural				urban background			
	RMSE	bias	R ²	regr. equation	RMSE	bias	R ²	regr. equation
EMEP, 50x50	18.12	-14.95	0.174	y = 0.199x + 15.02	31.12	-24.12	0.343	y = 0.335x + 9.60
MACC-ENS, 15x25	19.02	-14.98	0.296	y = 0.174x + 15.88	35.27	-26.77	0.122	y = 0.075x + 20.12

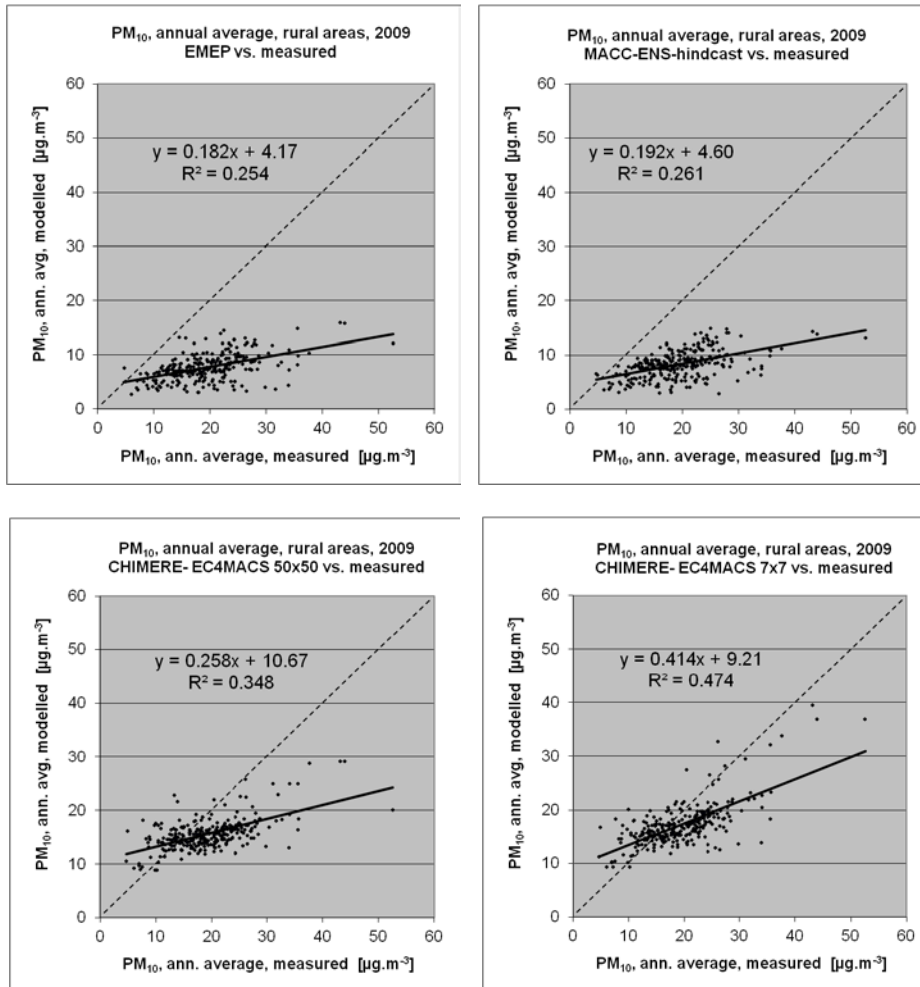


Figure A5.1 Scatter plots showing modelled vs. rural background measured data for EMEP (upper left), MACC-II Ensemble (upper right), CHIMERE-EC4MACS_50km (lower left) and CHIMERE-EC4MACS_7km (lower right) model outputs for PM₁₀ annual average 2009

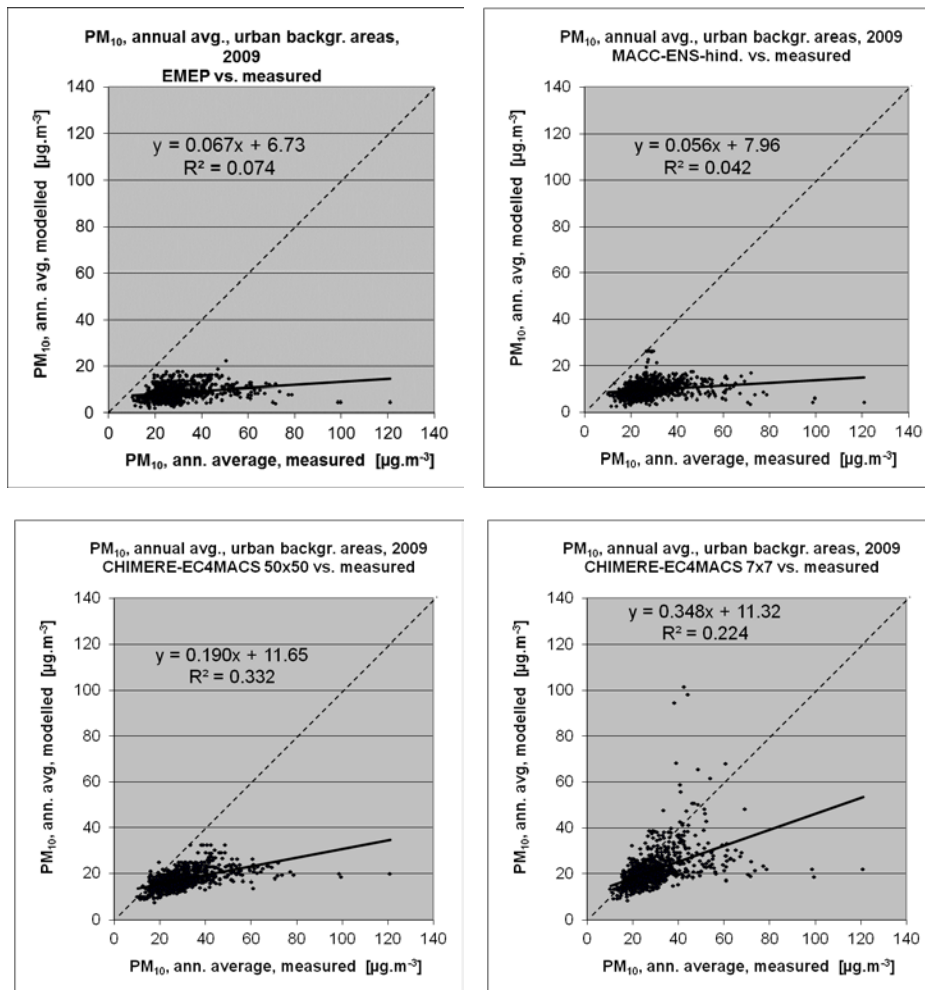


Figure A5.2 Scatter plots showing modelled vs. urban/suburban background measured data for EMEP (upper left), MACC-II Ensemble (upper right), CHIMERE-EC4MACS_50km (lower left) and CHIMERE-EC4MACS_7km (lower right) model outputs for PM₁₀ annual average 2009

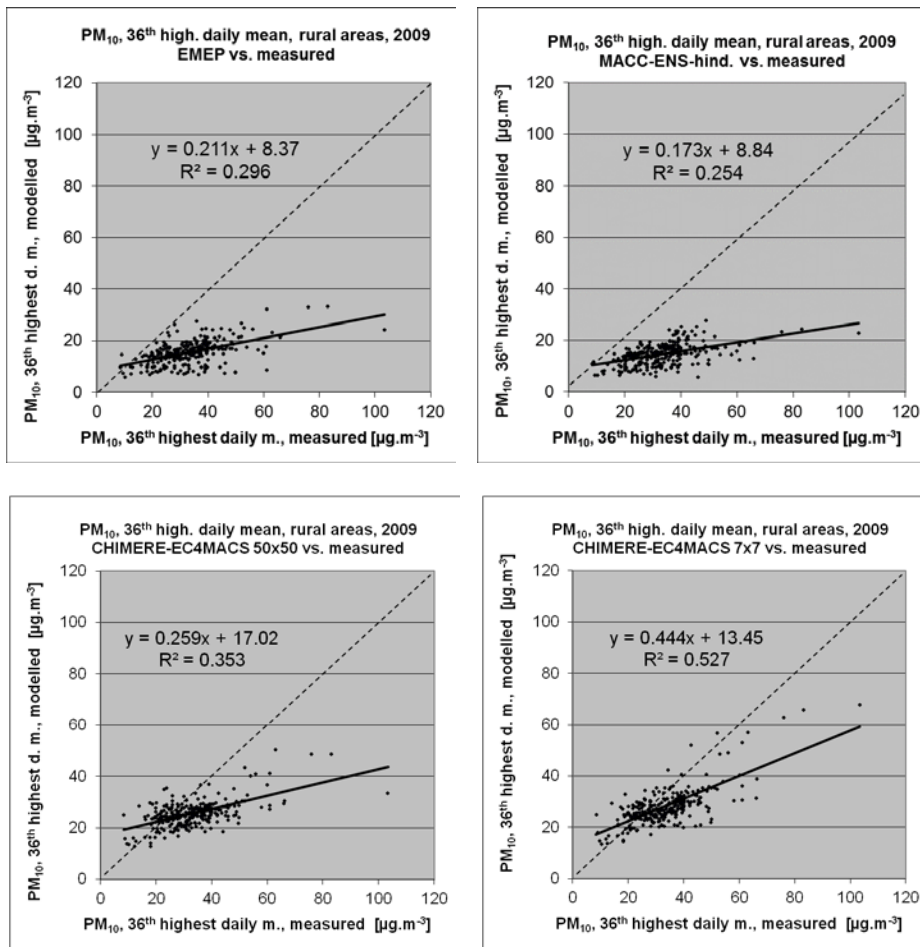


Figure A5.3 Scatter plots showing modelled vs. rural background measured data for EMEP (upper left), MACC-II Ensemble (upper right), CHIMERE-EC4MACS_50km (lower left) and CHIMERE-EC4MACS_7km (lower right) model outputs for PM₁₀ indicator 36th highest daily mean for 2009

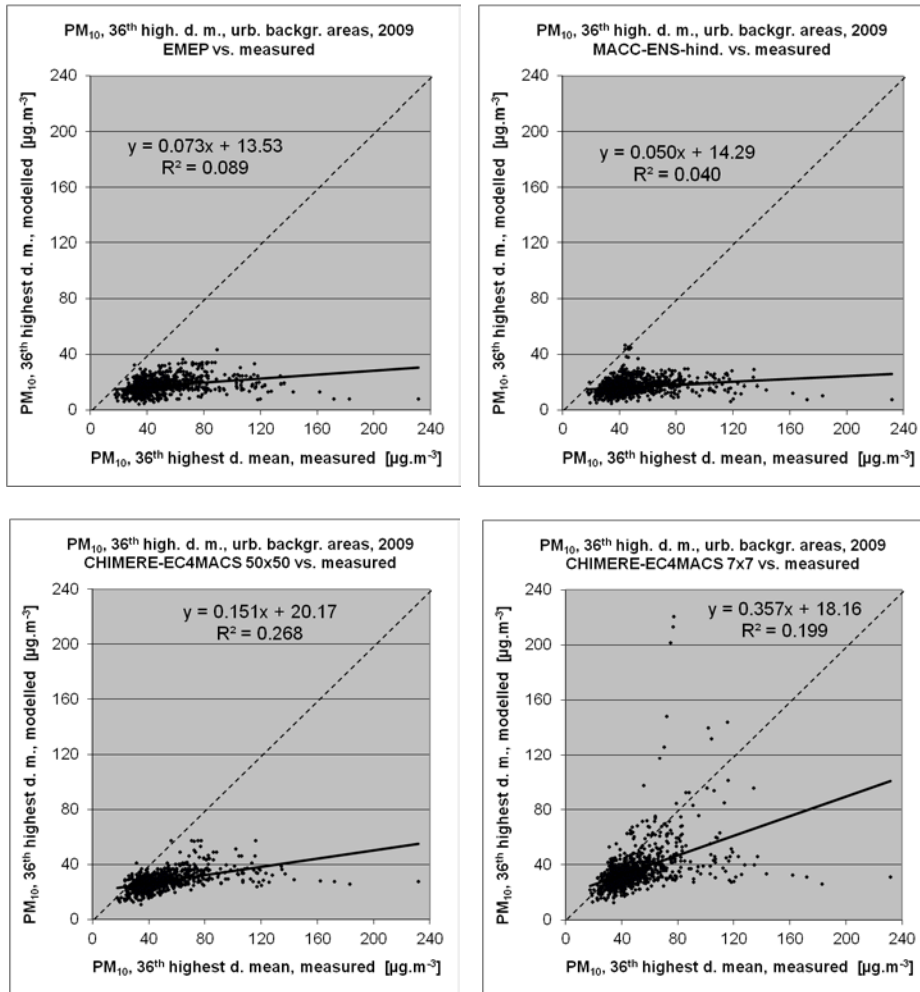


Figure A5.4 Scatter plots showing modelled vs. urban/suburban background measured data for EMEP (upper left), MACC-II Ensemble (upper right), CHIMERE-EC4MACS_50km (lower left) and CHIMERE-EC4MACS_7km (lower right) model outputs for PM₁₀ indicator 36th highest daily mean for 2009

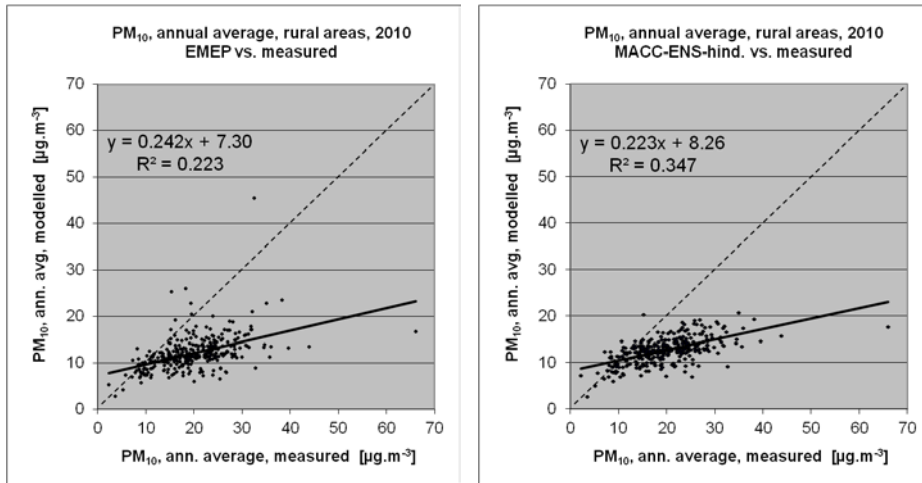


Figure A5.5 Scatter plots showing modelled vs. rural background measured data for EMEP (left) and MACC-II Ensemble (right) model outputs for PM₁₀ annual average 2010

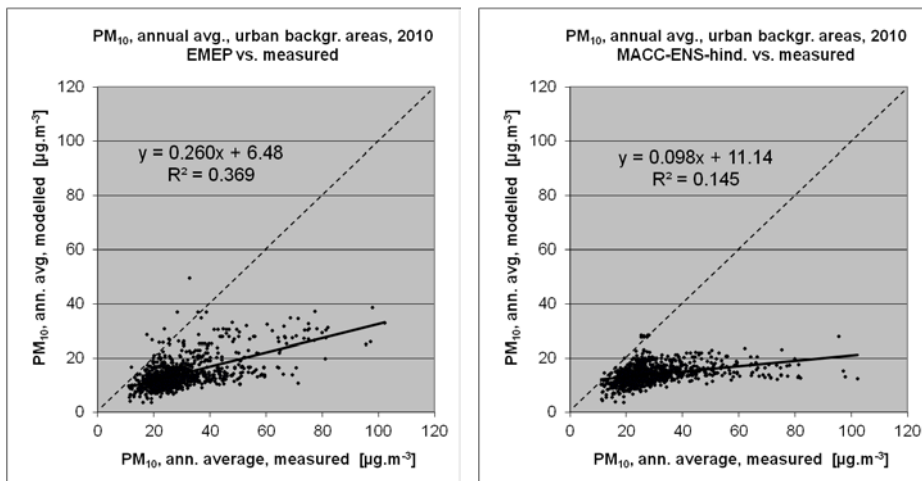


Figure A5.6 Scatter plots showing modelled vs. urban/suburban background measured data for EMEP (left) and MACC-II Ensemble (right) model outputs for PM₁₀ annual average 2010

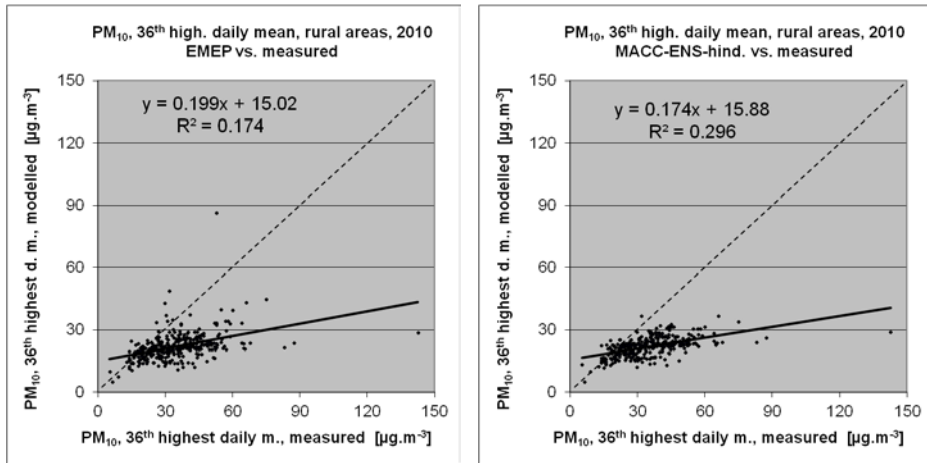


Figure A5.7 Scatter plots showing modelled vs. rural background measured data for EMEP (left) and MACC-II Ensemble (right) model outputs for PM₁₀ indicator 36th highest daily mean for 2010

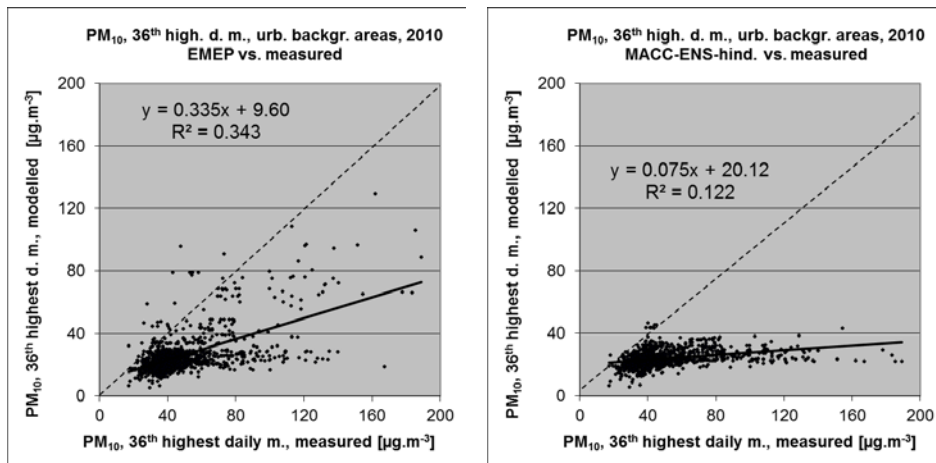


Figure A5.8 Scatter plots showing modelled vs. urban/suburban background measured data for EMEP (left) and MACC-II Ensemble (right) model outputs for PM₁₀ indicator 36th highest daily mean for 2010

Table A5.3 Statistical indicators for different chemical transport models outputs against measurement data – Ozone, 2009

chemical transport model	Ozone, 26 th highest daily 8-hourly maximum, 2009							
	rural				urban background			
	RMSE	bias	R ²	regr.equation	RMSE	bias	R ²	regr.equation
EMEP, 50x50	10.01	0.74	0.535	y = 0.587x + 48.24	12.79	6.06	0.505	y = 0.626x + 47.52
MACC-ENS, 20x30	14.24	-10.81	0.606	y = 0.690x + 24.85	11.96	-5.39	0.560	y = 0.691x + 28.92
CHIMERE-EC4M., 50x50	18.95	-14.61	0.333	y = 0.252x + 71.40	16.15	-9.70	0.325	y = 0.259x + 72.46
CHIMERE-EC4M., 7x7	13.35	-8.26	0.482	y = 0.513x + 47.79	12.07	-3.83	0.485	y = 0.597x + 40.87

chemical transport model	Ozone, SOMO35, 2009							
	rural				urban background			
	RMSE	bias	R ²	regr.equation	RMSE	bias	R ²	regr.equation
EMEP, 50x50	2084	1073	0.573	y = 0.684x + 2829	2923	2258	0.512	y = 0.765x + 3306
MACC-ENS, 20x30	2121	-1153	0.557	y = 0.589x + 1131	1626	90	0.570	y = 0.718x + 1349
CHIMERE-EC4M., 50x50	2482	-1222	0.344	y = 0.347x + 2408	1837	3	0.406	y = 0.454x + 2440
CHIMERE-EC4M., 7x7	1907	-267	0.499	y = 0.497x + 2527	1813	564	0.503	y = 0.627x + 2228

Table A5.4 Statistical indicators for different chemical transport models outputs against measurement data – Ozone, 2010

chemical transport model	Ozone, 26 th highest daily 8-hourly maximum, 2010							
	rural				urban background			
	RMSE	bias	R ²	regr.equation	RMSE	bias	R ²	regr.equation
EMEP, 50x50	11.05	1.44	0.523	y = 0.575x + 50.68	14.25	7.12	0.497	y = 0.607x + 51.30
MACC-ENS, 15x25	20.55	-17.03	0.470	y = 0.501x + 40.74	16.51	-10.78	0.461	y = 0.495x + 45.99

chemical transport model	Ozone, SOMO35, 2010							
	rural				urban background			
	RMSE	bias	R ²	regr.equation	RMSE	bias	R ²	regr.equation
EMEP, 50x50	2493	1569	0.523	y = 0.726x + 3054	3505	2895	0.491	y = 0.898x + 3337
MACC-ENS, 15x25	3097	-2348	0.395	y = 0.410x + 847	1802	-917	0.501	y = 0.608x + 775

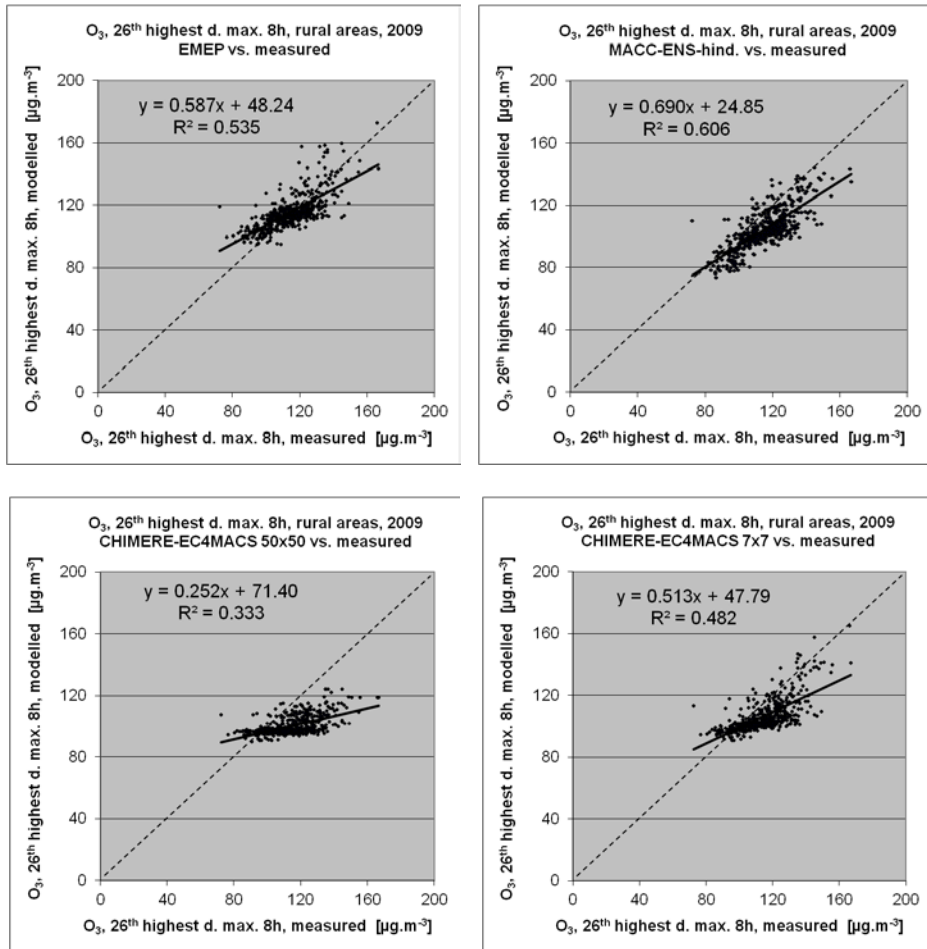


Figure A5.9 Scatter plots showing modelled vs. rural background measured data for EMEP (upper left), MACC-II Ensemble (upper right), CHIMERE-EC4MACS_50km (lower left) and CHIMERE-EC4MACS_7km (lower right) model outputs for ozone indicator 26th highest daily maximum 8-hourly mean for 2009

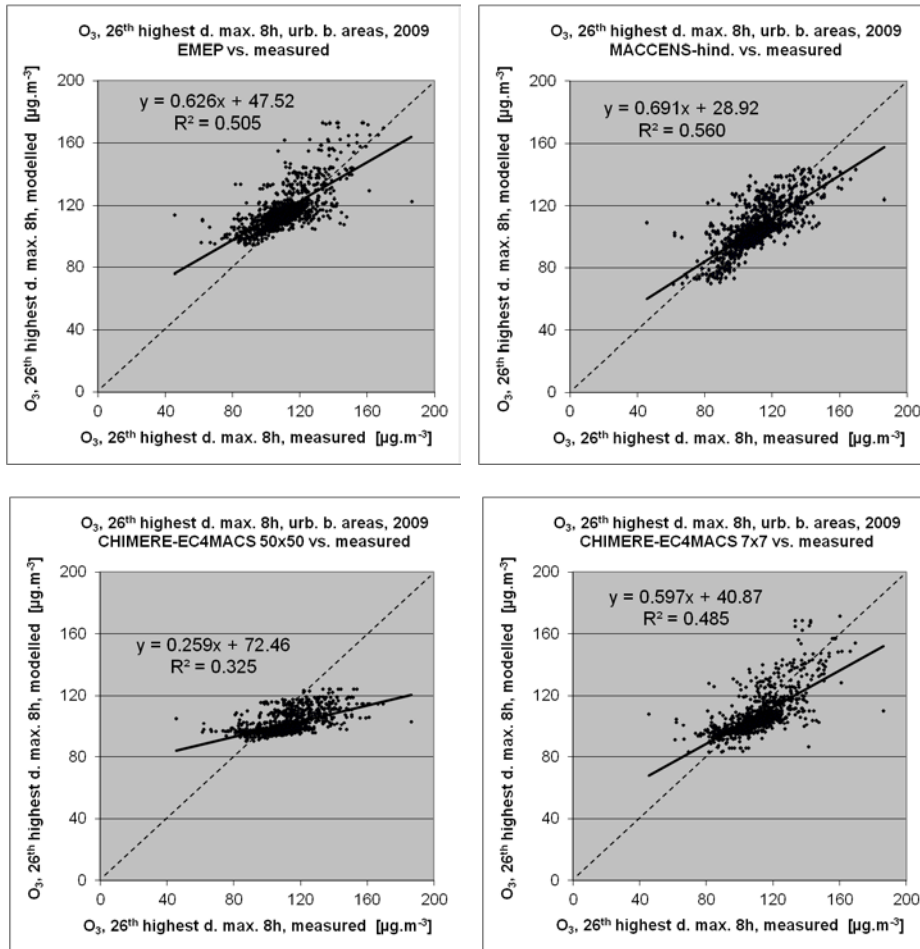


Figure A5.10 Scatter plots showing modelled vs. urban/suburban background measured data for EMEP (upper left), MACC-II Ensemble (upper right), CHIMERE-EC4MACS_50km (lower left) and CHIMERE-EC4MACS_7km (lower right) model outputs for ozone indicator 26th highest daily max. 8-hourly mean for 2009

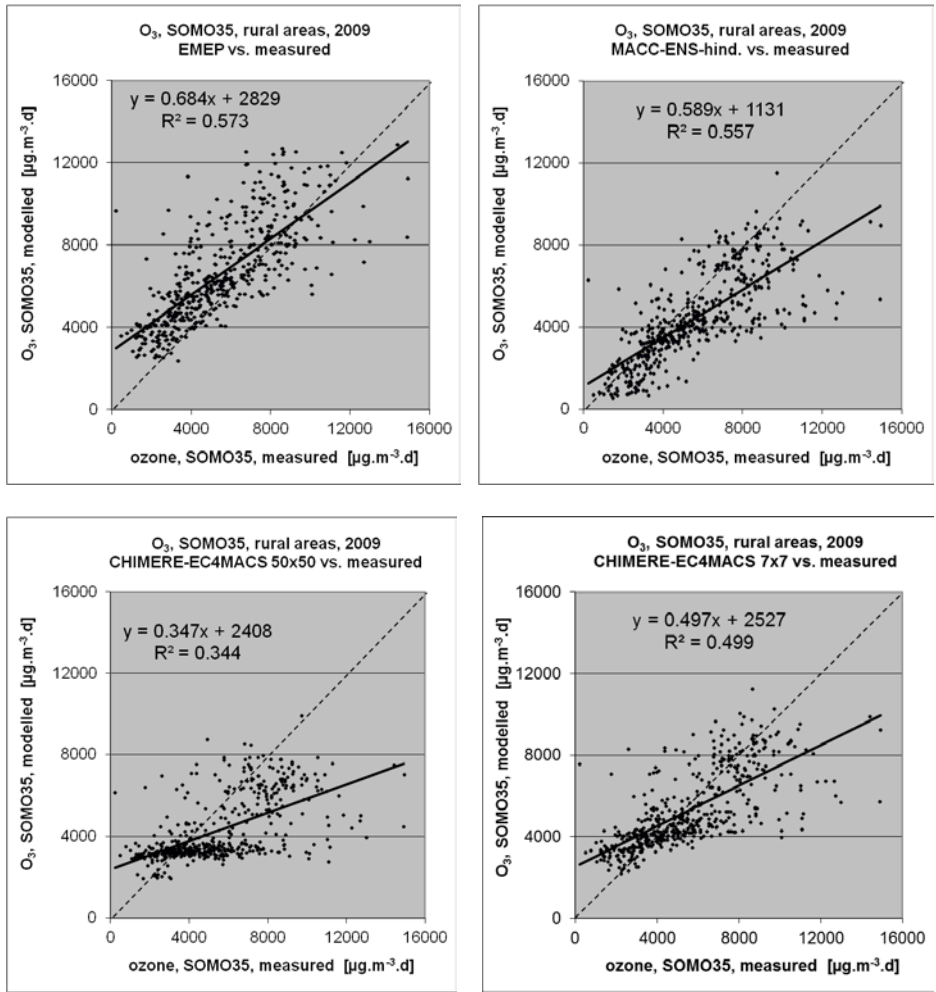


Figure A5.11 Scatter plots showing modelled vs. rural background measured data for EMEP (upper left), MACC-II Ensemble (upper right), CHIMERE-EC4MACS_50km (lower left) and CHIMERE-EC4MACS_7km (lower right) model outputs for ozone indicator SOMO35 for 2009

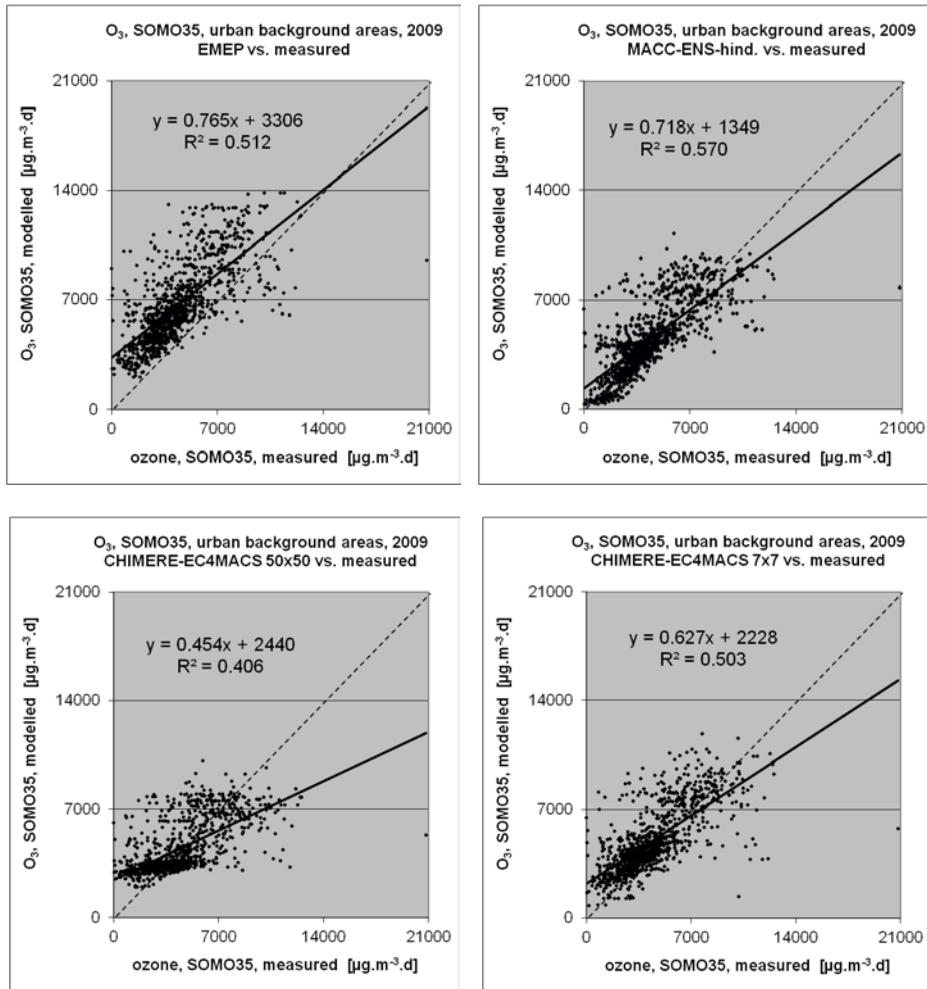


Figure A5.12 Scatter plots showing modelled vs. urban/suburban background measured data for EMEP (upper left), MACC-II Ensemble (upper right), CHIMERE-EC4MACS_50km (lower left) and CHIMERE-EC4MACS_7km (lower right) model outputs for ozone indicator SOMO35 for 2009

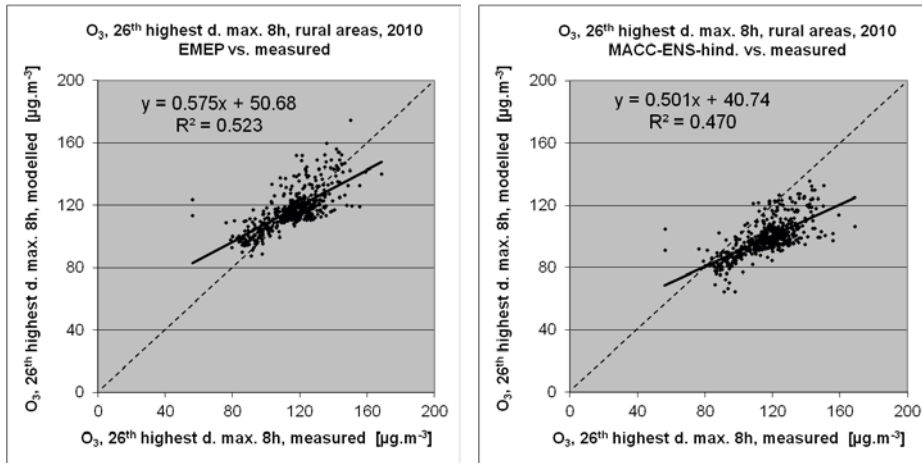


Figure A5.13 Scatter plots showing modelled vs. rural background measured data for EMEP (left) and MACC-II Ensemble (right) model outputs for ozone indicator 26th highest daily maximum 8-hourly mean for 2010

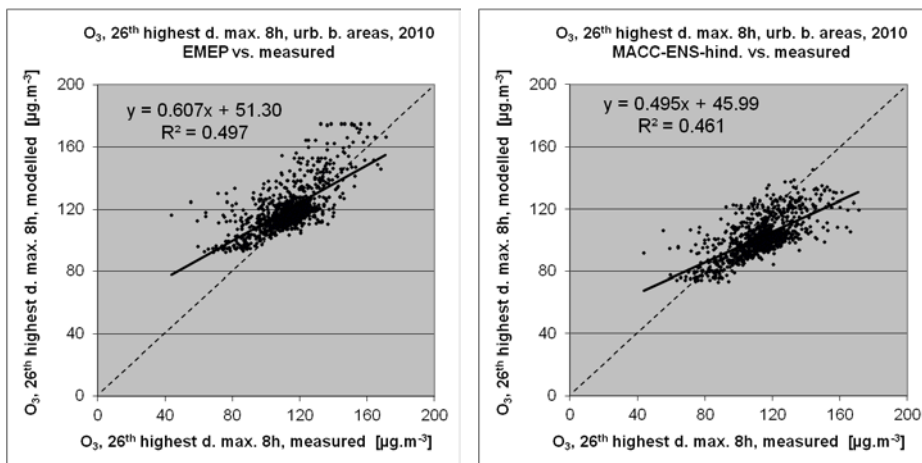


Figure A5.14 Scatter plots showing modelled vs. urban/suburban background measured data for EMEP (left) and MACC-II Ensemble (right) model outputs for ozone indicator 26th highest daily max. 8-hourly mean for 2010

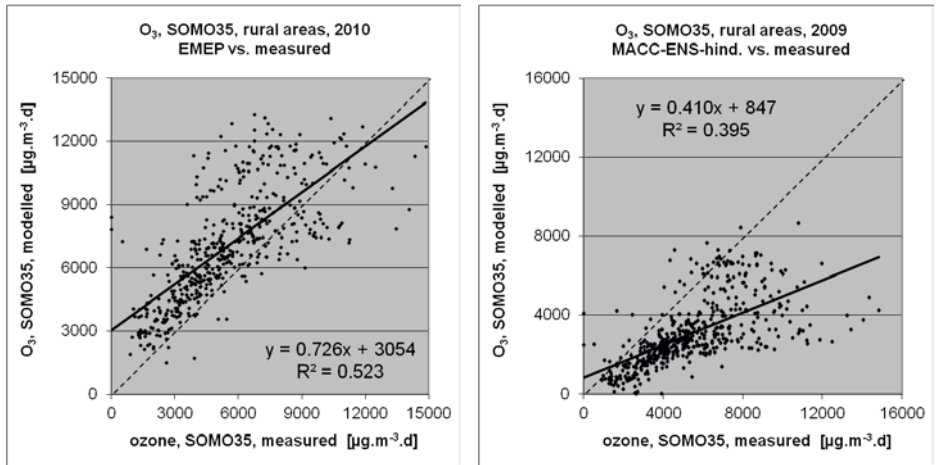


Figure A5.15 Scatter plots showing modelled vs. rural background measured data for EMEP (left) and MACC-II Ensemble (right) model outputs for ozone indicator SOMO35 for 2010

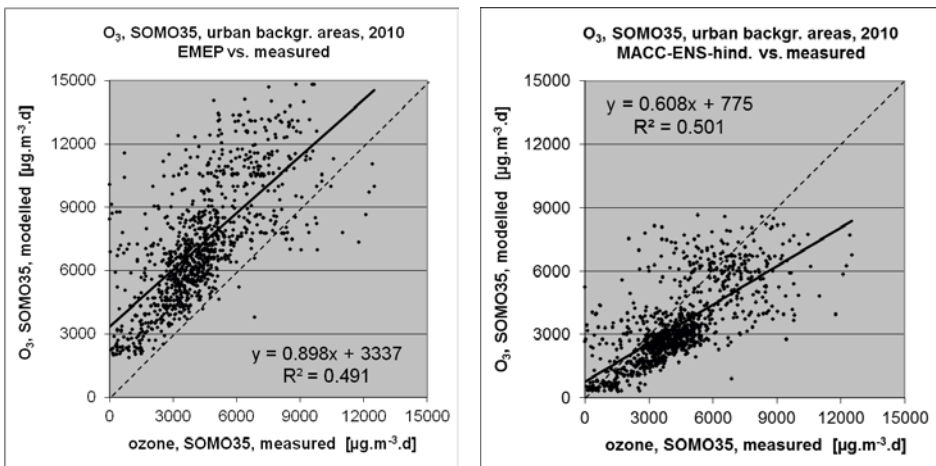


Figure A5.16 Scatter plots showing modelled vs. urban/suburban background measured data for EMEP (left) and MACC-II Ensemble (right) model outputs for ozone indicator SOMO35 for 2010

Annex 6. Comparison of scatter plots of reanalysed model and ETC/ACM mapping results

Section 5.2 presents the initial comparison of the ETC/ACM mapping and MACC-II Ensemble reanalysis results. Tables 5.1 to 5.2 show the statistical indicators relevant to this comparison. This annex contains, in addition to these tables, the correspondent scatter plots:

1. MACC-II Ensemble reanalysis results
 - scatter plots showing the results from the MACC-II Ensemble reanalysis modelling against the measured data (without distinction whether these data is used or not in the reanalysis),
2. ETC/ACM mapping results using EMEP model output
 - (i) *'leave-one-out' cross-validation* scatter plots of the ETC/ACM mapping (using EMEP model) for the separate (i.e. rural or urban background) map against the measured data,
 - (ii) *simple* scatter plots of the ETC/ACM mapping result (using EMEP model) for the separate (i.e. rural or urban background) map against the measured data,
 - (iii) *simple* scatter plots showing the ETC/ACM mapping result (using EMEP model) for the final merged map in the $1 \times 1 \text{ km}^2$ resolution against the measured data.
3. ETC/ACM mapping results using MACC-II Ensemble hindcast model output
 - (i) *'leave-one-out' cross-validation* scatter plots of the ETC/ACM mapping (using MACC-II Ensemble hindcast) for the separate (i.e. rural or urban background) map against the measured data,
 - (ii) *simple* scatter plots of the ETC/ACM mapping result (using MACC-II Ensemble) for the separate (i.e. rural or urban background) map against the measured data,

All the ETC/ACM mapping results are constructed in the same $10 \times 10 \text{ km}^2$ spatial resolution, with the exception of the final merged $1 \times 1 \text{ km}^2$ map. All the MACC-II Ensemble reanalysis results are converted into the same $10 \times 10 \text{ km}^2$ spatial resolution (see Section 3.2). For the rural areas, measured data of rural background stations is used, and for the urban background areas, measured data of urban and suburban background stations is used.

Figures A6.1 to A6.8 show the scatter plots for PM_{10} , and Figures A6.9 to A6.16 show the plots for ozone.

In all the figures, the MACC-II Ensemble reanalysis scatter plot (upper left) can be compared with cross-validated (centre) and simple (right) scatter plots of the ETC/ACM mapping results using either EMEP (top) or MACC-II Ensemble (bottom) model hindcast outputs. One may assume that the scatter plots, which would actually correspondent to the results of the MACC-II Ensemble reanalysis, could be found somewhere “in between” the cross-validated and the simple scatter plots of the ETC/ACM mapping results. Next to this, the simple scatter plot of the ETC/ACM final merged $1 \times 1 \text{ km}^2$ map (bottom left) can be compared on the one hand with the simple scatter plot of the separate ETC/ACM rural, resp. urban background map (top right), and on the other hand with the scatter plot of the MACC-II Ensemble reanalysis (top left).

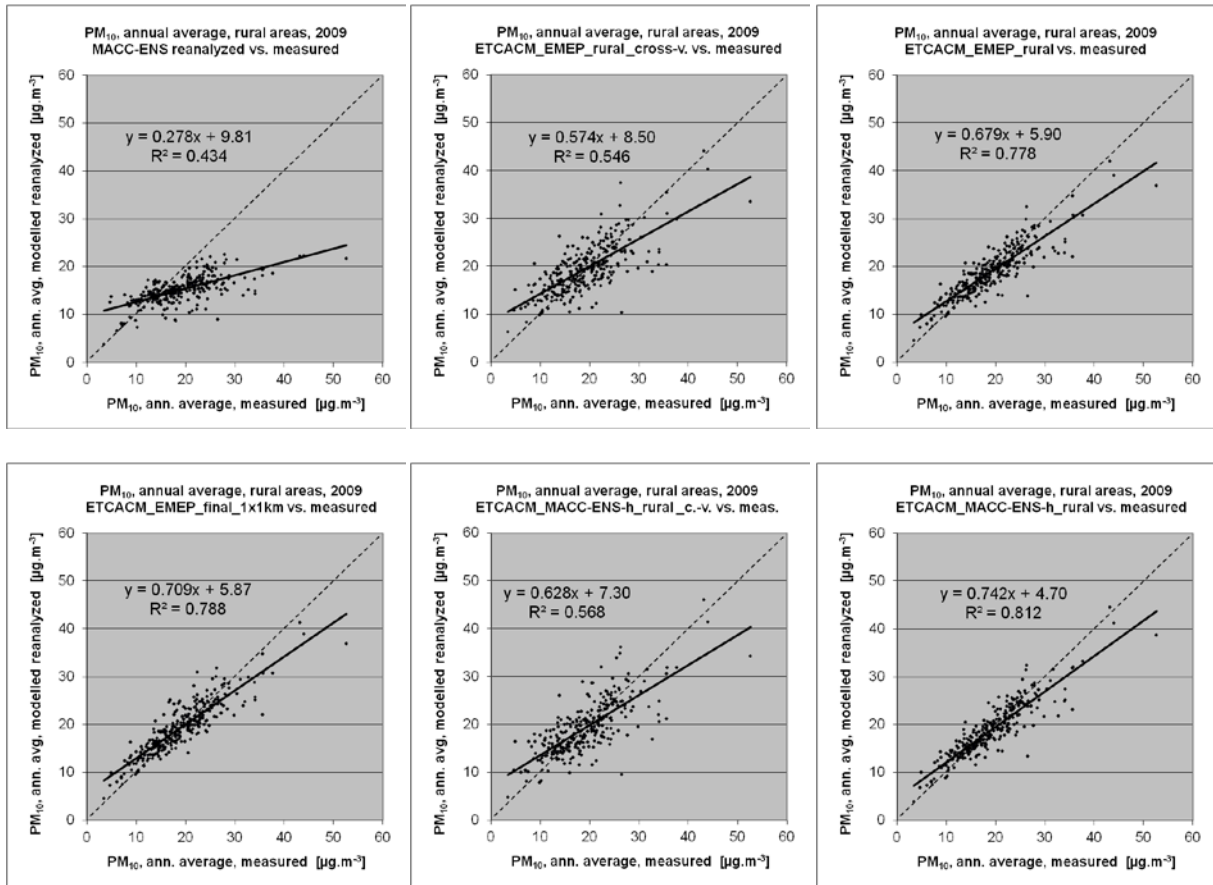


Figure A6.1 Scatter plots showing MACC-II Ensemble reanalysed vs. measured data (upper left) versus ETC/ACM mapping using EMEP vs. measured data using cross validation (upper middle) and simple comparison using rural (upper right) and final merged (lower left) map and ETC/ACM mapping using MACC-II Ensemble hindcast vs. measured data using cross validation (lower middle) and simple comparison (lower right) for PM_{10} annual average 2009 for rural background areas

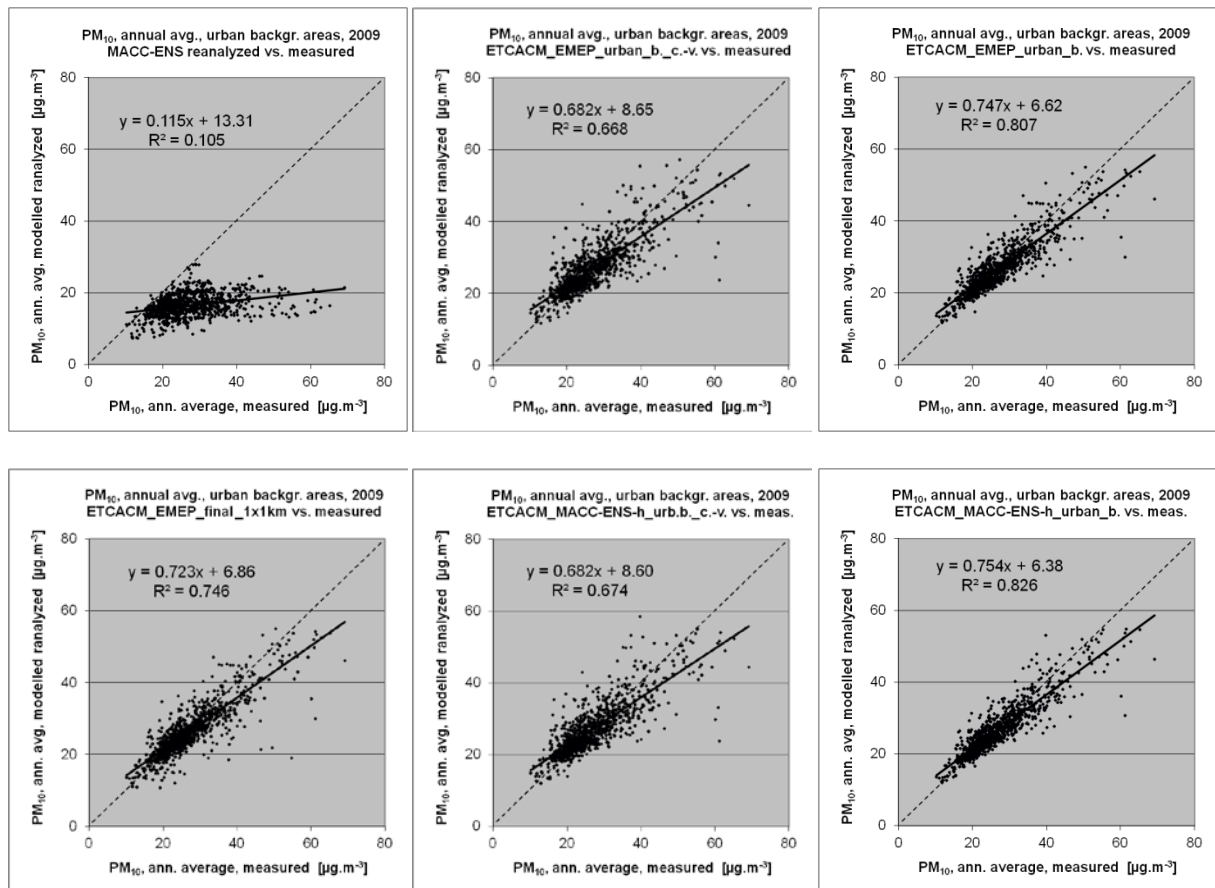


Figure A6.2 Scatter plots showing MACC-II Ensemble reanalysed vs. measured data (upper left) versus ETC/ACM mapping using EMEP vs. measured data using cross validation (upper middle) and simple comparison using urban background (upper right) and final merged (lower left) map and ETC/ACM mapping using MACC-II Ensemble hindcast vs. measured data using cross validation (lower middle) and simple comparison (lower right) for PM₁₀ annual average 2009 for urban background areas

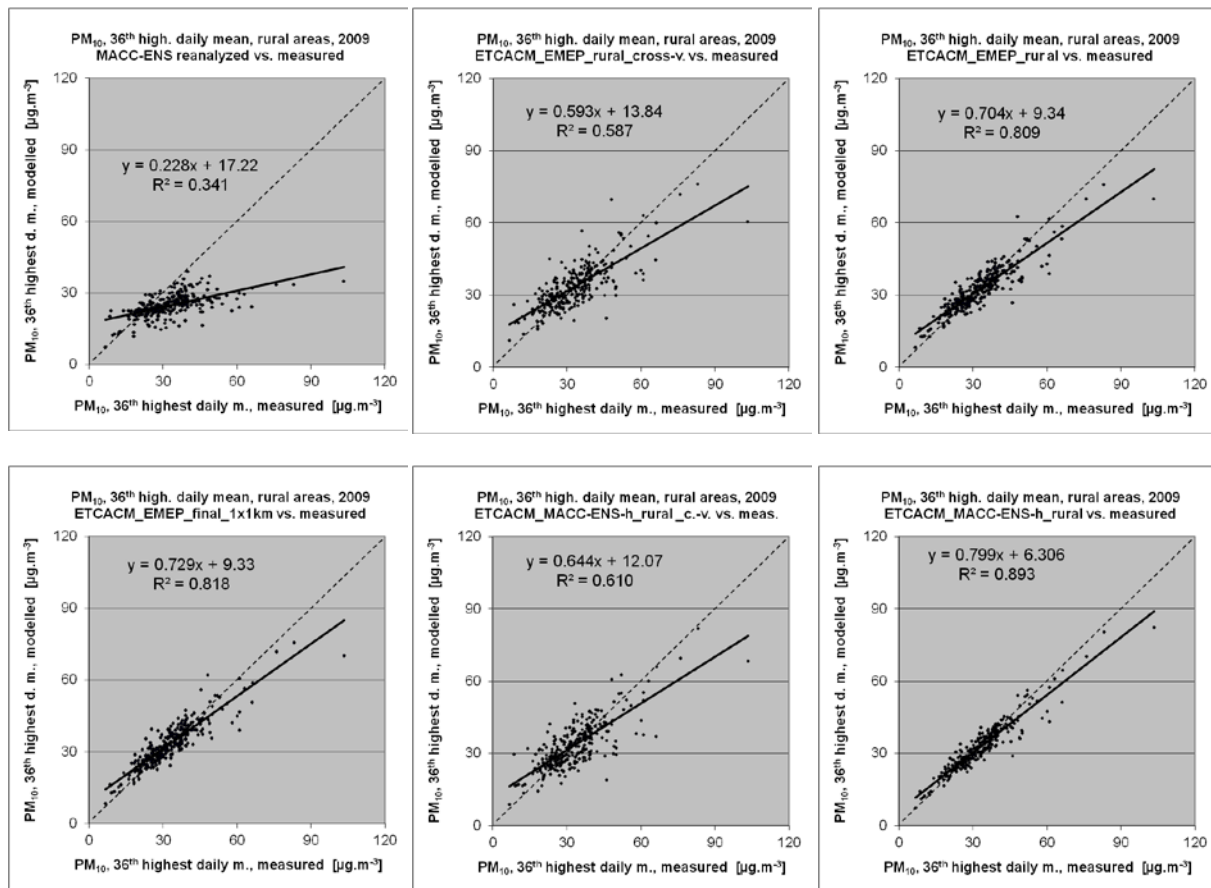


Figure A6.3 Scatter plots showing MACC-II Ensemble reanalysed vs. measured data (upper left) versus ETC/ACM mapping using EMEP vs. measured data using cross validation (upper middle) and simple comparison using rural (upper right) and final merged (lower left) map and ETC/ACM mapping using MACC-II Ensemble hindcast vs. measured data using cross validation (lower middle) and simple comparison (lower right) for PM₁₀ indicator 36th highest daily mean for 2009 for rural background areas

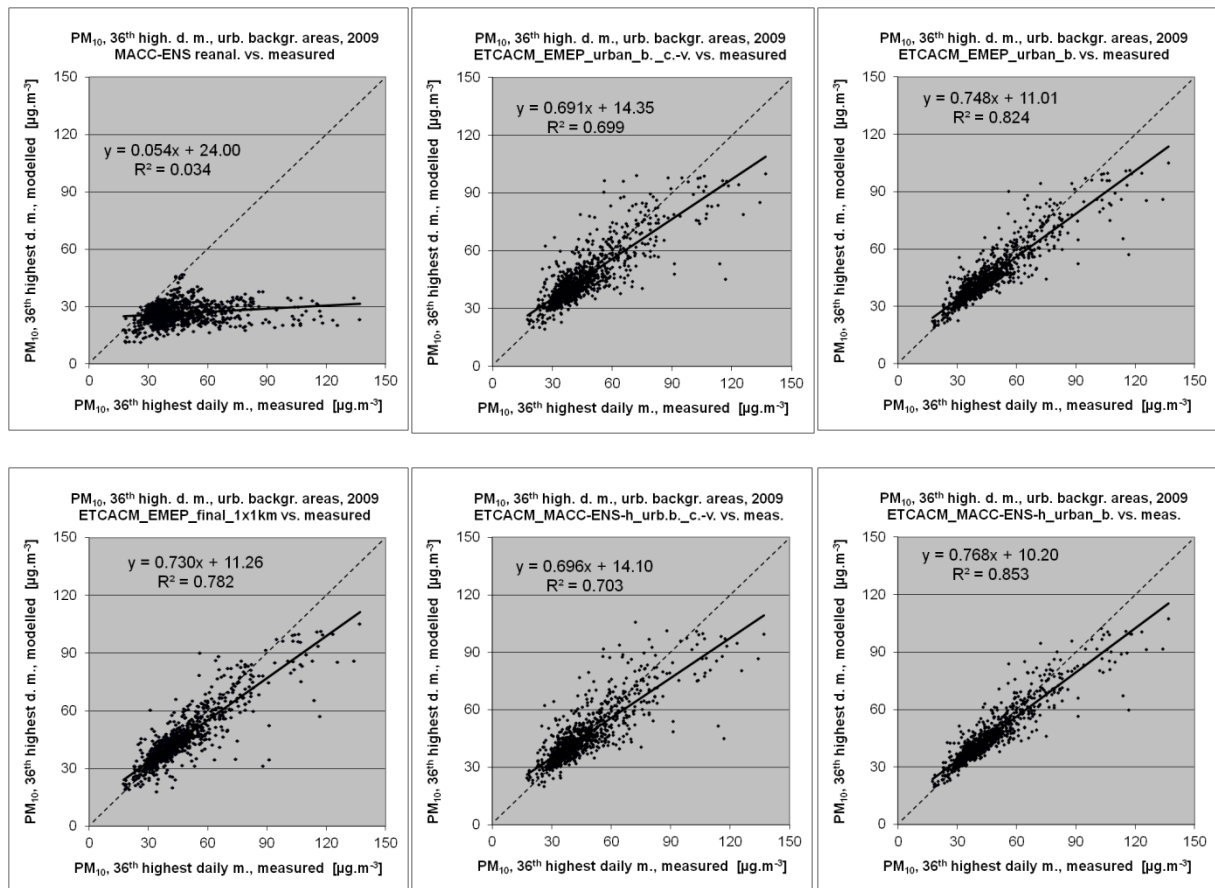


Figure A6.4 Scatter plots showing MACC-II Ensemble reanalysed vs. measured data (upper left) versus ETC/ACM mapping using EMEP vs. measured data using cross validation (upper middle) and simple comparison using urban background (upper right) and final merged (lower left) map and ETC/ACM mapping using MACC-II Ensemble hindcast vs. measured data using cross validation (lower middle) and simple comparison (lower right) for PM₁₀ indicator 36th highest daily mean for 2009 for urban background areas

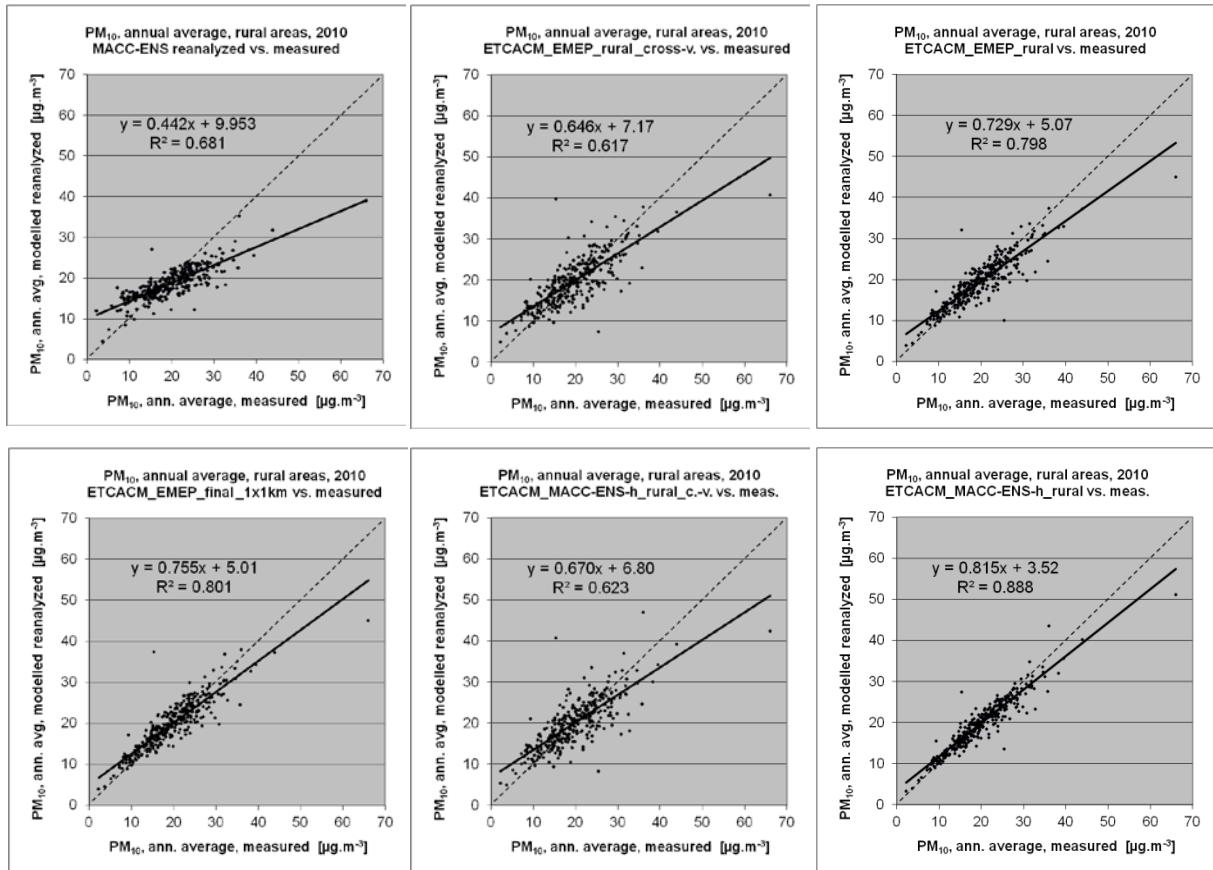


Figure A6.5 Scatter plots showing MACC-II Ensemble reanalysed vs. measured data (upper left) versus ETC/ACM mapping using EMEP vs. measured data using cross validation (upper middle) and simple comparison using rural (upper right) and final merged (lower left) map and ETC/ACM mapping using MACC-II Ensemble hindcast vs. measured data using cross validation (lower middle) and simple comparison (lower right) for PM₁₀ annual average 2010 for rural background areas (= Figure 5.9)

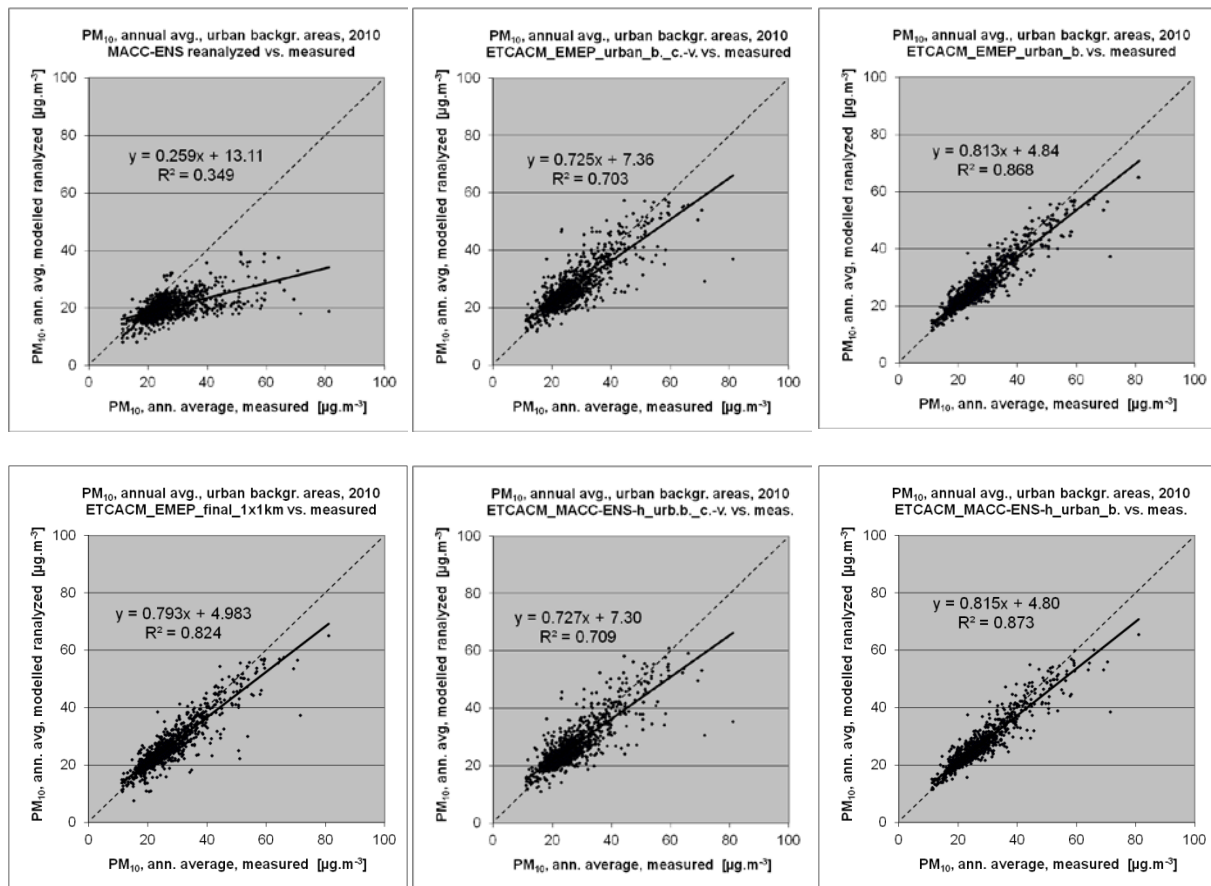


Figure A6.6 Scatter plots showing MACC-II Ensemble reanalysed vs. measured data (upper left) versus ETC/ACM mapping using EMEP vs. measured data using cross validation (upper middle) and simple comparison using urban background (upper right) and final merged (lower left) map and ETC/ACM mapping using MACC-II Ensemble hindcast vs. measured data using cross validation (lower middle) and simple comparison (lower right) for PM₁₀ annual average 2010 for urban background areas (= Figure 5.10)

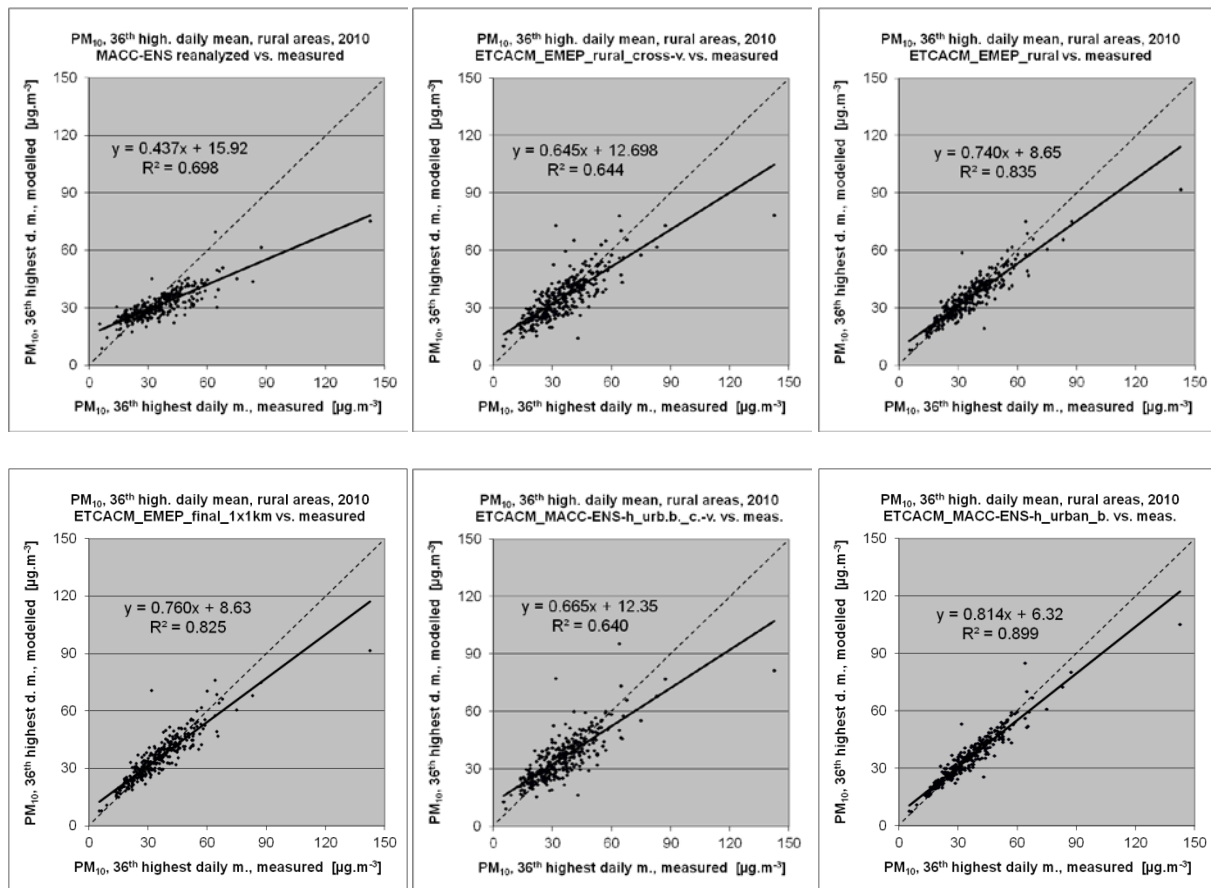


Figure A6.7 Scatter plots showing MACC-II Ensemble reanalysed vs. measured data (upper left) versus ETC/ACM mapping using EMEP vs. measured data using cross validation (upper middle) and simple comparison using rural (upper right) and final merged (lower left) map and ETC/ACM mapping using MACC-II Ensemble hindcast vs. measured data using cross validation (lower middle) and simple comparison (lower right) for PM_{10} indicator 36th highest daily mean for 2010 for rural background areas

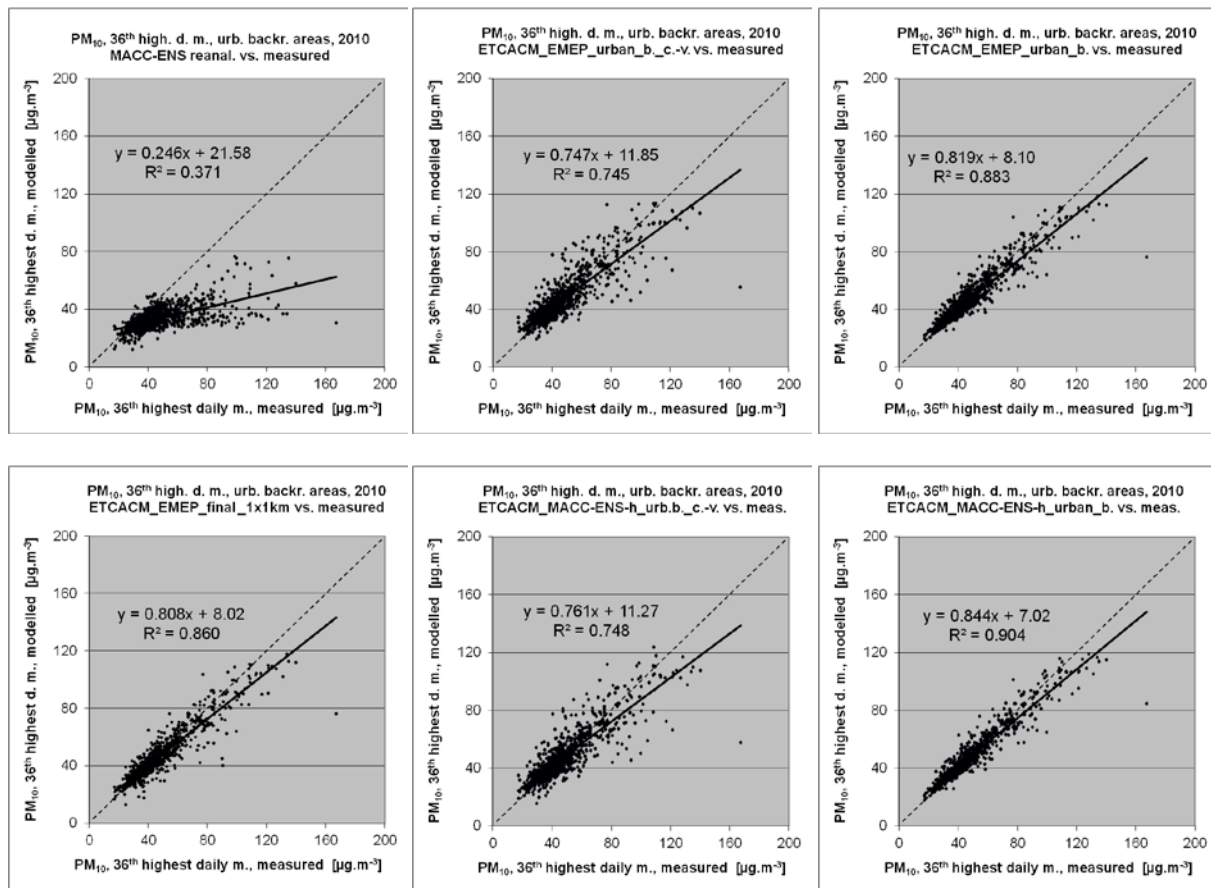


Figure A6.8 Scatter plots showing MACC-II Ensemble reanalysed vs. measured data (upper left) versus ETC/ACM mapping using EMEP vs. measured data using cross validation (upper middle) and simple comparison using urban background (upper right) and final merged (lower left) map and ETC/ACM mapping using MACC-II Ensemble hindcast vs. measured data using cross validation (lower middle) and simple comparison (lower right) for PM₁₀ indicator 36th highest daily mean for 2010 for urban background areas

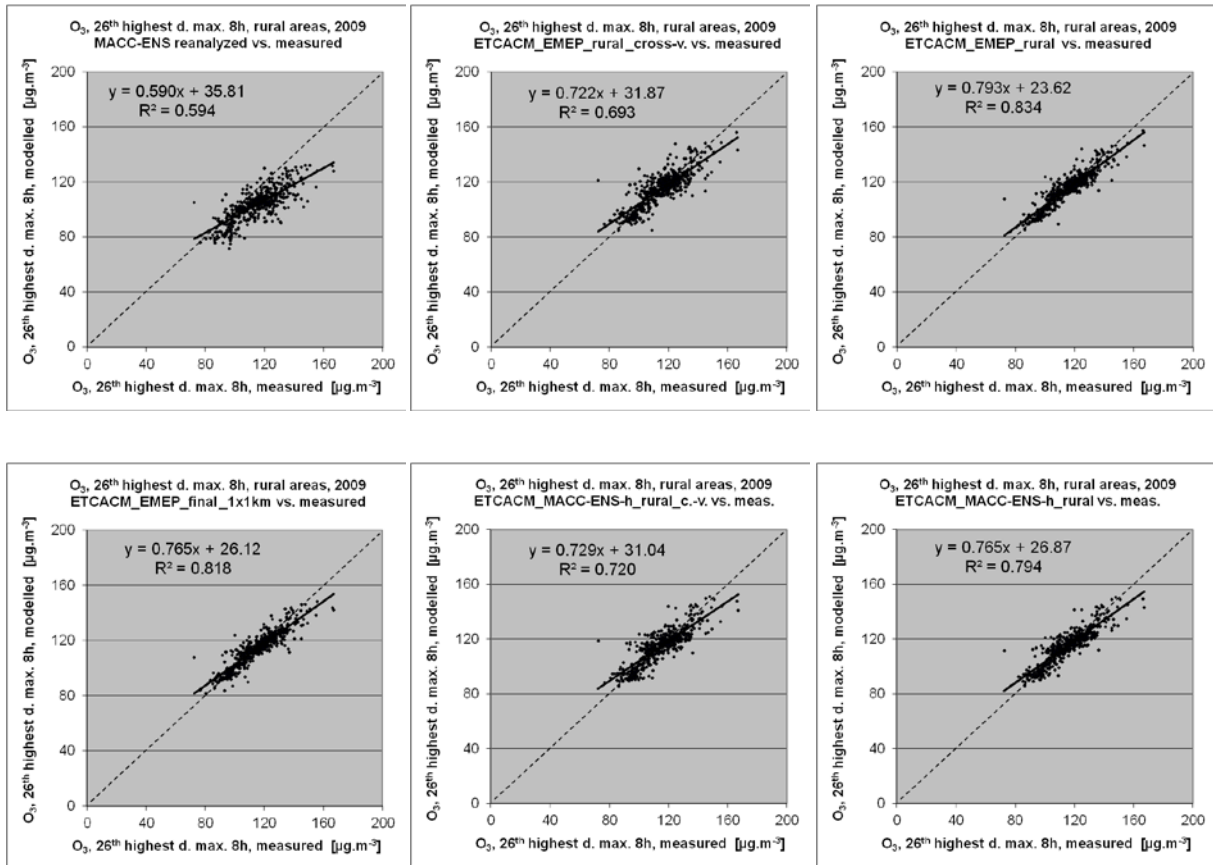


Figure A6.9 Scatter plots showing MACC-II Ensemble reanalysed vs. measured data (upper left) versus ETC/ACM mapping using EMEP vs. measured data using cross validation (upper middle) and simple comparison using rural (upper right) and final merged (lower left) map and ETC/ACM mapping using MACC-II Ensemble hindcast vs. measured data using cross validation (lower middle) and simple comparison (lower right) for ozone indicator 26th highest daily max. 8-hourly mean for 2009 for rural background areas

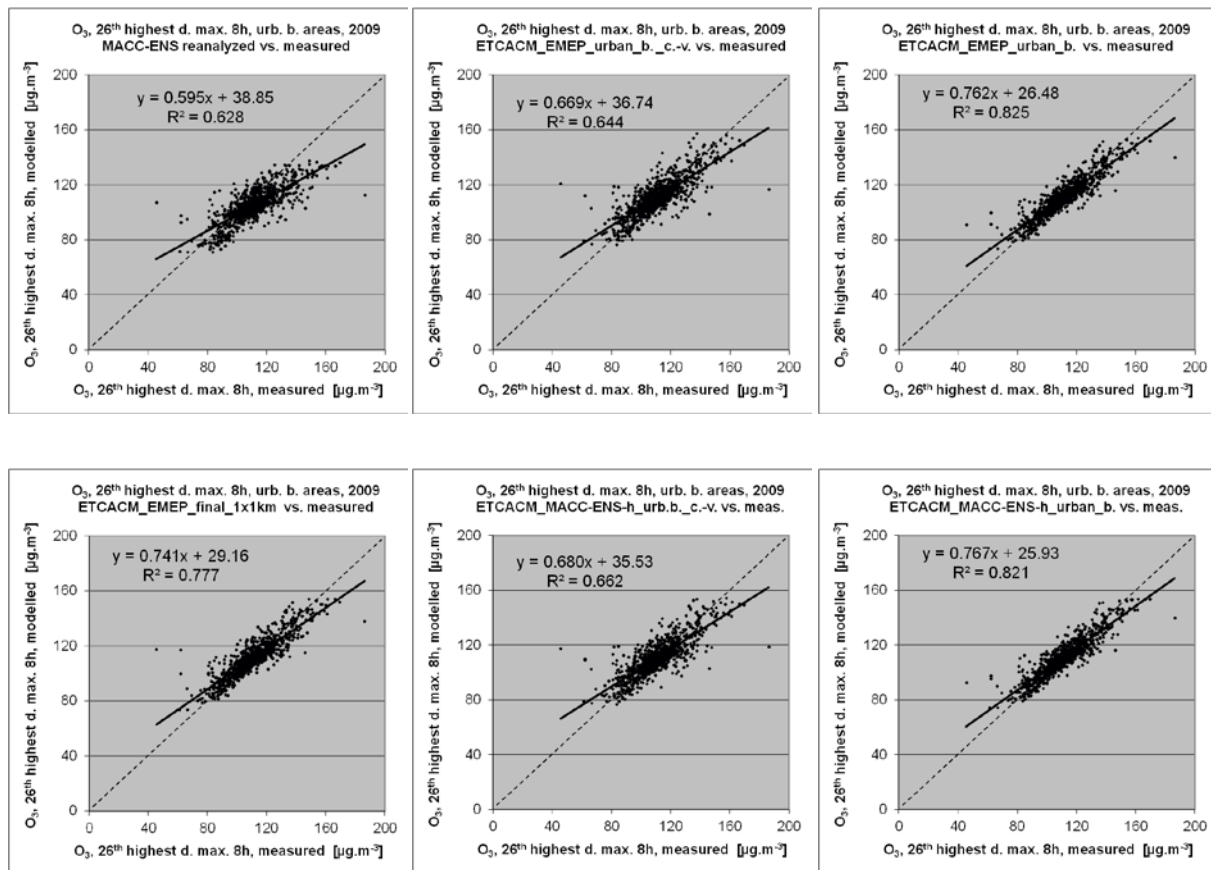


Figure A6.10 Scatter plots showing MACC-II Ensemble reanalysed vs. measured data (upper left) versus ETC/ACM mapping using EMEP vs. measured data using cross validation (upper middle) and simple comparison using urban background (upper right) and final merged (lower left) map and ETC/ACM mapping using MACC-II Ensemble hindcast vs. measured data using cross validation (lower middle) and simple comparison (lower right) for ozone indicator 26th highest daily max. 8-hourly mean for 2009 for urban background areas

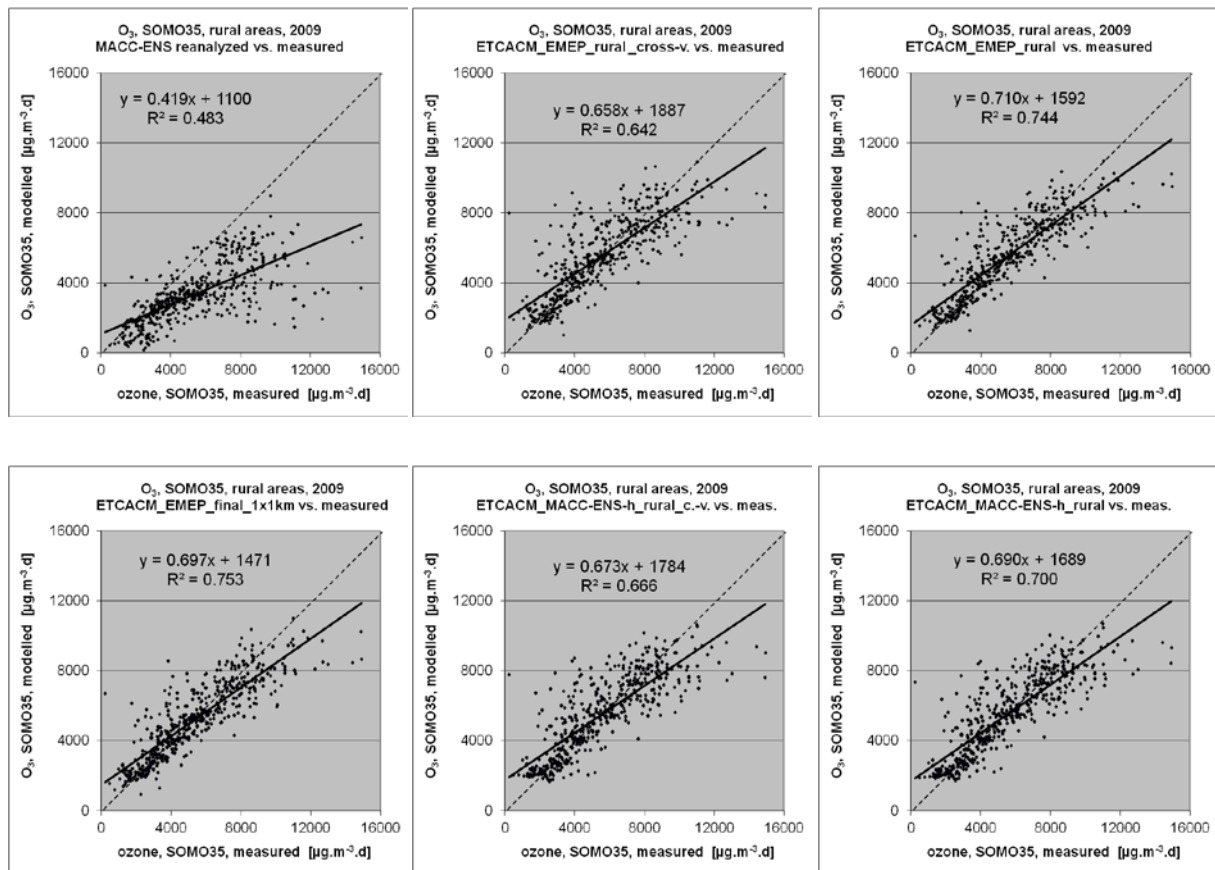


Figure A6.11 Scatter plots showing MACC-II Ensemble reanalysed vs. measured data (upper left) versus ETC/ACM mapping using EMEP vs. measured data using cross validation (upper middle) and simple comparison using rural (upper right) and final merged (lower left) map and ETC/ACM mapping using MACC-II Ensemble hindcast vs. measured data using cross validation (lower middle) and simple comparison (lower right) for ozone indicator SOMO35 for 2009 for rural background areas

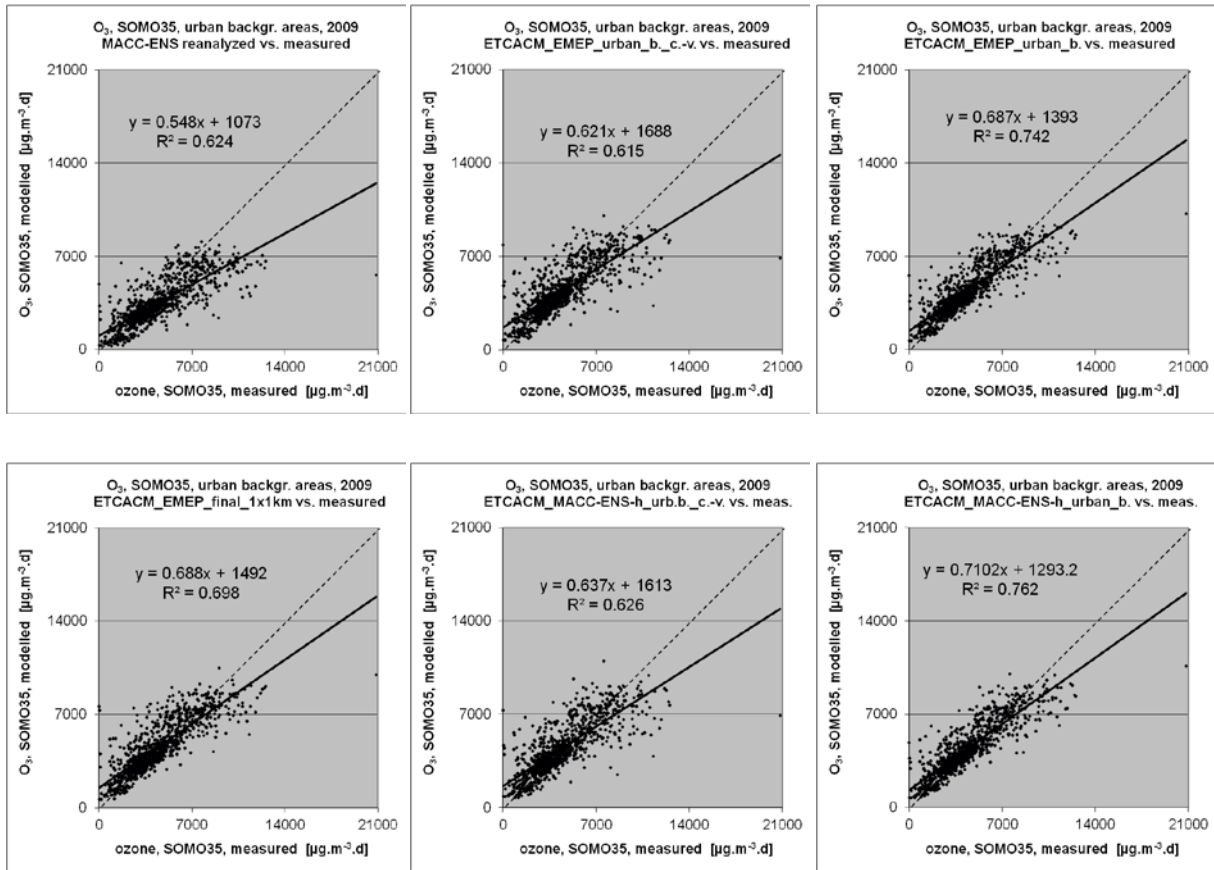


Figure A6.12 Scatter plots showing MACC-II Ensemble reanalysed vs. measured data (upper left) versus ETC/ACM mapping using EMEP vs. measured data using cross validation (upper middle) and simple comparison using urban background (upper right) and final merged (lower left) map and ETC/ACM mapping using MACC-II Ensemble hindcast vs. measured data using cross validation (lower middle) and simple comparison (lower right) for ozone indicator SOMO35 for 2009 for urban background areas

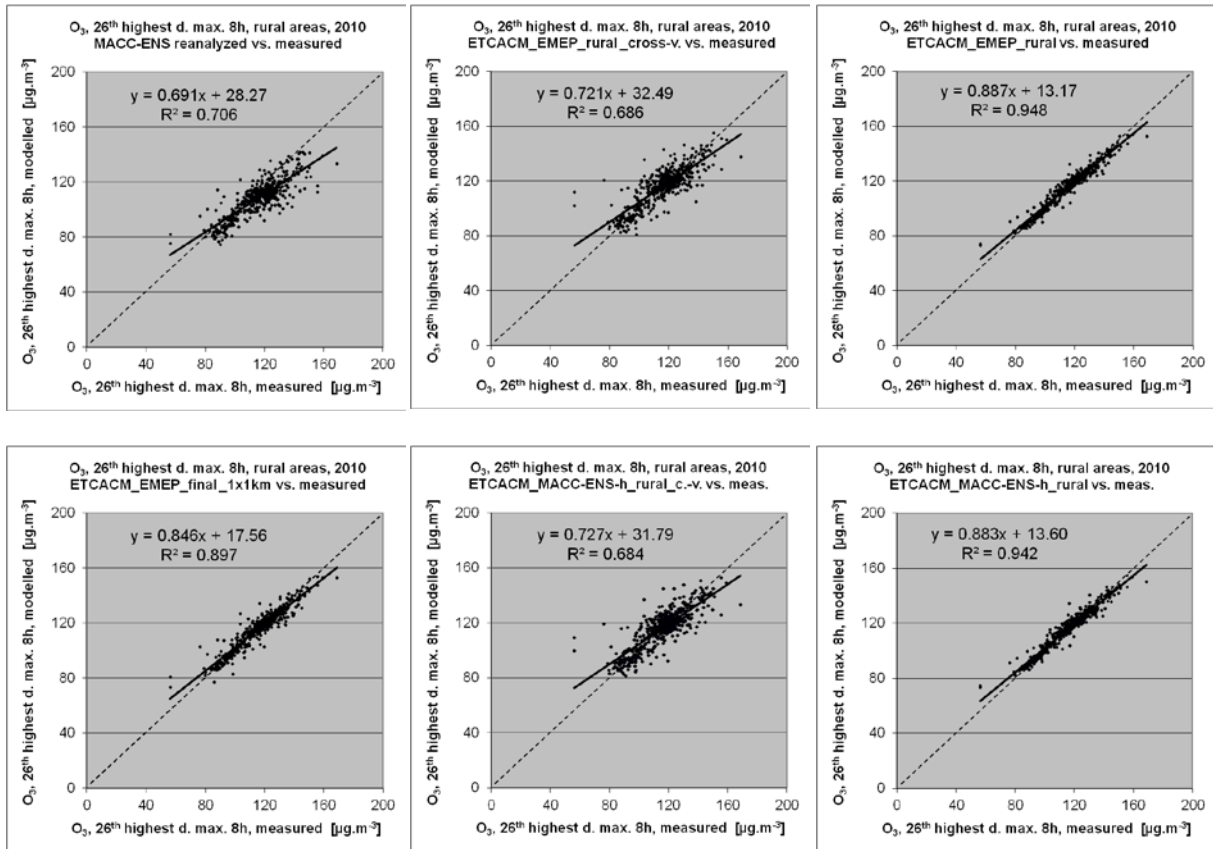


Figure A6.13 Scatter plots showing MACC-II Ensemble reanalysed vs. measured data (upper left) versus ETC/ACM mapping using EMEP vs. measured data using cross validation (upper middle) and simple comparison using rural (upper right) and final merged (lower left) map and ETC/ACM mapping using MACC-II Ensemble hindcast vs. measured data using cross validation (lower middle) and simple comparison (lower right) for ozone indicator 26th highest daily max. 8-hourly mean for 2010 for rural background areas

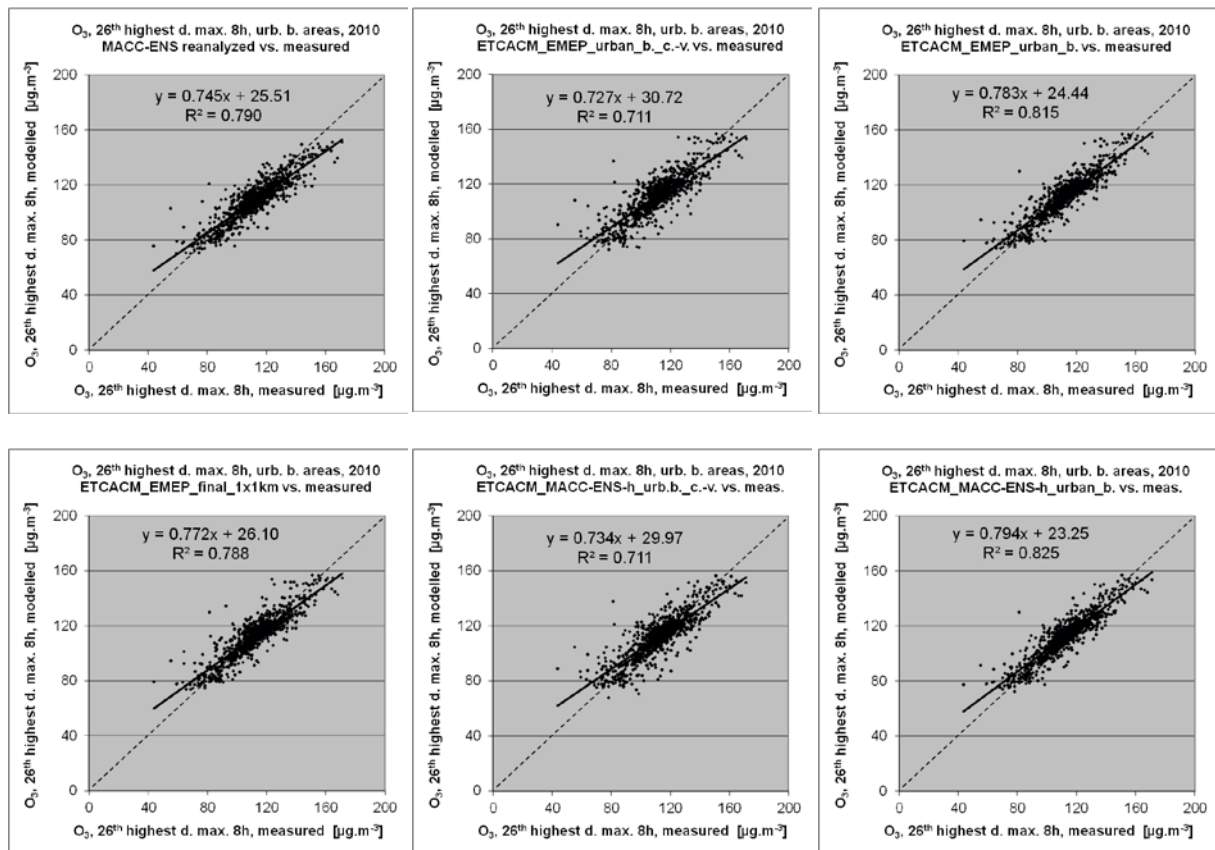


Figure A6.14 Scatter plots showing MACC-II Ensemble reanalysed vs. measured data (upper left) versus ETC/ACM mapping using EMEP vs. measured data using cross validation (upper middle) and simple comparison using urban background (upper right) and final merged (lower left) map and ETC/ACM mapping using MACC-II Ensemble hindcast vs. measured data using cross validation (lower middle) and simple comparison (lower right) for ozone indicator 26th highest daily max. 8-hourly mean for 2010 for urban background areas

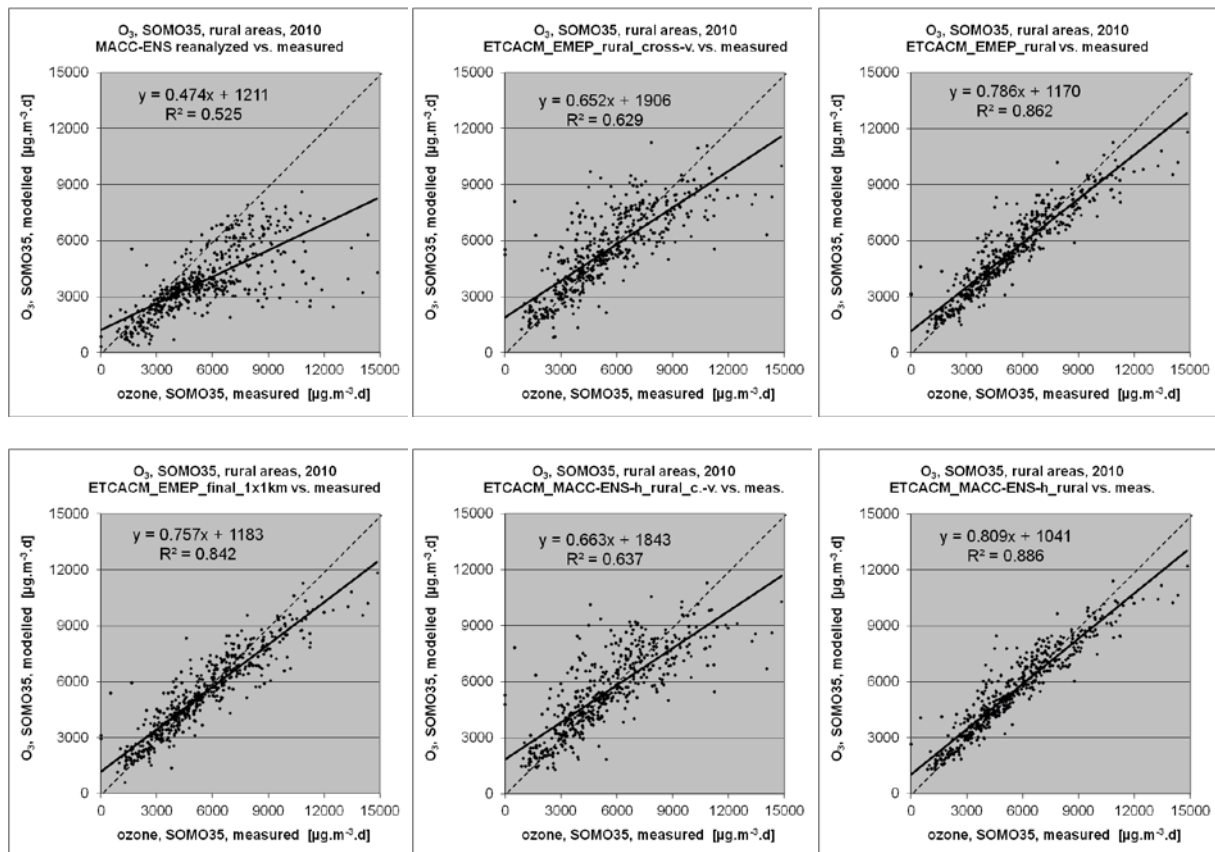


Figure A6.15 Scatter plots showing MACC-II Ensemble reanalysed vs. measured data (upper left) versus ETC/ACM mapping using EMEP vs. measured data using cross validation (upper middle) and simple comparison using rural (upper right) and final merged (lower left) map and ETC/ACM mapping using MACC-II Ensemble hindcast vs. measured data using cross validation (lower middle) and simple comparison (lower right) for ozone indicator SOMO35 for 2010 for rural background areas (= Figure 5.13)

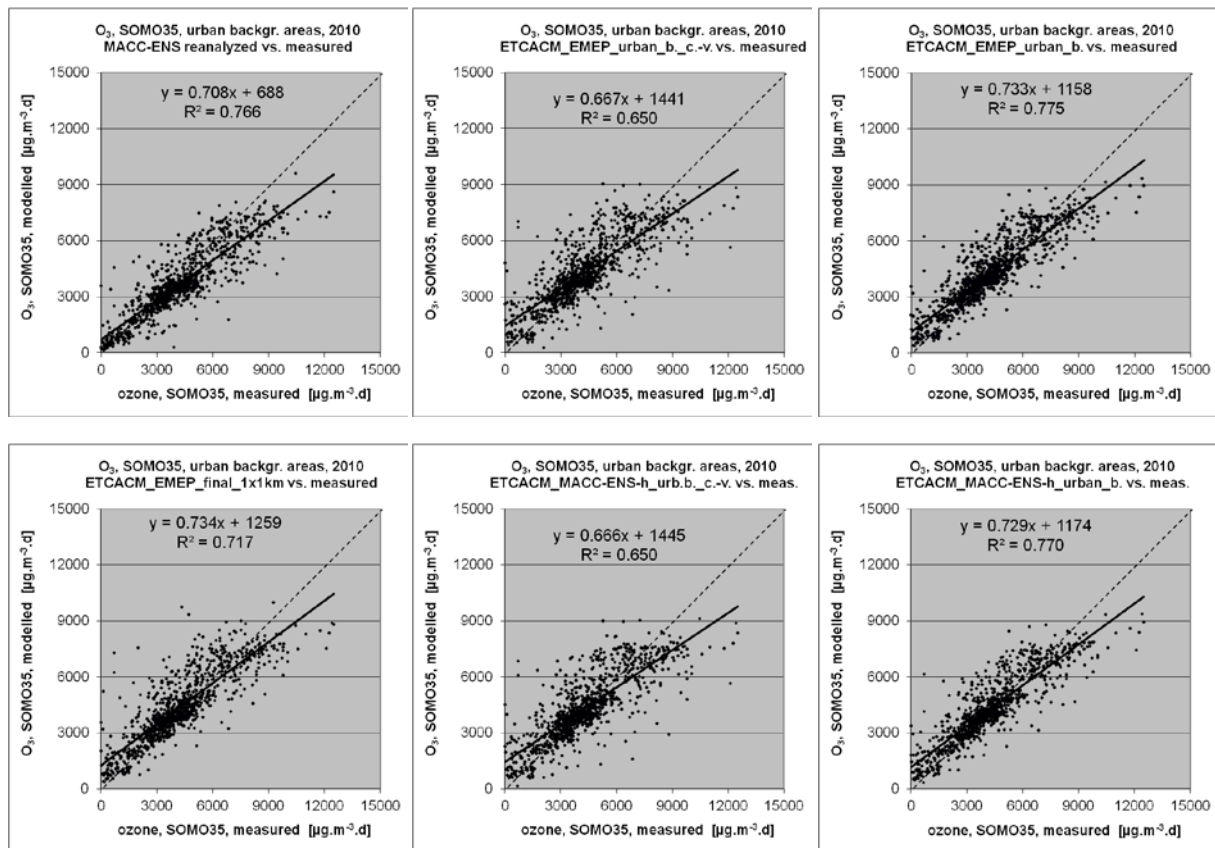


Figure A6.16 Scatter plots showing MACC-II Ensemble reanalysed vs. measured data (upper left) versus ETC/ACM mapping using EMEP vs. measured data using cross validation (upper middle) and simple comparison using urban background (upper right) and final merged (lower left) map and ETC/ACM mapping using MACC-II Ensemble hindcast vs. measured data using cross validation (lower middle) and simple comparison (lower right) for ozone indicator SOMO35 for 2010 for urban background areas (= Figure 5.14)

Annex 7. Explanation of Taylor diagram principle

Taylor diagram synthesizes on a unique quadrant various statistical indicators for various models: the radii correspond to the correlation coefficient values, the x-axis and the y-axis delimit arcs with standard deviation values and the internal semi-circles correspond to the RMSE values. The statistical indicators show the performance of the individual models in comparison with the observations. Correlation coefficient should be as close to one as possible, RMSE should be as small as possible and the standard deviation of the model results should be as close as possible to the standard deviation of the observations.

The Figure A7.1 below is a sample Taylor diagram (Taylor, 2001) which shows how it can be used to summarize the relative skill with which models simulate the spatial patterns. In this example statistics for eight models were computed, and a letter was assigned to each model considered. The position of each letter appearing on the plot quantifies how closely that model's simulation pattern matches observations. Consider model *F*, for example. Its pattern correlation with observations is about 0.65. The centred root-mean-square RMSE between the simulated and observed patterns is proportional to the distance to the point on the x-axis identified as “observed”. The green contours indicate the RMSE values and it can be seen that in the case of model *F* the centred RMSE is about 2.6 units. The standard deviation of the simulated pattern is proportional to the radial distance from the origin. For model *F* the standard deviation of the simulated field (about 3.3 units) is clearly greater than the observed standard deviation which is indicated by the dashed arc at the observed value of 2.9 units.

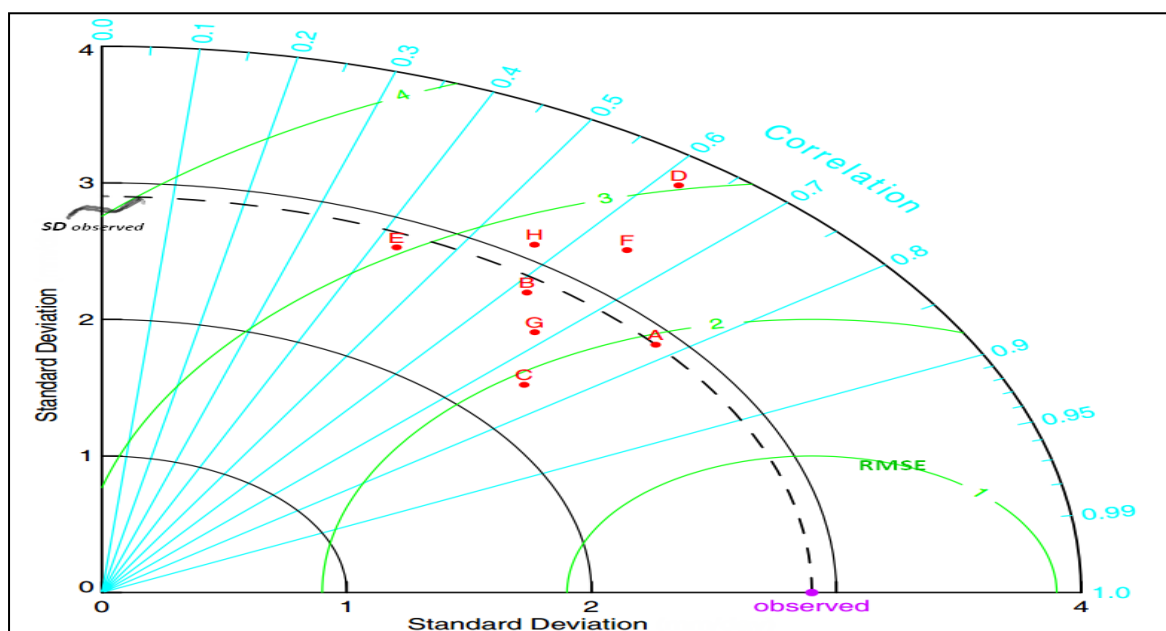


Figure A7.1 Sample Taylor diagram displaying a statistical comparison with observations of eight model estimates of the pattern of a quantity